The Impacts of Endocrine-disrupting Chemicals on Bacteria and Their Influences On the Cycling of Emerging Contaminants and Antibiotic-resistant Efflux Pump Proteins In Engineered Microbial Environments

by

Diego Erick Novoa

A Dissertation Presented in Partial Fulfillment
of the Requirements for the Degree
Doctor of Philosophy

Approved July 2022 by the
Graduate Supervisory Committee:

Otakuye Conroy-Ben, Chair
Morteza Abbazsadegan
Rosa Krajmalnik-Brown

ARIZONA STATE UNIVERSITY

August 2022

ABSTRACT

This dissertation encompasses the interaction of antimicrobial chemicals and emerging contaminants with multi-drug resistant (MDR) bacteria and their implications in engineered systems. The aim is to investigate the effect of combination antimicrobials on MDR bacteria *E. coli*, evaluate the extent of synergism and antagonism of utilizing two distinct biocidal chemicals, and evaluate the influence of endocrine-disrupting chemicals (EDCs) on protein production in response to stressors. Resistance mechanisms of bacteria such as *E. coli* include the use of protein systems that efflux excess nutrients or toxic compounds. These efflux proteins activate in response to environmental stressors such as contaminants and antimicrobials to varying degrees and are major contributors to antibiotic resistance in pathogenic bacteria. As is the case with engineered microbial environments, large quantities of emerging contaminants interact with bacteria, influencing antibiotic resistance and attenuation of these chemicals to an unknown degree. Interactions of antimicrobials on MDR bacteria such as *E. coli* have been extensively studied for pathogens, including synergistic combinations. Despite these studies in this field, a fundamental understanding of how chemicals influence antibiotic resistance in biological processes typical of engineered microbial environments is still ongoing. The impacts of EDCs on antibiotic resistance in *E. coli* were investigated by the characterization of synergism for antimicrobial therapies and the extrapolation of these metrics to the cycling of EDCs in engineered systems to observe the extent of antibiotic resistance proteins to the EDCs. The impact of this work provides insight into the delicate biochemistry and ongoing resistance phenomena regarding engineered systems.

DEDICATION

To my grandmother, Bertha Alayza Àguilar for being the first person to introduce me to the joys and wonders of science. She has been a pivotal source of inspiration in my life and this accumulation of work would not have been possible if it were not for her influence in my life. Gracias por todo abuelita, te quiero ahora y siempre.

To my mother and father, Sylvia Betty Alayza-Novoa, and Erich Moisés Novoa, for raising me to always work my hardest and supporting and redirecting me in the decisions that have led me to this work. Te quiero mucho mamá y papa.

To my brother Roberto Erich Novoa, for always being present and at the moment with me every time I needed him, and for his advice, encouragement, and for being my role model. I love you Toto.

Esto es para ustedes, y para mi

ACKNOWLEDGMENTS

I would like to thank Dr. Otakuye Conroy-Ben for her mentorship and endless support throughout my journey at Arizona State University (ASU). I am very grateful that you took a chance on me when I joined your lab. Thank you for all the feedback, encouragement, and knowledge you have given me. I would like to thank my committee member, Dr. Morteza Abbaszadegan, for making himself available to all my questions in the realm of microbiology and for all the great conversations we had. I would like to thank my other committee member, Dr. Rosa Krajmalnik-Brown, for teaching my favorite graduate class I took at ASU and for providing her with invaluable advice in the academic process. I would like to thank Stan Klonowski for providing and maintaining a safe laboratory to conduct experiments in and for his help with troubleshooting issues regarding equipment. I could not have finished my studies without your expertise and help. I would like to thank ASU's Fulton Schools of Engineering and the National Science Foundation for their financial and institutional support.

I would like to thank and acknowledge my friends and peers at ASU. There is no possibility of me arriving at this point in my graduate studies if it had not been for all the love and support, I have received from everyone. I would like to thank my mother, father, brother, sister-in-law, and niece for their love and support. I would like to give a special thanks to my future wife, Alondra Torres. Thank you for all your love and support. Te amo ahora, y siempre. This work has been an accumulation of all the encouragement, tears, laughs, grunts, and panic attacks I have shared with everyone that stood by me. Thank you all.

TABLE OF CONTENTS

Page

CHAPTER Page

CHAPTER Page

CHAPTER Page

APPENDIX Page

LIST OF TABLES

Table Page

Table Page

LIST OF FIGURES

Figure Page

Figure Page

Figure Page

Figure Page

Figure Page

Figure Page

CHAPTER 1

INTRODUCTION AND LITERATURE REVIEW

1.1. Introduction.

Antibiotic resistance in human bacterial pathogens is a critical concern to public and environmental health worldwide.[1] Bacteria can gain resistance intrinsically or attain it via gene transfer from other bacteria, as a result of exposure to inadequate concentrations of antibiotics resulting in sub-lethal exposure to the respective toxins.[2] Antibiotic-resistant bacteria can enter waterways from human and animal sources with many antibiotics originating from healthcare or agricultural industries.[3] In water systems, they are capable of easily spreading genes to other microbes. The flow and direction of antibiotic-resistant genes (ARGs) and emerging contaminants can be observed in Figure 1.1. The major pathways represent the primary sources and lifecycle of antibiotic usage in animal agriculture, and human healthcare as well as the direction and cycling of emerging contaminants. Each stage acts as a genetic reactor for antibiotic resistance allowing for the exchange and recycling of genetic material to shape the evolution of microbes in different stages of the system.[2, 4] Wastewater treatment plants (WWTP) are the focus of the cycling pathways of emerging contaminants and ARGs. During wastewater treatment, both genes and emerging contaminants can cycle through allowing for acute and chronic exposure of these pollutants to microbial life.

The biological wastewater treatment process present in modern WWTPs is an engineered ecosystem of microorganisms subject to controlled parameters influencing the microbial food network in favor of the reduction of biological oxygen demand (BOD). Fundamentals of typical biological treatment of wastewater involve a pretreatment step where coarse solids and grit are removed, a primary treatment step where sedimentation

or clarification is used to remove suspended solids, a secondary treatment step where a biological reactor is used to reduce the BOD, and lastly a tertiary treatment step that may involve filtration and disinfection of some kind depending on the need and if the finished water is to be reused.[5] Sludge settled from the primary and secondary clarifiers is referred to as waste activated sludge (WAS) and secondary sludge recycled into the biological treatment unit of the WWTP is referred two as returned activated sludge (RAS). The proliferation of emerging contaminants and or resistance genes can occur to various degrees depending on their fate and transport in a WWTP.

Bacterial antibiotic resistance has evolved to be redundant in bacterial cells increasing protection from biocides. Resistance mechanisms exist for virtually all classes of antibiotics across many species.[6-8] Mechanisms include modification of antibiotic molecules, destruction of an antibiotic molecule, decreased antibiotic penetration, changes in target sites, and chemical efflux of compounds among others.[9-13] The latter is of particular interest due to the multiple levels of resistance induced. Emerging contaminants may pose an issue to both public health and microbial ecology in built and natural environments based on the interactions that may occur between them and the mechanisms microbes employ for protection against contaminants and other environmental stressors.

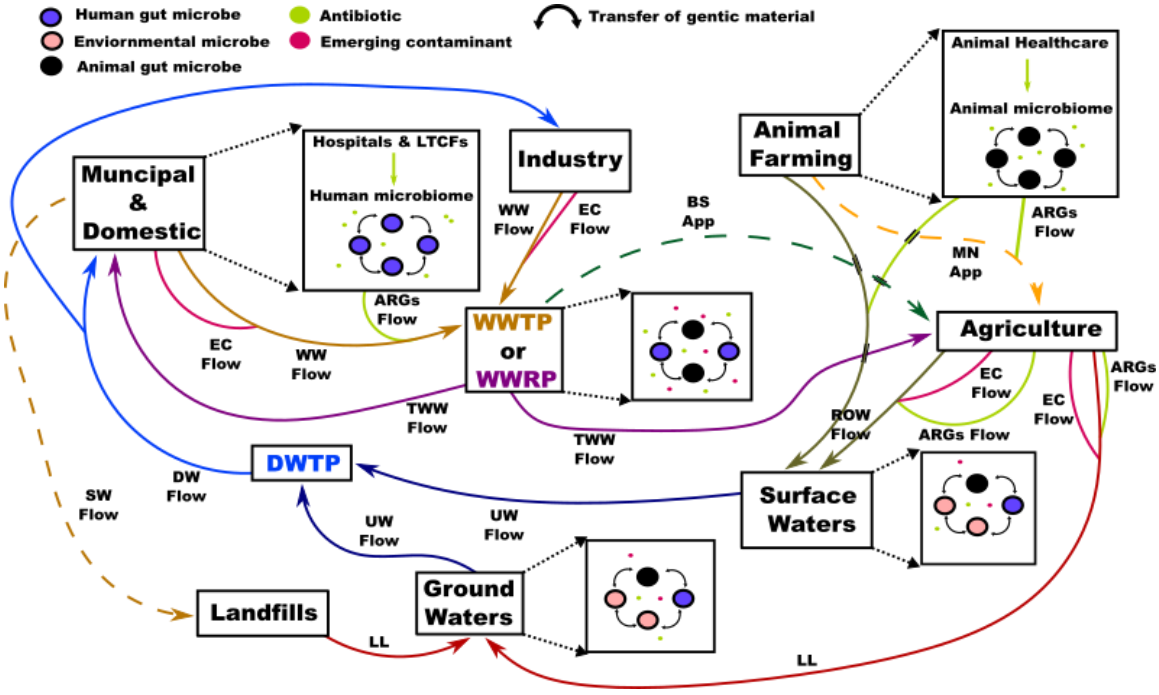

Figure 1.1. Genetic reactors of antibiotic resistance and the cycling pathways of contaminants. Solid lines represent aqueous flow via plumbing or natural flow. Dashed lines represent solid flow via transportation. LL is leeching of contaminants from surfaces. EC Flow is emerging contaminant flows, and ARGs Flow is antibiotics and ARGs flows into waste streams. WW Flow is wastewater movement from plumbing. UW Flow is the plumbing of untreated raw surface and ground waters. DW Flow is treated drinking water plumbing to consumers. SW Flow is solid waste movement. TWW Flow is treated wastewater plumbing for reuse applications. BS App is biosolid transportation for agricultural applications. MN App is solid manure transportation for agricultural applications. ROW Flow is the movement of runoff waters from farming and agriculture. Figure adapted from Baquero et al. 2015 and Petrović et al. 2003.

1.2. Multidrug-Efflux Pump Systems.

Multidrug-efflux pump systems in bacteria are resistance mechanisms of interest as they can confer resistance to several classes of biocides. These protein pumps may be substrate specific or transport a variety of chemically dissimilar compounds granting bacteria multidrug-resistance (MDR). Efflux pump genes are located chromosomally or encoded by transmissible genetic elements such as plasmids for horizontal gene transfer.[14-15] The five families of microbial efflux pump proteins to date include, the

major facilitator superfamily (MFS), the small multidrug-resistance (SMR) and the multidrug and toxic compound extrusion (MATE) the adenosine triphosphate (ATP)-binding cassette (ABC) superfamily, and the resistance nodulation division (RND) family (Figure 1.2.).[16-20]

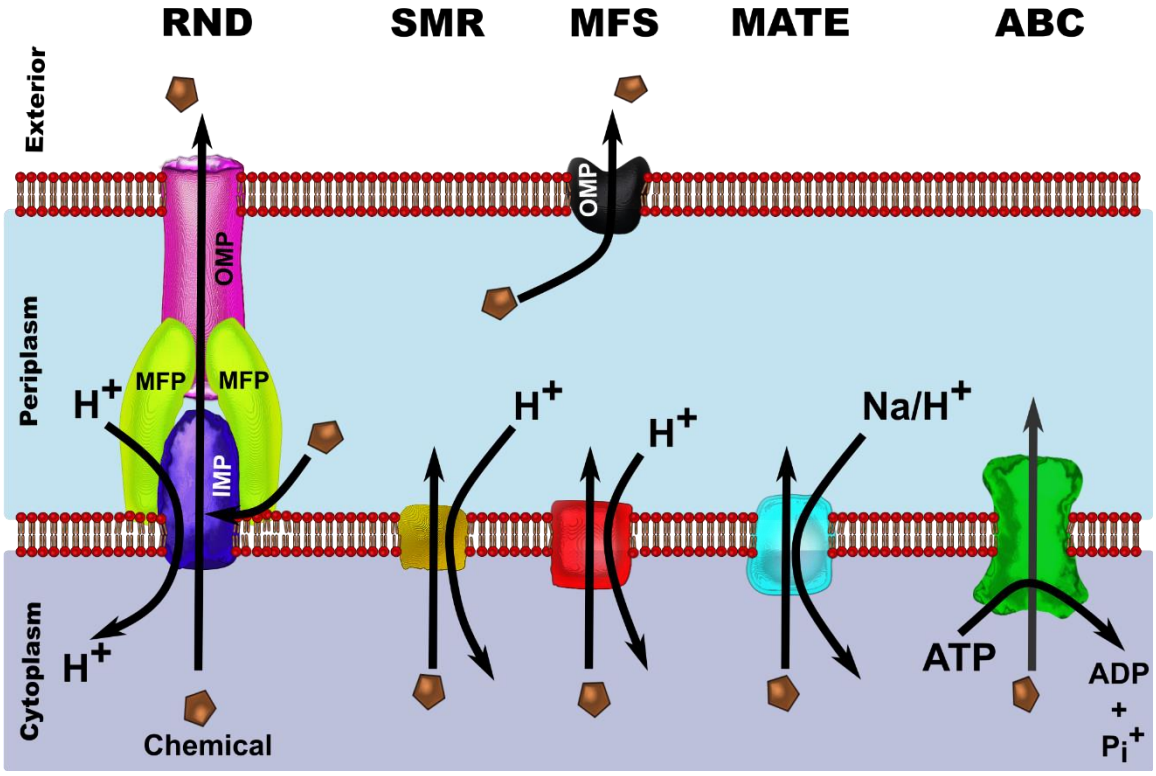

Figure 1.2. Schematic of the major family of efflux type proteins in bacterial cells. Electron usage for running the protein transporter is shown. OM is outer membrane and IM is inner membrane. Figure was inspired from Blanco et al. 2016.

MFS efflux pump family of proteins are the largest group of secondary membrane transporters and are present in bacteria plants and animals.[21] In gram-positive and gram-negative bacteria, these proteins contribute to chemical homeostasis as well as antibiotic resistance. MFS transporters import or export many substrates including ions, carbohydrates lipids, amino acids, peptides, and nucleosides.[22] Bacterial MFS proteins can export a wide range of drugs, antibiotics, and toxins by cation/substrates antiport

mechanisms because of their large substrate-binding pockets located in a central cavity that is facilitated by low H-bonding, primarily hydrophobic, van der Waals, and polar contacts between the pocket and substrate.[23-25]

The SMR protein family consists of small proteins that confer antibiotic resistance in bacteria. As the name implies SMR proteins are small (~12 kDa, 100-150 amino acid in length) proteins integrated with the inner membrane.[18, 26] SMR proteins are structured as four transmembranes stranded α-helical proteins that confers low-level resistance to a wide range of drugs using the proton motive force like other efflux families.[27] Substrates of the SMR protein family include antiseptics such as quaternary ammonium compounds (QAC), lipophilic compounds like DNA interchelating dyes, and antibiotics like tobramycin.[28-29]

Protein efflux pumps of the MATE family are important for bacterial antibiotic resistance. Originally, the first characterized MATE protein NorM was grouped in the MSF category because it possessed 12 putative hydrophobic regions but was later proposed to form a new family known as the MATE family.[30] The MATE proteins utilize energy from Na^+, unlike the other efflux pumps.[31] Bacterial MATE efflux proteins can export fluoroquinolones, cationic dyes, aminoglycosides, and a variety of unrelated compounds.[32] MATE proteins have a variety of compounds that are recognized but their substrate pool is narrower than RND-type pumps.

ABC drug transporters conferring MDR have been characterized in gram-positive and gram-negative bacteria.[33-34] In the *E. coli* genome, the genes that encode ABC transporters comprise almost 5% of the entire genome.[35] In bacteria, ABC transporters

operate by an enzymatic reaction that transduces the energy of ATP binding and hydrolysis transporting compounds across the membrane.[36] Bacterial ABC transporters typically consist of two ATP-binding cassette domains and two hydrophobic transmembrane segments encoded as independent polypeptides spanning the inner membrane of the cell, occasionally using additional proteins such as TolC during efflux.[35, 37] ABC proteins are a highly conserved ATP-binding motif domain that is involved in several roles in bacterial cells. In bacteria, ABC proteins import or export cellular components, toxins, metabolites, antibiotics, and other drugs.[38]

Homologs of RND-type proteins are ubiquitous in all three domains of life as they originate from an ancient family of efflux pumps.[16] Gram-negative pathogens such as *Escherichia coli* and *Pseudomonas aeruginosa* are well-studied bacteria that express the RND family of efflux pumps. These bacteria amongst others contain many RND pumps with overlapping substrates that can be exported. The RND family of proteins forms a tripartite complex of proteins that runs continuously from the cytoplasm through the inner membrane, to the periplasm and finally outside the outer membrane.[39] Substrates inside the cytoplasm are pumped across this channel of proteins outside of the cell reducing the concentration of the substrate inside of the cell.[40] Substrates can also be exported from the periplasm region by binding to the inner membrane-bound protein and be exported to the extracellular area.

The individual proteins that make up the RND transporter each serve a functional role in the process of exporting a compound. The inner membrane-bound energy-providing protein binds to the substrate and is either an ABC transporter or often a proton

antiporter of the RND family.[41] The protein anchored in the outer membrane functions as a non-specific channel in which the substrates are exported from the cytoplasm to the external area of the cell. The outer membrane channel-tunnel proteins for RND and MFS families of proteins are typically the TolC family.[42] The third protein, the membrane fusion protein, is primarily in the periplasm but is anchored by a single helix or an N or C-terminal lipid moiety to the outer membrane and serves as the adaptor protein.[43] These types of multicomponent protein complexes can transport a wide variety of substrates including antibiotics, dyes, detergents, and host-derived compounds.[44] The redundancy of these efflux pumps leads researchers to believe the functionality is not restricted to the exportation of antibiotics. RND-type efflux pumps have the broadest spectrum of substrates compared to the other family of efflux pump proteins.

1.3. Substrates of Multidrug-Efflux Pump Systems.

As mentioned prior, the substrates of MDR efflux pumps are broad and specific granting both gram-positive and gram-negative redundant layers of resistance to a variety of compounds. Despite decades of biochemical research there are still emerging substrates of RND-type efflux pumps. The major tripartite RND multidrug efflux pump of *E. coli*, the AcrAB-TolC, confers resistance to a multitude of compounds.

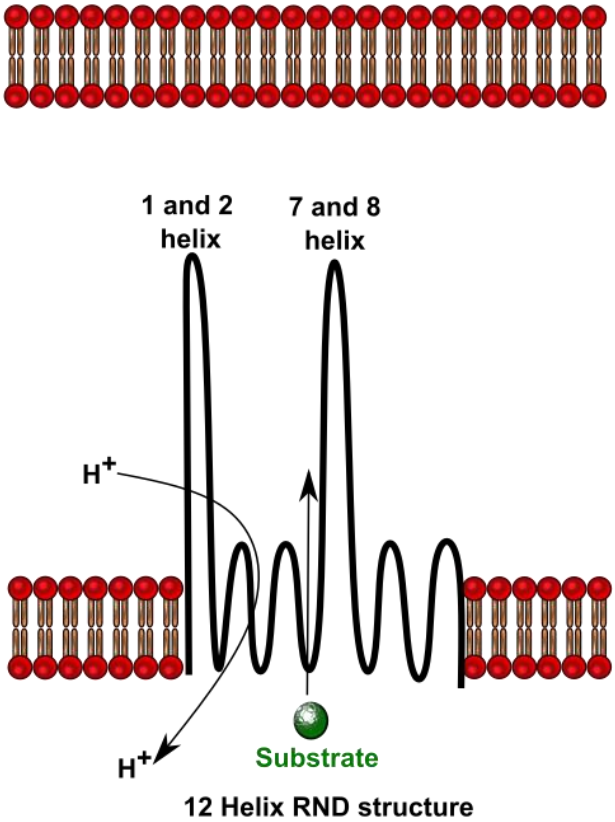

Figure 1.3. Schematic of the RND helix structure with large periplasmic or extracytoplasmic domains in the protein structure. Adapted from Borges-Walmsley et al. 2009.

RND transporters have 12-helical structures, possessing large periplasmic or extracytoplasmic domains between helices 1 and 2 and between helices 7 and 8 (Figure 1.3.).[45] The two large periplasmic loops that protrude between the two pair of helices form the headpiece of RND transporters and is what most likely allows for the broad substrate specificity in AcrB and AcrD.[46] Both proteins AcrB and AcrD share similarities yet have different substrate recognition. The deep pocket where tight bonding can occur in AcrB is more lipophilic than the other binding sites and the peripheral site where loose binding can occur known as the access pocket gives electrostatic funnel sourcing potentially for the recognition of monocationic compounds; these characteristics are most

likely the substrate recognition for AcrB and AcrD.[47] Whether it be ionic, small, or large molecules, efflux pumps have versatile binding sites for substrate recognition and several compounds including non-antibiotic will induce antibiotic resistance by MDR efflux pumps. A multitude of structurally and chemically dissimilar compounds are exported by these types of proteins (Table 1.1.).

Table 1.1. Substrates of selected major bacterial efflux pump proteins in MDR bacteria. Substrate chemicals are not inclusive, all studied, or all possible substrates.[48-51]

Bacterial Species	Efflux proteins	Substrates
Pseudomonas aeruginosa	MexAB-OprM	β-lactams, fluoroquinolones, chloramphenicol, tetracycline, novobiocin, trimethoprim, sulphonamides, macrolides, erythromycin, acriflavine, crystal violet, sodium dodecyl sulfate, aromatic hydrocarbons, homoserine lactones, cerulenin, thiolactomycin, irgasan, triclosan
	MexCD-OprJ	β-lactams, fluoroquinolones, chloramphenicol, tetracycline, novobiocin, trimethoprim, macrolides, crystal violet, ethidium bromide, acriflavine, sodium dodecyl sulfate, aromatic hydrocarbons, triclosan
	MexEF-OprN	fluoroquinolones, chloramphenicol, trimethoprim, aromatic hydrocarbons, triclosan
	MexXY-OprM	fluoroquinolones, aminoglycosides, tetracycline, erythromycin
Stenotrophomonas maltophilia	SmeABC	β-lactams, aminoglycosides, fluoroquinolones
	SmeDEF	tetracycline, erythromycin, fluoroquinolones, ethidium bromide
Escherichia coli	AcrAB-TolC	β-lactams, quinolones, tetracyclines, tigecycline, chloramphenicol, steroid hormones, lincosamides, benzene, cyclohexane, sodium dodecyl sulfate, Triton X-100, rifampicin, bile salts, free fatty acids, geraniol, enterobactin, triclosan, chlorhexidine, quaternary ammonium compounds, acriflavine, ethidium bromide

AcrAD-TolC	aminoglycosides, steroid hormones, enterobactin, β-lactams, quinolones, deoxycholate
AcrEF-TolC	quinolones, tigecycline, solvents
MdtABC-TolC	novobiocin, bile salts, enterobactin, quinolones, fosfomycin, benzalkonium, sodium dodecyl sulfate, zinc, myricetin
MdtEF-TolC	erythromycin, doxorubicin, benzalkonium, sodium dodecyl sulfate, deoxycholate, crystal violet, ethidium bromide, nitrosyl indole, rhodamine 6G, tetraphenylphosphonium bromide, free fatty acids
CusCFBA	silver, copper, fosfomycin, ethionamide, dinitrobenzene

1.4. Endocrine-Disrupting Chemicals as Emerging Contaminants.

The study of efflux pumps has primarily focused on the structural biology of the proteins, usage of clinically relevant antibiotics, and antibiotic resistance for pathogenic bacteria. Few focus on how these proteins change when experiencing emerging contaminants from the natural and built environment as potential substrates.

Estrogen mimics such as the synthetic hormones 17α-ethynylestradiol (EE2) and 17β-estradiol (E2), and plasticizers such as Bisphenol-A (BPS) and Bisphenol-S (BPS), are emerging contaminants that can interact with eukaryotic and prokaryotic life.[52-53] These compounds, known as endocrine-disrupting chemicals (EDCs), are part of a growing list of pollutants that make their way into built and natural environments. They are found in many common commercial products including plastic bottles, metal food cans, detergents, flame retardants, food additives and preservatives, pharmaceuticals, personal care products, cosmetics, toys, and other plastic goods, contaminated foods, and naturally in vegetation.[54-55]

As their name implies, EDCs have the potential to disrupt the endocrine system and metabolism of organisms. In multicellular organisms, hormones act as chemical messengers allowing communication between major organs and tissue in the regulation of physiological and behavioral activities.[56] EDCs can bind to nuclear hormone receptor sites including estrogen receptors, androgen receptors, progesterone receptors, thyroid receptors, and retinoid receptors.[57] This disruption can lead to adverse health effects in humans including increasing rates of cancers, altering adipose tissue promoting obesity, metabolic syndrome, diabetes, thyroid diseases, and infertility related to the sexual development of humans.[58-61]

EDCs are responsible for many long- and short-term impacts on multicellular organisms and are not limited to humans. Multigeneration effects of EDCs in birds and fish are evident, whereas mammalian impacts that are not from rodent studies derived are still relatively understudied.[62] Furthermore, it was postulated that EDCs cause transgenerational effects most likely by epigenetic mechanisms.[62]

Their complex and extensive impacts as environmental stressors are strongly linked to chronic diseases. Exposure to EDCs during early-life development may increase susceptibility to diseases later on in the life span of the affected organism.[63] In humans, early life EDCs exposure has been associated with breast or prostate cancer, endometriosis, infertility, diabetes/metabolic syndrome, early puberty, obesity, increased susceptibility to infections, autoimmune diseases, asthma, heart disease, stroke, Alzheimer's disease, Parkinson's disease, and ADHD and other learning disabilities.[64-69] Their complex and extensive impacts are even hypothesized to be a contributor to severe

cases of COVID-19 which are frequently linked to individuals suffering from chronic diseases that may have been induced by EDCs.[70]

1.5. EDCs and Microbes in WWTPs.

EDCs are extensively studied in eukaryotic organisms, while studies of EDCs interacting with prokaryotes focus on the biodegradability of EDCs by various microbes during wastewater treatment.[71-74] However, there are limited studies on the interference EDCs may have on microbes. Furthermore, there may be microbially mediated impacts of EDCs from prokaryotes to eukaryotes.

EDCs may bind to essential proteins in bacteria related to oxidation, transport, and communication. MDR-type genes in bacteria are over-expressed in the presence of natural and synthetic estrogens and estrogen mimics.[75] Exposure to E2, estriol, and estrone induced the expression of *acrB*, *acrF*, and *mdtF* (*yhiV*) in a qPCR analysis of *E. coli* strain K12, while exposed to the EDCs EE2, BPA, and nonylphenol (NP) similarly increased and induced the RND inner membrane genes *acrB* and *mdtF*.[76] NP has also been shown to reduce cell-to-cell communication by binding to the LasR protein blocking quorum sensing and reducing biofilm production in *Pseudomonas aeruginosa*.[77] The natural hormone progesterone was determined to have a direct inhibitory effect on *Coxiella burnetii* replication, an intracellular parasite that causes query fever in eukaryotic organisms.[78] In engineered systems, increased loadings of EDCs in wastewater treatment facilities are a problem in environmental endocrine disruption attenuation, as estrogens are incompletely removed during biological treatment and discharged at levels that impact aquatic animals.

In wastewater treatment plants (WWTP), EDCs have been quantified in a range of concentrations in the influent and effluent and can interact with the different phases of waste.[4, 79-81] A summary of worldwide concentrations of selected EDCs can be observed in Table 1.2. These concentrations of EDCs may not seem alarming due to the low concentration and high removal efficiencies of WWTPs. However, contrary to the standard monotonic dose-response curves used in evaluating the taxological impacts of chemicals, EDCs generate U-shaped and inverted U-shaped di-phasic dose-response curves.[57] This suggests that very low or very high endpoint concentrations can cause harm to human health and microbial ecology.

Table 1.2. Worldwide concentrations of EDCs quantified in the influent, effluent, and sludge of WWTPs within the last 15 years. Values marked as "--" were not reported from the respective study.

EDC	Influent (ng/L)	Sludge (ng/g)	Effluent (ng/L)	Year	Location	Reference
BPA	84,110	9,170	--	2009	Brazil	(82)
	1,960	231	477	2016	China	(83)
	412	64	--	2018	China	(52)
	90	961	43	2015	USA, NY	(84)
	--	--	4,367	2017	Saudi Arabia	(85)
	--	--	971	2017	Slovenia/ Croatia	(86)
	--	9,170	--	2009	Brazil	(82)
	--	1,520	--	2011	Korea	(87)
	--	140	--	2017	China	(88)
BPS	28	16	27	2015	USA, NY	(84)
	109	4	--	2018	China	(52)
	21	--	--	2015	Slovenia	(81)
	56	2	1	2016	China	(83)
	--	--	316	2017	Slovenia/ Croatia	(86)
	--	186	--	2012	India	(89)
	--	45	--	2011	Korea	(87)
	--	43	--	2017	China	(88)

EE2	7,890	--	390	2008-9	USA, TX	(90)
	491	102	268	2013	Tunisia	(91)
	474	--	14	2015-16	Kuwait	(92)
	80	--	4	2017	Tanzania	(93)
	5	--	0	2016	Malaysia	(94)
	--	410	--	2006-7	China	(95)
E2	93	--	85	2016	Malaysia	(94)
	62	793	25	2013	Tunisia	(91)
	5	4	2	2013	China	(96)
NP	7,000	--	--	2016	China	(97)
	2,319	3,579	676	2013	China	(96)
	5	--	--	2012	Portugal	(98)

Estrogen mimics like E2 and EE2 often accumulate in the solid phase including the RAS, WAS, and effluent biosolids of anaerobic digesters in WWTP due to their hydrophobic nature as their Log K_{ow} are 4.01 and 3.67 for E2 and EE2.[99-100] Although many other EDCs can share a similar fate, microbes responsible for aerobic and anaerobic biodegradation throughout wastewater treatment are in contact with EDCs before accumulation in the solid phase for the length of the HRT. The prolonged exposure to EDCs to bacteria typical of wastewater treatment is understudied. None of these EDCs are true antimicrobials, however anthropogenic bisphenol and nonylphenol have shown to exhibit biocidal activity in bacteria. The potential for EDCs to induce antibiotic resistance genes indirectly and directly causes harm to public health. Bacterial interactions with emerging contaminants like EDCs require further study to access impacts for potential eukaryotic and prokaryotic interferences.

1.6. Biocides to Bacteria.

1.6.1. Types of Biocides.

E. coli and other gram-negative and gram-positive bacteria found throughout WWTP possess multi-drug resistance (MDR) proteins that are responsible for the extrusion of toxic compounds from the cell and are exposed to emerging contaminants. MDR efflux proteins ensure their survival under harsh environments, such as high metal concentrations, anaerobic conditions, wastewater, and the human gut. Some compounds shown to be toxic to MDR bacteria are present at WWTPs, as an intentional effort to reduce microbial activity. Any compound in excess will be toxic, but some types of compounds fundamentally are biocides, whereas MDR bacteria will be resistant.

Biocides (antiseptics, disinfectants, antimicrobial, and preservatives) have been used in various forms for hundreds of years. Historically, humans have utilized biocides, such as the first reported biocide sulfur dioxide, chlorines and hypochlorites, alcohols, and metals like copper and silver for hygiene, food perseveration, and infection treatments.[101] Biocides that inhibit or inactivate bacteria can be categorized by their cellular target. These include interactions with outer cell parts, interactions at the cytoplasmic membrane level, and interactions within the cytoplasm.[102]

Table 1.3. Varied types of biocides and their primary classes regarding their target site or primary mechanism of action.[102-127]

Type of Biocide	Example Biocides
Chelating agents	1,10-Phenanthroline, 2,2'-Dipyridyl, 5,7-Dichloro-8-hydroxy-quinaldine, 5,7-Dichloro-8-hydroxyquinoline, 5-Chloro-7-iodo-8-hydroxy-quinoline, EDTA, 8-Hydroxy-quinoline, EGTA, Fusaric acid, Sodium pyrophosphate decahydrate
DNA and/or RNA targeting	6-Mercapto-purine, 5-Fluorouracil, Myricetin, Coumarin, Ciprofloxacin, Ofloxacin, Norfloxacin, Azathioprine
Folate synthesis targeting	Trimethoprim, Sulfamethoxazole

Ion channel inhibitor	Lidocaine, Procaine
Cell wall/membrane target	Dodine, Cetylpyridinium chloride, Methyltrioctyl-ammonium chloride, Phosphomycin, Cefmetazole, Cefamandole nafate, Cefsulodin, Cefuroxime, Cefoperazone, Cephalothin, Cefazolin, Cefotaxime, Cefoxitin, Moxalactam, Ceftriaxone, Amoxicillin, Ampicillin, Carbenicillin, Cloxacillin, Penicillin G
Oxidizing agents	Lawsone, Plumbagin, Chlorines
Protein Synthesis targeting	Amikacin, Streptomycin, Gentamicin, Tobramycin, Erythromycin, Spiramycin, Josamycin, Neomycin, Tylosin, Chlortetracycline, Tetracycline
Toxic ions	Potassium chromate, Potassium Tellurite, Cupric Chloride

1.6.2. Interactions With Outer Cell Parts.

Biocides may interact with outer cell components such as lipids although cell death may not necessarily occur. Aldehydes such as glutaraldehyde (GTA) do not necessarily require cell penetration to function as they utilize cross-linking reacting with the outer lipoproteins to inhibit enzymatic activity and other important survival functions.[128] Cationic compounds such as chlorhexidine and benzalkonium chloride can affect the hydrophobicity of gram-negative bacteria.[129-130] These compounds often also attack the membrane of bacteria and can increase their own uptake to reach additional target sites at the cell cytoplasmic membrane and substitutes in the cell cytoplasm.[131] Other chemicals such as hypochlorite, phenol, formalin, and mercuric chloride cause cell lysis by attacking the cell wall or impacting cell permeability.[132-134]

1.6.3. Interactions With the Cell Membrane.

The cell membrane of microbes is frequently a target for biocides. These compounds work to disrupt the membrane, block transporters in the membrane, interfere with electron transport (energy) or physically destroy the membrane. Compounds such as

penicillin-type antibiotics and cephalosporins bind to the penicillin-binding proteins (PBP) stopping the cross-linking of the peptidoglycan layer of the bacterial cell wall.[123, 135] Penicillin and other β-lactam antibiotics inhibit the catalytic activity of bacterial transpeptidases, and the activity of inhibition is based on the structural, geometric, and stereochemical similarities between the amide bonds of the antibiotic and the enzyme substrate.[126]

Quaternary ammonium compounds (QAC) are commonly used biocides that interact with the membranes of bacteria. Biocidal activity is based on the chain length of the QAC used.[136] QACs can bind by ionic and hydrophobic interactions with cell membranes causing a rearrangement of the membrane and leakage of intracellular constituents.[116] QACs can also bind and block essential ion channels of bacterial cells. Ion channel blockers bind to the narrow aqueous pore of ion channels interfering with conduction and preventing essential nutrients from entering the cell.[121] These compounds can include ions, anesthetics, and antidepressants.[121] Initially acting on the membrane, QACs can also find their way inside the cell and continue to interact with cytoplasmic constituents.

1.6.4. Interactions With Cytoplasmic Constituents.

Biocides can target or inhibit deoxyribonucleic acid (DNA) and ribonucleic acid (RNA) in bacteria to limit growth and induce fatal mutations.[137] These types of compounds can be analogs of nucleic acids acting as antagonists, directly damaging DNA, or inhibiting DNA enzymes.[103, 108, 110, 112, 114]

Oxidizing agents are biocides that can have several cellular effects on bacteria and can damage the internal structures of bacterial cells. Oxidizing agents can cause leakage of electrons from the electron transport chain, chain breaks in DNA damaging the structure and possibly producing point mutations, and modifications of amino acids leading to reduce protein function.[111]

Chelating agents are biocides that sequester metals such as iron, magnesium, calcium, and zinc necessary for certain essential microbial functions.[138-139] The chelation activity inhibits biological processes that require metal-dependent proteins.[140] This can result in an over or underload of metal ions that may normally be imported or exported.

Macrolide compounds containing 14-,15- or 16-membered lactone rings with one or more sugar moieties are chemicals commonly used as antibiotics.[113] Macrolide chemicals bind to the large ribosomal subunit and decrease cell growth by inhibiting protein synthesis.[141] Other antibiotics such as aminoglycosides used in clinical practice also act similarly. Aminoglycosides are a group of antibiotics that bind the aminoacyl site of the 16S ribosomal RNA (rRNA) within the 30S ribosomal subunit.[119] The structure of aminoglycosides is that one or several aminated sugars joined in glycosidic linkages to a dibasic cyclitol, their binding to the ribosome subunit impairs bacterial protein synthesis.[142] Tetracycline compounds also interact with the ribosome. Tetracyclines bind at the decoding center of the subunit ribosome where the codon of mRNA is recognized by the anticodon of the tRNA ultimately leading to inhibition of protein synthesis.[124]

As mentioned prior, cations can interact with external components of the cell, however, toxic anions and cations can also interact inside of the cell inhibiting biological

activity. Cu (I) is a cationic antimicrobial and disinfectant agent for the inactivation of several microbes.[115] Copper is toxic in aerobic conditions by redox-cycle generating reactive oxygen species that lead to lipid peroxidation and protein and DNA damage. Under anaerobic conditions, copper ions are toxic by their reducing capabilities by increasing iron acquisition and sulfur assimilation in bacteria such as *E. coli*.[143] Toxic anions such as chromate and ionic tellurite induce strong oxidizing effects that have mutagenic actions in bacterial systems targeting DNA or RNA substituents inside of the cell.[106, 117] A summary of some classes of biocides and their examples can be viewed in Table 1.3.

1.7. Synergism of Biocides.

Bacteria still evade the multitude of biochemical processes imparted by biocides. The differing mechanisms of biocide inactivation/inhibition can be coupled and are frequently done so to provide a synergistic effect toward the microbes.[144] This can be especially impactful for antibiotic-resistant bacteria. When MDR bacteria interact with biocides, adding one compound to limit resistance while the other targets the microbe for biocidal activity may allow for complete inactivation. These types of interactions can make previously obsolete antibiotics reusable again.

Synergistic combinations rely on two separate mechanisms of action acting independently or together to achieve stronger antimicrobial properties, utilizing the least amount of material of the synergistic compounds.[144] Several examples of these combinations have been used in previous studies. A synergistic combination of Cu (II), hydroxylamine, and hydrogen peroxide was shown to inhibit *P. aeruginosa* and its

biofilm growth and was able to clean RO membranes recovering lost flux from biofouling.[145] Pyrazine-2-carboxylic acid derivatives and kanamycin were able to effectively inactivate and remove biofilm growths of MDR *V. cholerae*.[146] Tetracycline and quercetin were shown to synergistically inhibit MDR *E. coli* growth by altering cell membrane permeability.[147] Efforts have been directed in looking into synergistic uses of efflux pump inhibitors (EPI) to combat MDR pathogens that typically overexpress and overproduce efflux pumps, an issue in clinical resistance.

1.8. Efflux Pump Inhibitors as Biocide Facilitators.

EPIs in combination with antibiotics or other biocides can induce synergistic effects on MDR bacteria by ceasing the exportation of MDR efflux pump substrates and maintaining the biocidal properties of the substrates.[148] EPIs are valuable as alternative therapeutics for MDR bacteria as they can increase intracellular biocide concentration when applied synergistically, restore antibiotic activity against MDR strains, and minimize progress towards antibiotic resistance.[149] The appeal of EPIs is that they can reinstate previously obsolete antibiotics and facilitate the mediation and preservation of antibiotics by mitigating further antibiotic resistance.

EPIs can be used on RND complex structures or MFPs and their outer membrane factor (OMF) proteins.[150] Typically, EPIs are designed to target an active site needed for the efflux pump conformational changes, limiting substrates transport, or they directly target single or multiple proteins that make up the efflux pumps complex.[150] Because of the nature of EPIs, they typically will be substrates of the target efflux pump themselves, but may not increase antibiotic resistance like other substrates, instead reducing intrinsic

resistance and reverse acquired resistance.[151] This shows promise in combating antibiotic-resistant bacteria.

Several EPIs have been discovered and continue to be studied over the last decade for applications with a variety of MDR bacteria. EPIs such as phenylalanyl arginyl β-naphthylamide (PAβN), globomycin, carbonyl cyanide m-chlorophenylhydrazone, various quinolines, EDTA, and arylpiperazine derivatives have been investigated with MDR gram-negative bacteria such as *E. coli*, *Enterobacter aerogenes*, *Klebsiella pneumoniae*, *Campylobacter jejuni*, *P. aeruginosa*, and *Salmonella enterica*.[152] The expression of AcrAB-TolC complex in *E. coli* was decreased when using a combination of EDTA ceftriaxone, and sulbactam as EDTA acted as an efflux pump inhibitor at a maximum inhibition concentration of 10 mM.[153] Abdali et al identified several novel EPIs that interact with at AcrA binding sites of the efflux protein complex AcrAB-TolC. The distinction between substrates and inhibitors was hypothesized to be from small differences in molecular contacts of the compounds with the AcrA and/or AcrB binding sites.[154] Direct binding to sites on efflux pump proteins are often mechanisms of EPIs.

Molecular modeling of EPIs and substrates of efflux pumps NorA and MexAB-OprM, and *p-glyco*-protein showed that the EPI and substrates can potentially form a complex.[155] The complex may cause the antibiotic to be unrecognized as a substrate of the MDR pumps. Chemicals such as PAβN bind to RND efflux pumps and act as a potentiator of the antibiotics: levofloxacin, erythromycin, and chloramphenicol, competitively binding to the RND efflux pumps in *P. aeruginosa*.[151, 156] Direct binding is a common mechanism amongst EPIs, but another mechanism is possible.

EPI may also work as energy disruptors that disrupt the proton motive force (PMF) or inhibit it by directly binding to the target efflux pump.[157] Compounds such as the ionophore carbonyl cyanide-m-chlorophenylhydrazone (CCCP) disrupt the PMF used by efflux pumps, although this compound could also make the bacterial cells metabolically inactive. Synergistic impacts with antibiotics and CCCP are most likely due to metabolic inactivity rather than efflux inhibition.[158] This may pose a problem for the usage of certain EPIs as they may not be clinically relevant if they can induce metabolic changes that could trigger resistance mechanisms.

Efflux pump inhibitors offer promising solutions for combatting and repealing antibiotic resistance. Much research has investigated their clinical relevance and potential to reverse antibiotic resistance reducing the need to abandon antibiotics. However, as genetic "hotspots" of antibiotic resistance, it is important from an environmental standpoint to explore EPIs for their impacts on microbes in engineered systems. Considering the interaction that may occur between MDR bacteria and emerging contaminants such as EDCs, EPI should be investigated for impacts to resistance mechanism.

1.9. Overarching Goal and Research Needs.

Antibiotic resistance is being investigated to address challenges presented by interactions of anthropogenic environmental stressors and MDR bacteria found in WWTPs. The overarching goal of this dissertation is to evaluate MDR efflux pumps from an environmental standpoint, to establish the relationship between EDCs as environmental stressors and MDR efflux pumps, and to evaluate how combating MDR synergistically can

reduce this interaction. *E. coli* was chosen as the test MDR organism throughout this work as it intrinsically carries efflux pumps of interest, is associated with clinical infections and is frequently found in built environments.

The primary research questions (Q) and hypotheses (H) addressed in this dissertation are:

Questions and hypotheses:

Q1) What types of biocides are recognized as substrates of the lesser studied efflux pump system MdtEF-TolC compared to the highly studied AcrAB-TolC in the MDR bacteria *E. coli*? (CHAPTER 2)

H1) If the protein structures are similar, the substrates will be highly comparable but dissimilar to an extent, based on the properties of the major binding sites on the proteins.

Q2) What levels of inhibition can be provided from applying synergistic combinations of biocides to MDR bacteria *E. coli*? (CHAPTER 3)

H2) Since several classes of biocides exist, synergistic results will vary to a degree; combinations of biocides with distinct mechanisms will induce the highest level of inhibition in MDR bacteria.

Q3) Can attempted synergistic combinations of biocides induce unwanted antagonistic responses in MDR bacteria such as *E. coli*? (CHAPTER 4)

H3) Some level of antagonism may be possible due to complex formation or binding that may occur such as when EPIs bind to substrates.

Q4) Do environmental contaminants such as synthetic EDCs induce antagonistic or synergistic inhibition of MDR bacteria such as *E. coli*? (CHAPTER 5)

H4) EDCs induce expression and are substrates of MDR efflux pumps, therefore high levels of antagonism will occur between EDCs and biocides to MDR bacteria.

Q5) Does the MDR proteins of *E coli.* change (relatively) when exposed to environmental stressors such as EDCs? (CHAPTER 5)

H5) High levels of MDR proteins should be detected since previous studies have shown EDCs to be substrates of efflux pump inhibitors and induce RND genes.

1.10. Dissertation Organization.

Chapter 1 provides the background information and overview of the concepts that are covered throughout the dissertation. Bacterial antibiotic resistance prevalence regarding built and natural systems are discussed. Multiple drug-resistance efflux pumps are discussed as the primary resistance mechanism of concern for this work. Additionally, it covers biocidal methods of inhibiting or inactivating MDR bacteria, including the mechanisms involved and the use of multiple antimicrobials. Furthermore, the applications of biocides that inhibit efflux pumps are discussed. The objective of this chapter is to provide information necessary for the readers to familiarize themselves with the major ideas explored in this dissertation.

Chapter 2 explores substrates of the lesser studied efflux pump system MdtEF-TolC and investigates how the structure of these pumps may dictate substrate specificity. Mutant strains of *E. coli* with triple gene deletions removing the AcrAB and MdtEF efflux pump

systems and mutant strains only containing the MdteEF efflux pump system were utilized with high-throughput screening, of 240 known biocides, to identify substrates. Trends amongst the identified substrates were observed and molecular simulations were utilized to describe differentiation between AcrB and MdtF proteins. The results of this chapter increase the knowledge of a lesser-studied efflux pump that may interact with emerging contaminants and byproducts to a lesser degree.

Chapter 3 investigates the high-throughput screening of 210 known biocides synergistically applied with group IB metal ions (Ag (I), Cu (II), Au (III)), for the discovery of new antimicrobial chemotherapy for the inactivation of MDR bacteria. *E. coli* was inactivated to various levels of degrees and the extent was quantified with the coefficient of drug interaction (CDI). The results confirm prior works and provide several novels Ag-biocide, and Au-biocide synergistic combinations that may be utilized for future competence against MDR bacteria.

Chapter 4 investigates further the results from Chapter 3 by investigating group IB metal ions application with the EPIs, chlorpromazine, promethazine, thioridazine, and trifluoperazine to *E. coli*. Novel Au (III)-phenothiazine complex formations occurred providing synergism or antagonism when applied toward *E. coli*. Additionally, the evaluation of synergistic or antagonistic quantification of inhibition is explored.

Chapter 5 investigates the role of emerging contaminants such as EDC in the production of antibiotic-resistance efflux pump proteins. The EDCs NP, E2, EE2, BPA, and BPS are applied at sublethal concentrations, and the extent of antibiotic resistance is investigated

using a chemical sensitivity assay. Proteins were extracted and a metaproteomic analysis was conducted to explore the impacts the EDCs have on protein changes in *E. coli*. All references are located at the end of this dissertation.

CHAPTER 2

THE ANAEROBIC EFFLUX PUMP MDTEF-TOLC CONFERS RESISTANCE TO CATIONIC BIOCIDES

Graphical Abstract

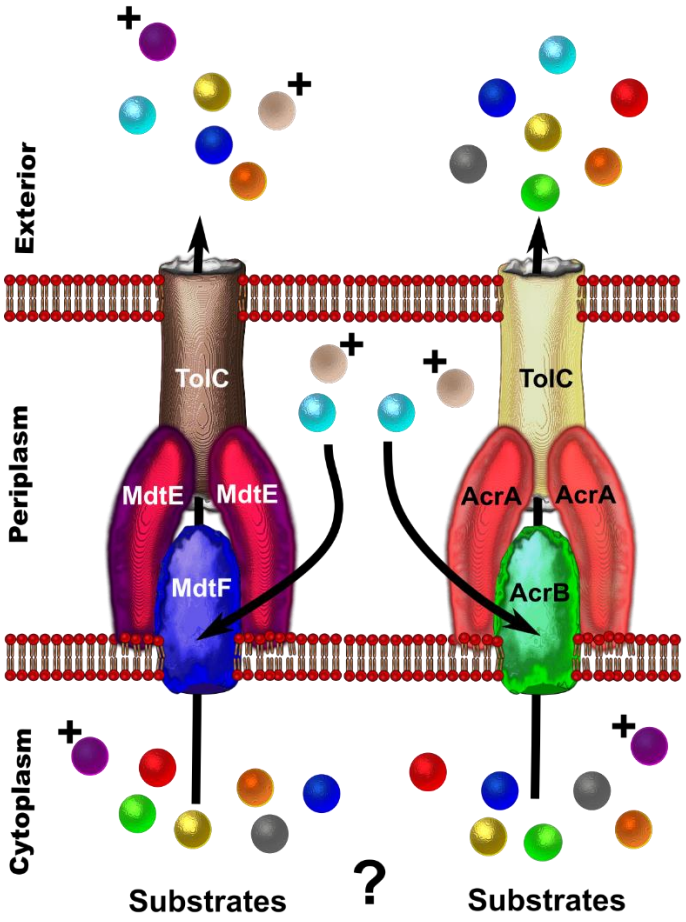

Abstract

The *E. coli* RND transporter MdtEF-TolC is a multi-drug efflux pump that exports substances in response to intracellular toxicity. Little is known of the complete substrate range of the anaerobic efflux pump. Still, the inner membrane protein responsible for differentiation, MdtF, is structurally homologous to and shares chemical specificity with the major RND efflux protein AcrB. To determine the substrate range of the anaerobic efflux pump MdtEF-TolC, *E. coli* mutants were exposed to 240 biocides, and growth was monitored. This approach was also used to validate existing and novel ligands of AcrAB-TolC. Results showed that overexpressed MdtEF conferred resistance to the same substrates as AcrAB-TolC, but were restricted primarily to cationic biocides, with some exceptions. To further elucidate differences within the distal and proximal binding pockets of these RND transporters, an *in silico* model of the MdtF triplex was constructed using AcrB as a template. Protein alignment and predicted structure revealed distinct regions within the distal binding pocket of MdtF that may contribute to a narrower substrate range do charge variations between it and AcrB. Binding prediction simulations confirmed dissimilar structural regions between MdtF and AcrB homotrimers that are probable substrate binding sites.

2.1. Introduction.

E. coli expresses multi-drug efflux proteins in response to intracellular toxin accumulation. These pumps are of the resistance nodulation division (RND), ATP-Binding-cassette (ABC-type), multi-drug and toxic compound extrusion (MATE), and small multi-drug resistance (SMR) types. The major multi-drug efflux protein, AcrAB-TolC, is an RND pump responsible for the extrusion of several chemicals, including bile salts, hormones, and antibiotics. The other six RND efflux pumps (CusCFBA, AcrEF, AcrD, MdtEF (YhiUV), and YegMNO) also work to export monovalent cations (CusCFBA), copper and zinc (AcrD), aminoglycosides (AcrD), and those similar to AcrAB and AcrEF.[159-164] The known substrates of MdtEF (also known as YhiUV)-TolC is limited in scope, but are similar to the major multidrug efflux pumps AcrAB-TolC of *E. coli* and MexAB-OprM in *Pseudomonas aeruginosa*. They include steroid hormones, deoxycholate, cationic detergents, crystal violet, ethidium, and erythromycin among others.[165] A protein blast of MdtF (Accession P37637) the inner membrane protein of the RND complex responsible for substrate recognition and binding, is most homologous to AcrB (71% identity) and MexB (63% identity). The protein identity is indicative of similar substrates across protein classes and bacteria species.

While AcrAB-TolC is the major multidrug efflux pump that is constitutively expressed in *E. coli*, the role of MdtEF-TolC is complex and lesser-known. GadX, a regulator of acid resistance, can induce MdtF expression through GadE.[166-169] MdtEF is also regulated by ArcA under anaerobic growth conditions.[166] MdtEF is expressed differentially during lag and stationary growth and under toxic stress.[170] A previous study

showed that the environmental pollutants 17α-ethynylestradiol, bisphenol-A, and nonylphenol induce expression of the genes *acrB* and *mdtF* that encode for the respective efflux pumps.[76] The efflux pump MdtEF has been observed to have increased expression and efflux of substrates under anaerobic conditions and has thus been termed an anaerobic efflux pump.[166-167, 171] Redundancy of efflux pumps that share similarities may give MDR bacteria high levels of resistance to harsh environmental stressors that may be experienced in built and natural environments.

To better understand the substrates of this lesser studied efflux pump system, a high-throughput chemical screening was applied to mutants expressing MdtF and AcrB. *E. coli* mutants with deletions and insertions of the inner membrane proteins were exposed to 240 biocides (Table 2.1.) to determine substrate specificity. Additional chemical data (pKA, molecular charge) were extracted from Chemicalize.[172] An alignment of the inner membrane proteins AcrB and MdtF and *in silico* construction provided insight into the surface chemistry of the binding pockets of the RND proteins. Probable binding sites were determined with molecular modeling of AcrB and MdtF.

Table 2.1. Chemical classes used in chemical sensitivity assay that were utilized to determine substrate range.

Type of Action	Antimicrobial Classes
Chelator	Carboxylic acids, hydroxyquinolines, N-heterocycles
DNA & RNA	Alkylation, fluoroquinolones, intercalators, nitrofuran analogs, purine/pyrimidine analogs, quinolones
Folate	Sulfonamides
Fungicide	Lipoxygenases, phenylsulfamides
Ion channel	K^+ inhibitors, Na^+ inhibitors
Membrane	Anionic/cationic/zwitterionic detergents, electron transport, guanidine (permeability), phenothiazines (efflux pump inhibitor),

Other biocides	Anti-capsules, acetylcholine antagonist, fatty acid synthesis, glycopeptides, nitroimidazoles, rifamycins, triazoles
Oxidation	Glutathiones, oxidizing agents, sulfhydryl
Protein	Aminoglycosides, lincosamides, macrolides, tetracyclines, tRNA synthetase
Respiration	Ca^{2+} transporters, ionphores, uncouplers
Wall	Cephalosporins, monobactams, β-lactams, peptidoglycan synthesis, polymyxins, glycopeptides

2.2. Materials and Methods.

2.2.1. Bacterial Strains.

Strains and plasmid descriptions and sources are found in Table 2.2. Electrocompetent *E. coli* W4680 (kan^R) and TKO (kan^R) were transformed with plasmids and plated on 100 mg/L ampicillin in LB agar. After selection, single colonies were pre-cultured in their appropriate antibiotics and inducers (IPTG, 1 mM) and grown to mid-log phase.

Table 2.2. *E. coli* mutants and plasmids were used in this study.

Strain	Genotype	Source
W4680A	K-12 ΔacrAB	(173)
TKO	K-12 ΔacrAB ΔacrF ΔyhiV	(174)
Plasmid		
pAB	AcrAB cloned into pUC18, amp^r	(161)
pUC18	Vector control, amp^r	
pYhiUV	MdtEF cloned into pUC119, amp^r	(160)
pUC119	Vector control, amp^r	(175)

2.2.2. Substrate Determination.

2.2.2.1. Chemical Sensitivity Assay.

Assay plates (Biolog chemical sensitivity panels PM11-20), seeded with LB media and *E. coli* mutants (5×10^5 cells/mL, 200 μL), were grown aerobically or anaerobically at 37 °C. A control plate containing no chemicals was also inoculated and grown. Anaerobic conditions were described by Zhang et al. 2011, where 10 mM nitrate

was supplied in LB media as the terminal electron acceptor.[166] Optical density (λ = 600 nm) was recorded at t = 0 and at t = 16 hours using a Biotek Synergy H1 multi-mode plate reader.

2.2.2.2. Assay Data Interpretation.

Relative growth was defined as the growth ($OD_{600,\ Biocide}$) of the strain with respective biocide after 16 hours of incubation, divided by growth ($OD_{600,\ Control}$) of the strain with no biocide applied. Results were interpreted by comparing growth at 16 hours for gene insert (*E. coli acrB*$^{+}$ or *mdtF*$^{+}$) and empty vector plasmid (*E. coli acrB*$^{-}$ or *mdtF*$^{-}$). Chemicals were considered substrates of the efflux pump if the growth of the strain with the pump insert was 2-fold greater than the plasmid control for the same chemical concentration in the corresponding well. One-way ANOVA followed by Fisher's least significant difference tests was performed to determine the statistical significance of the differences between relative bacterial growth conditions between test conditions using Origin 2018.

2.2.2.3. Substrate Properties.

Chemical data (formula, molecular weight, pKa, charge) for substrates of interest were extracted from the Chemicalize database.[172] pKa and charge were not properties of all biocides, as some chemicals did not possess acidic hydrogens. The pKa (pKa = -log of Ka, the acid dissociation constant) was compared to the test pH (pH = 7.2) to determine the biocide charge. Descriptive statistics on the charges determined for the respective substrates of both MdtEF and AcrAB were determined. A two-sample t-test was applied to determine the significance of the average charge of substrates determined in this study.

2.2.3. *In silico* Analysis of MdtF and AcrB Proteins.

Protein features of MdtF and AcrB were evaluated including hydropathy, sequence alignment with predicted protein structure, and prediction of substrate binding sites.

2.2.3.1. Sequence Alignments.

The UniProtKB BLAST algorithm was used to run a sequence similarity search to compare amino-acid sequences of the proteins MdtF and AcrB.[176] Protein sequences were input (accession numbers: P37637 and P31224) for an initial BLAST alignment of sequences and information was extracted for structural analysis to investigate similarities and differences.

2.2.3.2. Hydropathy and Isoelectric Point Analysis.

Whole protein hydropathy and isoelectric points (pI) were calculated with the Expasy ProtScale and ProtParam server web tools using the Kyte and Doolittle amino acid (AA) scale for both the inputted MdtF and AcrB sequences (accession numbers: P37637 and P31224).[177-178] Theoretical pI values were obtained to analyze surface charges of MdtF and AcrB. Hydropathy values were aligned and subject to least-squares linearization to evaluate hydrophobic/hydrophilic homology, mapped to major locations within the cell (cytoplasm, periplasm, and transmembrane) and protein secondary structure (helices, turns, and sheets). Similar and dissimilar regions' sequences were analyzed for residue class shifts (non-polar, polar, aromatic, aliphatic, cationic, and anionic).

2.2.3.3. Predicted Structure of MdtF.

The 3-D structure of MdtF was developed from existing high-resolution crystal structures of trimeric apo-AcrB using the platform Swiss-Model.[179] AcrB (accession number: P31224) was input to Swiss-Model to obtain a list of possible structural templates, which was then reduced to those proteins crystallized as intact homotrimers using X-ray crystallography, with no ligands or amino acid mutations, coverage greater than 97%, sequence identity of 71%, full coverage with all 1035 amino acid residues. Thus the structure 3AOA (GMQE 0.80 – 0.81), was chosen as the template to develop the MdtF homotrimer structure.[180] The predicted MdtF structure was compared to the secondary and tertiary structures of each AcrB trimer chain (A-C) to determine the overall fit and regions of similarity and dissimilarity. A Q_{mean} score of 0.60 or less was designated as having poor similarity to the model template and was used for this analysis. Residues from compared regions of structures were analyzed based on referenced properties of respective amino acids (AA).[181]

2.2.3.4. Predicted Substrate Binding Sites of MdtF and AcrB.

The PDB files produced from the Swiss-Model for the homotrimer structures of AcrB and MdtF were input into the P_2Rank tool to simulate and predict ligand binding sites of the protein structure.[182] P_2Rank was utilized as it is a rapid machine learning tool for rapid prediction of ligand binding sites from inputted PDB files or ascension numbers. P_2Rank simulations produced a ranked list of binding pockets that were characterized by the coordinates of the pocket centers and/or solvent-accessible protein atoms (pocket points) in the empty space and around the protein surface.[182] CSV files with an ordered list of predicted pockets, ranked scores, and amino acid residues that constitute the

predicted binding sites were generated for MdtF and AcrB homotrimers. Additionally, P_2Rank was used to develop visuals of the protein structures indicating potential binding sites.

2.3. Results and Discussion.

2.3.1. Overexpressed AcrAB.

Masses present in Biolog's pre-plated assays are proprietary, however, the span of the four concentrations was relevant for studying *E. coli* toxicity, as full growth, and no growth over the four concentrations was observed for nearly all analytes, except for tetrazolium violet and puromycin, which were fully toxic. However, the MIC nor the fold-difference concentration from the panel could be determined, a method typical of analyzing conferred resistance. The classes of chemicals transported by AcrAB-TolC are shown in Table 2.2. and many have been reported in prior studies.[75, 161, 165] With this screening, additional chemicals within the macrolides, tetracyclines, cationic membrane detergents, fenicols, fluoroquinolones, and quinolones classes of antimicrobials that are exported by this efflux pump were verified. New chemicals and classes uncovered by this assay were the metal-chelating 1,10-phenanthroline, unsubstituted and halogenated hydroxyquinolines, phenothiazines, glycopeptides, triclosan, and pentachlorophenol among others. With these reproducible results, and for those comparable to literature, interpretation of two-fold growth is an appropriate metric for evaluating antibiotic susceptibility.

2.3.2. Overexpressed MdtF.

The screen showed that MdtF substrates were the same substrates as AcrB (Table 2.3.) but were limited when the chemical was neutral to anionic. Growth was at least two-fold greater than control (empty vector) for overexpressed MdtF for cationic detergents, macrolides, the metal chelators clioquinol, and sanguinarine, 2,4-diamino-6,7-diisopropyl-pteridine, amitriptyline, the phenothiazines (efflux pump inhibitors), pridinol, chelerythrine, crystal violet, and cefmetazole. No differences were observed in substrate specificity at t = 16 hours for *E. coli* grown aerobically or anaerobically growth, except that anaerobically cultures grew slower (data not shown). The slower growth was accounted for by determining relative growth, where OD_{600} was normalized to bacteria grown with no biocides. Selected growth of mutant strains with biocides (with and without MdtEF) can be observed in Figure 2.1.

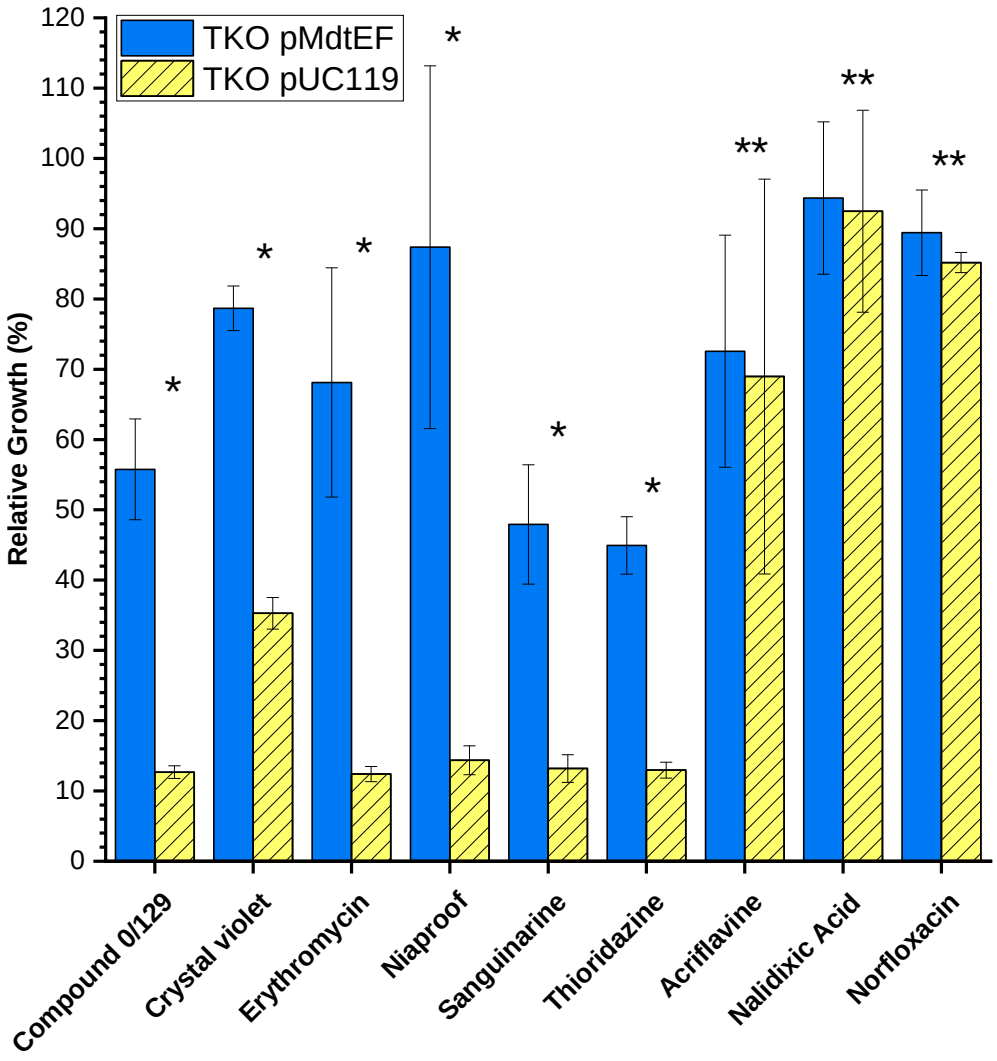

Figure 2.1. Selected relative growth of TKO pMdtEF and TKO pUC119 on select biocides from Biolog's chemical sensitivity panels. Antibiotics were considered substrates if the gene insert (solid, blue bars) allowed for two-fold greater growth than that by the empty vector (striped, yellow bars) and were statistically significant (* p-values < 0.05). Acriflavine, nalidixic acid, and norfloxacin were not considered substrates as there was no significant (** p-values > 0.05) difference in relative growth between tested strains, nor are they reported in literature. Error bars represent standard deviation of three independent experiments.

Table 2.3. Substrates of AcrAB and MdtEF determined from two-fold growth differences of *E. coli* mutants, with charges on molecule extracted from Chemicalize. **DNA intercalators acriflavine, proflavine, and 9-aminoacridine are likely substrates of MdtEF-TolC, however different hosts are needed to validate this.

Class	(Charge): Chemicals	AcrB	MdtF
Cationic detergent	(+1): benzethonium chloride, cetylpyridinium chloride, dequalinium chloride, dodecyltrimethyl ammonium bromide, domiphen bromide, methyltrioctylammonium chloride	●	●
Macrolide	(+1): josamycin, oleandomycin, spiramycin, troleandomycin, tylosin, erythromycin	●	●
Other biocides	(-1): niaproof; (0): 2,4-diamino-6,7-diisopropyl-pteridine (0/129); (+1): lidocaine, dodine, amitriptyline, pridinol, sanguinarine, chelerythrine, orphenadrine, trimethoprim	●	●
	(-1): hexachlorophene, rifamycin SV, lawsone, fusidic acid, pentachlorophenol; (0): nordihydroguaiaretic acid, lauryl sulfobetaine, triclosan, harmane, lincomycin	●	
Phenothiazine	(+1): thioridazine, trifluoperazine, chlorpromazine	●	●
Glycopeptide	(+1): phleomycin	●	
	(+2): bleomycin	●	●
Respiration uncoupler	(+1): crystal violet	●	●
	(0): iodonitrotetrazolium violet, menadione	●	
Chelator	(0): 5-chloro-7-iodo-8-hydroxyquinoline	●	●
	(0): 1,10-Phenanthroline, 5,7-dichloro-8-hydroxyquinaldine, 5,7-dichloro-8-hydroxyquinoline, 8-hydroxyquinoline	●	
DNA intercalator	(-1): novobiocin; (0): 2-phenylphenol; (+1): acriflavine, proflavine; (+2): 9-aminoacridine	●	**
Fenicol	(0): chloramphenicol, thiamphenicol	●	
Fluoroquinolone	(-1): ofloxacin; (0): ciprofloxacin, enoxacin, lomefloxacin, norfloxacin	●	
Quinolone	(-1): nalidixic acid, oxolinic acid	●	
Tetracycline	(0): chlortetracycline, doxycycline, oxytetracycline, rolitetracycline, tetracycline	●	

2.3.3. Chemical Variations of Substrates in MdtEF and AcrAB.

Closer analysis of the chemicals that were substrates of the pump MdtEF and not AcrAB showed a trend according to structure and chemical property. The properties of the AcrAB substrates were investigated further using the Chemicalize computational database, focusing on the pKa, structure, and charge at test pH of .[172, 183] It was discovered that substrates of MdtEF are also the substrates of AcrAB that have a +1 charge. A statistical analysis of the charge of MdtEF versus AcrAB substrates showed that the anaerobic efflux pump MdtEF, exports primarily cations, while AcrAB has broad substrate specificity of charged and neutral compounds (Figure 2.2.). The median of charge of the substrates for AcrAB was 0 while for MdtEF was 1. The distribution of the charges showed that AcrAB has broad substrate specificity of charged and neutral compounds. There were exceptions to the +1-charge rule (n = 2), however the average charge for AcrAB chemicals and that for MdtEF were statistically significant (p = 0.01876).

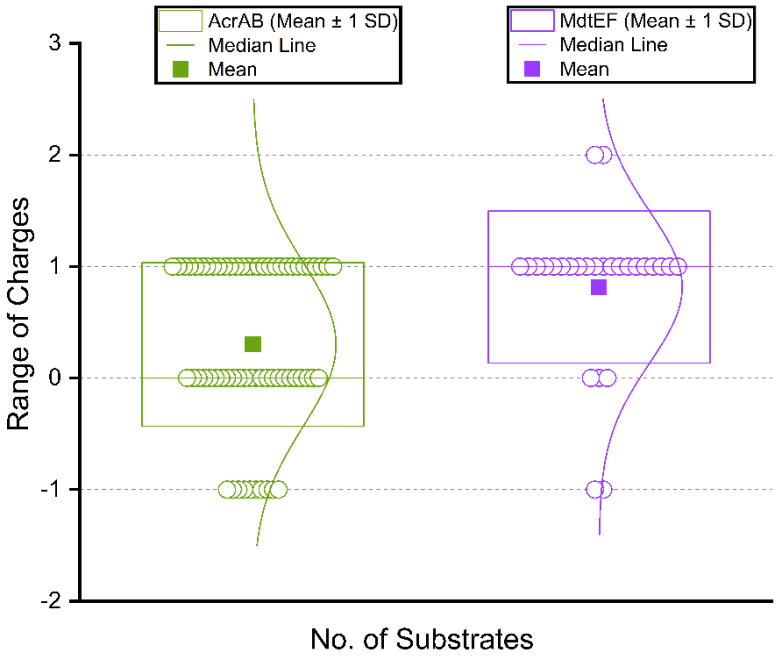

Figure 2.2. Charges of biocide classes exported by MdtEF and AcrAB. Boxes represent 1 standard deviation from the mean of charges. The median line showed the most reoccurring charge out of the substrate lists. The two outlying non-cationic points under "Other antibiotics" that are MdtEF substrates are Niaproof, an anionic surfactant, and 2,4-diamino-6,7-diisopropyl-pteridine.

Due to substrate similarity and known homology between various RND inner membrane proteins, the sequences of MdtF and AcrB were compared.[184] Protein alignment showed 71% identity, 84% positives, and two gaps (Appendix A) The periplasmic domain (residues (R) 33-335) alignment also showed homology, with 67% identity, 83% positive, and no gaps. The isoelectric points within this region were the same at 4.4. A second periplasmic region (R565-871 of AcrB) showed differences between the two proteins, but the overall isoelectric points (pI) for MdtF and AcrB are 4.9 and 4.8 with 65% identity and 79% positives.[185] Generally, these proteins exhibit similar chemistries, however, there are specific regions within the bulk protein that require further analysis based on *in silico* studies of AcrB channels.[186]

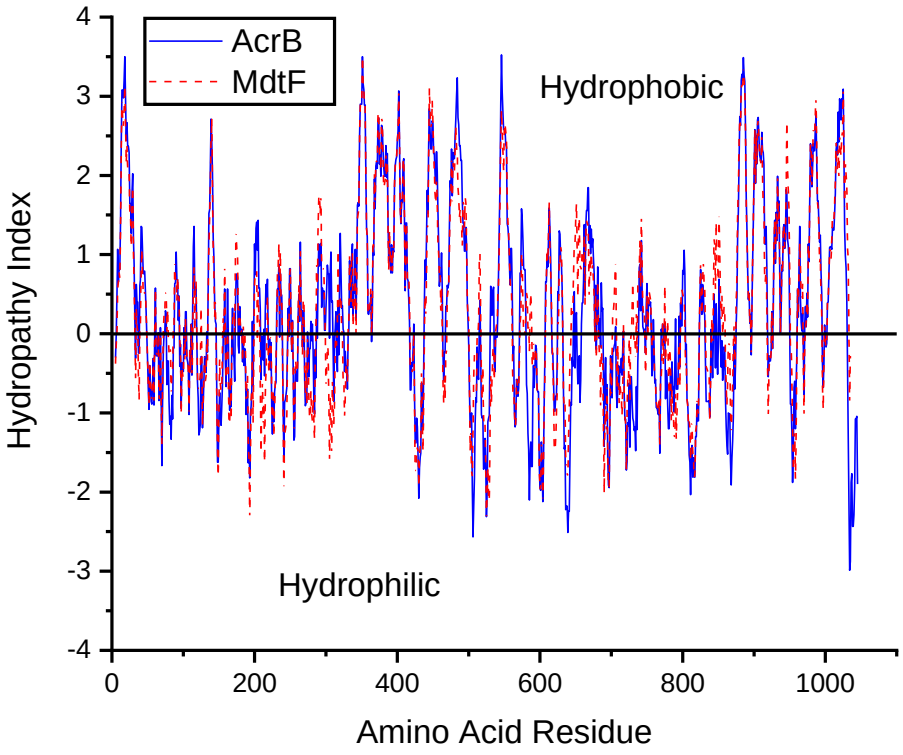

Figure 2.3. Hydropathy analysis of whole protein structures of AcrB and MdtF residue alignment. MdtF protein positions shifted by 2 residues.

Examination of the distal binding pocket, proximal binding pocket, and external cleft, identified as essential binding regions in AcrB, displayed similar homology overall (Figure 2.3.).[186] However, slight differences in the distal pocket, the site of terminal binding from CH1, CH2, and CH3 before export via the inner pore, suggest the local chemistry may play a role in substrate specificity. MdtF residues lining the distal pocket were more acidic (pI = 3.1) than AcrB (pI = 4.0). At pH = 7.4, the charge of MdtF surface residues was -3 (D130, E273, D274) creating a negative region at E273/D274/E180, while the net charge of AcrB was -2 (E130, E273, D276, R620). Concerning other essential binding regions, there are structural differences between MdtF

and AcrB in the proximal pocket, however, the amino acid classes were maintained over the four residues, with no change in the isoelectric point.

The substrates exported by AcrB are diverse in structure, size, charge, and hydrophobicity, while the substrates exported by MdtEF are more restricted to cations with exceptions. Reported exceptions include neutral and anionic substrates of MdtEF such as bile salts, steroid hormones, hormone mimics, and anionic detergents.[75-76] In this work, two neutral/anionic species were substrates of MdtEF-TolC: Niaproof (anion) and 2,4-Diamino-6,7-diisopropyl-pteridine (neutral). Niaproof is an anionic detergent similar in structure to sodium dodecyl sulfate (SDS), also transported by MdtEF. 2,4-Diamino-6,7-diisopropyl-pteridine possesses two basic amino functional groups attached to the pteridine ring that was not acidic (pKa 15.88) and the compound speciation would remain neutral in the typical physiological pH range (7.2-7.8.) of gram-negative bacteria.[172, 187]

Furthermore, not all cationic substrates of AcrB were substrates of MdtF with this screen. Four of the listed cationic substrates of AcrB are transported by MdtF as well: the similarly structured acriflavine, 9-aminoacridine, and proflavine, and the glycopeptide phleomycin. The former are antiseptics that are substrates of at least five other membrane-bound transporters in *E. coli*, and to truly study conferred resistance in a live host, multiple gene deletions are likely needed.[160, 188-190] Phleomycin, on the other hand, is a polyprotic glycopeptide with a +1/+2 charge at neutral pH values and is predominantly neutral at pH = 7.7. An *E. coli* efflux pump does exist for glycopeptides (AmpG), and perhaps this protein is more efficient at phleomycin removal than the presence of MdtF.[191]

Analysis suggests that pH, which determines acid-base speciation and surface charge of the distal pocket, plays a role in MdtF substrate specificity. Isoelectric point analyses showed that the MdtF surface charge is more negative than AcrB. This would allow stronger electrostatic interactions to occur between the channel and cationic substrates. The pKa also determines the charge of the analyte at a given pH. Twenty-five out of 27 (93%) of the confirmed substrates of MdtEF were cations. However, the two anion/neutral biocides, along with other reported human hormones (neutral) and bile salts (carboxylic and sulfonic acids) are also substrates of MdtEF. This may be due to redundancy in substrate specificity since hormones and bile salts are known substrates of the AcrAB-TolC system.[160, 192-193] Bile salts cause widespread protein unfolding and disulfide stress in *E. coli*.[194] MdtEF could export such compounds as a response to this added stress. The MdtEF structure may also be responsible for waste metabolite transport.[195] MdtEF could recognize metabolites from carbon metabolism which may be why some neutral compounds are exported as well.

Results from the phenotypic chemical sensitivity assay revealed a narrower substrate range for MdtF compared to AcrB. Interestingly, the substrates of MdtF are the same as AcrB, but are limited to cationic and polar neutral biocides, but not anionic. Channel and binding pocket differences likely contribute to the efflux of cations in MdtF over neutral and anionic substrates.

2.3.4. Structural Differences of MdtF and AcrB proteins.

Structural analysis of the predicted MdtF structure (Figure 2.4.), revealed distinct regions that differ from the AcrB structure. The external cleft and vestibule, distal and

proximal pockets of MdtF were dissimilar to AcrB, pointing to areas where sequential, topological, and structural differences may play a role in substrate differentiation between the two efflux pumps. Selected sections of MdtF and AcrB homotrimer structure constructed from the Swiss-Model provided additional insight into substrate differences.

Table 2.4. Sequences where structural similarities and dissimilarities of AcrB and MdtF protein structures were discovered. Residue regions are from the homotrimer structures and approximate locations regarding structural features. Highlighted AA are of interest based on variations between respectively compared sequences.

Structure Location	Protein	Sequence	Residue Region
External Cleft	MdtF	FMSGATGE	459-465
	AcrB	FFGGSTGA	459-465
Cytoplasm	MdtF	KA-APEGGHK-PNALFAR	498-513
	AcrB	KPIAKGDHGEGKKGFFGW	498-515
Distal proximal pockets	MdtF	FSGQ	615-618
	AcrB	FAGR	617-620
C-Loop	MdtF	LGTASGFD	672-679
	AcrB	LGTATGFD	673-680
Hoist Loop	MdtF	TGLSYQEALSSNQ	858-870
	AcrB	TGMSYQERLSGNQ	860-872

The amino acid differences in protein sequence can be referenced to biomolecular differences in the individual residues providing insight into substrate preferences between AcrB and MdtF.[181] In the external cleft there are notable sequence differences in residues between the efflux pumps. In R465 there is an anionic glutamate, located on the surface of the monomer of MdtF, whereas the additional phenylalanine in AcrB at R460 is a hydrophobic, aromatic AA. All these residues are located within proximity to the proximal cleft, where ciprofloxacin, a zwitterion, interacts.

In the hoist loop location, the MdtF structure has an uncharged, aliphatic, hydrophobic alanine, whereas AcrB has a cationic arginine. Disorder of peptides in AcrB

creates a pore in the monomer structure in which the AA alanine at R867, is exposed. The peptide differences at AcrB change the respective residue from cationic to neutral. This region is where negative substrates may interact with AcrB, but not with MdtF as it does not transport anions.

Another distinct structural difference between predicted MdtF and the AcrB structure is a sequence in the cytoplasmic section of the RND proteins, where alignment of this highly dissimilar region showed a two AA deletion in MdtF. This region in AcrB is highly ordered and compact whereas for MdtF a pore is evident. Simulations of the homotrimer structure predicted an α-helix in MdtF at this pore whereas no such helix formed in AcrB. The deletion of the two AA and the differences in sequences lead to the formation of the α-helix in MtdF but not in AcrB. The AcrB sequence has two additional aromatic residues, suggesting a less diverse pathway for substrates to traverse MdtF. This region of the structure may play a role in the transport of substrates from the cytoplasm. The extra cationic residues in AcrB may facilitate the transport of antibiotics from the cytoplasm.

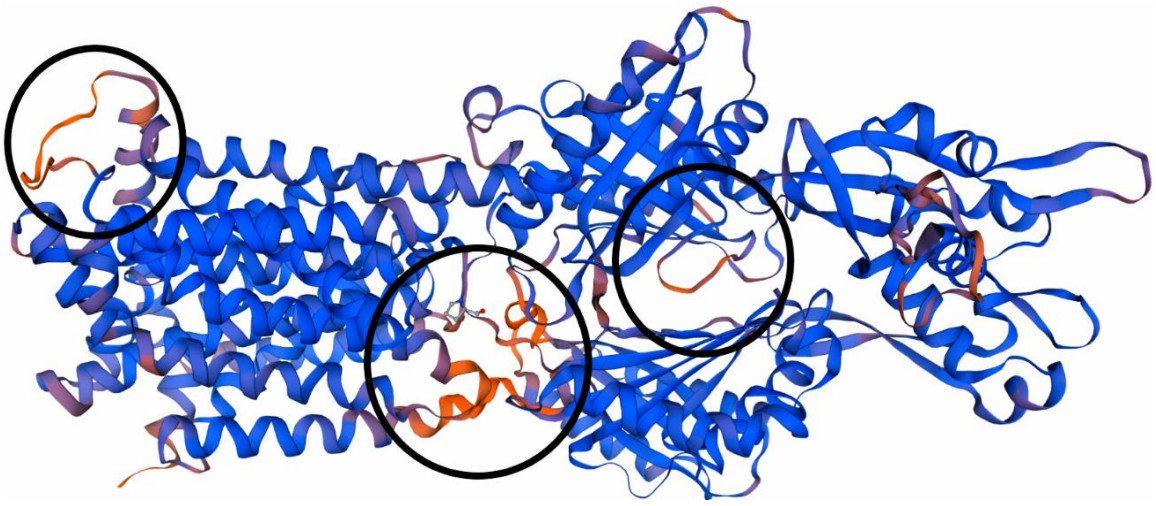

Figure 2.4. Predicted structure of MdtF. The external cleft and vestibule, distal pocket, and proximal pocket with distinct dissimilarities when compared to AcrB are encircled.

The peptide sequences in the distal binding pocket for MdtF differ in polarity and charge from AcrB. The MdtF pore region contains the polar AA serine in R616, glycine in R617, and the neutral AA glutamine in R618, while the AcrB pore region contains the aliphatic, neutral, and non-polar AA alanine in R617, glycine in R618, and the cationic AA arginine in R619. These residues line the pore region, where AcrB has a cation and MdtF is polar/neutral. At R274 of the monomer structures, the MdtF structure is negatively charged with an aspartic acid residue, while AcrB is polar/neutral with an asparagine residue in the same position of the monomer.

Binding site simulations reveal highly probable substrate recognition sites associated with the dissimilar regions of interest between MdtF and AcrB. Some binding site models are biased towards only precise predictions as a majority utilized residue-centric methods which favor smaller spatial pockets as binding sites with highly accurate predictions.[182, 196-198] However, this may lead to high levels of false positives. The utilization of P_2Rank as a pocket-centric method, where larger pockets on the structure

are ranked as potential binding sites, is the most suited simulation to apply for MDR efflux pump proteins that have broad-substrate specificity. Large binding pockets have been shown to act as binding sites for substrate recognition of ligands, their substructures, and superstructures within the same pocket.[199-200] Substrates of MdtF and AcrB can be broad but noticeable trends are apparent.

The PDB file created in the Swiss-Model for the homotrimer structure of AcrB and MdtF was input into the P_2Rank tool. Predictions of binding sites revealed probable binding that coincided with the distinct structural dissimilarities between the efflux pump proteins discussed prior. High ranking (1-10) binding sites coincide with the external cleft, vestibule, and distal and proximal pockets for both MdtF and AcrB (Figure 2.5.). A complete list of major binding sites associated with regions in Table 2.4., can be seen in Table A.1. The highest and most probable ranking binding site for both structures occurred in the distal pocket regions (MdtF R615-618, AcrB R617-620) where the key structural differences support the transport of cationic substrates by MdtF compared to the substrate potential of AcrB. These results suggest the negative charge at R274 of the monomer structure and loss of cation (from R618 to R620) in MdtF at the pore region of the distal binding pocket results in easier transport of cationic substances through the G-loop where large polyprotic substrates such as tetracyclines interact. This demonstrates another feature that can hinder neutral/anionic chemicals yet facilitates the transport of cationic biocides by MdtF.

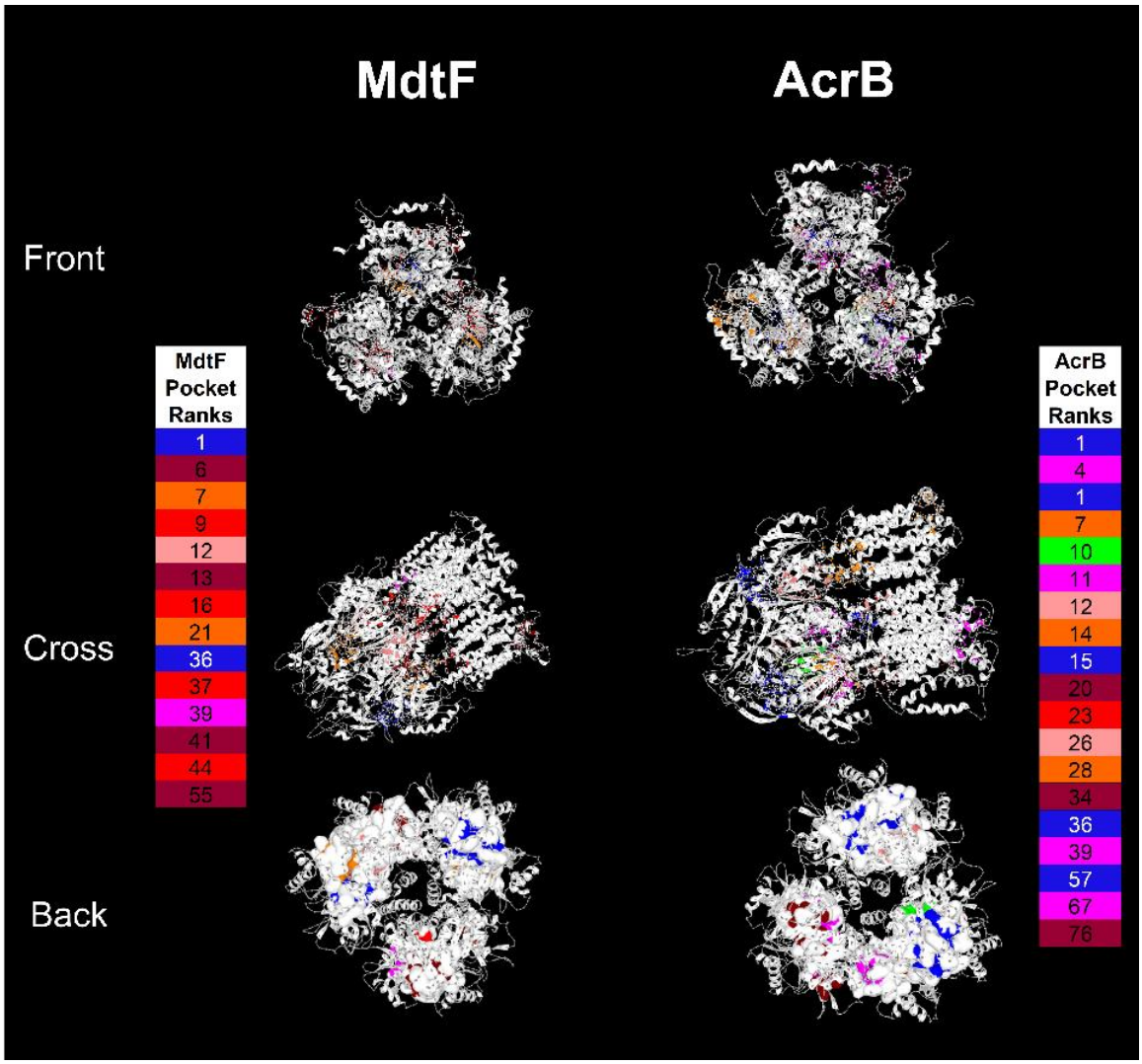

Figure 2.5. Homotrimer protein structures with predicted binding. Binding sites shown are not indicative of total predicted sites but are associated with major structural dissimilarities between MdtF and AcrB. Protein structures are displayed from three profiles.

2.5. Conclusion.

In this work, a high-throughput method was utilized to determine MdtF substrates, which were primarily cationic biocides derived from AcrAB-TolC analytes. Using two-fold growth as a metric for assessing sensitivity, these results validated previously published substrates and discovered new substrates. The results from the *in*

silico analysis of MdtF and AcrB homotrimer and monomer structures revealed insights into the differences in substrate recognition. The results of this study demonstrate that the presence of MdtEF-TolC renders *E. coli* less sensitive to cationic biocides, suggesting the role of MdtEF-TolC as a proton/cation antiporter. The significance of these findings is that under acidic conditions, the lower pI of essential binding residues in the distal pocket would deprotonate, allowing for stronger interactions between cation and anion. These findings suggest that acidic conditions influence the transport of cationic substrates for the MDR efflux pump, MdtEF.

Variations in pH of built microbial communities may alter the cycling of emerging contaminants that may be substrates of the MdtEF-TolC efflux pump. Furthermore, as an anaerobic efflux pump, the recognition of substrates to this efflux pump may vary in different types of biological treatment such as aerobic, anoxic, and aerobic biological reactors or aerobic and anaerobic digesters. Under aerobic conditions, AcrAB may be the primary transporter cycling chemicals, whereas under anaerobic conditions MdtEF may allow for different substrates to be cycled depending on the pH. The substrate differences between MdtEF and AcrAB demonstrate the robustness of *E. coli* and its potential to influence the transport of chemicals in various conditions and types of WWTPs.

CHAPTER 3

HIGH-THROUGHPUT SCREENING OF SYNERGISTIC GROUP IB-BIOCIDE COMBINATIONS FOR E. COLI INACTIVATION

Graphical Abstract

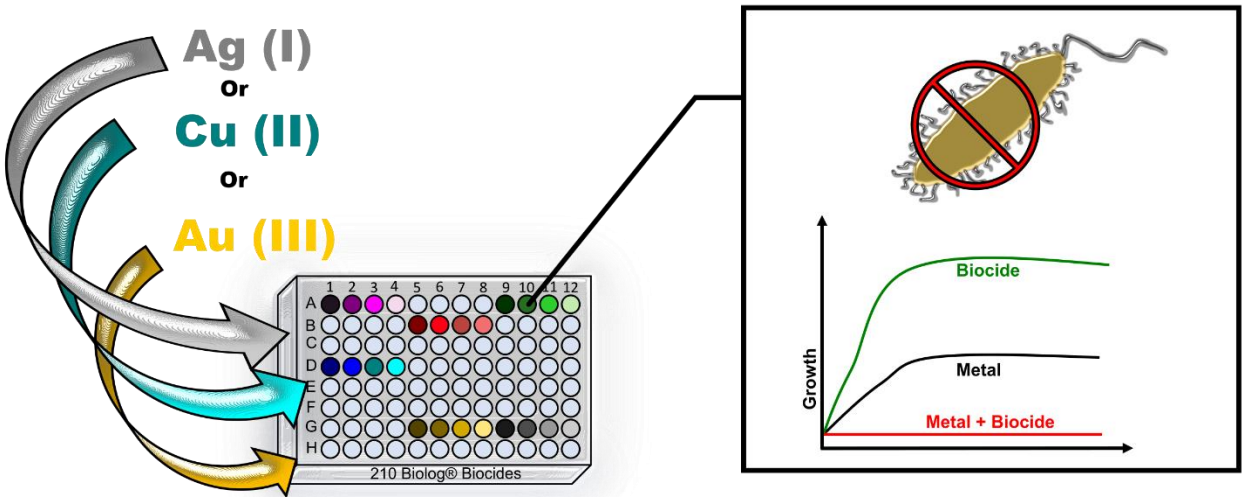

Abstract

The over-prescription of antibiotics, use of biocides in commercial products, and misuse of antimicrobials have generated drug-resistant microbes, resulting in the need for stronger pharmaceuticals to fight infections. In this work, a high-throughput screen to assess synergistic metal-biocide combinations for pathogen inactivation was investigated. Group IB metal ions (Ag(I), Cu (II), and Au (III)) were mixed with various classes of pre-plated biocides (210 total). Wild-type *E. coli* (strain W3110) were exposed to metal ions, biocides, and the metal-biocide mixture. The coefficient of drug interaction (CDI) was used to quantify the possible extent of synergism. Novel biocide and Ag^{+}, Cu^{2+}, and Au^{3+} combinations including silver-hydroxyquinolines, copper-oxidizing agents, gold-macrolides and, gold-phenothiazines were discovered by this study, while also validating previously reported metallo-organic combinations.

3.1. Introduction.

Multi-drug resistance (MDR) conferred by *E. coli* and other microbes has resulted in extensive and rigorous approaches to pathogen inactivation. These include the use of physical methods such as thermo-spectral energy, electrochemical means, plasma discharges, and biochemical means such as antibiotics, metals, enzymes, phages, peptides, efflux pump inhibitors, nanoparticles (NPs), alone, and in combination synergistically.[201-204] Synergism, where more than one inactivating agent can be utilized, is a promising method to combat MDR bacteria such as *E. coli*, by using less material to achieve the same lethality. This approach can be used to enhance the toxicity of individual biocides and provide a means to combat MDR bacteria that have several efflux pumps to defend themselves from environmental stressors.

Due to the toxic nature of silver and copper ions towards bacteria, synergistic combinations with these Group IB metals show promise as treatment options. Copper ions show biocidal activity in combination with β-lactams, aminoglycosides, and quinolones.[205-207] Silver ions can also act synergistically in combination with biocides working to inactivate MDR bacteria such as *E. coli*. These include combinations with efflux pump inhibitors, aminoglycosides, glycopeptides, and fluoroquinolones.[208-209] Synergistic studies of gold ion interactions with antibiotics are limited but have been reported for phenothiazines, salicylates, and polymyxins.[210-211]

When used in combinations with antimicrobials, metal ions such as Ag (I), Cu (II), and Au (III) could be a beneficial strategy for multidrug resistance, by enhancing antimicrobial properties. A high-throughput method to inactivate wild-type *E. coli* was

utilized to identify potential drug combinations, screening approximately 210 organic biocides covering aminoglycosides, efflux pump inhibitors, glycopeptides, β-lactams, and detergents, among others. Strict limits placed on the combination index for cell growth at 16 hours revealed highly synergistic combinations that were also verified with growth curves, offering insight into new combinations of silver, copper, and gold ions with biocides that can be further explored for novel therapeutics for MDR bacteria.

3.2. Materials and Methods.

3.2.1. Chemicals and Cell Lines

Metals were obtained from Sigma Aldrich as salts ($AgNO_3$, $CuSO_4$, $HAuCl_4$) and prepared as stock solutions in nanopore water, then filter sterilized. Bacteria (*E. coli* W3110) [212] were pre-cultured in LB media or chloride-free LB (to prevent silver chloride precipitation) and grown to mid-log (OD_{600} 0.8-1.00, 37 ºC). Cells were seeded (5×10^5 cell/mL) in serially diluted metal ion and respective LB media and grown for 16 hours The minimum inhibitory concentration (MIC) was determined for each metal (Table B.1.).

3.2.2. Chemical Sensitivity Assays.

Biolog's chemical sensitivity assays were used per the manufacturer's procedure to evaluate combinations of biocides and either Ag (I), Cu (II), or Au (III). Biocides were tested with three concentrations of $AgNO_3$ (0.5, 1, and 5µM), $CuSO_4$ (0.1, 0.1, and 1 mM), and $HAuCl_4$ (5, 25, and 50 µM). The plates were incubated at 37°C and the absorbance (590 nm) was recorded for 24 hours on a microplate reader spectrophotometer (Biotek Synergy H1) to generate growth curves.

3.2.3. Data Analysis.

The coefficient of drug interaction (CDI) quantifies combination responses as either additive, synergistic, or antagonistic (Equation 3.1.).[213] Combinations were labeled additive if CDI ≈ 1, synergistic if CDI < 1, and antagonistic if CDI > 1. Relative growth, defined as the growth normalized to *E. coli* grown without chemicals, was calculated for cultures grown in the biocides alone (A), the metal ion alone (B), or the metal-biocide mixture (AB). Assays were tested in duplicate.

$$\mathbf{CDI} = \frac{\mathbf{A+B}}{\mathbf{AB}} \qquad \textbf{Equation 3.1.}$$

An upper CDI limit of 0.5 was chosen as the metric to define a highly synergistic pair of metal biocides.

3.3. Results.

3.3.1. Synergism of Metal and Biocide Combinations.

A CDI heat map (shown are CDI < 0.5) for all synergistic combinations tested, organized by metal and antibiotic class (Figure 3.1.), with select growth curves is presented. The results validated published results of synergistic pairs, discussed below, with this assay (Figure 3.1., Table 3.1.), indicating that the biocide classes and plated concentrations were applicable in the combinatory tests. Novel synergistic mixtures of metals and antibiotics were also discovered that are notable for future *in vitro* toxicity, metal chelation, and clinical trials. Growth curves (Figure 3.2.) for select combinations are shown, further supporting the use of the high-throughput assay to rapidly screen synergism using CDI. Additive and antagonistic combinations are not shown.

Table 3.1. Synergistic silver/copper/gold-biocide combinations that inactivated *E. coli* (W3110). Chemicals are organized by class of biocide or target of action. Chemicals in *italics* are combinations with respective metals that have not been previously reported to date.

Target or class	Silver synergism	Copper synergism	Gold synergism
Chelator	EDTA, EGTA, *5,7-dichloro-8-hydroxyquinaldine, 5,7-dichloro-8-hydroxyquinoline, 5-chloro-7-iodo-8-hydroxyquinoline, 8-hydroxyquinoline,* 1,10-phenanthroline, and sodium pyrophosphate decahydrate	fusaric acid, and 1,10-phenanthroline	EDTA
DNA & RNA	4-hydroxycoumarin, *9-aminoacridine, acriflavine, novobiocin, proflavine,* 5-nitro-2-furaldehyde semicarbazone, furaltadone, nitrofurantoin, disulphiram, myricetin azathioprine and 5-fluorouracil	2-phenylphenol, 4-hydroxycoumarin, disulphiram, myricetin, and azathioprine	novobiocin and *disulphiram*
Folate	2,4-Diamino-6,7-diisopropylpteridine, hydroxyurea, sulfachloropyridazine, sulfadiazine, sulfamethazine, sulfamonomethoxine, sulfathiazole		
Fungicide	*nordihydroguaiaretic acid, dichlofluanid,* and *tolylfluanid*	*nordihydroguaiaretic acid* and dichlofluanid	

Ion channel	*lidocaine* and *procaine*	*lidocaine*	lidocaine and procaine
Membrane	benzethonium chloride, dequalinium chloride, dodecyltrimethyl ammonium bromide, alexidine, *dodine*, *guanidine hydrochloride*, 1-hydroxypyridine-2-thione, amitriptyline, *chlorpromazine*, *promethazine*, *thioridazine*, and *trifluoperazine*	benzethonium chloride, methyltrioctylammoniu m chloride, *Niaproof*, guanidine hydrochloride, trifluoperazine, and *lauryl sulfobetaine*	methyltrioctyl ammonium bromide, domiphen bromide,dodine, guanidine hydrochloride, 1-hydroxypyridine -2-thione, protamine sulfate, and chlorpromazine
Other Biocides	ketoprofen, *atropine*, *orphenadrine*, *2-nitroimidazole*, *ornidazole*, chelerythrine, Compound 48/80, *D,L-propranolol*, ethionamide, *patulin*, *sanguinarine*, tannic acid, rifamycin SV, and 3-Amino-1,2,4-triazole	ketoprofen, sodium salicylate, atropine, pridinol, ornidazole, tinidazole, captan, semicarbazide, rifampicin, rifamycin SV, and *3-amino-1,2,4-triazole*	thiosalicylic acid and rifampicin

Protein	amikacin, apramycin, capreomycin, geneticin (G418), gentamicin, hygromycin B, kanamycin, paromomycin, sisomicin, spectinomycin, streptomycin, tobramycin, lincomycin, *erythromycin*, *josamycin*, *oleandomycin*, *troleandomycin*, *tylosin*, benserazide, PMSF, β-Chloro-L-alanine HCl, chloramphenicol, fusidic acid, puromycin, thiamphenicol, penimepicycline, *D,L-serine hydroxamate*, *DL-methionine hydroxamate*, and *L-glutamic-g-hydroxamate*	capreomycin, dihydrostreptomycin, geneticin (G418), paromomycin, oleandomycin, PMSF, blasticidin S, *fusidic acid*, puromycin, *thiamphenicol*, demeclocycline, and glycine hydroxamate	*erythromycin*, *oleandomycin*, *spiramycin*, *troleandomycin*, *tylosin* and fusidic acid
Respiration	ruthenium red, 18-crown-6 ether, CCCP, FCCP, pentachlorophenol, sorbic acid, *tetrazolium violet*	ruthenium red, 2,4-dintrophenol, 3,5-dinitrobenzene, CCCP, FCCP, pentachlorophenol, sodium, caprylate, *iodonitro tetrazolium violet*,*menadione*, and *tetrazolium violet*	CCCP, and tetrazolium violet

Cell Wall	oxacillin, cefotaxime, cephalothin, bleomycin, phleomycin, vancomycin, phosphomycin, colistin, and polymyxin B	colistin	*bleomycin, vancomycin, phleomycin*, phosphomycin, colistin, and polymyxin B
Oxidation			methyl viologen

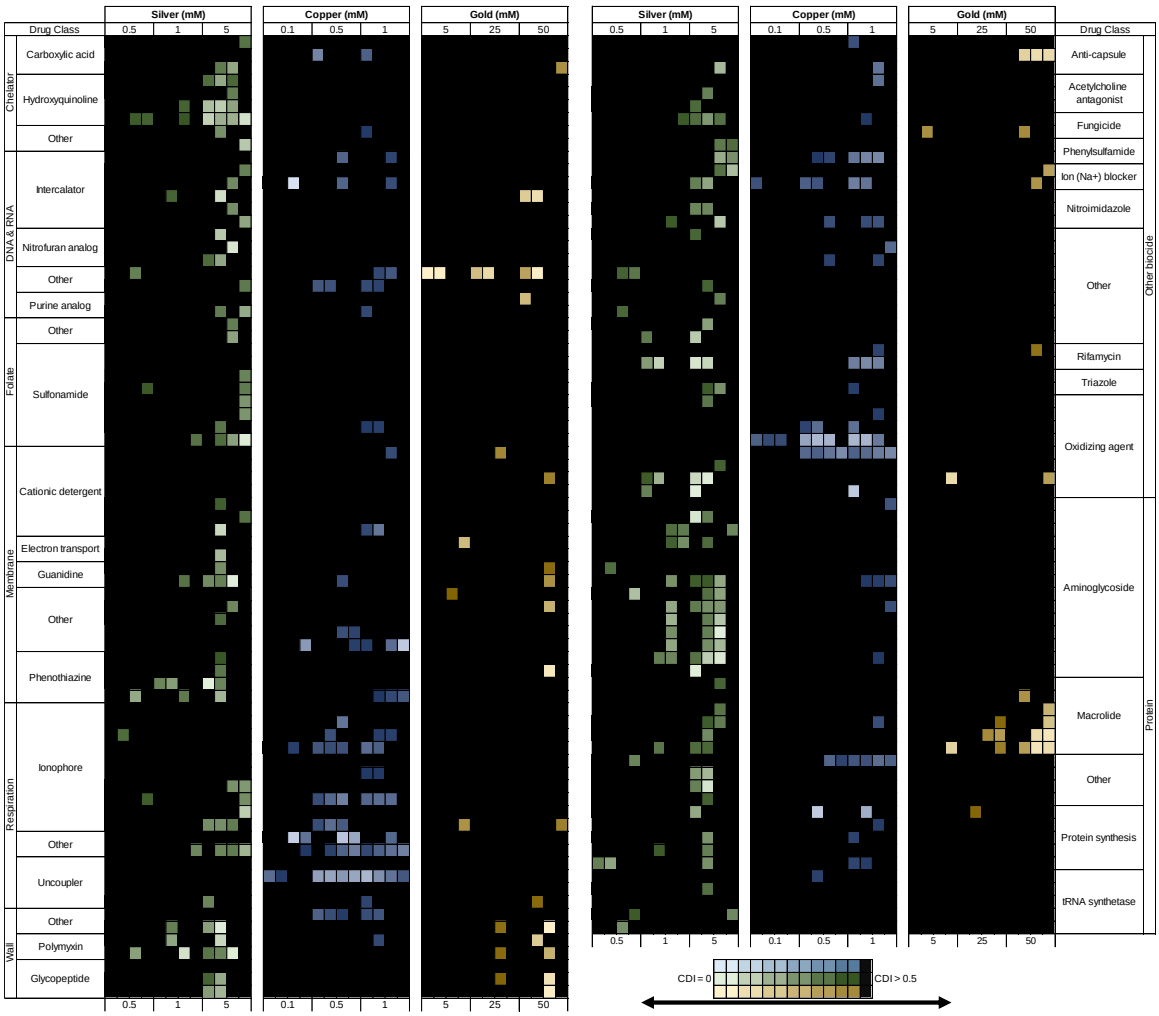

Figure 3.1. Coefficient of drug interaction heat map of 630 combinations of Group IB metals with biocides present in a commercially available 96-well panel set. 196 combinations with silver, 149 combinations with copper, and 53 gold combinations with biocides resulted in elevated levels of synergism (CDI < 0.5) Blackened areas include values considered to be low synergistic (0.5 > CDI < 1), additive, antagonistic, or undefined by the CDI equation as the case when the AB (metal-biocide combination) resulted in no growth.

3.3.2. Ag (I)/Biocide Interactions.

Highly synergistic combinations (CDI < 0.5) of silver ions with biocides were observed for several antibiotic classes and individual chemicals (Figure 3.1., Table 3.1.), including metal chelators, DNA intercalators, nitrofurans, phenothiazines, acetylcholine antagonists, nitroimidazoles, aminoglycosides, macrolides, and tRNA synthetase

inhibitors, among others. Previously reported synergistic mixtures were verified with CDI values and 24-hour growth curves. These include interactions with aminoglycosides, β-lactams, phenothiazines, sulfonamides, and tetracyclines, as discussed below. Growth of sulfonamide (sulfadiazine), amikacin (an aminoglycoside), and tetracycline with and without silver are shown, depicting enhanced toxicity when the antibiotic was mixed with the metal, compared to the antibiotic and metal alone (Figure 3.2.A).

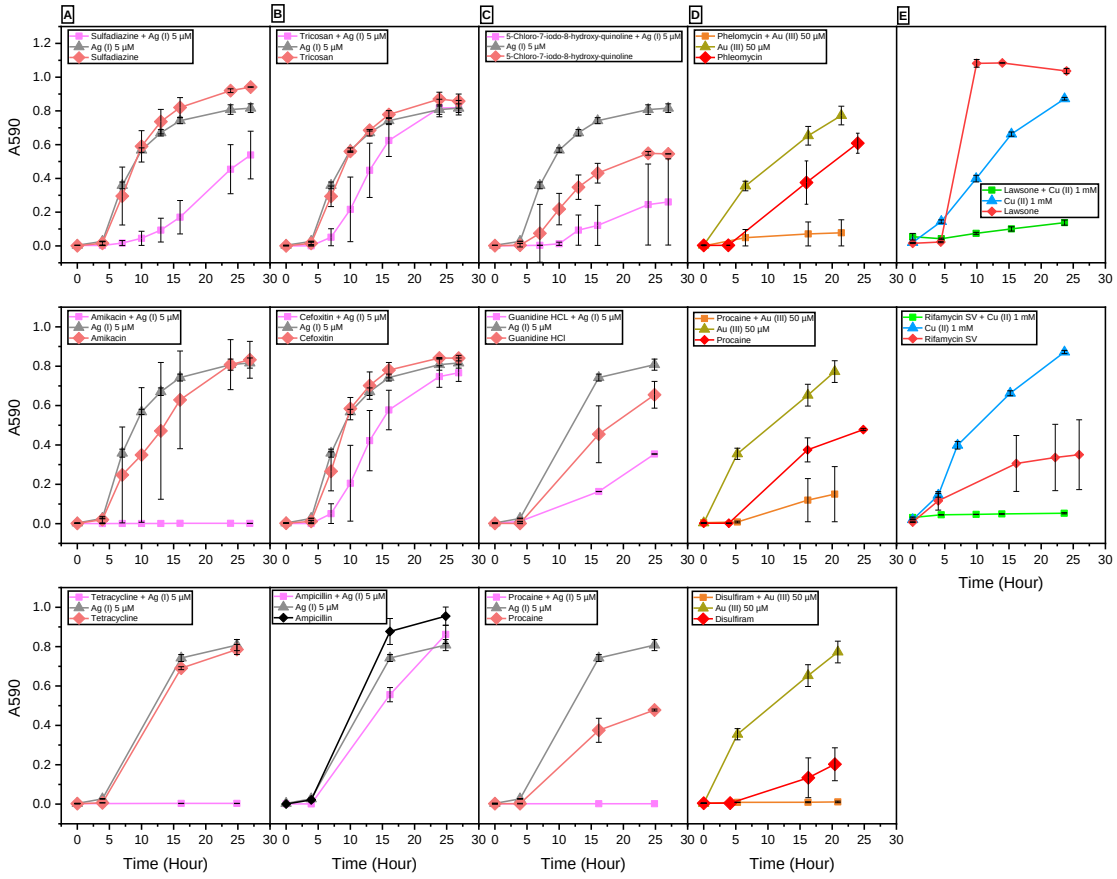

Figure 3.2. Selected growth curves of metal-biocide combinations. A: 24-hour growth curves of previously reported synergistic combinations of silver ions and antibiotics. B: 24-hour growth curves of additive combinations of silver ions and biocides. C: 24-hour growth curves of novel synergistic combinations with silver ions, discovered with this screen. D: 24-hour growth curves of gold ions with selected biocides. The combination was toxic, while *E. coli* grew on the individual gold ions or biocide. E: 24-hour growth curves of novel copper ions with selected antibiotics yielding synergistic inhibition of growth.

Several novel silver-biocide combinations that synergistically inactivated *E. coli* (Table 3.1.) and select 24-hour growth curves are shown (Figure 3.2.C) were discovered from this screening. These include silver with hydroxyquinolines, intercalators, phenothiazines, nitroimidazoles, macrolides, and aminoacyl hydroxamates, among others. Additional tests are needed to deduce if growth inhibition is due to the metal and biocide acting via similar or different mechanisms, or if a metal-biocide complex is responsible for reduced growth.

3.3.3. Cu (II)/Biocide Interactions.

Copper-biocide interactions that resulted in synergistic CDI values included mixtures with oxidizing agents and respiration ionophores and uncouplers (Figure 3.1, Table 3.1.). Novel biocide-copper mixtures discovered with this screen include copper with chlorodinitrobenzene, thioctic acid, iodonitrotetrazolium violet, fusidic acid, nordihydroguaiaretic acid, triazole, thiamphenicol, zwitterionic (lauryl sulfobetaine) detergents, anionic detergents (niaproof), menadione, and lidocaine. Selected growth curves were plotted (Figure 3.2.E.).

3.3.4. Au (III)/Biocide Interactions.

In this screen, toxic combinations were observed between gold ions and macrolides, guanidines, glycopeptides, polymyxins, and other individual chemicals (Figure 3.1., Figure 3.2.D). Gold ions with glycopeptides, polymyxins, macrolides, and the individual chemicals disulfiram (a purine analog), this salicylic acid, novobiocin, and chlorpromazine generated strongly synergistic (CDI < 0.1) effects. Novel combinations

uncovered here included those with macrolides, glycopeptides, and sodium channel blockers.

3.4. Discussion.

3.4.1. Rapid Screening of Metal Biocide Combinations with CDI.

The high-throughput screening validated published reports and resulted in new combinations of antimicrobials for future investigations. This high-throughput approach can be utilized to study biocide mixtures efficiently. The approach outlined includes (1) determining the minimum inhibitory concentration of Group IB metals with *E. coli*, (2) conducting a combinatory drug assay, (3) analyzing results for synergism using the coefficient of drug interaction, and (4) qualifying CDI values with growth curves for individual chemicals and the combination. This approach can function as the genesis of synergistic, additive, and/or antagonist investigations on MDR bacteria.

The selection of sub-lethal concentrations was important in the study of synergism to determine whether the toxicity was due to the mixture or antibiotic. Metal concentrations greater than the MIC would render results uninterpretable as there could not be a distinction between metal and biocide toxicity at concentrations beyond the metal MIC. To determine if there was a concentration trend, three increasing metal concentrations were selected, with the smallest 10-fold less than the greatest, non-toxic level.

3.4.2. Biocides with Silver Ions.

Silver's toxic characteristic is the basis for many combinatory studies with antibiotics. Previous studies have reported that silver activity was enhanced when used

with aminoglycosides, fluoroquinolones, cephalosporins, and fusidic acid among others.[214] The results from this chemical assay confirm these synergistic combinations and reveal new combinations including, those that act as chelating agents, DNA and RNA targeting compounds, fungicides, protein inhibiting or targeting, membrane targeting, and respiration inhibiting chemicals (Figure 3.1., Table 4.1.).

As a transition metal, silver can form complexes with heteroatoms, leading to a complicated mechanism of lethality, where the complex itself is toxic, or the molecule is retained internally, preventing efflux. However, it may be possible for complex formations to reduce toxicity (antagonism, CDI > 1.0) as was the case with Ag (I)-phenothiazine complex that inhibited the growth of several pathogenic microbes including *E. coli*, yet the complex was not as effective compared to the control (phenothiazine alone).[215] It is probable that antagonistic responses (Figure B.1.) could occur with some metal-biocide combinations due to complexation, reducing antimicrobial activity. Further investigation into the chemistry and mechanism of action of the silver metal combinations will be required to understand the extent of the synergism or antagonism to maximize toxicity.

3.4.3. Biocides with Copper Ions.

Though copper is a cofactor and essential nutrient in bacteria, excess intracellular concentrations are toxic to the cell. As a result, bacteria have evolved resistance mechanisms to maintain intracellular copper homeostasis and mitigate damage caused by excess copper. In excess, copper can damage macromolecules within the vicinity of the metal via oxidative stress or bind to essential proteins damaging multiple cellular

functions.[216] Copper may be exported under sublethal concentrations due to normal cell function, but added biocides such as ionophores/uncouplers reduce the resistance mechanism, increased the toxicity of the combinations, and prevent the export of Cu ions, resulting in synergism.

In combination with ionophores, uncouplers, and oxidizing agents, copper exhibited synergism, suggesting multiple methods of inactivation at play. Ionophores and uncoupling agents can disrupt energy systems in the cells, impacting essential resistance mechanisms such as efflux pumps that protect the cell from intracellular toxicity of compounds by exporting and decreasing toxic concentrations.[217] Synergism with oxidizing agents and copper ion is likely due to increased oxidative stress on the bacterial cell as copper itself is an oxidizing agent. Oxidizing agents may play multiple roles in increasing toxicity when applied with copper, including maintaining copper in the environmentally available form of Cu (II), preventing the export of the monovalent ion Cu (I) by CusCFBA, and forming complexes that increase toxicity by DNA damage.[218] It is probable that oxidizing agents and copper combinations result in dual oxidative stress toward the cell resulting in the synergism observed. Future work should be pursued into investigating concentrations of copper ions above MIC values in combinations with ionophores and uncouplers to observe possible toxicity and explore mechanisms of action.

3.4.4. Biocides with Gold Ions.

The least quantity of synergistic combinations was obtained with gold ions (Figure 3.2., Table 3.1.). This may be due to the lower toxicity of gold ions in the cell

compared to other metal ions (MIC_{90} of 50 μM Table B.1). Limited studies have evaluated gold ion combinations for antimicrobial purposes, possibly because of the economic limitations in utilizing precious metals. However, noteworthy synergism between biocides and gold ions should be explored as a possible "last resort" in treating severe infections.[219]

Gold acted synergistically with several macrolide combinations of the chemical assay (Figure 3.1.). Macrolides act by binding to the ribosomal subunit preventing protein synthesis.[202] Gold ions may also form complexes with these compounds, preventing recognition of the biocide and/or resistance mechanism, or perhaps gold adds additional stress by oxidation imbalance as reported more recently.[220] However, considering the high levels of antagonism observed (Figure B.1), it is also possible complexation of gold ions with the biocides can reduce toxicity by chemical alterations. Additional studies in gold organo-metallic structural and coordination chemistry will reveal if complexes are promising leads.

3.5. Conclusion.

In conclusion, the screening of synergistic combinations of soluble Group IB metal ions with biocides to inactivate *E. coli* was explored, confirming prior discovered synergistic silver, copper, or gold ion/biocide combinations while also discovering novel combinations. Results were reproducible when compared to studies that used conventional MIC, checkerboard, and time-kill tests reviewed in literature. Silver ions not only acted synergistically with antimicrobials but also with chelators and efflux pump inhibitors. Further results validated copper ion synergism with ionophores and oxidizing

agents. Lastly, gold ion synergy with macrolides and glycopeptides reveals a new direction in antimicrobial therapy. Because these findings support previous studies, the high-throughput method can be used as a preliminary screen to evaluate other combinations of antimicrobials, including those with radiation, nanomaterials, and plasmid curing agents. The result of the study lays the foundation for future exploration of more novel and potentially synergistic combinations of metal and biocides to reinstate obsolete antibiotics and other pharmaceuticals to combat MDR pathogens.

CHAPTER 4

SYNERGY AND ANTAGONISM OF GROUP IB METAL AND PHENOTHIAZINE COMPLEXES AND MIXTURES ON E. COLI

Graphical Abstract

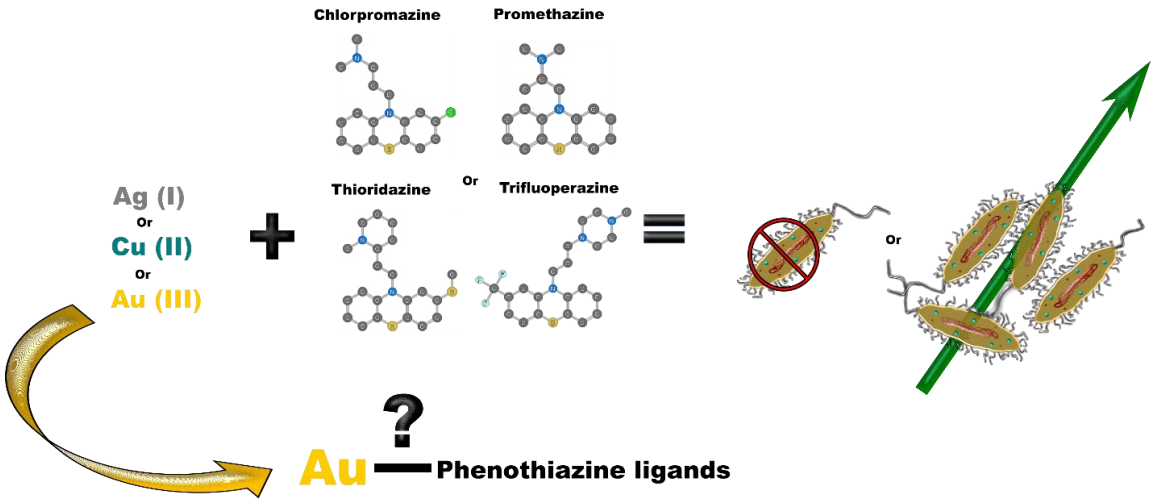

Abstract

Antibiotic-resistant bacteria are a concern to public health and the maintenance of microbial ecology. Novel approaches are required to combat multi-drug resistant bacteria such as *E. coli*. The phenothiazine class of drugs promethazine, trifluoperazine, chlorpromazine, and thioridazine, which act as efflux pump inhibitors, were mixed with either Cu (II), Ag (I), or Au (III) ions at various molar ratios of drug to metal to determine organometallic complexation and toxicity towards *E. coli*. The mole ratio method was applied to estimate the degree of complexation, providing the ligand-metal stoichiometry. UV-vis and FT-IR spectra confirmed complex formation between phenothiazines and Au (III) through λ_{max} peak shifts and the disappearance of sulfur bond peaks. Minimum inhibitory concentration and checkerboard assays were conducted to assess the toxicity and provide metrics to quantify synergism toward *E. coli*. Silver and copper ion and drug combinations produced synergistic results to varying degrees, in addition to trifluoperazine and Au (III). Complex formations were observed with Au (III) and promethazine, trifluoperazine, chlorpromazine, and thioridazine at various concentrations and were tested for antimicrobial capabilities to *E. coli*. The results suggest that phenothiazine/silver, phenothiazine/copper, and the trifluoperazine/gold dual combinations may act as synergistic antimicrobial agents toward *E. coli*.

4.1. Introduction.

Antibiotic-resistant bacteria are a worldwide problem to public health and the maintenance of both natural and engineered environmental microbial communities. Several options of antimicrobial agents are becoming increasingly limited due to the increase of multidrug resistance in microorganisms. Drugs like phenothiazines have been pharmacologically repurposed for their antimicrobial capabilities. Phenothiazines (PTZ) was originally designed and commonly prescribed as psychotropic drugs.[221] The popularity of these drugs declined due to strong adverse side effects in humans, but studies have been conducted to understand the biological activity of phenothiazines in the treatment of pathogenic infections.[222] The phenothiazine class of psychotropic drugs has a fused tricyclic phenothiazine ring scaffold.[223] This class of chemicals includes promethazine (PMZ), trifluoperazine (TFPZ) chlorpromazine (CPZ), and thioridazine (TDZ) which have varied functional groups attached at the 2 and 10 positions (Figure 4.1.). Phenothiazines such as chlorpromazine, trifluoperazine, and thioridazine have shown antimycobacterial and antimicrobial properties as efflux pump inhibitors (EPIs).[222, 224] Studies reveal that thioridazine in small dosages can effectively treat tuberculosis caused by *mycobacterium tuberculosis* in the lungs.[225] Antibacterial properties of different phenothiazines have also been reported for both gram-positive and gram-negative bacteria. However, reported concentrations were values higher than the highest plasma concentration achievable. This would make phenothiazines impractical as antimicrobials alone, but promising results in other studies suggest synergistic applications may be possible.[222]

A variety of gram-negative bacteria may become susceptible to antibiotics despite previous drug resistance.[226] The multi-drug resistance (MDR) can be primarily credited to the over-expression of efflux pump systems in bacteria.[226] Phenothiazines inhibit the transport of calcium reducing the energy driving force of the cells that power the efflux pumps systems in MDR bacteria.[226] Through inhibition of the efflux pump systems, phenothiazines may allow previously void antibiotics to effectively treat resistant bacteria.

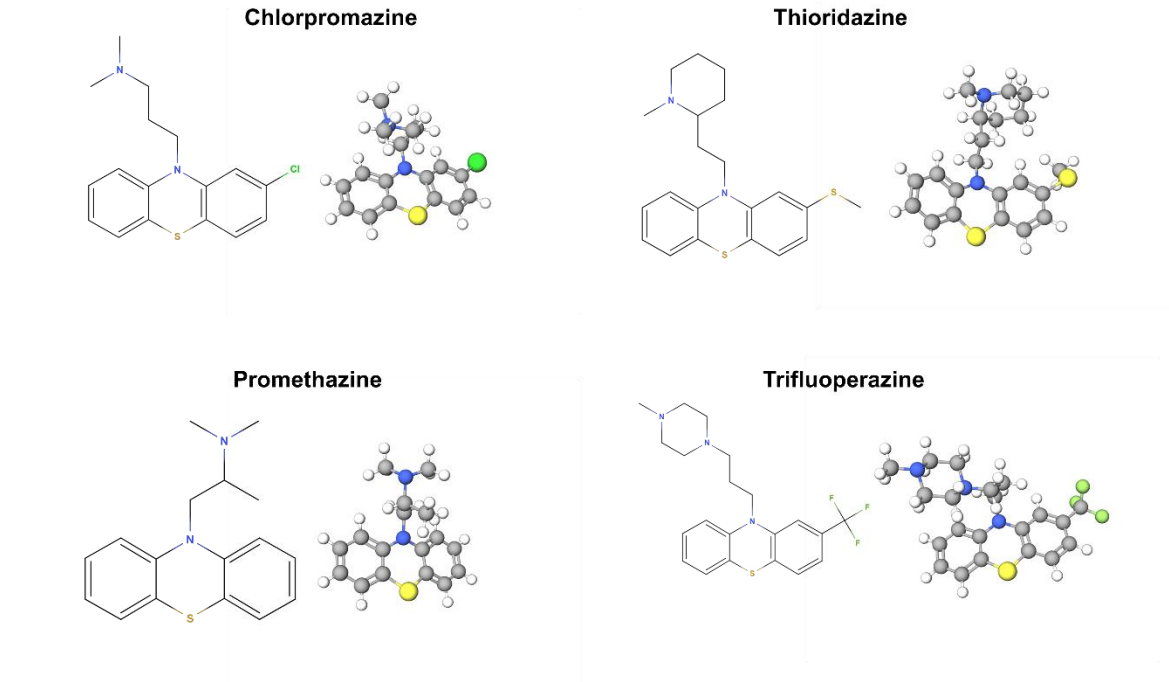

Figure 4.1. 2D and 3D Molecular structures of the PTZs, CPZ, TDZ, PMZ, and TFPZ. The bright green dots represent chlorine atoms, blue dots represent nitrogen atoms, the lime green dots represent fluorine atoms, and the yellow dots represent sulfur atoms.

Metal ions of copper gold and silver have been studied for decades for their antimicrobial properties [227-229]. Cu (II), Ag (I), or Au (III) ions exhibit toxicity to bacteria in a variety of ways, including the removal of electrons from the respiratory transport train of bacterial cells, free radical production, or enzyme inhibition leading to added

oxidative stress.[230-232] The synergistic capabilities of phenothiazine coupled with antimicrobial properties of silver metal ions have been studied.[215] The results from this study on phenothiazines may suggest a more appropriate action would be to investigate phenothiazines as synergistic compounds.

Synergism scoring was assessed and compared by utilizing the Bliss, Loewe, and ZIP methods. Conflicting arguments arise when quantifying synergistic combinations of dose-response and the scientific community has not come to a consensus on models that can be utilized for assessing the synergism of two or more drugs applied together.[233] The Loewe additivity model utilizes the dose equivalence principle (DEP) and defines the expected effect of drug combinations as if a drug was combined with itself.[233-234] the Bliss independence model utilizes the multiplicative survival principle (MEP) and defines the effects of individual drugs in a combination as mutually non-exclusive competing events.[233, 235] The zero-interaction potential (ZIP) utilizes the advantages of Bliss and Loewe models and assumes that two non-interacting drugs will have negligible changes to their individual dose responses.[236] Combination index (CI) is also frequently used and heavily cited to quantify synergy. CI is based on the Loewe method, utilizing isobologram analysis (based on the Michaelis-Menten, Hill, Henderson-Hasselbalch, and Scatchard equations), quantifying syngersim.[213, 237]

To better understand the role of synergistic binding of phenothiazine with metal ions, PMZ, TFPZ, CPZ, and TDZ were prepared with either Cu (II), Ag (I), or Au (III) ions at various molar ratios of drug to metal. Mixtures and complexes were observed, and toxicity was assessed with checkerboard assays to optimize dosages to inhibit wild-type

E. coli. The usage of synergism models for dual drug applications is discussed and discrepancies between models are explored based on the chemical properties of the tested compounds. For the first time to the knowledge of this study, Au (III) and promethazine, trifluoperazine, chlorpromazine, and thioridazine complex formations were observed and tested for antimicrobial capabilities to *E. coli*.

4.2. Materials and Methods.

4.2.1. Chemical Reagents.

Promethazine, trifluoperazine, chlorpromazine, thioridazine, gold chloride, copper sulfate, and silver nitrate were commercially obtained as salts from Millipore Sigma. The phenothiazine and metal ionic solutions were prepared in nanopure DI water using volumetric flasks and stored in wrapped containers at 4°C to prevent photoreactions.

4.2.2. Bacterial Media Preparation.

The *E. coli* strain used was wild-type W3110.[238] Bacterial strains were grown in Luria-Bertani (LB) agar from stocks. Liquid cultures of W3110 were prepared in LB media as described.[239] Modified LB media was prepared as chloride-free to limit AgCl precipitation.

4.2.3. Organo-Metallic Chemistry.

4.2.3.1. Mole-Ratio Method.

UV-vis absorbance spectroscopy was conducted using a Biotek Synergy H1 multi-mode reader. UV-vis scans were performed across a 96-well UV plate using wavelengths from 230 nm to 700 nm at 2 nm increments, prepared with 2-fold dilutions of the mixtures to test various concentrations. Phenothiazines were initially mixed with

either Cu (II), Ag (I), or Au (III) ions at 32 mM of metal ion up to 1.6, 1.07, 1.44, 1.26 M of PMZ, TFPZ, CPZ, and TDZ in a 96-well plate. Additional scans of Au (III) and the PTZ were performed, focusing on molar ratios of 0.5, 1, 1.5, 2, 2.5, 3, 3.5, and 4 of PTZs to Au (III), at either 150 mM for CPZ, TDZ, and TFPZ or 100 mM Au (III) for PMZ, along with Au (III) and the PTZ alone. The mole ratio method was used to determine the stoichiometry of metal-ligand complexes of Au (III) and the respective phenothiazine complexes.[240]

4.2.3.2. Fourier-transform Infrared Spectroscopy (FT-IR).

Samples were prepared by dispensing 10 µL at a time of the 2:1 ratios of 20 mM of PTZ to 10 mM Au (III) solutions onto the center of a glass microscope slide. Slides were prepared while on a hotplate set to 70 ºC to assist with solvent evaporation. Additional slides of the PTZ at 20 mM were prepared. Dispensing of the corresponding solution on the slides was repeated until a sufficient layer (> 0.5 cm x 0.5 cm) of the coating was obtained. Samples were processed using a Bruker IFS66 V/S FT-IR system installed with a mercury cadmium telluride detector and a KBr beam splitter equipped with a diamond attenuated total reflectance module. Indexes of N-C and S-C bonds were used to analyze potential complexation sites of Au ions with the PTZ.

4.2.4. Microbiology.

4.2.4.1. Minimum Inhibitory Concentration Assay.

Minimum inhibitory concentration (MIC) assays were run on metal ions and phenothiazines by the microtiter broth dilution method. The *E. coli* W3110 was pre-cultured in LB media or chloride-free LB and seeded to 5 x 10^5 CFU/mL, final

concentration in a two-fold serial-dilution, down seven rows of a 96-well plate, of silver nitrate, copper sulfate, and gold chloride. Plates were read (OD_{600}) after 16 hours of incubation at 37 ºC and the MICs were determined. The same procedure was conducted for the PTZs.

4.2.4.2. Checkerboard Assays.

Checkerboard assays were run on PTZs with the metal ions. Bacteria were pre-cultured in 5 mL of LB media or chloride-free LB, to prevent silver chloride precipitation. Cultures were seeded to 20 mL of fresh LB media to obtain a concentration of $1.33x10^5$ cells/mL. The PTZs were serial-diluted two-fold across the first ten columns of a 96-well plate by dispensing and mixing 25 µL of corresponding PTZ to 25 µL of nanopure autoclaved DI water. Whereas the metal solutions were serial-diluted two-fold separately in centrifuge tubes. The metal solutions were then dispensed across 7 rows of the plate adding 25 µL of metal per well. Column 12 served as positive control by having only bacteria and autoclaved water. Wells H11 and H12 were used as negative control having only autoclaved water and LB media with no bacteria. The bacterial solution was then applied to the dilutions (94 of the wells) for a final concentration of 10^5 cells/well and a total in-well volume of 200 µL. Plates were read (OD_{600}) after 16 hours of incubation at 37 ºC using the Biotek Synergy H1 reader.

4.2.4.3. Toxicity, Synergism, Antagonism, and Statistical Analysis.

A comparison of synergism was determined by the zero-interaction potency model (ZIP), Bliss Independence, and Lowe Additivity methods. The open-source software SynergyFinder was used to analyze the synergism or antagonism of the metal

ions and PTZ mixtures or complexes from the checkerboard assays.[241] The software was used to generate and analyze response curves using log-logistic 4-parameter curve fittings and calculate the synergy scores based on the three methods mentioned. One-way ANOVA followed by Fisher's least significant difference tests were performed to determine statistically significant differences between bacterial growth conditions using Origin 2018 software.

4.3. Results and Discussion.

4.3.1 Metal - PTZ Complexes and Mixtures.

Promethazine (PMZ), trifluoperazine (TFPZ) chlorpromazine (CPZ), and thioridazine (TDZ) were initially mixed with either Cu (II), Ag (I), or Au (III) ions undergoing two-fold dilutions on a 96-well plate. Initial UV-vis scans were conducted from 230 nm to 700 nm. No UV-vis shifts were observed with mixture preparation of Cu (II) and Ag (I) and the phenothiazines. Scans showed peak shifts for all phenothiazine and Au (III) parings. Molar ratios of 0.5 to 4 at 0.5 increment phenothiazine to Au (III) solutions were prepared for further analysis. UV-vis spectroscopy scans of the mixtures were performed at a range of 230 to 700nm at 2 nm increments. The spectra of Au (III) and all PTZ mixed solutions exhibited varied shifts in the UV-vis spectrum. All tested ratios exhibited peak shifts with Au (III). Selected 1:1 ratio spectra for the PTZs and Au (III) can be seen in Figure 2. PMZ, TFPZ, and TDZ exhibited red shifts in the UV-vis spectrum when combined with equal molar concentrations of Au (III). Chlorpromazine exhibited a blue shift in the UV-vis spectrum.

Trifluoperazine and thioridazine exhibited bathochromic shifts in the UV-vis spectrum when combined with equal molar concentrations of Au (III). Bathochromic shifts in the spectra can be associated with the addition of metal ions to the phenothiazines due to an effective intramolecular charge transfer [242]. The nitrogen and sulfur substituents on the trifluoperazine and thioridazine structures may induce an electron-donating effect and transfer the electron density toward the Au (III) causing the red shifts observed in the Au(III) and PTZ complexes.[243-246]

Chlorpromazine and promethazine exhibited hypsochromic shifts in the UV-vis spectrum when combined with Au (III). Hypsochromatic shifts are typically associated with ridgidochromism of the structure of the metal-ligand complex [247-249]. The Au(III) and CPZ complex may induce an intense lowest energy metal to ligand charge transfer absorption bands as apparent with the red shifts observed [250]. The bulkier structure of CPZ and PMZ may result in a rigid structure when binding to the Au (III) resulting in the hypsochromatic shifts observed.

4.3.2. Mole-Ratios.

The mole ratio method was used to determine the stoichiometry of metal-ligand complexes of Au (III) and the respective phenothiazine complexes [240]. The ratios of ligand to metal varied increasingly, holding the metal concentration constant at either 150 mM for CPZ, TDZ, and TFPZ or 100 mM Au (III) for PMZ. The major peaks in the UV-vis spectrums of the respective phenothiazine alone (Figure 4.2.) were selected as wavelengths to scan the mixtures selected for the mole ratio method. At lower ratios, the absorbance increases as more respective phenothiazine bind to the Au (III). The

absorbance of the respective phenothiazines at various ratios of ligand to metal was plotted (Figure 4.3.). The point where the two lines intersect is the ligand-binding ratio. The ligand-binding ratios are summarized in Table 4.1.

The mole-ratio method can be used to understand the stoichiometry of the complex formation between the Au(III) and the respective phenothiazine.[251] At high ratios, all metal-binding sites are occupied in theory, and no further absorbance increase is observed. Each phenothiazine and Au (III) complex exhibited two major peaks in the UV-vis spectra at various mole ratios tested, corresponding to a pi-bond alteration from metal binding in the low-UV range and color formation in the visible range (Figures C.1-4.). Chlorpromazine and trifluoperazine complexes yielded the most consistent binding ratio for both major peaks tested. Thioridazine and promethazine had variations in the binding ratios of the major peaks evaluated.

Gold (III) ion forms complexes with square-planar geometry and has a coordination number of 4.[252-253] Ligands that may react with Au (III) forming complexes are typically subject to gold-trans-ligand bonds; strongly electron-donating ligands form weak gold-*trans*-ligand bonds, ligands with a weak electron donor strength form strong gold-*trans*-ligand bonds.[254-255] The complexation that is occurring may be from the electron-withdrawing groups associated with the PTZ molecules binding to the Au (III) in *trans*-location.

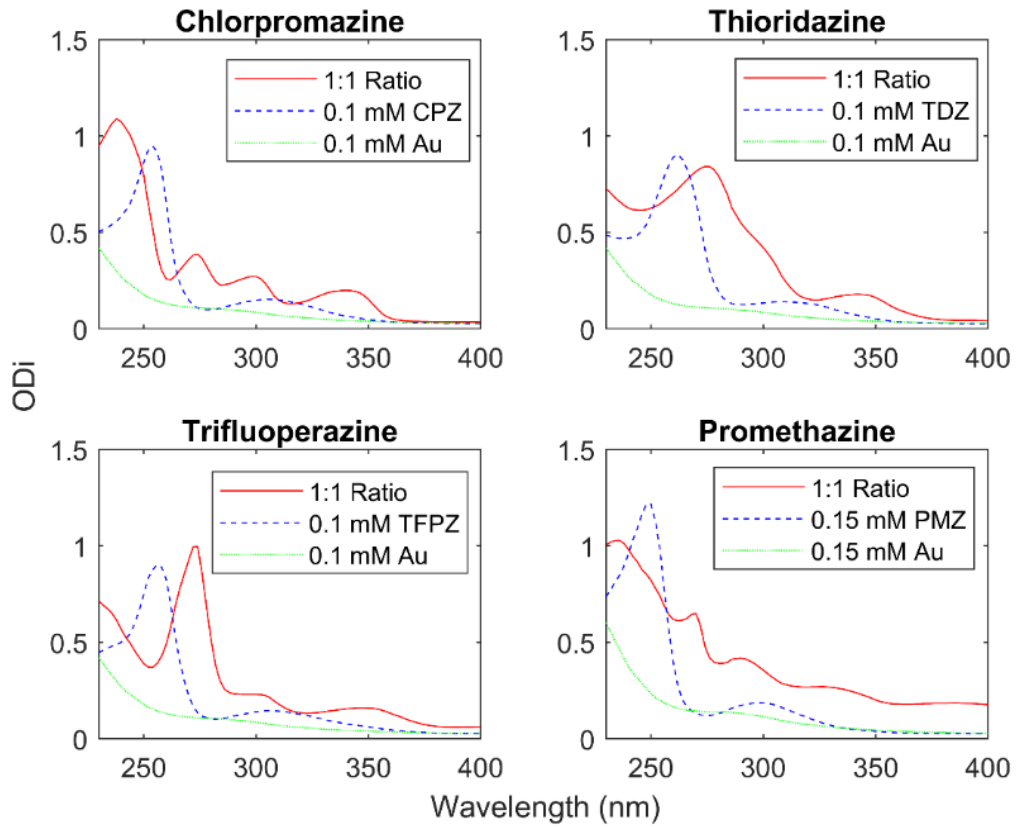

Figure 4.2. Selected UV-vis absorption spectra of phenothiazine and Au (III) complexes at 1:1 molar ratios. The dashed lines represent the individual molar concentrations used for the phenothiazine and the Au (III) in the complex solution. Solid line represents the ratio. Dotted line represents the Au (III) alone.

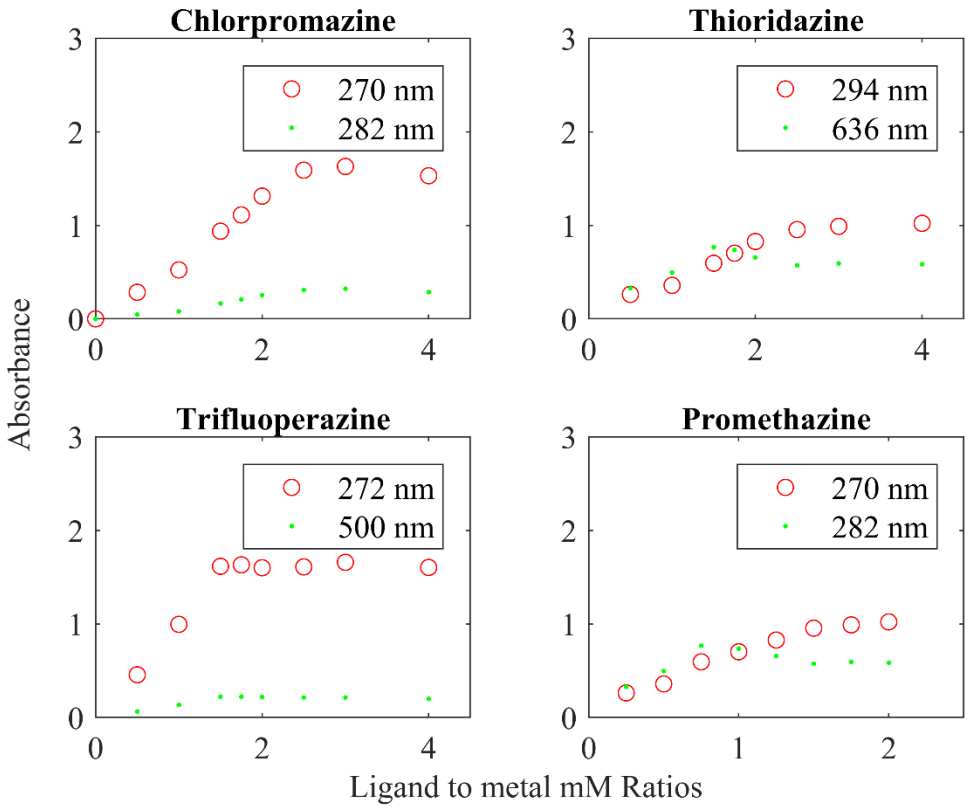

Figure 4.3. Mole ratios of phenothiazine complexes at select peaks. Major peaks were selected for determining the complex ratio.

Table 4.1: Ligand to metal binding ratios for phenothiazine and Au (III) complexes. Values are calculated from intersectional points from where the two lines of the corresponding scans meet (Figure 4.4.).

	Wavelength (nm)	Line intersection PTZ/Au Ratio
Chlorpromazine	270	2.21
	282	2.21
Thioridazine	294	2.26
	636	2.59
Trifuoperazine	272	1.52
	500	1.53
Promethazine	270	0.98
	282	0.78

Figure 4.4. shows the FT-IR-spectra of 2:1 molar ratio of CPZ, PMZ, TDZ, and TFPZ with Au (III). A weak band at 2550 cm^{-1} corresponds to the presence of the S-H group in the phenothiazine ring structure of CPZ, PMZ, TDZ, and TFPZ. The S-H band was not observed in the spectra of the PTZ, upon the addition of Au (III). Prominent bands associated with N^{+3}-H stretching is also visible on the spectra around 3,000-3,500 cm^{-1}. The decrease in the S-H peak in all the PTZ structures confirms interactions of Au (III) with an electron-withdrawing group producing the peak shifts in the UV-vis spectra, suggesting S-Au coordination.[256] These results provide evidence that a metal-ligand complex structure has formed between CPZ, PTZ, TFPZ, TDZ and TFPZ, and Au (III) at various molar ratios (Table 4.1).

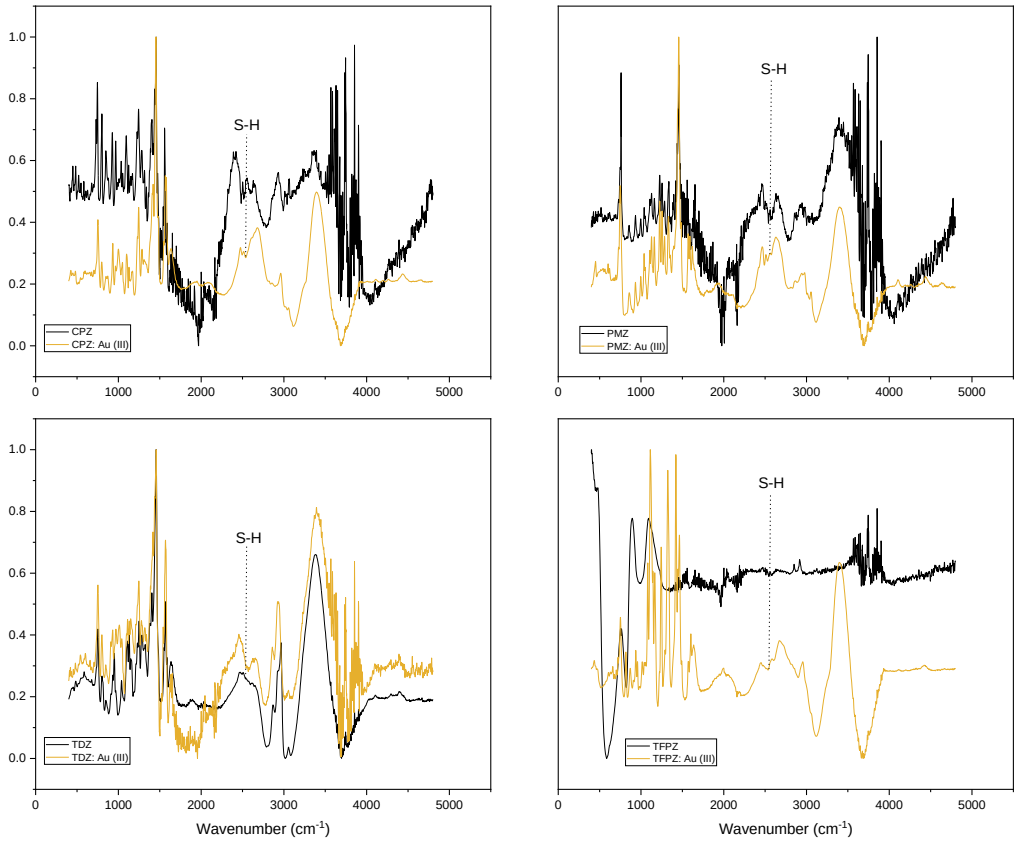

Figure 4.4. FTIR spectra of PTZ/Au (III) complexes at a 2:1 ligand to metal ratio.

4.3.3. Toxicity of the Metal and PTZ Mixtures or Complexes.

The MIC of all individual phenothiazines and metals in *E. coli* was determined by the microtitre broth dilution method (Table D.1.). Checkerboard assays were performed to evaluate toxicity to the bacterial cells and synergistic potential. Various concentrations of two-fold dilutions of phenothiazine to metal were tested yielding MIC_{90} under various drug to metal combinations. The Ag (I), Cu (II), and Au (III) exhibited toxicity in combination with different phenothiazines to varying levels.

Significant increased or decreased growth, and non-significant tested combinations, can be seen in Table 4.2. Lower concentrations of Ag (I), Cu (II), and Au (III) in combination with the highest concentrations of PTZ tended to result in a significant (p-value < 0.05) decrease in bacterial growth in comparison to the respective application of the metal ions alone. The higher concentrations of Ag (I) and Cu (II) applied dually with nearly all PTZ concentrations tended to result in no significant difference (p-values > 0.05) in bacterial growth. Mid to high Au (III) concentrations applied with all PTZ had instances of significantly increased growth of bacteria in comparison to the application of the respective Au (III) concentrations alone. Selected relative growths after 16 hours of incubation can be seen in Figure 4.5.

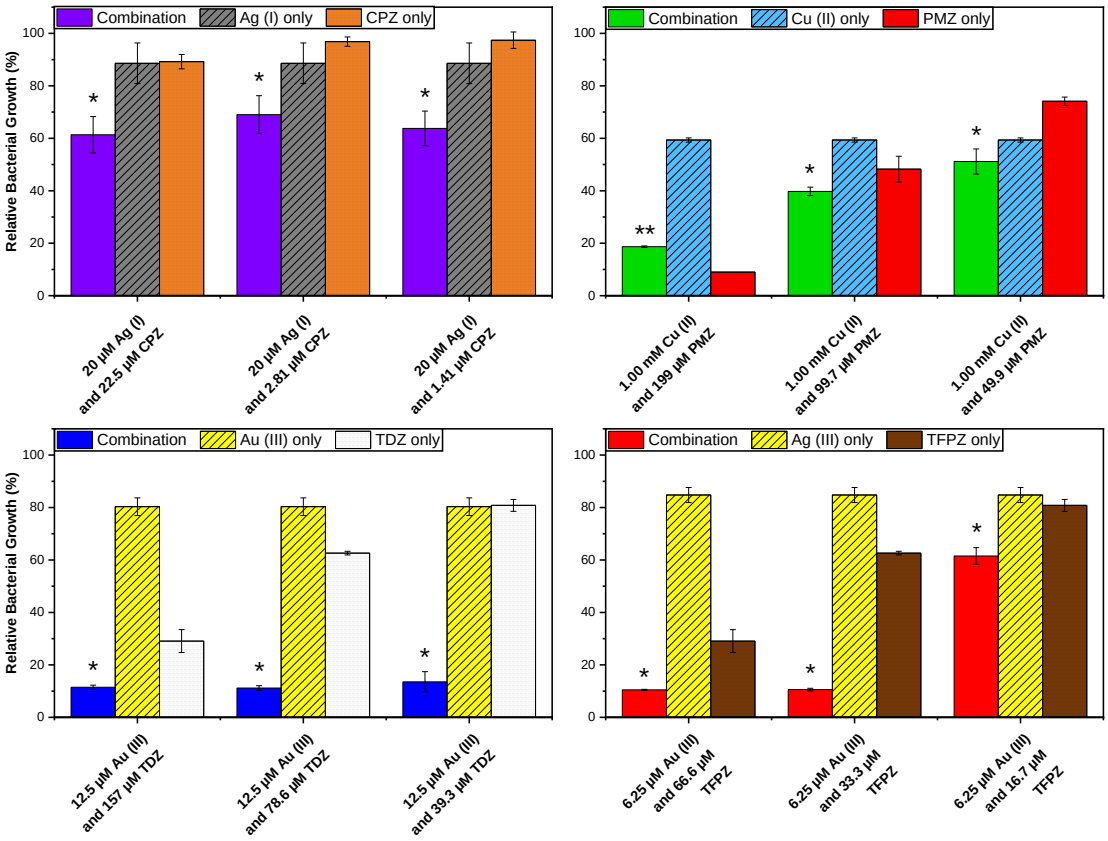

Figure 4.5. Selected relative growths after 16 hours of incubation of Ag (I), Cu (II), and Au (III) applied with either CPZ, PMZ, TDZ, or TFPZ resulting in a significant (p-value < 0.05) decrease* in relative *E. coli* growth in comparison to application of both PTZ and metal concentrations individually or significant (p-value < 0.05) decrease of growth in comparison to the application of at least **one of either PTZ or metal concentrations alone. Relative growth is based on OD_{600} in comparison to control of bacteria grown without chemical addition.

Table 4.2. Combinations of concentrations of PTZ and metal ions result in an increase or decrease in *E. coli* growth relative to the metal concentration alone. The green downward triangle represents a statistically significant decrease in *E. coli* growth (inhibition). Red upward triangles represent a statistically significant increase in bacterial growth.

		CPZ										PMZ										TDZ										TFPZ									
	μM	180	90.1	45.0	22.5	11.3	5.63	2.81	1.41	0.704	0.352	199	99.7	49.9	24.9	12.5	6.23	3.12	1.56	0.779	0.390	314	157.2	78.6	39.3	19.7	9.83	4.91	2.46	1.228	0.614	133	66.6	33.3	16.7	8.3	4.16	2.08	1.04	0.520	0.260
Ag (I)	40																					▲																			
	20	▼	▼	▼	▼	▼	▼	▼	▼	▼	▼	▼	▼	▼	▼	▼	▼	▼	▼	▼												▼	▼	▼							
	10																																							
	5	▼	▼	▼								▼	▼										▼	▼																	
	2.5	▼	▼	▼								▼	▼									▼	▼	▼								▼	▼	▼							
	1.3	▼	▼	▼								▼	▼									▼	▼	▼								▼	▼	▼							
	0.625	▼	▼	▼								▼	▼									▼	▼	▼								▼	▼	▼							
Cu (II)	4000															▼	▼	▼																							
	2000																																							
	1000	▼	▼	▼								▼	▼	▼								▼	▼	▼								▼	▼	▼							
	500.0	▼	▼	▼								▼	▼	▼								▼	▼	▼								▼	▼	▼							
	250.0	▼	▼	▼								▼	▼	▼								▼	▼	▼								▼	▼	▼							
	125.0	▼	▼	▼								▼	▼	▼								▼	▼	▼								▼	▼	▼							
	62.50	▼	▼	▼								▼	▼	▼								▼	▼	▼								▼	▼	▼							
Au (III)	100		▲										▲	▲									▲										▲								
	50		▲										▲	▲	▲	▲	▲							▲												▲					
	25		▼									▼	▼					▲				▼	▼		▲																
	12.5	▼	▼									▼	▼									▼	▼			▲	▲	▲				▼	▼	▼	▼						
	6.3	▼	▼									▼	▼									▼	▼	▼								▼	▼	▼	▼			▲		▲	
	3.1	▼	▼	▼								▼	▼									▼	▼	▼	▼							▼	▼	▼							
	1.56	▼	▼									▼	▼									▼	▼	▼								▼	▼	▼							

4.3.4. Synergism and Antagonism of Metal-Phenothiazine Combinations.

A comparison of synergism was determined by the zero-interaction potency model (ZIP), Bliss Independence, and Lowe Additivity methods. The open-source software SynergyFinder was used to determine the synergy scores for the checkerboard assays.[241] The software was used to plot dose-response curves using log-logistic 4-parameter curve fittings. The average synergy scores for the various conditions for each phenothiazine and metal combination tested (Table 4.3.) were calculated.

Table 4.3. Dual drug scoring from three methods of synergism calculations. Bliss and ZIP >1 = synergism, <1 = antagonism; Loewe <1 = synergism >1 = antagonism.

Metal Ions	Phenothiazines	Bliss	Loewe	ZIP
Ag (I)	CPZ	6.461	-2.628	6.792
	PMZ	-1.543	-11.602	0.198
	TDZ	0.216	3.237	1.165
	TFPZ	1.538	-0.834	3.25
Cu (II)	CPZ	1.097	-5.541	1.166
	PMZ	-0.888	-7.538	-0.266
	TDZ	0.782	-7.085	1.276
	TFPZ	0.782	-5.618	1.277
Au (III)	CPZ	-13.628	-16.507	-10.726
	PMZ	-11.131	-20.079	-11.289
	TDZ	0.782	-10.113	1.275
	TFPZ	-1.456	-14.663	0.89

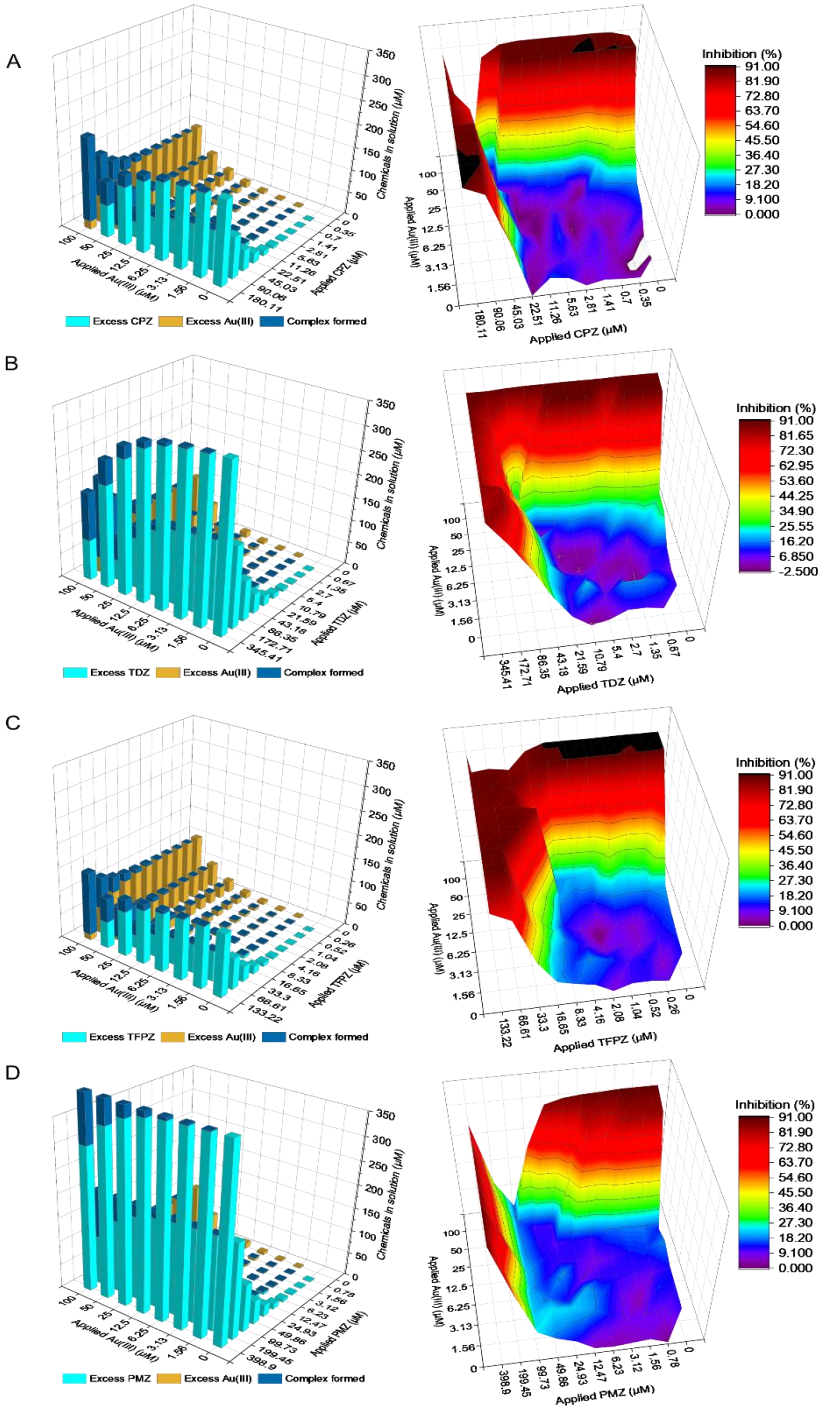

Figure 4.6 Au-PTZ complex, excess Au (III), and excess PTZ in solution of checkerboard assays (left). Surface plots showing inhibition of bacterial growth (right). A is chlorpromazine, B is thioridazine, C is trifluoperazine, D is promethazine.

Silver and all phenothiazines tested resulted in high ZIP synergy scores suggesting high levels of synergism between the drug combination toward *E. coli*. Bliss scores also suggested synergism with Ag (I) and all the phenothiazines. Loewe had contradicting antagonistic results for Ag (I) and CPZ and PMZ compared to Bliss and ZIP synergy methods. The Cu (II) synergy scores agreed for antagonism for all phenothiazines tested using the Loewe and ZIP methods. The Bliss method confirms all PTZ tested except for PTZ which scored antagonistically. The Au (III) and TFPZ complex ZIP scores suggested synergism. Gold complexes with CPZ, THZ, and PMZ all showed antagonism toward the ZIP method. The Bliss method scores suggested all PTZ combinations with Au (III) were antagonistic. The Loewe scores suggested all Au (III) and PTZ complexes were synergistic.

Silver ions have well-established antimicrobial properties and have been extensively studied with more research in the last decade going toward nanoparticle silver.[230] The primary mechanism of Ag ion toxicity is DNA and RNA damage by binding and condensing preventing transcription and replication and limiting protein synthesis and cell division.[229, 257] Additionally, silver ions, and silver NPs have been known to generate reactive oxygen species (ROS) which can damage and destroy bacteria cells.[258] The primary methods of action from CPZ are at the cellular membrane, causing elongation and then filamentation of the cell as well as disruption of the electron transport systems by reducing superoxide dismutases (SOD) that detoxify the cells from superoxide radicals.[259-260] Furthermore, CPZ is both a substrate and inhibitor of the efflux pump AcrB protein found in *E Coli.*, which is responsible for RND multi-drug antibiotic

resistance [261]. Bliss and ZIP methods agreed for synergism compared to an antagonistic score for the Loewe method. The Loewe model works as an additivity model from the concept that the compounds in question do not interact with themselves and both compounds can be interchanged if they have the same effect.[262] The Bliss model assumes the individual compounds have independent events of actions when applied simultaneously.[241, 262] The ZIP model assumes that two non-interacting drugs will have negligible changes to individual dose responses.[236] The ZIP model utilizes advantages from both models and is appropriate for high-throughput screening of compounds.[236] The discrepancies in the Loewe synergy scores can be attributed to the indirect interactions of Ag (I) and CPZ. Silver's mode of action may cause a reduction in *E. coli's* ability to detoxify from CPZ causing the dose experienced by the bacterium to differ. The assumption that the Loewe model incurs about the additive activity of the doses of the compound cannot be made in this case. TDZ synergy scores suggested synergism across all models.

TDZ has been shown to act as antimicrobial and antiplasmid toward *E. coli*.[224, 263] Additionally, TDZ can inhibit RND efflux pumps leading to a decrease in biofilm formations.[264-265] The toxicity of Ag (I) and TDZ mixture may be attributed to additive toxicity to the cell. All three models showed synergism in TFPZ and Ag (I) mixtures. TFPZ is known to inhibit calmodulin, a calcium-binding protein that is essential to cellular processes such as cell cycle and cell division.[266-267] However, *E. coli* is much less sensitive to the toxicity of this compound compared to other types of microbes.[268] This may explain the higher synergy scores across all models tested.

The Ag (I) and PMZ mixtures showed synergism for the Bliss and ZIP methods but antagonism for Loewe. PMZ can inhibit major efflux pumps and alter membrane permeability in bacterial cells [269]. Additionally, PMZ can act as an antiplasmid agent.[270-271] Similar to the case of CPZ, Ag (I) may be indirectly influencing the dosage voiding the assumption for the Loewe method.

Copper is known to be both an essential nutrient acting as a cofactor for many biochemical reactions, and a toxic molecule to the cell of *E. coli*.[272] Copper is environmentally available as Cu (II) under aerobic conditions but Cu (I) is the predominant form that is utilized for metal homeostasis in bacteria.[231] Electrons from respiratory chain components are utilized in Cu (II) reduction Cu (I).[273] Additionally, copper is involved in free radical superoxide formation.[227, 274-275] The Cu (II) and CPZ, TDZ, and TFPZ mixture combinations suggested synergism based on all three models. Cu (II) and PMZ mixtures were synergistic for the Loewe and ZIP models but antagonistic for the Bliss model. The ZIP score reported is the expected response matching the effect as if the individual drugs did not influence the toxicity of one another.[241] The ZIP score for Cu (II) and PMZ is not very synergistic based on the model criteria for synergism and antagonism. This may be reported as synergistic based on overestimates from the calculations of the model. The Loewe method has Cu (II) and PMZ combination very synergistic based on the criteria and based on its additive effect of treating the individual compounds as if they were one single drug and may overestimate the synergism as Cu (II) alone is highly toxic to *E. coli.*

The largest discrepancies between the three methods were in the Au (III) and PTZ complexes. Gold ions have been often tested as complexes with other biocidal compounds and are relevant to microbial toxicity of Gold NPs.[228, 232] In aquatic systems Au (III) has been shown to inhibit the growth of bacteria, algae, and euglena [276]. Au (III) is toxic to *E. coli* by creating an imbalance of the bacterium's oxidative status by decreasing intracellular thiol levels that increase superoxide concentrations and facilitating the production of SOD enzymes [220]. The Au (III) and CPZ, TDZ, TFPZ, and PMZ complexes were all antagonistic based on the Bliss method, while Au (III) PTZ complexes were synergistic in the Loewe model, and CPZ, TDZ, and PMZ were antagonistic for the ZIP model while TFPZ was synergistic.

The underlying discrepancies are most likely due to the base assumptions of each model. The ZIP method expects the response to correspond to the fact that the individual drugs do not specifically affect the drug response potency of each other [241]. Complex formation between Au (III) and all the PTZs tested would null this assumption as complex formation would change the compound making the bioavailable gold and phenothiazine less than what the bacterium was initially dosed with. The confirmed complex formation would explain a third compound which could vary the results of the two-drug run of all three methods to calculate synergism. The complex calculations from the mol-ratios can be used to calculate excess phenothiazine and remaining Au (III) in the wells across the checkerboard assays.

When addressing synergism, models with base assumptions that compounds will not interact have the potential to misdirect the discovery of novel chemotherapies for

MDR bacteria. Studies involving dual application of compounds require an initial understanding of the chemical interactions the compounds may have before dual application for bacterial inactivation. The complexation occurring between Au (III) and the PTZ reduces the actual ionic concentrations to which the bacteria would be exposed. This makes the utilization of the models to quantify synergism challenging for compounds that may have initial reactions leaving the test conditions with unintentional quantities of drug combinations (i.e. metal, ligand, and complex) in which different models that were initially utilized may need to be applied or developed. The scientific community needs to come to a more standardized procedural method of testing for synergism from the usage of 2 or more antimicrobial compounds applied simultaneously. Methods should include the initial study of the biological and chemical interactions which may influence bioavailable concentrations of test compounds altering the true dose-response curve. Additionally, the utilization of robust standardized models that can accommodate multiple drug applications with various levels of interaction between drugs and between bacterial cells and drugs would allow for the standardization of multiple drug testing in drug applications for MDR bacterial inactivation.

4.4. Conclusion.

In this study, the phenothiazine class of drugs promethazine, trifluoperazine, chlorpromazine, and thioridazine, which act as efflux pump inhibitors, were mixed with either Cu (II), or Ag (I), or Au (III) ions and applied for *E. coli* inactivation. Ag (I) and Cu (II) drug combinations produced synergistic inhibitions to varying degrees. The TFPZ and Au (III) combinations were synergistic with *E. coli*.

There was toxicity and increased synergism, particularly with Ag (I) and Cu (III) that may have occurred because of the inhibition of major transporters that provided relief from the environmental stressors. Au (III) complexation formation with the PTZ may inhibit the irreversible binding of the EPIs to the efflux pumps and limit toxicity. This suggests that the changes in substrate chemicals may reduce toxicity as the efflux pump no longer recognizes the EPI. The toxicity observed may be associated with increased loadings of PTZ and metal respectively. The results of this study suggest that phenothiazine/silver, phenothiazine/copper, and the trifluoperazine/gold dual combinations may act as synergistic antimicrobial agents toward *E. coli*. Future studies should refine the complexation process and purify compounds to ensure synergism is from the novel complex and not from excess un-complexed Au (III) or PTZ.

CHAPTER 5

MEMBRANE PROTEOMIC ANALYSIS REVEALS ENDOCRINE-DISRUPTING CHEMICALS INDUCE ANTIBIOTIC-RESISTANCE TOWARD KNOWN BIOCIDES

Graphical Abstract

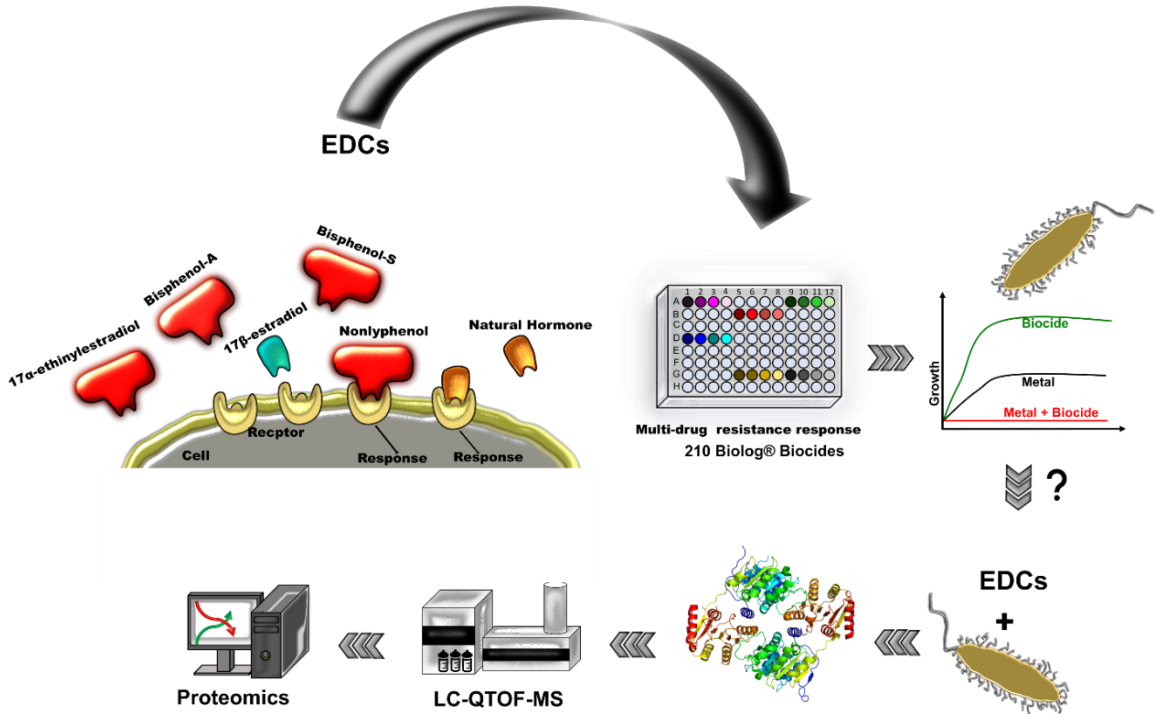

Abstract

Constitutively and chemical-induced expression of multi-drug resistant (MDR) proteins render bacteria resistant to harsh environments, metals, biocides, and other non-conventional chemicals. Endocrine-disrupting chemicals (EDCs) such as nonylphenol (NP), 17β-estradiol (E2), 17α- ethynylestradiol (EE2), bisphenol-A (BPA), and bisphenol-S (BPS) may induce membrane-bound multi-drug resistant (MDR) genes and are substrates of MDR efflux pumps found in bacteria. To understand the effect of estrogens on *E. coli* grown with prolonged exposure of the EDCs NP, E2, EE2, BPA, and BPS (0.01% *w*/*v*) and evaluated for induced antimicrobial resistance with a chemical sensitivity assay. NP exposed cells resulted in the highest quantity of antagonistic response (induced resistance) with cells becoming resistant to 105 of the chemicals, followed by EE2 (n = 88), BPA (n = 80), BPS (n = 61), and E2 (n = 38). Membrane proteins from exposed cells were extracted and relatively quantified using unlabeled, untargeted LC-QTOF mass spectrometry. Regulatory (repression), RND-type, and ABC-type efflux proteins were upregulated after exposure to specific environmental estrogens (MdtB in NP, EE2, BPA and BPS treated cells, AcrD in EE2, BPA and BPS treated cells, ArsB in EE2, BPA, and BPS treated cells, MarR in NP, E2, BPA and BPS, MdtN in NP treated cells). Non-target analysis of membrane proteins confirmed elevated expression of antibiotic-resistant proteins.

5.1. Introduction.

Estrogen mimics such as the synthetic hormones 17α-ethynylestradiol (EE2) and 17β-estradiol (E2), plasticizers such as Bisphenol-A (BPS), and Bisphenol-S (BPS), and the detergent nonylphenol (NP) are environmental pollutants responsible for various endocrine-disrupting effects in humans and aquatic and terrestrial animal life.[63, 277] These contaminants are found in consumer products, prescriptions, at historically polluted sites, and increasingly in tap water and wastewater.[52-53] Because of the increased use of chemicals for industrial, residential, and pharmaceutical usage, EDCs continue to be a large and growing group of compounds. The United States Environmental Protection Agency (EPA) defines endocrine-disrupting chemicals (EDCs) as exogenous substances or mixtures that alter functions of the endocrine systems of humans and wildlife in both the exposed organism and its offspring.[58, 278] EDCs have a significant acute and chronic impact on human and wildlife health and the microbial ecology of built and natural environments.[279-280] Research suggests that because the actions of EDCs are not limited to a single endocrine axis or organ, they can be responsible for increasing rates of cancers, altering adipose tissue promoting obesity, metabolic syndrome, diabetes, thyroid diseases, and infertility related to the sexual development of humans.[58-61] This accentuates the role EDCs partake in exacerbation of bacteria virulence involved in clinical infections, environmental ecology, and engineered microbial systems.

Studies have shown that natural sex hormones such as estradiol, can increase growth and virulence factors in multi-drug resistant (MDR) bacteria such as *E. coli*, and *P. aeruginosa*, increasing the persistence of these bacteria during infections.[281-283]

Synthetic estrogen mimics, plasticizers, and detergents that act as EDCs can play similar roles in MDR bacteria and induce other virulence factors such as antibiotic resistance.

E. coli and other gram-negative bacteria possess MDR efflux pump proteins that are responsible for the extrusion of toxic chemicals from the cytoplasm and periplasm as a resistance response to environmental stressors.[284] These efflux pumps facilitate the survival of gram-negative bacteria in harsh environments, such as high metals, anaerobic conditions, wastewater, and the human gut. Chemicals pumped from the cell vary due to the wide substrates of the efflux pumps in total and include bile salts, antibiotics, biocides, detergents, and heavy metals, among others.[285-290]

MDR proteins are over-expressed in the presence of natural and synthetic estrogens and estrogen mimics.[75] Exposure to E2, estriol, and estrone induced the expression of *acrB*, *acrF*, and *mdtF* (*yhiV*) in a qPCR analysis of *E. coli* strain K12, while exposure to anthropogenic estrogens EE2, BPA, and NP similarly increased and induced the RND inner membrane genes *acrB* and *mdtF*.[76] None of these chemicals are true antimicrobials, however, anthropogenic bisphenols and nonylphenol have been shown to exhibit biocidal activity in bacteria. Loadings of EDCs in natural and built environments may pose a direct and indirect risk to public health and microbial ecology as the cycling of these contaminants in built and natural microbial communities may induce antibiotic resistance.

To better understand the role EDCs may play in antibiotic resistance in MDR bacteria, generationally EDC-exposed *E. coli* was evaluated against 210 biocides (Table 5.1) for high-throughput relative testing of potential antagonism. To determine if

antibiotic-resistant proteins are overexpressed in response to prolonged exposure to anthropogenic EDCs NP, E2, EE2, BPA, and BPS, membrane proteins were extracted and quantified on LC-QTOF mass spectrometry. The resulting conferred resistance to 210 antibiotics was determined using the coefficient of drug interaction, a type of combination index (CDI) for antagonism, and protein expression was investigated to observe the role of EDC-induced antibiotic resistance.

5.2. Materials and Methods

5.2.1. Chemicals and Cell Line.

All the EDCs for all test conditions were commercially obtained from Millipore Sigma. The chemicals NP, EE2, BPA, and BPS were prepared in molecular grade 190 proof ethanol (Sigma Aldrich) using volumetric flasks and stored in glass containers at 4 °C. The chemical E2 was prepared in molecular grade DMSO (Sigma Aldrich) in the same manner and stored. All chemical stocks were prepared at 100X and made fresh before biological application.

The *E. coli* strain wild-type W3110 was used and served as the control and test strain.[238] Plates were prepared using stock EDC solutions and LB agar (EDCs at 0.01% w/v). *E. coli* was streaked on the respective EDC plate for NP, E2, EE2, BPA, and BPS (all EDCs at 0.01% w/v) and incubated overnight at 37°C for 16 hours. The process was repeated two additional times to acclimate cells to the respective EDC across three successive agar plates.

5.2.2. Chemical Sensitivity Assays

Biolog's chemical sensitivity assays (PM11-PM-20) were used to evaluate high-throughput screening of the effects of combinations of multiple classes of biocides and the environmental estrogens NP, E2, EE2, BPA, and BPS. Assays were conducted per the manufacturer's procedure with modifications. A bacteria colony was pre-cultured in either 5mL of LB media containing either NP, E2, EE2, BPA, BPS (EDCs at 0.01% *w/v*) or no estrogen and incubated at 37°C till mid-log growth (OD_{600} 0.8-1.00). Cultures were seeded to 120 mL of fresh LB media being estrogen free or with their respective estrogens at the same concentration for a final bacterial concentration of 10^6 cells/mL. The cultures were dispensed (100 µL per well) in Biolog's microbial chemical sensitivity panels (Biolog, Inc., PM11-20) for a final in-well concentration of 10^5 cells/mL. The plates were incubated at 37 °C and the growth (OD_{600}) was recorded on a microplate reader spectrophotometer (Biotek Synergy H1) at t = 0 and t = 16 hr.

5.2.3. Analysis of Combinatory Effects.

The coefficient of drug interaction was used to determine if estrogen exposure resulted in decreased antibiotic susceptibility. Bacteria growth (OD_{600}) on the estrogen mimic was normalized relative to the control (LB media only) over the same period. Normalized growth, often used in CDI calculations was used in the calculation for Equation 5.1.

$$\mathbf{CDI} = \frac{\mathbf{A+B}}{(\mathbf{AB})} \qquad \textbf{Equation 5.1.}$$

Where AB is the growth of *E. coli* in the estrogen-biocide mixture, A is the growth of *E. coli* on the estrogen alone, and B was the growth on the Biolog biocide alone. The combination was designated synergistic at CDI < 1, additive at CDI = 1, and

antagonistic at CDI > 1. The lower limit of CDI > 1.5 was used for antagonistic combination, though slight antagonism at CDI = 1.1 is a valid starting point.[291-292] CDI values greater than or equal to 1.5 were set to indicate elevated levels of antagonism since the growth of the EDC plus biocide was greater than at least one of the individual chemicals by 16.7-56.7%. CDI values represent the average of duplicate experiments.

5.2.4. Protein Extraction.

Overnight 5 mL precultures of LB media containing either NP, E2, EE2, BPA, or BPS (EDCs at 0.01% *w/v*) and no chemicals were prepared and incubated at 37°C. Bacteria from precultures were seeded into 250 mL of fresh LB media with respective EDCs or no chemicals for a final bacterial concentration of 10^5 cells/mL. The cultures were grown to mid-log (OD_{600} 0.8-1.00) and centrifuged at 3500 x g (Sorvall RC 5C Plus) at 4°C. Pellets were processed immediately for protein extraction. Membrane proteins were fractionated and isolated using BioRad's ReadyPrep™ Protein Extraction Kit (membrane II, sodium carbonate extraction methods) per the manufacturer's procedure.[293] Bacterial sample tissues under triplicate growth and extractions for all EDCs and controls were processed. In a microcentrifuge tube on ice, 2 mL of lysis buffer solution was added to ~100 mg of sample. To disrupt the cells, samples were sonicated on ice with an ultrasonic probe (Qsonica Ultrasonic Processor Q500) 4 times with bursts of 30 seconds on and 30 seconds rest intervals for a total time of 8 min at 20% amplitude. Samples were centrifuged at 3,000 x g at 4°C. The supernatant was diluted into a chilled beaker on ice containing 60 mL of membrane protein concentration reagent and stirred for 60 min. Samples were then ultracentrifuged (Bechman Coulter Optima XPN-100

Ultracentrifuge) at 100,000 x g for 60 min at 4°C. The supernatant was decanted and discarded, and the pellets were washed with 3 mL of chilled lysis buffer and rested for 2 min. The samples were washed a second time with lysis buffer and iced for 1 min. Pellets were resuspended with 2 mL of 2-D rehydration sample buffer containing a tributylphosphine reducing agent, ampholyte (0.2% *w/v*), and an ASB-14 detergent to efficiently solubilize the proteins. Samples were centrifuged at 16,000 x g for 20 min at room temperature and the supernatant was transferred to clean tubes. Samples were tested on nano-drop addon on the microplate reader (Biotek Synergy H1) and proteins were quantified. Samples were stored at -80 °C for downstream applications.

5.3.5. Protein Mass-Spectroscopy and Proteomics Analysis.

Non-target relative quantitative proteomics was performed on protein extracts. Triplicate biological extract samples were submitted to be processed for protein mass-spectroscopy. Samples were digested in trypsin and proteins and peptides were relatively (label-free) quantified using an Agilent 1290 HPLC coupled to the Agilent 6530 Quadrupole TOF LC-MS. Proteins were identified with the FASTA format alogrithim[294] Tryptic peptides were also targeted based on a prediction list to maximize detection during untargeted analysis. The data were analyzed, and statistics were applied using the Proteome Discoverer software.[295] Data were statistically analyzed by one-way ANOVA. Significantly increased abundance of proteins was determined to be values with a fold-change (FC) > 4 and p-value < 0.05. A significantly decreased abundance of proteins was determined to be values with a FC < 0.25 and a p-value < 0.05. The resulting statistical

data can be visualized on $\log_{10}$-$\log_2$ volcano plots for each EDC test condition (Figure D.1.)

5.3. Results

5.3.1. EDC Chemical Sensitivity Assay.

Antimicrobial susceptibility of wild-type *E. coli* (W3110) was performed by a high-throughput screen using Biolog's chemical sensitivity assay. Biolog's pre-plated chemicals allowed for the testing of 210 chemicals covering 7 classes of biocides (Table 5.1.) and are frequently used to test the toxicity of conventional antibiotics in a 96-well microplate format. Each plate contains 24 chemicals of four increasing masses of each biocide across 10 plates (PM11-PM20, Table 5.1.). Relative growth (OD_{600}) was used to calculate the CDI for each well of the bioassay plate (Equation 5.1.). The number of antagonistic combinations from each class of biocide with the corresponding EDCs is presented in Figure 5.1. and 5.2. Of the EDCs assessed, NP combinations resulted in the highest quantity of antagonism and showed elevated growth when mixed with 105 chemicals, followed by EE2 at 88, BPA at 80, BPS at 61, and E2 at 38 antagonistic combinations.

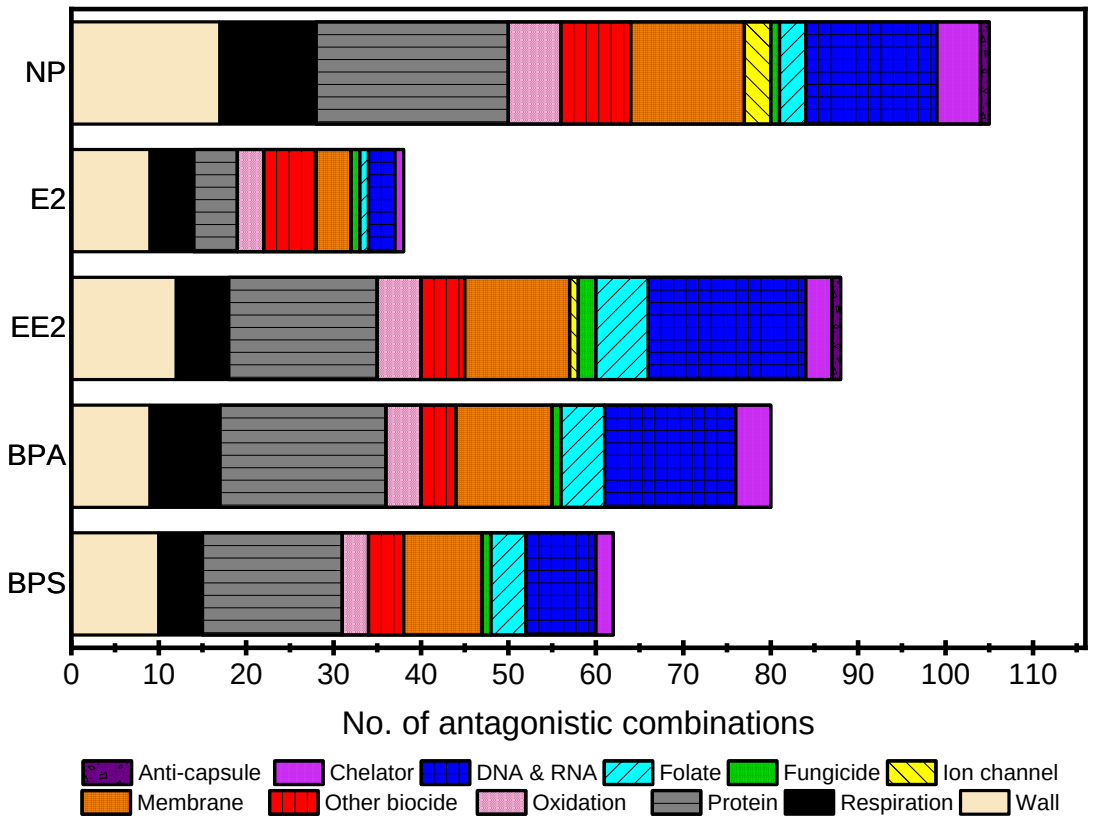

Figure 5.1. Antagonistic biocide and EDC combinations within classes of chemical tested. Antagonistic combinations were counted in this figure if the CDI values were ≥ 1.5. Multiple concentrations may induce but were only counted once for each respective EDC in this figure.

Table 5.1. Biocide chemical class or target of biocide in Biolog's chemical sensitivity assay. Metal biocides are another class of Biolog's chemical sensitivity assay but were excluded from this study. A total of 210 were evaluated with various subtypes of chemicals

No. of chemicals	Subtype of chemical	Class or target of action
2	Glutathione	Oxidation
5	Oxidizing agent	
1	Sulfhydryl	
14	Aminoglycoside	Protein
1	Linocosamide	
6	Macrolide	
6	Protein synthesis	
8	Tetracycline	
5	tRNA synthetase	
3	Other	
1	Ca^{2+} transporter	Resperation
10	Ionphore	
4	Uncoupler	
2	Other	
11	Cephalosporin	Cell wall
1	Monobactam	
11	β-lactam	
3	Peptidogylcan synthesis	
3	Polymyxin	
1	Other	
3	Acetylcholine antagonist	Other biocides
1	Fatty acid synthesis	
3	Glycopeptide	
3	Nitroimidzaole	
2	Rifamycin	
2	Triazole	
13	Other	
3	Anti-capsule	
		Total tested

Class or target of action	Subtype of chemical	No. of chemicals
Chelator	Carboxylic acid	3
	Hydroxyguinoline	4
	N-heterocycle	2
	Other	1
DNA & RNA	DNA alkylation	2
	Fluoroquinolone	5
	Intercalator	8
	Nitrofuran analog	3
	Purine analog	2
	Pyrimidine analog	5
	Quinoline	4
	Other	4
Folate	Sulfonamide	8
	Other	3
Ion channel	K^+ inhibitor	2
	Na^+ inhibitor	2
Membrane	Anionic detergent	1
	Cationic detergent	6
	Electron transport	3
	Guanidine (permeability)	2
	Phenothizaine	4
	Other	3
	Zwitterionic detergent	1
Fungalcide	Lipoxygenase	1
	phenylsulfamide	2
	Other	1
	210	

Figure 5.2. Heatmap of CDI values of EDC (0.01% w/v) induced antagonism to Biolog Chemicals. Major groups (shaded in green) were greater than 50 % of the classes of biocide resulting in elevated levels of antagonism (AC is anticapsule and Fungi are fungicides, Ach Recp is Ach Receptors, Ion is Ion channel inhibitors, and Folate Syn is folate synthesis).

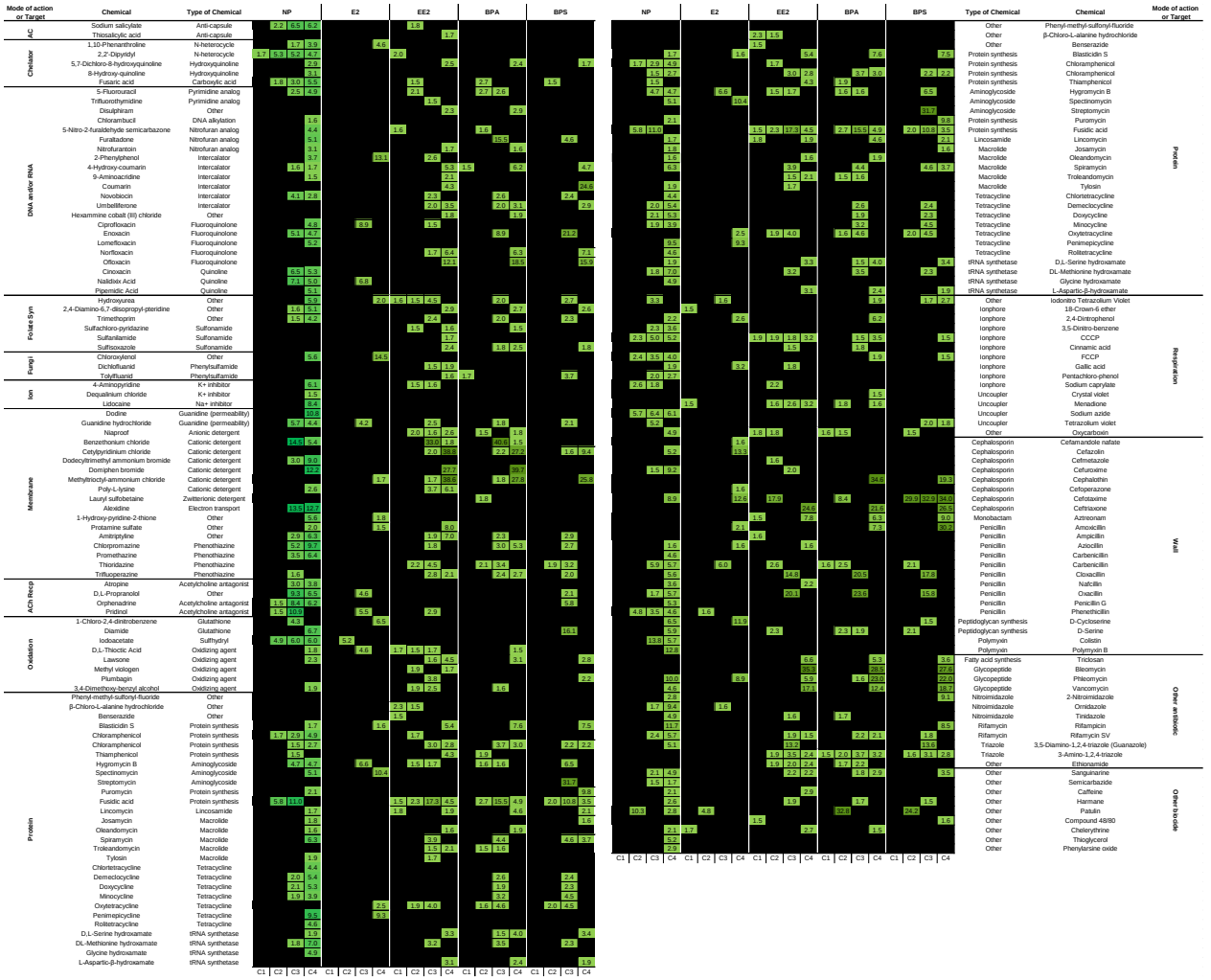

5.3.2. Proteomic Analysis of EDC Induced Antibiotic Resistance.

To further investigate the basis of EDC-induced resistance to 54 types of biocides, a metaproteomic analysis of *E. coli* membrane proteins was conducted. This proteomics study was conducted using untargeted, label-free mass spectrometry, semi-quantified. From the analysis of the proteomic data, 13,923 unique peptides were identified matching 2,012 proteins (Figure 5.3.). Of the proteins identified across biological replicates (n = 3), 1483 were shared between control (unacclimated) cells and NP treated cells (93.6% W3110, 81.2% NP). The shared identified proteins between the synthetic estrogens E2 and EE2 treated cells and control was 1261 between E2 and W3110 (79.6% W3110, 88.0% E2), 1503 between EE2 and W3310 (94.9% W3110, 87.6% EE2), and 1220 between E2 and EE2 (92.1% E2, 78.2% EE2). The shared identified proteins between the plasticizers BPA and BPS treated cells and control was 1493 between BPA and W3110 (94.3% W3110, 77.1% BPA), 1358 between BPS and W3310 (85.7% W3110, 85.7% EE2), and 1503 between BPA and BPS (81.9% BPA, 94.9% BPS).

Significant proteins detected were sorted by biological process, molecular function, and cellular location using the Proteome Discoverer software (Figure 5.4.). For all tested EDCs, the two highest abundant upregulated proteins belonged to metabolic processes and responses to stimuli. Downregulated proteins varied between EDCs, with the most abundant being metabolic processes due to NP, E2, EE2, and BPS exposure. Significant up and downregulated proteins were also sorted by molecular function and location of a cellular component. For all EDC-treated cells, the most abundant upregulated proteins detected by molecular function demonstrated catalytic activity. Most of the proteins detected were associated with the membrane, cytosol, and cytoplasm.

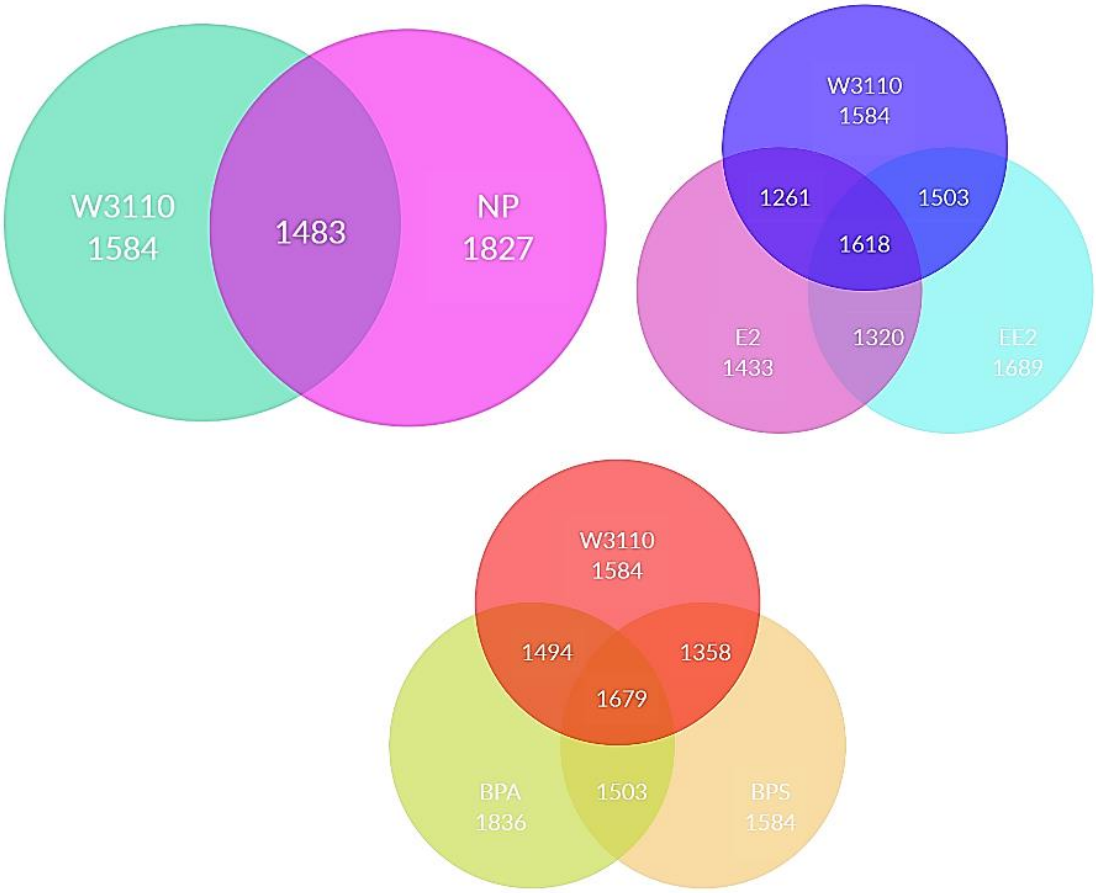

Figure 5.3. Venn diagrams of total detected, and protein overlap between different tested EDC (0.01% w/v) types. Unique proteins for each EDC exposed and wild-type (strain W3110, control) were: NP 47, E2 39, EE2 18, BPA 31 and W3110 21. No unique proteins were obtained for BPS-treated cells.

5.3.3. Significant Antibiotic Resistant Proteins Identified.

Exposure to EDCs resulted in increased and decreased protein production of several resistant classes of proteins when compared to their respective controls. Proteins detected were considered increased in abundance when the relative expression level showed a fold-change (FC) ≥ 4 (p-value < 0.05). Proteins were considered decreased in abundance when the relative expression level exhibited a FC $\leq$ 0.25 (p-value < 0.05) (Table 5.2.). NP, EE2, and BPA-treated

cells had a mostly increased relative abundance of significantly identified antibiotic-resistant proteins, whereas E2 and BPS had a mostly decreased abundance of antibiotic-resistant proteins.

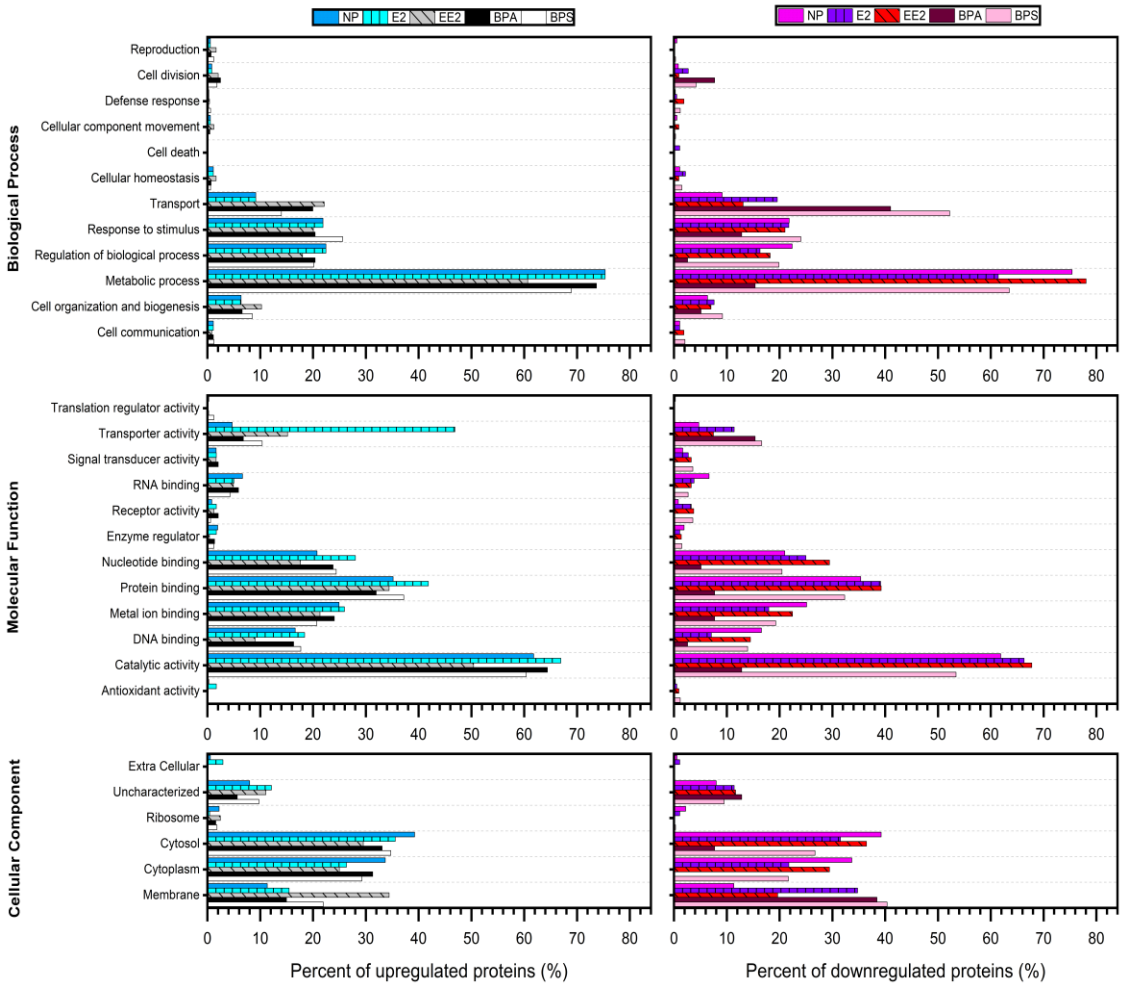

Figure 5.4. Protein ontology of significantly up or downregulated proteins**.** Percentage of upregulated and downregulated proteins detected and categorized by gene ontology. Biological process (top), molecular function (middle), cellular component (bottom), and upregulated (Blue colors; Left) and downregulated (Red colors; Right)

Table 5.2. Major antibiotic resistance proteins significantly detected from treatment from EDCs. Increased protein abundances are highlighted in blue (solid) and decreased are highlighted in red (spotted).

ID	Classification	Protein Name		NP	E2	EE2	BPA	BPS
P37637	Multidrug resistance protein	MdtF	Log2 FC					-2.94
			-Log P-Value					1.95
P37636	Multidrug resistance protein	MdtE	Log2 FC					-2.52
			-Log P-Value					1.49
P24177	Probable aminoglycoside efflux pump	AcrD	Log2 FC	-6.644	-6.644	6.64	6.64	4.58
			-Log P-Value	16.43	16.43	16.43	16.43	3.33
P76398	Multidrug resistance protein	MdtB	Log2 FC	6.64	-6.644	6.64	6.64	6.64
			-Log P-Value	7.64	16.43	16.43	16.43	16.49
P0AFP9	Probable multidrug ABC transporter permease	YbhR	Log2 FC					-6.644
			-Log P-Value					16.43
P25744	Multidrug resistance protein	MdtG	Log2 FC		-6.644	-6.644		-3.40
			-Log P-Value		16.43	16.43		2.527
P0AEJ0	Multidrug export protein	EmrB	Log2 FC	-6.644	-6.644			-3.035
			-Log P-Value	16.43	16.43			1.85
P37340	Multidrug resistance protein	MdtK	Log2 FC					-6.644
			-Log P-Value					16.49
P0AE78	Magnesium and cobalt efflux protein	YbeX	Log2 FC			-5.059		-2.427
			-Log P-Value			6.802		1.388
P0AB93	Arsenical pump membrane protein	ArsB	Log2 FC			6.64	6.64	6.64
			-Log P-Value			16.43	16.43	16.43
P27245	Multiple antibiotic resistance protein	MarR	Log2 FC	6.64	6.64	-6.644	6.64	2.907
			-Log P-Value	16.43	16.43	16.43	16.43	1.532
P76397	Multidrug resistance protein	YbhS	Log2 FC			6.64		
			-Log P-Value			16.43		
P0AFQ2	Probable multidrug ABC transporter	MdtN	Log2 FC	6.64				
			-Log P-Value	16.43				
P32716	Multidrug resistance protein	MdtA	Log2 FC		-6.644			
			-Log P-Value		16.43			

5.4. Discussion.

5.4.1. EDC and Chemical Sensitivity Assays.

Combinations of NP and biocides yielded high antagonistic levels with anticapsule, chelating agents, DNA and/or RNA targeting, folate synthesis targeting, fungicidal, ion channel inhibiting, membrane targeting, Ach receptor targeting, oxidizing, protein inhibiting, respiration targeting, a cell wall targeting and other biocidal and

antibiotic chemical classes of compounds (Table 5.1.). Exposure to nonylphenol made *E. coli* more drug resistant. Nonylphenol products are toxic detergents and are responsible for superoxide formation that leads to severe inhibition of bacterial growth unless resistant mechanisms such as radical scavenging enzymes are present.[296] Previous work has shown that NP, EE2, and BPA induced antibiotic resistant genes (*acrB* and *mdtF*) encoding the inner membrane protein of RND chemical efflux pumps found in *E. coli* and the hormones E2, estriol, and estrone induced genes (*acrB*, *acrF*, and *mdtF*).[76] Substrates of the protein AcrB include lipophilic beta-lactams, multiple pharmaceutical drugs, detergents, bile salts, organic solvents, disinfectants, dyes, steroid hormones, phospholipids, ethidium, and lipophilic carboxylates.[46, 75, 165, 297] Substrates of the efflux protein MdtF include acriflavin, doxorubicin, ethidium, rhodamine 6G, and deoxycholate,[165-166, 174, 298] while AcrD efflux substrates include amikacin, gentamycin, neomycin, kanamycin, tobramycin, sodium dodecyl sulfate (SDS), deoxycholate, estradiol, progesterone, aminoglycosides, Cu^{2+}, Zn^{2+}, and L-cysteine.[46, 163, 299-301] The high levels of antagonism observed in NP-exposed cells may be due to the chemical efflux caused by NP in *E coli*. Increased protein production from gene expression likely results in increased efflux, reducing the effectiveness of these types of chemicals.

Bisphenols, as the parent compound or replacement, caused phenotypic antibiotic resistance across an array of chemicals. The plasticizer BPA, when mixed with antimicrobials and biocides, resulted in several antagonistic combinations, most notably with DNA/RNA targeting antibiotics, chelating agents, folate synthesis targeting, oxidating agents, protein synthesis, respiration targeting, wall targeting, and membrane

targeting classes of chemicals (Table 5.2.). As substrates of major efflux pumps in bacteria, induction of efflux may be a cause for higher levels of antagonism with chemicals such as membrane targeting an oxidizing agent that requires penetration of the cell or membrane proximity to be biologically active. BPS shared the same antagonistic class of biocides but also showed antagonism with Ach receptor inhibiting whereas BPA did not. Neither BPA nor BPS combinations showed antagonism with ion channel inhibitors.

Synthetic hormones such as E2 and EE2 produced low and high numbers of antagonistic combinations. Of the 210 chemicals evaluated, E2 exposure resulted in 38 antagonistic combinations. Estrogenic compounds such as E2 are often readily biodegraded by bacteria and are hypothesized to act as a carbon source for metabolism.[302-303] Reduced antagonism with the tested biocides is likely due to assimilation of E2 into cellular carbon, resulting in no negative interaction with biocide or cell. However, the synthetic hormone EE2 reduced antibiotic effectiveness, and cells survived on biocides compared to no exposure. Since hormones are substrates of major multi-drug efflux pumps in *E. coli*, the induction of antibiotic resistance genes that export many compounds would result in prominent levels of observed antagonism, due to acquired resistance.

5.4.2. Proteomic Analysis of EDC-exposed Cells.

Biological processes and molecular functions can give insight into the influence of the EDCs on the membrane proteins of *E. coli.* As expected, there is an enrichment of upregulated proteins associated with transporter activity compared to their relative

controls for E2, EE2, BPS, and BPA acclimated cells. Transporter activity involves the import and export of biomolecules in response to environmental factors using the energy of ATP hydrolysis and electro-chemical gradients.[288, 304] As substrates of major transporters E2 and BPA should increase transporter activity as proteins responsible for energy transport and detoxifications are upregulated. Increased metabolic activity and response to stimuli signify the bacteria's attempts to matin homeostasis from the stress of exposure to the EDCs.[305]

Cells treated with NP, E2, and EE2 had a significant decrease in nucleotide-binding proteins compared to their respective controls. The abundance of nucleotide-binding proteins decreased in downregulated proteins treated with BPA compared to its respective control. Nucleotide-binding proteins shape bacterial chromosome changes in response to environmental conditions and are essential in bacterial cell function through stabilization and protection of DNA.[306-307] An increase in the downregulated proteins could be a response to the stress the EDCs impose on the cell. A decrease in proteins categorized as nucleotide-binding may suggest fewer proteins are being downregulated compared to the respective control increasing DNA protection and stabilization from stressors such as BPA.

EE2, BPA, and BPS-treated cells increased upregulated proteins associated with biological processes, more specifically transporter activity. Transport proteins such as MDR efflux pumps are responsible for the traffic of biomolecules inside or outside the cell including essential molecules and toxins.[308] The increase in these proteins may be due to stimulus from the EDC needing to allocate compounds and energy for defense or

continued function of the cell. Additionally, this increased protein production can be for the efflux of chemicals via protein transporters to protect cells from toxic compounds.

5.4.3. Upregulated and Downregulated Antibiotic Regulation and Efflux.

The antibiotic-resistance proteins detected can provide insight into the extent of resistance occurring due to pollutant exposure (Table 5.3.). The MarR protein represses the transcription of the MarORAB operon, limiting antibiotic resistance of *E. coli*.[309] The *marRAB* that encodes for the MarORAB protein system, is stochastic and its expression is enhanced by the presence of antimicrobial compounds.[310] MarRAB operon expression is repressed by the MarR protein, but phenolic compounds such as salicylic acid, dissociate the binding between MarR and PmarO by binding directly to the MarR protein ending the repression.[311-312] The increased abundance of MarR in EDC exposed cells could indicate an attempt by the cells to maintain homeostasis with stressors. As a phenolic compound, NP can bind to MarR protein causing the regulation of several resistance proteins, observed here, and could explain the high counts of antagonism with the 210 biocides assessed and NP accumulated *E. coli*. Interestingly, despite previous studies indicating expression of acrAB-TolC related genes, no significant (relative to the controls) AcrB proteins were detected for NP, BPA, and E2 treated cells. The MarR protein also regulates the AcrAB efflux pump responsible for exporting a variety of structurally and chemically unrelated compounds outside of the cell. [313-314] The upregulation of the MarR protein can explain why no significant detection of AcrB proteins occurred as initially expected consequently other MDR proteins were expressed and discussed below.

The protein AcrD is an RND transporter and homolog of the AcrB protein that forms a tripartite complex responsible for the efflux of aminoglycosides and anionic β-lactams [163, 299, 315-316] Like AcrB, the protein AcrD works with AcrA and TolC to export a more selective variety of compounds than compared with the AcrAB-TolC efflux pump system. [315, 317] Upregulation in AcrD in EE2, BPA, and BPS cells can be associated with an upregulation of BaeR, (data not shown) a regulator of AcrD. However, BaeR expression increased for NP and E2 treated cells, yet AcrD was downregulated in these cases. There is conflicting research that shows BaeR is required for the regulation of AcrD under kanamycin treatment.[318-320] Further work is needed to better understand the protein regulations in the EDC-treated cells.

The protein MdtB was significantly upregulated in NP, EE2, BPA, and BPS-treated cells. MdtB can form a complex with MdtA, MdtC, and TolC to confer resistance to novobiocin, β-lactams, and bile salt derivatives, forming a more selective heterotrimeric efflux transporter $MdtB_2C$ complex.[160, 321-323] The upregulation of MdtB can be a reason for elevated antagonistic combinations seen in several categories of biocides tested with the NP, EE2, BPA and BPS treated cells. The protein MdtN was only upregulated in NP and may confer resistance to sulfur-based drugs.[324] This protein is understudied and further research from the community is needed to better understand the potential implications.

E2, EE2, BPA, and BPS treated cells had significantly upregulated ArsB protein. The ArsB protein is thought to assist in the efflux of arsenite and antimonite by the formation of an arsenic transporter pump.[325]. A homolog of MarR in *Achromobacter* sp.

was recently identified and regulates arsenic resistance through *arsB*.[326] Further exploration is needed to see if the EDCs induce arsenic resistance proteins in *E coli*.

5.5. Conclusion.

The estrogen-mimics NP, E2, EE2, BPA, and BPS are chemicals of interest in health and engineering. From a health perspective, *E. coli* is the dominant strain responsible for urinary tract infections, and exposure to estrogen has been suggested as the underlying factor in elevated antibiotic resistance in clinical cultures. In engineered systems, increased loadings of estrogen mimics are a problem in wastewater attenuation, as estrogens are incompletely removed during secondary treatment. It was shown that generational contact of EDCs to bacteria typical of built and natural systems, confers resistance to a variety of antibiotics and other biocidal chemicals. Upon growth under EDCs, *E. coli* exhibited increased resistance toward biocides that would otherwise normally neutralize or inactivate the cells.

Elevated levels of regulatory proteins involved in antibiotic resistance were detected. It is unclear why some protein efflux pumps remained significantly upregulated while others were not detected. The chronic exposure to the EDCs although at high concentrations, created regulation of the cell that coincides with acclimation to the environmental stressor. This is evident by the lack of any significant increase or decreases to efflux pump proteins upon chronic generational exposure to the EDCs. The significance of these results demonstrates a need to better understand the complexities of the biochemistry involved during wastewater biological treatment, where many natural and anthropogenic chemicals can make prolonged contact with multi-drug resistant

bacteria. Future work will investigate a range of environmentally relevant EDCs exposed to bacteria, while whole-cell proteomics allows for the assessment of chronic or acute exposure to MDR bacteria.

CHAPTER 6

CONCLUSION AND IMPLICATIONS

6.1. Substrates of the MdtEF-TolC Efflux Pump.

Gram-negative pathogens such as *Escherichia coli* express the RND family of efflux pumps. This bacterium contains RND pumps with overlapping substrates that can be exported. In Chapter 2, substrates were determined for the proteins AcrAB and MdtEF using a chemical sensitivity assay. In the case of MdtEF and AcrAB, substrates can be similar with AcrAB having a more diverse substrate recognition while MdtEF tended to prefer cationic substrates. The results from the *in silico* analysis of MdtF and AcrB structures revealed variations that could explain the differing substrate recognition between the protein pumps.

The significance of this chapter is that under acidic conditions, the lower pI of essential binding residues in the distal pocket would deprotonate, allowing for stronger interactions between cationic substrate and anionic surface of the distal pocket in MdtEF. These findings suggested that acidic conditions influence the transport of cationic substrates for the MDR efflux pump, MdtEF. This has implications for the need to better understand the influence of operating conditions on antibiotic resistance in the built microbial communities of WWTPs.

Variations in pH and oxygenation of biological reactors in WWTPs may alter the cycling of emerging contaminants that may be substrates of the MdtEF-TolC efflux pump. Under aerobic conditions, AcrAB may be the primary transporter cycling chemicals, under anaerobic conditions MdtEF may allow for different substrates to be cycled depending on the pH. Both protein systems are ubiquitous with *E. coli* and grant the organism levels of redundant resistance to chemical stressors, while differences in the

substrate recognition between the pumps provide robustness to *E. coli*. As a result, it is probable that the operating conditions of WWTPs may influence antibiotic resistance and dictate which protein pumps may be operating and involved in the cycling of emerging contaminants.

6.2. Novel Antimicrobials.

Applying unique techniques such as dual biocide application can provide useful inactivation or inhibition of the MDR bacteria that carry efflux pump proteins as part of their arsenal of antibiotic-resistant mechanisms. In chapter 3, dual applications of metals and 210 known biocides provided insight into the possible synergistic combinations that can reduce bacterial growth in *E. coli*.

The screening of synergistic combinations of the Group IB metal ions Ag (I), Cu (II), and Au (III) with biocides to inactivate *E. coli* was explored. The significance of these results was that it confirmed prior discovered synergistic silver, copper, or gold ion/biocide combinations while also discovering new never previously reported combinations that may be promising antimicrobials when applied in combination. Because these findings support previous studies, the high-throughput method can be used as a preliminary screen to evaluate other combinations of biocides in dual applications to combat MDR bacteria.

The implications of this study were that this type of screening and the discovery of novel synergistic combinations lays the framework for future exploration of more potential antimicrobials that can inactivate or inhibit MDR bacteria allowing the continued use of declining effective antibiotics and other pharmaceuticals.

6.3. Synergism and Antagonism During Drug Discovery.

Understanding the type of chemicals that influence antibiotic-resistant mechanisms such as efflux pump proteins, can further guide in understanding what type of biocides can be used to inhibit or inactivate MDR bacteria such as *E. coli*. Chapter 4 further investigated the concept of synergism by studying the specific biocides chlorpromazine (CPZ), promethazine (PMZ), thioridazine (TDZ), and trifluoperazine (TFPZ) derived from the results of chapter 3, dually applied with silver, copper, and gold ions for synergism toward *E. coli.*

Ag (I) and Cu (II) drug combinations produced synergistic inhibitions to varying degrees. The TFPZ and Au (III) combinations were synergistic with *E. coli*.
As phenothiazines (PTZ), the chemicals CPZ, PMZ, TDZ, and TFPZ may act as efflux pump inhibitors. There toxicity and increased synergism particularly with Ag (I) and Cu (III) may be the result of the limitations to MDR efflux pump proteins placed by the PTZs allowing for the toxic ions to limit *E. coli* growth. Complex formation between ligands and metal (PTZ and Au (III)) may inhibit the irreversible binding of the EPIs to the efflux pumps and limit toxicity. The complexation may reduce toxicity as the efflux pump will no longer recognize the PTZ as a substrate. This suggests that the changes in substrate chemicals may reduce toxicity as the efflux pump no longer recognizes the EPI.

Quantification of synergism is relative to how test compounds interact with a biocide. The assumption that most synergism models make is that dually applied chemicals for the inactivation of microorganisms do not interact or interfere with each other's dose-response curve. However, this assumption is fundamentally flawed as

chemicals will interact with test organisms and possibly each other to varying degrees. The implications of this chapter highlight the importance of the nescisidaty to understand the chemical and biological interactions that dually applied antimicrobials may have on themselves, the other test antimicrobial, or the target organisms.

6.4. Emerging Contaminant Influences on Antibiotic-Resistant Bacteria.

The endocrine-disrupting chemicals (EDCs), nonylphenol (NP), 17β-estradiol (E2), 17α- ethynylestradiol (EE2), bisphenol-A (BPA), and bisphenol-S (BPS) may induce membrane-bound multi-drug resistant (MDR) genes and were substrates of MDR efflux pumps found in bacteria. As EDCs, these chemicals are of interest in WWTP due to their influences in public health and microbial ecology. In built systems such as WWTPs, increased loadings of EDC are an issue in wastewater attenuation, since estrogens are not fully degraded and removed during biological treatment.

Chapter 5 showed that through generational contact of EDCs to *E. coli*, the induction of antibiotic resistance proteins occurred and provided resistance to several biocides that were previously studied in chapters 3 and 4. Upon growth under EDCs, *E. coli* exhibited decreased susceptibility toward biocides that performed better prior to EDC exposure. Upregulated regulatory proteins involved in antibiotic resistance were detected. It was probable that the chronic exposure to the EDCs causes regulation of antibiotic resistance proteins as the cells become acclimated to the environmental stressors. The implications of these results showed that emerging contaminants that are substrates of MDR efflux pump proteins, may provide increased antibiotic resistance to bacteria such as *E. coli*. This is of particular concern as the reality of built systems and

environments that are experienced by MDR bacteria in WWTPs will have a multitude of emerging contaminants that may or may not be substrates of MDR efflux pumps. Attenuation of the chemicals and cycling of the chemicals can influence the bioavailability of these contaminants and may reduce the effectiveness of biological treatment.

REFERENCES

1. Huttner, A.; Harbarth, S.; Carlet, J.; Cosgrove, S.; Goossens, H.; Holmes, A.; Jarlier, V.; Voss, A.; Pittet, D.; for the World Healthcare-Associated Infections Forum, p., Antimicrobial resistance: a global view from the 2013 World Healthcare-Associated Infections Forum. *Antimicrobial Resistance and Infection Control* **2013,** *2* (1), 31.

2. Baquero, F.; Martínez, J.-L.; Cantón, R., Antibiotics and antibiotic resistance in water environments. *Current Opinion in Biotechnology* **2008,** *19* (3), 260-265.

3. Done, H. Y.; Venkatesan, A. K.; Halden, R. U., Does the Recent Growth of Aquaculture Create Antibiotic Resistance Threats Different from those Associated with Land Animal Production in Agriculture? *The AAPS Journal* **2015,** *17* (3), 513-524.

4. Petrović, M.; Gonzalez, S.; Barceló, D., Analysis and removal of emerging contaminants in wastewater and drinking water. *TrAC Trends in Analytical Chemistry* **2003,** *22* (10), 685-696.

5. Rittmann, B.; McCarty, P., Environmental Biotechnology: Principles and Applications. McGraw-Hill Education: 2020.

6. Andersson, D. I., Persistence of antibiotic resistant bacteria. *Current Opinion in Microbiology* **2003,** *6* (5), 452-456.

7. McArthur, A. G.; Waglechner, N.; Nizam, F.; Yan, A.; Azad, M. A.; Baylay, A. J.; Bhullar, K.; Canova, M. J.; Pascale, G. D.; Ejim, L.; Kalan, L.; King, A. M.; Koteva, K.; Morar, M.; Mulvey, M. R.; O'Brien, J. S.; Pawlowski, A. C.; Piddock, L. J. V.; Spanogiannopoulos, P.; Sutherland, A. D.; Tang, I.; Taylor, P. L.; Thaker, M.; Wang, W.; Yan, M.; Yu, T.; Wright, G. D., The Comprehensive Antibiotic Resistance Database. *Antimicrobial Agents and Chemotherapy* **2013,** *57* (7), 3348-3357.

8. Benveniste, R.; Davies, J., Mechanisms of antibiotic resistance in bacteria. *Annual review of biochemistry* **1973,** *42* (1), 471-506.

9. Cox, G.; Wright, G. D., Intrinsic antibiotic resistance: Mechanisms, origins, challenges and solutions. *International Journal of Medical Microbiology* **2013,** *303* (6), 287-292.

10. Blair, J. M. A.; Webber, M. A.; Baylay, A. J.; Ogbolu, D. O.; Piddock, L. J. V., Molecular mechanisms of antibiotic resistance. *Nature Reviews Microbiology* **2015,** *13* (1), 42-51.

11. Munita, J. M.; Arias, C. A.; Kudva, I. T.; Zhang, Q., Mechanisms of Antibiotic Resistance. *Microbiology Spectrum* **2016,** *4* (2), 4.2.15.

12. Vega, N. M.; Gore, J., Collective antibiotic resistance: mechanisms and implications. *Current Opinion in Microbiology* **2014,** *21*, 28-34.

13. Yelin, I.; Kishony, R., Antibiotic resistance. *Cell* **2018,** *172* (5), 1136-1136. e1.

14. Blanco, P.; Hernando-Amado, S.; Reales-Calderon, A. J.; Corona, F.; Lira, F.; Alcalde-Rico, M.; Bernardini, A.; Sanchez, B. M.; Martinez, L. J., Bacterial Multidrug Efflux Pumps: Much More Than Antibiotic Resistance Determinants. *Microorganisms* **2016,** *4* (1).

15. Piddock Laura, J. V., Clinically Relevant Chromosomally Encoded Multidrug Resistance Efflux Pumps in Bacteria. *Clinical Microbiology Reviews* **2006,** *19* (2), 382-402.

16. Tseng, T. T.; Gratwick, K. S.; Kollman, J.; Park, D.; Nies, D. H.; Goffeau, A.; Saier, M. H., Jr., The RND permease superfamily: an ancient, ubiquitous and diverse family that includes human disease and development proteins. *J Mol Microbiol Biotechnol* **1999,** *1* (1), 107-25.

17. Lubelski, J.; Konings, W. N.; Driessen, A. J. M., Distribution and physiology of ABC-type transporters contributing to multidrug resistance in bacteria. *Microbiol Mol Biol Rev* **2007,** *71* (3), 463-476.

18. Chung, Y. J.; Saier, M. H., SMR-type multidrug resistance pumps. *Curr Opin Drug Discov Devel* **2001,** *4* (2), 237-245.

19. Law, C. J.; Maloney, P. C.; Wang, D.-N., Ins and outs of major facilitator superfamily antiporters. *Annu Rev Microbiol* **2008,** *62*, 289-305.

20. Nikaido, H., Structure and mechanism of RND-type multidrug efflux pumps. *Adv Enzymol Relat Areas Mol Biol* **2011,** *77*, 1-60.

21. Pasqua, M.; Grossi, M.; Zennaro, A.; Fanelli, G.; Micheli, G.; Barras, F.; Colonna, B.; Prosseda, G., The Varied Role of Efflux Pumps of the MFS Family in the Interplay of Bacteria with Animal and Plant Cells. *Microorganisms* **2019,** *7* (9), 285.

22. Yan, N., Structural advances for the major facilitator superfamily (MFS) transporters. *Trends in Biochemical Sciences* **2013,** *38* (3), 151-159.

23. Saidijam, M.; Benedetti, G.; Ren, Q.; Xu, Z.; Hoyle, C. J.; Palmer, S. L.; Ward, A.; Bettaney, K. E.; Szakonyi, G.; Meuller, J., Microbial drug efflux proteins of the major facilitator superfamily. *Current drug targets* **2006,** *7* (7), 793-811.

24. Saidijam, M.; Bettaney, K. E.; Leng, D.; Ma, P.; Xu, Z.; Keen, J. N.; Rutherford, N. G.; Ward, A.; Henderson, P. J.; Szakonyi, G., The MFS efflux proteins of gram-

positive and gram-negative bacteria. *Adv Enzymol Relat Areas Mol Biol* **2011,** *77*, 147-166.

25. Wu, H.-H.; Symersky, J.; Lu, M., Structure and mechanism of a redesigned multidrug transporter from the Major Facilitator Superfamily. *Scientific Reports* **2020,** *10* (1), 3949.

26. Paulsen, I. T.; Skurray, R. A.; Tam, R.; Saier Jr, M. H.; Turner, R. J.; Weiner, J. H.; Goldberg, E. B.; Grinius, L. L., The SMR family: a novel family of multidrug efflux proteins involved with the efflux of lipophilic drugs. *Molecular Microbiology* **1996,** *19* (6), 1167-1175.

27. Bay, D. C.; Rommens, K. L.; Turner, R. J., Small multidrug resistance proteins: A multidrug transporter family that continues to grow. *Biochimica et Biophysica Acta (BBA) - Biomembranes* **2008,** *1778* (9), 1814-1838.

28. Bay, D. C.; Turner, R. J., Diversity and evolution of the small multidrug resistance protein family. *BMC Evolutionary Biology* **2009,** *9* (1), 140.

29. Bellmann-Sickert, K.; Stone, T. A.; Poulsen, B. E.; Deber, C. M., Efflux by small multidrug resistance proteins is inhibited by membrane-interactive helix-stapled peptides. *Journal of Biological Chemistry* **2015,** *290* (3), 1752-1759.

30. Brown, M. H.; Paulsen, I. T.; Skurray, R. A., The multidrug efflux protein NorM is a prototype of a new family of transporters. *Molecular Microbiology* **1999,** *31* (1), 394-395.

31. Kumar, S.; Floyd, J. T.; He, G.; Varela, M. F., Bacterial antimicrobial efflux pumps of the MFS and MATE transporter families: a review. *Recent Res Dev Antimicrob Agents Chemother* **2013,** *7*, 1-21.

32. Kuroda, T.; Tsuchiya, T., Multidrug efflux transporters in the MATE family. *Biochimica et Biophysica Acta (BBA) - Proteins and Proteomics* **2009,** *1794* (5), 763-768.

33. Huda, N.; Lee, E.-W.; Chen, J.; Morita, Y.; Kuroda, T.; Mizushima, T.; Tsuchiya, T., Molecular cloning and characterization of an ABC multidrug efflux pump, VcaM, in Non-O1 Vibrio cholerae. *Antimicrobial agents and chemotherapy* **2003,** *47* (8), 2413-2417.

34. Feng, Z.; Liu, D.; Wang, L.; Wang, Y.; Zang, Z.; Liu, Z.; Song, B.; Gu, L.; Fan, Z.; Yang, S.; Chen, J.; Cui, Y., A Putative Efflux Transporter of the ABC Family, YbhFSR, in Escherichia coli Functions in Tetracycline Efflux and Na+(Li+)/H+ Transport. *Front Microbiol* **2020,** *11* (556).

35. Linton, K. J.; Higgins, C. F., The Escherichia coli ATP-binding cassette (ABC) proteins. *Molecular microbiology* **1998,** *28* (1), 5-13.

36. Wilkens, S., Structure and mechanism of ABC transporters. *F1000Prime Rep* **2015,** *7*, 14-14.

37. Davidson, A. L.; Nikaido, H., Purification and characterization of the membrane-associated components of the maltose transport system from Escherichia coli. *Journal of Biological Chemistry* **1991,** *266* (14), 8946-8951.

38. Fath, M. J.; Kolter, R., ABC transporters: bacterial exporters. *Microbiological Reviews* **1993,** *57* (4), 995-1017.

39. Fernando, D. M.; Kumar, A., Resistance-Nodulation-Division Multidrug Efflux Pumps in Gram-Negative Bacteria: Role in Virulence. *Antibiotics* **2013,** *2* (1), 163-181.

40. Zgurskaya, H. I., Multicomponent drug efflux complexes: architecture and mechanism of assembly. *Future Microbiology* **2009,** *4* (7), 919-32.

41. Eswaran, J.; Koronakis, E.; Higgins, M. K.; Hughes, C.; Koronakis, V., Three's company: component structures bring a closer view of tripartite drug efflux pumps. *Current Opinion in Structural Biology* **2004,** *14* (6), 741-747.

42. Koronakis, V.; Sharff, A.; Koronakis, E.; Luisi, B.; Hughes, C., Crystal structure of the bacterial membrane protein TolC central to multidrug efflux and protein export. *Nature* **2000,** *405* (6789), 914-919.

43. Pos, K. M., Trinity revealed: Stoichiometric complex assembly of a bacterial multidrug efflux pump. *Proceedings of the National Academy of Sciences* **2009,** *106* (17), 6893-6894.

44. Blair, J. M. A.; Piddock, L. J. V., Structure, function and inhibition of RND efflux pumps in Gram-negative bacteria: an update. *Current Opinion in Microbiology* **2009,** *12* (5), 512-519.

45. Borges-Walmsley, M. I.; McKeegan, K. S.; Walmsley, A. R., Structure and function of efflux pumps that confer resistance to drugs. *Biochemical Journal* **2003,** *376* (2), 313-338.

46. Elkins, C. A.; Nikaido, H., Substrate specificity of the RND-type multidrug efflux pumps AcrB and AcrD of Escherichia coli is determined predominantly by two large periplasmic loops. *Journal of bacteriology* **2002,** *184* (23), 6490-6498.

47. Ramaswamy, V. K.; Vargiu, A. V.; Malloci, G.; Dreier, J.; Ruggerone, P., Molecular Rationale behind the Differential Substrate Specificity of Bacterial RND Multi-Drug Transporters. *Scientific Reports* **2017,** *7* (1), 8075.

48. Nikaido, H., Multidrug efflux pumps of gram-negative bacteria. *Journal of bacteriology* **1996,** *178* (20), 5853-5859.

49. Zhang, L.; Li, X. Z.; Poole, K., SmeDEF multidrug efflux pump contributes to intrinsic multidrug resistance in Stenotrophomonas maltophilia. *Antimicrobial agents and chemotherapy* **2001,** *45* (12), 3497-3503.

50. Poole, K., Multidrug efflux pumps and antimicrobial resistance in Pseudomonas aeruginosa and related organisms. *Journal of molecular microbiology and biotechnology* **2001,** *3* (2), 255-264.

51. Masuda, N.; Sakagawa, E.; Ohya, S.; Gotoh, N.; Tsujimoto, H.; Nishino, T., Substrate Specificities of MexAB-OprM, MexCD-OprJ, and MexXY-OprM Efflux Pumps in *Pseudomonas aeruginosa*. *Antimicrobial Agents and Chemotherapy* **2000,** *44* (12), 3322-3327.

52. Sun, X.; Peng, J.; Wang, M.; Wang, J.; Tang, C.; Yang, L.; Lei, H.; Li, F.; Wang, X.; Chen, J., Determination of nine bisphenols in sewage and sludge using dummy molecularly imprinted solid-phase extraction coupled with liquid chromatography tandem mass spectrometry. *Journal of Chromatography A* **2018,** *1552*, 10-16.

53. Luo, Y.; Guo, W.; Ngo, H. H.; Nghiem, L. D.; Hai, F. I.; Zhang, J.; Liang, S.; Wang, X. C., A review on the occurrence of micropollutants in the aquatic environment and their fate and removal during wastewater treatment. *Science of The Total Environment* **2014,** *473-474*, 619-641.

54. Darbre, P. D., *Endocrine disruption and human health*. academic press: 2021.

55. Autrup, H.; Barile, F. A.; Berry, S. C.; Blaauboer, B. J.; Boobis, A.; Bolt, H.; Borgert, C. J.; Dekant, W.; Dietrich, D.; Domingo, J. L., Human exposure to synthetic endocrine disrupting chemicals (S-EDCs) is generally negligible as compared to natural compounds with higher or comparable endocrine activity: how to evaluate the risk of the S-EDCs? *Archives of Toxicology* **2020,** *94*, 2549-2557.

56. Darbre, P. D., The history of endocrine-disrupting chemicals. *Current Opinion in Endocrine and Metabolic Research* **2019,** *7*, 26-33.

57. Schug, T. T.; Janesick, A.; Blumberg, B.; Heindel, J. J., Endocrine disrupting chemicals and disease susceptibility. *J Steroid Biochem Mol Biol* **2011,** *127* (3-5), 204-215.

58. Costa, E. M. F.; Spritzer, P. M.; Hohl, A.; Bachega, T. A., Effects of endocrine disruptors in the development of the female reproductive tract. *Arquivos Brasileiros de Endocrinologia & Metabologia* **2014,** *58*, 153-161.

59. Lauretta, R.; Sansone, A.; Sansone, M.; Romanelli, F.; Appetecchia, M., Endocrine Disrupting Chemicals: Effects on Endocrine Glands. *Frontiers in Endocrinology* **2019,** *10* (178).

60. Birnbaum, L. S., State of the Science of Endocrine Disruptors. *Environmental Health Perspectives* **2013,** *121* (4), a107-a107.

61. Colborn, T.; vom Saal, F. S.; Soto, A. M., Developmental effects of endocrine-disrupting chemicals in wildlife and humans. *Environmental Health Perspectives* **1993,** *101* (5), 378-384.

62. Robaire, B.; Delbes, G.; Head, J. A.; Marlatt, V. L.; Martyniuk, C. J.; Reynaud, S.; Trudeau, V. L.; Mennigen, J. A., A cross-species comparative approach to assessing multi- and transgenerational effects of endocrine disrupting chemicals. *Environmental Research* **2022,** *204*, 112063.

63. Diamanti-Kandarakis, E.; Bourguignon, J.-P.; Giudice, L. C.; Hauser, R.; Prins, G. S.; Soto, A. M.; Zoeller, R. T.; Gore, A. C., Endocrine-disrupting chemicals: an Endocrine Society scientific statement. *Endocrine reviews* **2009,** *30* (4), 293-342.

64. Yaoi, T.; Itoh, K.; Nakamura, K.; Ogi, H.; Fujiwara, Y.; Fushiki, S., Genome-wide analysis of epigenomic alterations in fetal mouse forebrain after exposure to low doses of bisphenol A. *Biochemical and biophysical research communications* **2008,** *376* (3), 563-567.

65. Perera, F.; Tang, W.-y.; Herbstman, J.; Tang, D.; Levin, L.; Miller, R.; Ho, S.-m., Relation of DNA Methylation of 5′-CpG Island of ACSL3 to Transplacental Exposure to Airborne Polycyclic Aromatic Hydrocarbons and Childhood Asthma. *PLOS ONE* **2009,** *4* (2), e4488.

66. Novikova, S. I.; He, F.; Bai, J.; Cutrufello, N. J.; Lidow, M. S.; Undieh, A. S., Maternal Cocaine Administration in Mice Alters DNA Methylation and Gene Expression in Hippocampal Neurons of Neonatal and Prepubertal Offspring. *PLOS ONE* **2008,** *3* (4), e1919.

67. Heindel, J.; Newbold, R., Developmental origins of health and disease: the importance of environmental exposures. *Early Life Origins of Human Health and Disease* **2009**, 42-51.

68. Skinner, M. K.; Manikkam, M.; Guerrero-Bosagna, C., Epigenetic transgenerational actions of environmental factors in disease etiology. *Trends in Endocrinology & Metabolism* **2010,** *21* (4), 214-222.

69. Skinner, M. K., Role of epigenetics in developmental biology and transgenerational inheritance. *Birth Defects Research Part C: Embryo Today: Reviews* **2011,** *93* (1), 51-55.

70. Wu, Q.; Coumoul, X.; Grandjean, P.; Barouki, R.; Audouze, K., Endocrine disrupting chemicals and COVID-19 relationships: A computational systems biology approach. *Environment International* **2021,** *157*, 106232.

71. Liu, Z.-h.; Kanjo, Y.; Mizutani, S., Removal mechanisms for endocrine disrupting compounds (EDCs) in wastewater treatment — physical means, biodegradation, and chemical advanced oxidation: A review. *Science of The Total Environment* **2009,** *407* (2), 731-748.

72. Cajthaml, T., Biodegradation of endocrine-disrupting compounds by ligninolytic fungi: mechanisms involved in the degradation. *Environmental microbiology* **2015,** *17* (12), 4822-4834.

73. Al-Hashimi, A. M., Biodegradation Effect of some Bacterial Isolates on some Endocrine Disruptors (EDCS). *Endocrine* **2018,** *17*, 01.

74. Castellanos, R. M.; Bassin, J. P.; Bila, D. M.; Dezotti, M., Biodegradation of natural and synthetic endocrine-disrupting chemicals by aerobic granular sludge reactor: Evaluating estrogenic activity and estrogens fate. *Environmental Pollution* **2021,** *274*, 116551.

75. Elkins, C. A.; Mullis, L. B., Mammalian Steroid Hormones Are Substrates for the Major RND- and MFS-Type Tripartite Multidrug Efflux Pumps of Escherichia coli. *Journal of Bacteriology* **2006,** *188* (3), 1191-1195.

76. Li, X.; Teske, S.; Conroy-Ben, O., Estrogen mimics induce genes encoding chemical efflux proteins in gram-negative bacteria. *Chemosphere* **2015,** *128*, 327-331.

77. Jayaprada, T.; Hu, J.; Zhang, Y.; Feng, H.; Shen, D.; Geekiyanage, S.; Yao, Y.; Wang, M., The interference of nonylphenol with bacterial cell-to-cell communication. *Environmental Pollution* **2020,** *257*, 113352.

78. Howard, Z. P.; Omsland, A.; Roy, C. R., Selective Inhibition of Coxiella burnetii Replication by the Steroid Hormone Progesterone. *Infection and Immunity* **2020,** *88* (12), e00894-19.

79. Stasinakis, A. S.; Gatidou, G.; Mamais, D.; Thomaidis, N. S.; Lekkas, T. D., Occurrence and fate of endocrine disrupters in Greek sewage treatment plants. *Water Research* **2008,** *42* (6), 1796-1804.

80. Gabet-Giraud, V.; Miège, C.; Choubert, J. M.; Ruel, S. M.; Coquery, M., Occurrence and removal of estrogens and beta blockers by various processes in wastewater treatment plants. *Science of The Total Environment* **2010,** *408* (19), 4257-4269.

81. Česen, M.; Lenarčič, K.; Mislej, V.; Levstek, M.; Kovačič, A.; Cimrmančič, B.; Uranjek, N.; Kosjek, T.; Heath, D.; Dolenc, M. S.; Heath, E., The occurrence and source identification of bisphenol compounds in wastewaters. *Science of The Total Environment* **2018,** *616-617*, 744-752.

82. Froehner, S.; Piccioni, W.; Machado, K. S.; Aisse, M. M., Removal Capacity of Caffeine, Hormones, and Bisphenol by Aerobic and Anaerobic Sewage Treatment. *Water, Air, & Soil Pollution* **2011,** *216* (1), 463-471.

83. Sun, Q.; Wang, Y.; Li, Y.; Ashfaq, M.; Dai, L.; Xie, X.; Yu, C.-P., Fate and mass balance of bisphenol analogues in wastewater treatment plants in Xiamen City, China. *Environmental Pollution* **2017,** *225*, 542-549.

84. Xue, J.; Kannan, K., Mass flows and removal of eight bisphenol analogs, bisphenol A diglycidyl ether and its derivatives in two wastewater treatment plants in New York State, USA. *Science of The Total Environment* **2019,** *648*, 442-449.

85. Al-Saleh, I.; Elkhatib, R.; Al-Rajoudi, T.; Al-Qudaihi, G., Assessing the concentration of phthalate esters (PAEs) and bisphenol A (BPA) and the genotoxic potential of treated wastewater (final effluent) in Saudi Arabia. *Science of The Total Environment* **2017,** *578*, 440-451.

86. Česen, M.; Ahel, M.; Terzić, S.; Heath, D. J.; Heath, E., The occurrence of contaminants of emerging concern in Slovenian and Croatian wastewaters and receiving Sava river. *Science of The Total Environment* **2019,** *650*, 2446-2453.

87. Lee, S.; Liao, C.; Song, G.-J.; Ra, K.; Kannan, K.; Moon, H.-B., Emission of bisphenol analogues including bisphenol A and bisphenol F from wastewater treatment plants in Korea. *Chemosphere* **2015,** *119*, 1000-1006.

88. Pang, L.; Yang, H.; Lv, L.; Liu, S.; Gu, W.; Zhou, Y.; Wang, Y.; Yang, P.; Zhao, H.; Guo, L.; Dong, J., Occurrence and Estrogenic Potency of Bisphenol Analogs in Sewage Sludge from Wastewater Treatment Plants in Central China. *Archives of Environmental Contamination and Toxicology* **2019,** *77* (3), 461-470.

89. Karthikraj, R.; Kannan, K., Mass loading and removal of benzotriazoles, benzothiazoles, benzophenones, and bisphenols in Indian sewage treatment plants. *Chemosphere* **2017,** *181*, 216-223.

90. Karnjanapiboonwong, A.; Suski, J. G.; Shah, A. A.; Cai, Q.; Morse, A. N.; Anderson, T. A., Occurrence of PPCPs at a Wastewater Treatment Plant and in Soil and Groundwater at a Land Application Site. *Water, Air, & Soil Pollution* **2011,** *216* (1), 257-273.

91. Belhaj, D.; Athmouni, K.; Jerbi, B.; Kallel, M.; Ayadi, H.; Zhou, J. L., Estrogenic compounds in Tunisian urban sewage treatment plant: occurrence, removal and

ecotoxicological impact of sewage discharge and sludge disposal. *Ecotoxicology (London, England)* **2016,** *25* (10), 1849-1857.

92. Saeed, T.; Al-Jandal, N.; Abusam, A.; Taqi, H.; Al-Khabbaz, A.; Zafar, J., Sources and levels of endocrine disrupting compounds (EDCs) in Kuwait's coastal areas. *Marine Pollution Bulletin* **2017,** *118* (1), 407-412.

93. Damkjaer, K.; Weisser, J. J.; Msigala, S. C.; Mdegela, R.; Styrishave, B., Occurrence, removal and risk assessment of steroid hormones in two wastewater stabilization pond systems in Morogoro, Tanzania. *Chemosphere* **2018,** *212*, 1142-1154.

94. Yien Fang, T.; Praveena, S. M.; Aris, A. Z.; Syed Ismail, S. N.; Rasdi, I., Quantification of selected steroid hormones (17β-Estradiol and 17α-Ethynylestradiol) in wastewater treatment plants in Klang Valley (Malaysia). *Chemosphere* **2019,** *215*, 153-162.

95. Zhou, Y.; Zha, J.; Wang, Z., Occurrence and fate of steroid estrogens in the largest wastewater treatment plant in Beijing, China. *Environ Monit Assess* **2012,** *184* (11), 6799-813.

96. Zhu, B.; Ben, W.; Yuan, X.; Zhang, Y.; Yang, M.; Qiang, Z., Simultaneous detection of endocrine disrupting chemicals including conjugates in municipal wastewater and sludge with enhanced sample pretreatment and UPLC-MS/MS. *Environmental Science: Processes & Impacts* **2015,** *17* (8), 1377-1385.

97. Gao, D.; Li, Z.; Guan, J.; Liang, H., Seasonal variations in the concentration and removal of nonylphenol ethoxylates from the wastewater of a sewage treatment plant. *Journal of Environmental Sciences* **2017,** *54*, 217-223.

98. Carvalho, A. R.; Cardoso, V.; Rodrigues, A.; Benoliel, M. J.; Duarte, E., Fate and Analysis of Endocrine-Disrupting Compounds in a Wastewater Treatment Plant in Portugal. *Water, Air, & Soil Pollution* **2016,** *227* (6), 202.

99. Rose, K.; Farenhorst, A.; Claeys, A.; Ascef, B., *17 β-estradiol and 17 α-ethinylestradiol mineralization in sewage sludge and biosolids*. 2014; Vol. 49.

100. EPA, U., Estimation programs interface suite™ for Microsoft® windows, v 4.11. *United States Environmental Protection Agency, Washington, DC, USA* **2012**.

101. Block, S. S., *Disinfection, sterilization, and preservation*. Lippincott Williams & Wilkins: 2001.

102. Maillard, J.-Y., Bacterial target sites for biocide action. *Journal of Applied Microbiology* **2002,** *92* (s1), 16S-27S.

103. Bolton, E. T.; Mandel, H. G., The effects of 6-mercaptopurine on biosynthesis in Escherichia coli. *Journal of Biological Chemistry* **1957,** *227* (2), 833-844.

104. Pabst, M. J.; Somerville, R. L., A Comparison of Hydroxylamine and N-Methylhydroxylamine as Probes for the Mechanism of Action of the Anthranilate Synthetase of Escherichia coli. *Journal of Biological Chemistry* **1971,** *246* (23), 7214-7216.

105. Krishnaswamy, M.; Purushothaman, K. K., Plumbagin: a study of its anticancer, antibacterial and antifungal properties. *Indian J Exp Biol* **1980,** *18* (8), 876-877.

106. LaVelle, J. M., Potassium chromate potentiates frameshift mutagenesis in E. coli and S. typhimurium. *Mutation Research/Genetic Toxicology* **1986,** *171* (1), 1-10.

107. Tsuchiya, H.; Sato, M.; Kameyama, Y.; Takagi, N.; Namikawa, I., Effect of lidocaine on phospholipid and fatty acid composition of bacterial membranes. *Letters in Applied Microbiology* **1987,** *4* (6), 141-144.

108. Voogd, C. E., Azathioprine, a genotoxic agent to be considered non-genotoxic in man. *Mutation Research/Reviews in Genetic Toxicology* **1989,** *221* (2), 133-152.

109. Kuyyakanond, T.; Quesnel, L. B., The mechanism of action of chlorhexidine. *FEMS Microbiology Letters* **1992,** *100* (1-3), 211-215.

110. Ong, K. C.; Khoo, H.-E., Biological effects of myricetin. *General Pharmacology: The Vascular System* **1997,** *29* (2), 121-126.

111. Lushchak, V. I., Oxidative Stress and Mechanisms of Protection Against It in Bacteria. *Biochemistry (Moscow)* **2001,** *66* (5), 476-489.

112. Yamane, A., MagiProbe: a novel fluorescence quenching-based oligonucleotide probe carrying a fluorophore and an intercalator. *Nucleic Acids Research* **2002,** *30* (19), e97-e97.

113. Gaynor, M.; Mankin, A. S., Macrolide antibiotics: binding site, mechanism of action, resistance. *Current topics in medicinal chemistry* **2003,** *3* (9), 949-960.

114. Blondeau, J. M., Fluoroquinolones: mechanism of action, classification, and development of resistance. *Survey of Ophthalmology* **2004,** *49* (2, Supplement 2), S73-S78.

115. Borkow, G.; Gabbay, J., Putting copper into action: copper-impregnated products with potent biocidal activities. *The FASEB Journal* **2004,** *18* (14), 1728-1730.

116. Ioannou, C. J.; Hanlon, G. W.; Denyer, S. P., Action of Disinfectant Quaternary Ammonium Compounds against *Staphylococcus aureus*. *Antimicrobial Agents and Chemotherapy* **2007,** *51* (1), 296-306.

117. Pérez, J. M.; Calderón, I. L.; Arenas, F. A.; Fuentes, D. E.; Pradenas, G. A.; Fuentes, E. L.; Sandoval, J. M.; Castro, M. E.; Elías, A. O.; Vásquez, C. C., Bacterial Toxicity of Potassium Tellurite: Unveiling an Ancient Enigma. *PLOS ONE* **2007,** *2* (2), e211.

118. Sauriasari, R.; Wang, D.-H.; Takemura, Y.; Tsutsui, K.; Masuoka, N.; Sano, K.; Horita, M.; Wang, B.-L.; Ogino, K., Cytotoxicity of lawsone and cytoprotective activity of antioxidants in catalase mutant Escherichia coli. *Toxicology* **2007,** *235* (1), 103-111.

119. Durante-Mangoni, E.; Grammatikos, A.; Utili, R.; Falagas, M. E., Do we still need the aminoglycosides? *International Journal of Antimicrobial Agents* **2009,** *33* (3), 201-205.

120. Jeyachandran, R.; Mahesh, A.; Cindrella, L.; Sudhakar, S.; Pazhanichamy, K., Antibacterial activity of plumbagin and root extracts of Plumbago zeylanica L. *Acta Biologica Cracoviensia Series Botanica* **2009,** *51* (1), 17-22.

121. Hilf, R. J. C.; Bertozzi, C.; Zimmermann, I.; Reiter, A.; Trauner, D.; Dutzler, R., Structural basis of open channel block in a prokaryotic pentameric ligand-gated ion channel. *Nature Structural & Molecular Biology* **2010,** *17* (11), 1330-1336.

122. Prachayasittikul, V.; Prachayasittikul, S.; Ruchirawat, S.; Prachayasittikul, V., 8-Hydroxyquinolines: a review of their metal chelating properties and medicinal applications. *Drug Des Devel Ther* **2013,** *7*, 1157-1178.

123. Worthington, R. J.; Melander, C., Overcoming Resistance to β-Lactam Antibiotics. *The Journal of Organic Chemistry* **2013,** *78* (9), 4207-4213.

124. Nguyen, F.; Starosta, A. L.; Arenz, S.; Sohmen, D.; Dönhöfer, A.; Wilson, D. N., Tetracycline antibiotics and resistance mechanisms. *Biological Chemistry* **2014,** *395* (5), 559-575.

125. Virk, B.; Jia, J.; Maynard, C. A.; Raimundo, A.; Lefebvre, J.; Richards, S. A.; Chetina, N.; Liang, Y.; Helliwell, N.; Cipinska, M.; Weinkove, D., Folate Acts in E. coli to Accelerate C. elegans Aging Independently of Bacterial Biosynthesis. *Cell Reports* **2016,** *14* (7), 1611-1620.

126. Lima, L. M.; Silva, B. N. M. d.; Barbosa, G.; Barreiro, E. J., β-lactam antibiotics: An overview from a medicinal chemistry perspective. *European Journal of Medicinal Chemistry* **2020,** *208*, 112829.

127. Mao, X.; Auer, D. L.; Buchalla, W.; Hiller, K.-A.; Maisch, T.; Hellwig, E.; Al-Ahmad, A.; Cieplik, F., Cetylpyridinium Chloride: Mechanism of Action, Antimicrobial Efficacy in Biofilms, and Potential Risks of Resistance. *Antimicrobial Agents and Chemotherapy* **2020,** *64* (8), e00576-20.

128. Gorman, S. P.; Scott, E. M.; Russell, A. D., Antimicrobial Activity, Uses and Mechanism of Action of Glutaraldehyde. *Journal of Applied Bacteriology* **1980,** *48* (2), 161-190.

129. Grace, J. L.; Huang, J. X.; Cheah, S.-E.; Truong, N. P.; Cooper, M. A.; Li, J.; Davis, T. P.; Quinn, J. F.; Velkov, T.; Whittaker, M. R., Antibacterial low molecular weight cationic polymers: Dissecting the contribution of hydrophobicity, chain length and charge to activity. *RSC advances* **2016,** *6* (19), 15469-15477.

130. Savage, P. B., Multidrug-resistant bacteria: overcoming antibiotic permeability barriers of Gram-negative bacteria. *Annals of Medicine* **2001,** *33* (3), 167-171.

131. Gilbert, P.; Pemberton, D.; Wilkinson, D. E., Barrier properties of the gram-negative cell envelope towards high molecular weight polyhexamethylene biguanides. *The Journal of applied bacteriology* **1990,** *69* (4), 585-92.

132. Pulvertaft, R. J. V.; Lumb, G. D., Bacterial lysis and antiseptics. *J Hyg (Lond)* **1948,** *46* (1), 62-64.

133. Kristoffersen, T., Mode of Action of Hypochlorite Sanitizers with and without Sodium Bromide1. *Journal of Dairy Science* **1958,** *41* (7), 942-949.

134. Venkobachar, C.; Iyengar, L.; Prabhakara Rao, A. V. S., Mechanism of disinfection: Effect of chlorine on cell membrane functions. *Water Research* **1977,** *11* (8), 727-729.

135. Darville, T.; Yamauchi, T., The Cephalosporin Antibiotics. *Pediatrics In Review* **1994,** *15* (2), 54-62.

136. Tomlinson, E.; Brown, M. R.; Davis, S. S., Effect of colloidal association on the measured activity of alkylbenzyldimethylammonium chlorides against Pseudomonas aeruginosa. *Journal of medicinal chemistry* **1977,** *20* (10), 1277-82.

137. Roy-Burman, P., *Analogues of nucleic acid components: Mechanisms of action*. Springer Science & Business Media: 2012; Vol. 25.

138. Finnegan, S.; Percival, S. L., EDTA: An Antimicrobial and Antibiofilm Agent for Use in Wound Care. *Adv Wound Care (New Rochelle)* **2015,** *4* (7), 415-421.

139. Zhou, Y.-J.; Zhang, M.-X.; Hider, R. C.; Zhou, T., In vitro antimicrobial activity of hydroxypyridinone hexadentate-based dendrimeric chelators alone and in combination with norfloxacin. *FEMS Microbiology Letters* **2014,** *355* (2), 124-130.

140. L.S. Santos, A.; L. Sodre, C.; S. Valle, R.; A. Silva, B.; A. Abi-chacra, E.; V. Silva, L.; L. Souza-Goncalves, A.; S. Sangenito, L.; S. Goncalves, D.; O.P. Souza, L.; F. Palmeira, V.; d, M.; apos; Avila-Levy, C.; F. Kneipp, L.; Kellett, A.; McCann, M.; H. Branquinha, M., Antimicrobial Action of Chelating Agents: Repercussions on the Microorganism Development, Virulence and Pathogenesis. *Current Medicinal Chemistry* **2012,** *19* (17), 2715-2737.

141. Tenson, T.; Lovmar, M.; Ehrenberg, M., The Mechanism of Action of Macrolides, Lincosamides and Streptogramin B Reveals the Nascent Peptide Exit Path in the Ribosome. *Journal of molecular biology* **2003,** *330* (5), 1005-1014.

142. Mingeot-Leclercq, M.-P.; Glupczynski, Y.; Tulkens, P. M., Aminoglycosides: Activity and Resistance. *Antimicrobial Agents and Chemotherapy* **1999,** *43* (4), 727-737.

143. Macomber, L.; Imlay, J. A., The iron-sulfur clusters of dehydratases are primary intracellular targets of copper toxicity. *Proceedings of the National Academy of Sciences* **2009,** *106* (20), 8344-8349.

144. Acar, J. F., Antibiotic Synergy and Antagonism. *Medical Clinics of North America* **2000,** *84* (6), 1391-1406.

145. Lee, H.-J.; Kim, H.-E.; Lee, C., Combination of cupric ion with hydroxylamine and hydrogen peroxide for the control of bacterial biofilms on RO membranes. *Water Research* **2017,** *110*, 83-90.

146. Hema, M.; Princy, S. A.; Sridharan, V.; Vinoth, P.; Balamurugan, P.; Sumana, M., Synergistic activity of quorum sensing inhibitor, pyrizine-2-carboxylic acid and antibiotics against multi-drug resistant V. cholerae. *RSC advances* **2016,** *6* (51), 45938-45946.

147. Qu, S.; Dai, C.; Shen, Z.; Tang, Q.; Wang, H.; Zhai, B.; Zhao, L.; Hao, Z., Mechanism of Synergy Between Tetracycline and Quercetin Against Antibiotic Resistant Escherichia coli. *Front Microbiol* **2019,** *10* (2536).

148. Askoura, M.; Mattawa, W.; Abujamel, T.; Taher, I., Efflux pump inhibitors (EPIs) as new antimicrobial agents against Pseudomonas aeruginosa. *Libyan Journal of Medicine* **2011,** *6* (1), 5870.

149. Lamut, A.; Peterlin Mašič, L.; Kikelj, D.; Tomašič, T., Efflux pump inhibitors of clinically relevant multidrug resistant bacteria. *Medicinal Research Reviews* **2019,** *39* (6), 2460-2504.

150. Zgurskaya, H. I.; Walker, J. K.; Parks, J. M.; Rybenkov, V. V., Multidrug Efflux Pumps and the Two-Faced Janus of Substrates and Inhibitors. *Accounts of Chemical Research* **2021,** *54* (4), 930-939.

151. Lomovskaya, O.; Warren, M. S.; Lee, A.; Galazzo, J.; Fronko, R.; Lee, M.; Blais, J.; Cho, D.; Chamberland, S.; Renau, T.; Leger, R.; Hecker, S.; Watkins, W.; Hoshino, K.; Ishida, H.; Lee, V. J., Identification and Characterization of Inhibitors of Multidrug Resistance Efflux Pumps in Pseudomonas aeruginosa: Novel Agents for Combination Therapy. *Antimicrobial Agents and Chemotherapy* **2001,** *45* (1), 105-116.

152. Pagès, J.-M.; Masi, M.; Barbe, J., Inhibitors of efflux pumps in Gram-negative bacteria. *Trends in Molecular Medicine* **2005,** *11* (8), 382-389.

153. Chaudhary, M., A novel approach to combat acquired multiple resistance in Escherichia coli by using EDTA pump inhibitor. *J. Microb. Biotech.* **2012,** *4*, 126-130.

154. Abdali, N.; Parks, J. M.; Haynes, K. M.; Chaney, J. L.; Green, A. T.; Wolloscheck, D.; Walker, J. K.; Rybenkov, V. V.; Baudry, J.; Smith, J. C.; Zgurskaya, H. I., Reviving Antibiotics: Efflux Pump Inhibitors That Interact with AcrA, a Membrane Fusion Protein of the AcrAB-TolC Multidrug Efflux Pump. *ACS Infectious Diseases* **2017,** *3* (1), 89-98.

155. Zloh, M.; Kaatz, G. W.; Gibbons, S., Inhibitors of multidrug resistance (MDR) have affinity for MDR substrates. *Bioorganic & Medicinal Chemistry Letters* **2004,** *14* (4), 881-885.

156. Tohidpour, A.; Najar Peerayeh, S.; Mehrabadi, J. F.; Rezaei Yazdi, H., Determination of the Efflux Pump-Mediated Resistance Prevalence in Pseudomonas aeruginosa, Using an Efflux Pump Inhibitor. *Current Microbiology* **2009,** *59* (3), 352-355.

157. Sharma, A.; Gupta, V. K.; Pathania, R., Efflux pump inhibitors for bacterial pathogens: From bench to bedside. *Indian J Med Res* **2019,** *149* (2), 129-145.

158. Osei Sekyere, J.; Amoako, D. G., Carbonyl Cyanide m-Chlorophenylhydrazine (CCCP) Reverses Resistance to Colistin, but Not to Carbapenems and Tigecycline in Multidrug-Resistant Enterobacteriaceae. *Front Microbiol* **2017,** *8*, 228-228.

159. Franke, S.; Grass, G.; Rensing, C.; Nies, D. H., Molecular Analysis of the Copper-Transporting Efflux System CusCFBA of *Escherichia coli*. *Journal of Bacteriology* **2003,** *185* (13), 3804-3812.

160. Nishino, K.; Yamaguchi, A., Analysis of a complete library of putative drug transporter genes in Escherichia coli. *Journal of bacteriology* **2001,** *183* (20), 5803-5812.

161. Tikhonova, E. B.; Zgurskaya, H. I., AcrA, AcrB, and TolC of *Escherichia coli* Form a Stable Intermembrane Multidrug Efflux Complex. *Journal of Biological Chemistry* **2004,** *279* (31), 32116-32124.

162. Lau, S. Y.; Zgurskaya, H. I., Cell Division Defects in *Escherichia coli* Deficient in the Multidrug Efflux Transporter AcrEF-TolC. *Journal of Bacteriology* **2005,** *187* (22), 7815-7825.

163. Aires, J. R.; Nikaido, H., Aminoglycosides are captured from both periplasm and cytoplasm by the AcrD multidrug efflux transporter of Escherichia coli. *Journal of bacteriology* **2005,** *187* (6), 1923-1929.

164. Baranova, N.; Nikaido, H., The baeSR two-component regulatory system activates transcription of the yegMNOB (mdtABCD) transporter gene cluster in Escherichia coli and increases its resistance to novobiocin and deoxycholate. *Journal of bacteriology* **2002,** *184* (15), 4168-4176.

165. Saier, M. H., Jr; Reddy, V. S.; Moreno-Hagelsieb, G.; Hendargo, K. J.; Zhang, Y.; Iddamsetty, V.; Lam, Katie Jing K.; Tian, N.; Russum, S.; Wang, J.; Medrano-Soto, A., The Transporter Classification Database (TCDB): 2021 update. *Nucleic Acids Research* **2020,** *49* (D1), D461-D467.

166. Zhang, Y.; Xiao, M.; Horiyama, T.; Zhang, Y.; Li, X.; Nishino, K.; Yan, A., The Multidrug Efflux Pump MdtEF Protects against Nitrosative Damage during the Anaerobic Respiration in Escherichia coli. *Journal of Biological Chemistry* **2011,** *286* (30), 26576-26584.

167. Deng, Z.; Shan, Y.; Pan, Q.; Gao, X.; Yan, A., Anaerobic expression of the gadE-mdtEF multidrug efflux operon is primarily regulated by the two-component system ArcBA through antagonizing the H-NS mediated repression. *Front Microbiol* **2013,** *4*.

168. Nishino, K.; Senda, Y.; Yamaguchi, A.; Nishino, K.; Yamaguchi, A.; Nishino, K.; Yamaguchi, A., The AraC-family regulator GadX enhances multidrug resistance in Escherichia coli by activating expression of mdtEF multidrug efflux genes. *Journal of Infection and Chemotherapy* **2008,** *14* (1), 23-29.

169. Masuda, N.; Church, G. M., Regulatory network of acid resistance genes in Escherichia coli. *Molecular Microbiology* **2003,** *48* (3), 699-712.

170. Kobayashi, A.; Hirakawa, H.; Hirata, T.; Nishino, K.; Yamaguchi, A., Growth Phase-Dependent Expression of Drug Exporters in Escherichia coli and Its Contribution to Drug Tolerance. *Journal of Bacteriology* **2006,** *188* (16), 5693-5703.

171. Sun, J.; Deng, Z.; Fung, D. K. C.; Yan, A., Study of the Expression of Bacterial Multidrug Efflux Pumps in Anaerobic Conditions. In *Bacterial Multidrug Exporters:*

Methods and Protocols, Yamaguchi, A.; Nishino, K., Eds. Springer New York: New York, NY, 2018; pp 253-268.

172. Swain, M., Chemicalize. org. ACS Publications: 2012.

173. Ma, D.; Cook, D. N.; Alberti, M.; Pon, N. G.; Nikaido, H.; Hearst, J. E., Genes acrA and acrB encode a stress-induced efflux system of Escherichia coli. *Molecular Microbiology* **1995,** *16* (1), 45-55.

174. Bohnert, J. A.; Schuster, S.; Fähnrich, E.; Trittler, R.; Kern, W. V., Altered spectrum of multidrug resistance associated with a single point mutation in the Escherichia coli RND-type MDR efflux pump YhiV (MdtF). *Journal of Antimicrobial Chemotherapy* **2006,** *59* (6), 1216-1222.

175. Yanisch-Perron, C.; Vieira, J.; Messing, J., Improved M13 phage cloning vectors and host strains: nucleotide sequences of the M13mp18 and pUC19 vectors. *Gene* **1985,** *33* (1), 103-19.

176. Pundir, S.; Martin, M. J.; O'Donovan, C., UniProt protein knowledgebase. In *Protein Bioinformatics*, Springer: 2017; pp 41-55.

177. Artimo, P.; Jonnalagedda, M.; Arnold, K.; Baratin, D.; Csardi, G.; de Castro, E.; Duvaud, S.; Flegel, V.; Fortier, A.; Gasteiger, E.; Grosdidier, A.; Hernandez, C.; Ioannidis, V.; Kuznetsov, D.; Liechti, R.; Moretti, S.; Mostaguir, K.; Redaschi, N.; Rossier, G.; Xenarios, I.; Stockinger, H., ExPASy: SIB bioinformatics resource portal. *Nucleic Acids Research* **2012,** *40* (W1), W597-W603.

178. Kyte, J.; Doolittle, R. F., A simple method for displaying the hydropathic character of a protein. *Journal of molecular biology* **1982,** *157* (1), 105-132.

179. Waterhouse, A.; Bertoni, M.; Bienert, S.; Studer, G.; Tauriello, G.; Gumienny, R.; Heer, F. T.; de Beer, T. A. P.; Rempfer, C.; Bordoli, L., SWISS-MODEL: homology modelling of protein structures and complexes. *Nucleic acids research* **2018,** *46* (W1), W296-W303.

180. Nakashima, R.; Sakurai, K.; Yamasaki, S.; Nishino, K.; Yamaguchi, A., Structures of the multidrug exporter AcrB reveal a proximal multisite drug-binding pocket. *Nature* **2011,** *480* (7378), 565-569.

181. Haynes, W. M.; Lide, D. R.; Bruno, T. J., *CRC handbook of chemistry and physics*. CRC press: 2016.

182. Krivák, R.; Hoksza, D., P2Rank: machine learning based tool for rapid and accurate prediction of ligand binding sites from protein structure. *Journal of Cheminformatics* **2018,** *10* (1), 39.

183. ChemAxon, ChemAxon–Software solutions and services for chemistry and biology. ChemAxon: 2016.

184. Gasteiger, E.; Gattiker, A.; Hoogland, C.; Ivanyi, I.; Appel, R. D.; Bairoch, A., ExPASy: the proteomics server for in-depth protein knowledge and analysis. *Nucleic Acids Research* **2003,** *31* (13), 3784-3788.

185. Kozlowski, L. P., IPC–isoelectric point calculator. *Biology direct* **2016,** *11* (1), 1-16.

186. Vargiu, A. V.; Nikaido, H., Multidrug binding properties of the AcrB efflux pump characterized by molecular dynamics simulations. *Proceedings of the National Academy of Sciences* **2012,** *109* (50), 20637-20642.

187. Wilks, J. C.; Slonczewski, J. L., pH of the Cytoplasm and Periplasm of *Escherichia coli*: Rapid Measurement by Green Fluorescent Protein Fluorimetry. *Journal of Bacteriology* **2007,** *189* (15), 5601-5607.

188. Koita, K.; Rao, C. V., Identification and Analysis of the Putative Pentose Sugar Efflux Transporters in Escherichia coli. *PLOS ONE* **2012,** *7* (8), e43700.

189. Sulavik, M. C.; Houseweart, C.; Cramer, C.; Jiwani, N.; Murgolo, N.; Greene, J.; DiDomenico, B.; Shaw, K. J.; Miller, G. H.; Hare, R.; Shimer, G., Antibiotic Susceptibility Profiles of Escherichia coli Strains Lacking Multidrug Efflux Pump Genes. *Antimicrobial Agents and Chemotherapy* **2001,** *45* (4), 1126-1136.

190. Adler, J.; Bibi, E., Determinants of Substrate Recognition by the *Escherichia coli* Multidrug Transporter MdfA Identified on Both Sides of the Membrane *. *Journal of Biological Chemistry* **2004,** *279* (10), 8957-8965.

191. Cheng, Q.; Park, J. T., Substrate Specificity of the AmpG Permease Required for Recycling of Cell Wall Anhydro-Muropeptides. *Journal of Bacteriology* **2002,** *184* (23), 6434-6436.

192. Geer, L. Y.; Marchler-Bauer, A.; Geer, R. C.; Han, L.; He, J.; He, S.; Liu, C.; Shi, W.; Bryant, S. H., The NCBI biosystems database. *Nucleic acids research* **2010,** *38* (suppl_1), D492-D496.

193. Rosenberg, E. Y.; Bertenthal, D.; Nilles, M. L.; Bertrand, K. P.; Nikaido, H., Bile salts and fatty acids induce the expression of Escherichia coli AcrAB multidrug efflux pump through their interaction with Rob regulatory protein. *Molecular Microbiology* **2003,** *48* (6), 1609-1619.

194. Cremers, C. M.; Knoefler, D.; Vitvitsky, V.; Banerjee, R.; Jakob, U., Bile salts act as effective protein-unfolding agents and instigators of disulfide stress in vivo. *Proceedings of the National Academy of Sciences* **2014,** *111* (16), E1610-E1619.

195. Hirakawa, H.; Inazumi, Y.; Senda, Y.; Kobayashi, A.; Hirata, T.; Nishino, K.; Yamaguchi, A., N-Acetyl-d-Glucosamine Induces the Expression of Multidrug Exporter Genes, mdtEF, via Catabolite Activation in Escherichia coli. *Journal of Bacteriology* **2006,** *188* (16), 5851-5858.

196. Gallo Cassarino, T.; Bordoli, L.; Schwede, T., Assessment of ligand binding site predictions in CASP10. *Proteins: Structure, Function, and Bioinformatics* **2014,** *82*, 154-163.

197. Haas, J.; Roth, S.; Arnold, K.; Kiefer, F.; Schmidt, T.; Bordoli, L.; Schwede, T., The Protein Model Portal—a comprehensive resource for protein structure and model information. *Database* **2013,** *2013*.

198. Neuvirth, H.; Raz, R.; Schreiber, G., ProMate: A Structure Based Prediction Program to Identify the Location of Protein–Protein Binding Sites. *Journal of molecular biology* **2004,** *338* (1), 181-199.

199. Ma, B.; Shatsky, M.; Wolfson, H. J.; Nussinov, R., Multiple diverse ligands binding at a single protein site: a matter of pre-existing populations. *Protein science* **2002,** *11* (2), 184-197.

200. Arkin, M. R.; Wells, J. A., Small-molecule inhibitors of protein–protein interactions: progressing towards the dream. *Nature reviews Drug discovery* **2004,** *3* (4), 301-317.

201. Paul, D.; Chakraborty, R.; Mandal, S. M., Biocides and health-care agents are more than just antibiotics: Inducing cross to co-resistance in microbes. *Ecotoxicology and Environmental Safety* **2019,** *174*, 601-610.

202. Ribeiro da Cunha, B.; Fonseca, L. P.; Calado, C. R. C., Antibiotic Discovery: Where Have We Come from, Where Do We Go? *Antibiotics* **2019,** *8* (2), 45.

203. Ye, M.; Sun, M.; Huang, D.; Zhang, Z.; Zhang, H.; Zhang, S.; Hu, F.; Jiang, X.; Jiao, W., A review of bacteriophage therapy for pathogenic bacteria inactivation in the soil environment. *Environment International* **2019,** *129*, 488-496.

204. Soni, A.; Choi, J.; Brightwell, G., Plasma-Activated Water (PAW) as a Disinfection Technology for Bacterial Inactivation with a Focus on Fruit and Vegetables. *Foods* **2021,** *10* (1), 166.

205. Živec, P.; Perdih, F.; Turel, I.; Giester, G.; Psomas, G., Different types of copper complexes with the quinolone antimicrobial drugs ofloxacin and norfloxacin: Structure, DNA-and albumin-binding. *Journal of inorganic biochemistry* **2012,** *117*, 35-47.

206. Fernández-González, A.; Badía, R.; Díaz-García, M. E., Insights into the reaction of β-lactam antibiotics with copper (II) ions in aqueous and micellar media: Kinetic and spectrometric studies. *Analytical biochemistry* **2005,** *341* (1), 113-121.

207. Szczepanik, W.; Kaczmarek, P.; Jeżowska-Bojczuk, M., Oxidative activity of copper (II) complexes with aminoglycoside antibiotics as implication to the toxicity of these drugs. *Bioinorganic chemistry and applications* **2004,** *2* (1-2), 55-68.

208. Herisse, M.; Duverger, Y.; Martin-Verstraete, I.; Barras, F.; Ezraty, B., Silver potentiates aminoglycoside toxicity by enhancing their uptake. *Molecular microbiology* **2017,** *105* (1), 115-126.

209. Morones-Ramirez, J. R.; Winkler, J. A.; Spina, C. S.; Collins, J. J., Silver enhances antibiotic activity against gram-negative bacteria. *Science translational medicine* **2013,** *5* (190), 190ra81-190ra81.

210. Morioka, H.; Tachibana, M.; Machino, M.; Suganuma, A., Polymyxin B binding sites in Escherichia coli as revealed by polymyxin B-gold labeling. *Journal of Histochemistry & Cytochemistry* **1987,** *35* (2), 229-231.

211. Dinger, M. B.; Henderson, W., Organogold (III) metallacyclic chemistry. Part 4. Synthesis, characterisation, and biological activity of gold (III)-thiosalicylate and-salicylate complexes. *Journal of organometallic chemistry* **1998,** *560* (1), 233-243.

212. Bachmann, B. J., Derivations and genotypes of some mutant derivatives of Escherichia coli K-12. *Escherichia coli and Salmonella: cellular and molecular biology, 2nd ed. ASM Press, Washington, DC* **1996**, 2460-2488.

213. Chou, T.-C., Theoretical Basis, Experimental Design, and Computerized Simulation of Synergism and Antagonism in Drug Combination Studies. *Pharmacological Reviews* **2006,** *58* (3), 621-681.

214. Lestari, M. F. W. L. A., Synergism Effect of Antibiotics and Silver Nanoparticles to Control Antibiotic Resistant Bacteria: A Mini Review. **2021**.

215. Kumar, V.; Upadhyay, N.; Manhas, A., Designing, syntheses, characterization, computational study and biological activities of silver-phenothiazine metal complex. *Journal of Molecular Structure* **2015,** *1099*, 135-141.

216. Giachino, A.; Waldron, K. J., Copper tolerance in bacteria requires the activation of multiple accessory pathways. *Molecular Microbiology* **2020,** *114* (3), 377-390.

217. Griffith, J. M.; Basting, P. J.; Bischof, K. M.; Wrona, E. P.; Kunka, K. S.; Tancredi, A. C.; Moore, J. P.; Hyman, M. R. L.; Slonczewski, J. L.; Parales, R. E., Experimental Evolution of Escherichia coli K-12 in the Presence of Proton Motive Force (PMF) Uncoupler Carbonyl Cyanide *m*-Chlorophenylhydrazone Selects for Mutations

Affecting PMF-Driven Drug Efflux Pumps. *Applied and environmental microbiology* **2019,** *85* (5), e02792-18.

218. Babula, P.; Vanco, J.; Krejcova, L.; Hynek, D.; Sochor, J.; Adam, V.; Trnkova, L.; Hubalek, J.; Kizek, R., Voltammetric characterization of Lawsone-Copper (II) ternary complexes and their interactions with dsDNA. *International Journal of Electrochemical Science* **2012,** *7* (8), 7349-7366.

219. Huttner, B.; Jones, M.; Rubin, M. A.; Neuhauser, M. M.; Gundlapalli, A.; Samore, M., Drugs of Last Resort? The Use of Polymyxins and Tigecycline at US Veterans Affairs Medical Centers, 2005–2010. *PLOS ONE* **2012,** *7* (5), e36649.

220. Muñoz-Villagrán, C.; Contreras, F.; Cornejo, F.; Figueroa, M.; Valenzuela-Bezanilla, D.; Luraschi, R.; Reinoso, C.; Rivas-Pardo, J.; Vásquez, C.; Castro, M.; Arenas, F., Understanding gold toxicity in aerobically-grown Escherichia coli. *Biol Res* **2020,** *53* (1), 26-26.

221. Sudeshna, G.; Parimal, K., Multiple non-psychiatric effects of phenothiazines: A review. *European Journal of Pharmacology* **2010,** *648* (1), 6-14.

222. Kristiansen, J. E.; Dastidar, S. G.; Palchoudhuri, S.; Roy, D. S.; Das, S.; Hendricks, O.; Christensen, J. B., Phenothiazines as a solution for multidrug resistant tuberculosis: From the origin to present. *International microbiology : the official journal of the Spanish Society for Microbiology* **2015,** *18* (1), 1-12.

223. Rao, P. P.; Pham, A. T.; Shakeri, A., Discovery of small molecules for the treatment of Alzheimer's disease. In *Small Molecule Drug Discovery*, Elsevier: 2020; pp 289-322.

224. Das Gupta, A.; Dastidar, S.; Shirataki, Y.; Motohashi, N., Antibacterial Activity of Artificial Phenothiazines and Isoflavones from Plants. 2008; Vol. 15, pp 67-132.

225. Amaral, L.; Kristiansen, J. E.; Viveiros, M.; Atouguia, J., Activity of phenothiazines against antibiotic-resistant Mycobacterium tuberculosis: a review supporting further studies that may elucidate the potential use of thioridazine as anti-tuberculosis therapy. *The Journal of antimicrobial chemotherapy* **2001,** *47* (5), 505-11.

226. Martins, M.; Dastidar, S. G.; Fanning, S.; Kristiansen, J. E.; Molnar, J.; Pagès, J.-M.; Schelz, Z.; Spengler, G.; Viveiros, M.; Amaral, L., Potential role of non-antibiotics (helper compounds) in the treatment of multidrug-resistant Gram-negative infections: mechanisms for their direct and indirect activities. *International Journal of Antimicrobial Agents* **2008,** *31* (3), 198-208.

227. Dupont, C. L.; Grass, G.; Rensing, C., Copper toxicity and the origin of bacterial resistance—new insights and applications†. *Metallomics* **2011,** *3* (11), 1109-1118.

228. Zhang, Y.; Shareena Dasari, T. P.; Deng, H.; Yu, H., Antimicrobial Activity of Gold Nanoparticles and Ionic Gold. *Journal of Environmental Science and Health, Part C* **2015,** *33* (3), 286-327.

229. Liau, S. Y.; Read, D. C.; Pugh, W. J.; Furr, J. R.; Russell, A. D., Interaction of silver nitrate with readily identifiable groups: relationship to the antibacterialaction of silver ions. *Letters in Applied Microbiology* **1997,** *25* (4), 279-283.

230. Ivask, A.; ElBadawy, A.; Kaweeteerawat, C.; Boren, D.; Fischer, H.; Ji, Z.; Chang, C. H.; Liu, R.; Tolaymat, T.; Telesca, D.; Zink, J. I.; Cohen, Y.; Holden, P. A.; Godwin, H. A., Toxicity Mechanisms in Escherichia coli Vary for Silver Nanoparticles and Differ from Ionic Silver. *ACS Nano* **2014,** *8* (1), 374-386.

231. Volentini, S. I.; Farías, R. N.; Rodríguez-Montelongo, L.; Rapisarda, V. A., Cu(II)-reduction by Escherichia coli cells is dependent on respiratory chain components. *Biometals : an international journal on the role of metal ions in biology, biochemistry, and medicine* **2011,** *24* (5), 827-35.

232. Shareena Dasari, T. P.; Zhang, Y.; Yu, H., Antibacterial Activity and Cytotoxicity of Gold (I) and (III) Ions and Gold Nanoparticles. *Biochem Pharmacol (Los Angel)* **2015,** *4* (6), 199.

233. Wooten, D. J.; Meyer, C. T.; Lubbock, A. L. R.; Quaranta, V.; Lopez, C. F., MuSyC is a consensus framework that unifies multi-drug synergy metrics for combinatorial drug discovery. *Nature Communications* **2021,** *12* (1), 4607.

234. Loewe, S., The problem of synergism and antagonism of combined drugs. *Arzneimittelforschung* **1953,** *3*, 285-290.

235. Bliss, C. I., The toxicity of poisons applied jointly 1. *Annals of applied biology* **1939,** *26* (3), 585-615.

236. Yadav, B.; Wennerberg, K.; Aittokallio, T.; Tang, J., Searching for Drug Synergy in Complex Dose–Response Landscapes Using an Interaction Potency Model. *Computational and Structural Biotechnology Journal* **2015,** *13*, 504-513.

237. Zhao, L.; Au, J. L. S.; Wientjes, M. G., Comparison of methods for evaluating drug-drug interaction. *Front Biosci (Elite Ed)* **2010,** *2*, 241-249.

238. Bachmann, B. J., Pedigrees of some mutant strains of Escherichia coli K-12. *Bacteriological Reviews* **1972,** *36* (4), 525-557.

239. Sambrook, J.; Fritsch, E. F.; Maniatis, T., *Molecular cloning: a laboratory manual*. Cold spring harbor laboratory press: 1989.

240. Meyer Jr, A. S.; Ayres, G. H., The Mole Ratio Method for Spectrophotometric Determination of Complexes in Solution1. *Journal of the American Chemical Society* **1957,** *79* (1), 49-53.

241. Ianevski, A.; Giri, A. K.; Aittokallio, T., SynergyFinder 2.0: visual analytics of multi-drug combination synergies. *Nucleic Acids Research* **2020,** *48* (W1), W488-W493.

242. Lin, W.; Yuan, L.; Cao, X.; Tan, W.; Feng, Y., A Coumarin-Based Chromogenic Sensor for Transition-Metal Ions Showing Ion-Dependent Bathochromic Shift. *European Journal of Organic Chemistry* **2008,** *2008* (29), 4981-4987.

243. Yu, T.; Zhao, Y.; Fan, D., Synthesis, crystal structure and photoluminescence of 3-(1-benzotriazole)-4-methyl-coumarin. *Journal of Molecular Structure* **2006,** *791* (1), 18-22.

244. Puodziukynaite, E.; Wang, L.; Schanze, K. S.; Papanikolas, J. M.; Reynolds, J. R., Poly(fluorene-co-thiophene)-based ionic transition-metal complex polymers for solar energy harvesting and storage applications. *Polymer Chemistry* **2014,** *5* (7), 2363-2369.

245. Shahabadi, N.; Mohammadi, S.; Alizadeh, R., DNA Interaction Studies of a New Platinum(II) Complex Containing Different Aromatic Dinitrogen Ligands. *Bioinorganic Chemistry and Applications* **2011,** *2011*, 429241.

246. Chohan, Z. H.; Scozzafava, A.; Supuran, C. T., Zinc Complexes of Benzothiazole-derived Schiff Bases with Antibacterial Activity. *Journal of Enzyme Inhibition and Medicinal Chemistry* **2003,** *18* (3), 259-263.

247. Itokazu, M. K.; Polo, A. S.; Iha, N. Y. M., Luminescent rigidochromism of fac-[Re(CO)3(phen)(cis-bpe)]+ and its binuclear complex as photosensors. *Journal of Photochemistry and Photobiology A: Chemistry* **2003,** *160* (1), 27-32.

248. Giordano, P. J.; Wrighton, M. S., The nature of the lowest excited state in fac-tricarbonylhalobis(4-phenylpyridine)rhenium(I) and fac-tricarbonylhalobis(4,4'-bipyridine)rhenium(I): emissive organometallic complexes in fluid solution. *Journal of the American Chemical Society* **1979,** *101* (11), 2888-2897.

249. Zhao, Q.; Li, F.; Huang, C., Phosphorescent chemosensors based on heavy-metal complexes. *Chemical Society Reviews* **2010,** *39* (8), 3007-3030.

250. Lees, A. J., Organometallic complexes as luminescence probes in monitoring thermal and photochemical polymerizations. *Coordination Chemistry Reviews* **1998,** *177* (1), 3-35.

251. Chriswell, C.; Schilt, A., New and improved techniques for applying the mole ratio method to the identification of weak complexes in solution. *Analytical Chemistry* **1975,** *47* (9), 1623-1629.

252. Kharasch, M. S.; Isbell, H. S., The Chemistry Of Organic Gold Compounds. III. Direct Introduction Gold Into The Aromatic Nucleus (Preliminary Communication). *Journal of the American Chemical Society* **1931,** *53* (8), 3053-3059.

253. Radisavljević, S.; Petrović, B., Gold(III) Complexes: An Overview on Their Kinetics, Interactions With DNA/BSA, Cytotoxic Activity, and Computational Calculations. *Frontiers in Chemistry* **2020,** *8* (379).

254. Rocchigiani, L.; Bochmann, M., Recent Advances in Gold(III) Chemistry: Structure, Bonding, Reactivity, and Role in Homogeneous Catalysis. *Chemical Reviews* **2021,** *121* (14), 8364-8451.

255. Basova, T. V.; Hassan, A.; Morozova, N. B., Chemistry of gold(I, III) complexes with organic ligands as potential MOCVD precursors for fabrication of thin metallic films and nanoparticles. *Coordination Chemistry Reviews* **2019,** *380*, 58-82.

256. Aryal, S.; B, K. C. R.; Dharmaraj, N.; Bhattarai, N.; Kim, C. H.; Kim, H. Y., Spectroscopic identification of S-Au interaction in cysteine capped gold nanoparticles. *Spectrochimica acta. Part A, Molecular and biomolecular spectroscopy* **2006,** *63* (1), 160-3.

257. Mohamed, D. S.; Abd El-Baky, R. M.; Sandle, T.; Mandour, S. A.; Ahmed, E. F., Antimicrobial Activity of Silver-Treated Bacteria against other Multi-Drug Resistant Pathogens in Their Environment. *Antibiotics* **2020,** *9* (4), 181.

258. Choi, Y.; Kim, H.-A.; Kim, K.-W.; Lee, B.-T., Comparative toxicity of silver nanoparticles and silver ions to Escherichia coli. *Journal of Environmental Sciences* **2018,** *66*, 50-60.

259. Amaral, L.; Lorian, V., Effects of chlorpromazine on the cell envelope proteins of Escherichia coli. *Antimicrobial agents and chemotherapy* **1991,** *35* (9), 1923-1924.

260. Zhang, Q. M.; Yonei, S., Induction of manganese-superoxide dismutase by membrane-binding drugs in Escherichia coli. *Journal of bacteriology* **1991,** *173* (11), 3488-3491.

261. Grimsey, E. M.; Fais, C.; Marshall, R. L.; Ricci, V.; Ciusa, M. L.; Stone, J. W.; Ivens, A.; Malloci, G.; Ruggerone, P.; Vargiu, A. V.; Piddock, L. J. V., Chlorpromazine and Amitriptyline Are Substrates and Inhibitors of the AcrB Multidrug Efflux Pump. *mBio* **2020,** *11* (3), e00465-20.

262. Tallarida, R. J., Quantitative methods for assessing drug synergism. *Genes & cancer* **2011,** *2* (11), 1003-1008.

263. Radhakrishnan, V.; Ganguly, K.; Ganguly, M.; Dastidar, S. G.; Chakrabarty, A. N., Potentiality of tricyclic compound thioridazine as an effective antibacterial and antiplasmid agent. *Indian J Exp Biol* **1999,** *37* (7), 671-675.

264. Kvist, M.; Hancock, V.; Klemm, P., Inactivation of Efflux Pumps Abolishes Bacterial Biofilm Formation. *Applied and environmental microbiology* **2008,** *74* (23), 7376-7382.

265. Viveiros, M.; Martins, A.; Paixão, L.; Rodrigues, L.; Martins, M.; Couto, I.; Fähnrich, E.; Kern, W. V.; Amaral, L., Demonstration of intrinsic efflux activity of Escherichia coli K-12 AG100 by an automated ethidium bromide method. *International Journal of Antimicrobial Agents* **2008,** *31* (5), 458-462.

266. Prozialeck, W. C.; Weiss, B., Inhibition of calmodulin by phenothiazines and related drugs: structure-activity relationships. *Journal of Pharmacology and Experimental Therapeutics* **1982,** *222* (3), 509-516.

267. Massom, L. R.; Lukas, T. J.; Persechini, A.; Kretsinger, R. H.; Watterson, D. M.; Jarrett, H. W., Trifluoperazine binding to mutant calmodulins. *Biochemistry* **1991,** *30* (3), 663-667.

268. Mazumder, R.; Ganguly, K.; Dastidar, S. G.; Chakrabarty, A. N., Trifluoperazine: a broad spectrum bactericide especially active on staphylococci and vibrios. *International Journal of Antimicrobial Agents* **2001,** *18* (4), 403-406.

269. Lehtinen, J.; Lilius, E.-M., Promethazine renders Escherichia coli susceptible to penicillin G: real-time measurement of bacterial susceptibility by fluoro-luminometry. *International Journal of Antimicrobial Agents* **2007,** *30* (1), 44-51.

270. Motohashi, N.; Sakagami, H.; Kurihara, T.; Ferenczy, L.; Csuri, K.; Molnar, J., Antimicrobial activity of phenothiazines, benzo[a]phenothiazines and benz[c]acridines. *Anticancer Res* **1992,** *12* (4), 1207-1210.

271. Molnar, J.; Mandi, Y.; Holland, I. B.; Schneider, G., Antibacterial effect, plasmid curing activity and chemical structure of some tricyclic compounds. *Acta Microbiologica Academiae Scientiarum Hungaricae* **1977,** *24* (1), 1-6.

272. Linder, M. C.; Hazegh-Azam, M., Copper biochemistry and molecular biology. *The American journal of clinical nutrition* **1996,** *63* (5), 797s-811s.

273. Rodríguez-Montelongo, L.; Farías, R. N.; Massa, E. M., Sites of Electron Transfer to Membrane-Bound Copper and Hydroperoxide-Induced Damage in the Respiratory Chain ofEscherichia coli. *Archives of Biochemistry and Biophysics* **1995,** *323* (1), 19-26.

274. Harris, Z. L.; Gitlin, J. D., Genetic and molecular basis for copper toxicity. *The American journal of clinical nutrition* **1996,** *63* (5), 836S-841S.

275. Gutteridge, J. M. C.; Halliwell, B., Free Radicals and Antioxidants in the Year 2000: A Historical Look to the Future. *Annals of the New York Academy of Sciences* **2000,** *899* (1), 136-147.

276. Nam, S.-H.; Lee, W.-M.; Shin, Y.-J.; Yoon, S.-J.; Kim, S. W.; Kwak, J. I.; An, Y.-J., Derivation of guideline values for gold (III) ion toxicity limits to protect aquatic ecosystems. *Water Research* **2014,** *48*, 126-136.

277. Lee, H.-B.; Peart, T. E.; Svoboda, M. L., Determination of endocrine-disrupting phenols, acidic pharmaceuticals, and personal-care products in sewage by solid-phase extraction and gas chromatography–mass spectrometry. *Journal of Chromatography A* **2005,** *1094* (1), 122-129.

278. Kavlock, R. J.; Daston, G. P.; DeRosa, C.; Fenner-Crisp, P.; Gray, L. E.; Kaattari, S.; Lucier, G.; Luster, M.; Mac, M. J.; Maczka, C., Research needs for the risk assessment of health and environmental effects of endocrine disruptors: a report of the US EPA-sponsored workshop. *Environmental health perspectives* **1996,** *104* (suppl 4), 715-740.

279. Latini, G.; Knipp, G.; Mantovani, A.; Marcovecchio, M.; Chiarelli, F.; Soder, O., Endocrine disruptors and human health. *Mini-Reviews in Medicinal Chemistry* **2010,** *10* (9), 846.

280. Matsui, S.; Takigami, H.; Matsuda, T.; Taniguchi, N.; Adachi, J.; Kawami, H.; Shimizu, Y., Estrogen and estrogen mimics contamination in water and the role of sewage treatment. *Water Science and Technology* **2000,** *42* (12), 173-179.

281. Gümüş, D.; Kalaycı Yüksek, F.; Sefer, Ö.; Yörük, E.; Uz, G.; Anğ Küçüker, M., The roles of hormones in the modulation of growth and virulence genes' expressions in UPEC strains. *Microbial Pathogenesis* **2019,** *132*, 319-324.

282. Vidaillac, C.; Yong, V. F. L.; Aschtgen, M.-S.; Qu, J.; Yang, S.; Xu, G.; Seng, Z. J.; Brown, A. C.; Ali, M. K.; Jaggi, T. K.; Sankaran, J.; Foo, Y. H.; Righetti, F.; Nedumaran, A. M.; Aogáin, M. M.; Roizman, D.; Richard, J.-A.; Rogers, T. R.; Toyofuku, M.; Luo, D.; Loh, E.; Wohland, T.; Czarny, B.; Horvat, J. C.; Hansbro, P. M.; Yang, L.; Li, L.; Normark, S.; Henriques-Normark, B.; Chotirmall, S. H.; Sperandio, V., Sex Steroids Induce Membrane Stress Responses and Virulence Properties in Pseudomonas aeruginosa. *mBio* **2020,** *11* (5), e01774-20.

283. Engelsöy, U.; Svensson, M. A.; Demirel, I., Estradiol Alters the Virulence Traits of Uropathogenic Escherichia coli. *Front Microbiol* **2021,** *12*.

284. Meena, V.; Dotaniya, M.; Saha, J.; Patra, A., Antibiotics and antibiotic resistant bacteria in wastewater: impact on environment, soil microbial activity and human health. *African Journal of Microbiology Research* **2015,** *9* (14), 965-978.

285. Nishino, K.; Nikaido, E.; Yamaguchi, A., Regulation and physiological function of multidrug efflux pumps in Escherichia coli and Salmonella. *Biochimica et Biophysica Acta (BBA) - Proteins and Proteomics* **2009,** *1794* (5), 834-843.

286. Teelucksingh, T.; Thompson, L. K.; Cox, G.; Margolin, W., The Evolutionary Conservation of Escherichia coli Drug Efflux Pumps Supports Physiological Functions. *Journal of Bacteriology* **2020,** *202* (22), e00367-20.

287. Sun, J.; Deng, Z.; Yan, A., Bacterial multidrug efflux pumps: Mechanisms, physiology and pharmacological exploitations. *Biochemical and Biophysical Research Communications* **2014,** *453* (2), 254-267.

288. Sabrialabed, S.; Yang, J. G.; Yariv, E.; Ben-Tal, N.; Lewinson, O., Substrate recognition and ATPase activity of the E. coli cysteine/cystine ABC transporter YecSC-FliY. *J Biol Chem* **2020,** *295* (16), 5245-5256.

289. Elkins, C. A.; Nikaido, H., Substrate Specificity of the RND-Type Multidrug Efflux Pumps AcrB and AcrD of *Escherichia coli* Is Determined Predominately by Two Large Periplasmic Loops. *Journal of Bacteriology* **2002,** *184* (23), 6490-6498.

290. Nikaido, H.; Zgurskaya, H. I., AcrAB and related multidrug efflux pumps of Escherichia coli. *Journal of molecular microbiology and biotechnology* **2001,** *3* (2), 215-218.

291. Chen, L.; Ye, H.-L.; Zhang, G.; Yao, W.-M.; Chen, X.-Z.; Zhang, F.-C.; Liang, G., Autophagy Inhibition Contributes to the Synergistic Interaction between EGCG and Doxorubicin to Kill the Hepatoma Hep3B Cells. *PLOS ONE* **2014,** *9* (1), e85771.

292. Huang, R.-y.; Pei, L.; Liu, Q.; Chen, S.; Dou, H.; Shu, G.; Yuan, Z.-x.; Lin, J.; Peng, G.; Zhang, W.; Fu, H., Isobologram Analysis: A Comprehensive Review of Methodology and Current Research. *Frontiers in Pharmacology* **2019,** *10* (1222).

293. Molloy, M. P.; Herbert, B. R.; Slade, M. B.; Rabilloud, T.; Nouwens, A. S.; Williams, K. L.; Gooley, A. A., Proteomic analysis of the Escherichia coli outer membrane. *European Journal of Biochemistry* **2000,** *267* (10), 2871-2881.

294. Pearson, W. R., Searching protein sequence libraries: comparison of the sensitivity and selectivity of the Smith-Waterman and FASTA algorithms. *Genomics* **1991,** *11* (3), 635-650.

295. Orsburn, B. C., Proteome Discoverer-A Community Enhanced Data Processing Suite for Protein Informatics. *Proteomes* **2021,** *9* (1), 15.

296. Okai, Y.; Sato, E. F.; Higashi-Okai, K.; Inoue, M., Effect of endocrine disruptor para-nonylphenol on the cell growth and oxygen radical generation in Escherichia coli

mutant cells deficient in catalase and superoxide dismutase. *Free Radical Biology and Medicine* **2004,** *37* (9), 1412-1418.

297. Yu, E. W.; McDermott, G.; Zgurskaya, H. I.; Nikaido, H.; Koshland, D. E., Structural Basis of Multiple Drug-Binding Capacity of the AcrB Multidrug Efflux Pump. *Science* **2003,** *300* (5621), 976-980.

298. Schuster, S.; Vavra, M.; Greim, L.; Kern, W. V., Exploring the Contribution of the AcrB Homolog MdtF to Drug Resistance and Dye Efflux in a Multidrug Resistant E. coli Isolate. *Antibiotics* **2021,** *10* (5), 503.

299. Kobayashi, N.; Tamura, N.; van Veen, H. W.; Yamaguchi, A.; Murakami, S., β-Lactam selectivity of multidrug transporters AcrB and AcrD resides in the proximal binding pocket. *Journal of Biological Chemistry* **2014,** *289* (15), 10680-10690.

300. Yamada, S.; Awano, N.; Inubushi, K.; Maeda, E.; Nakamori, S.; Nishino, K.; Yamaguchi, A.; Takagi, H., Effect of drug transporter genes on cysteine export and overproduction in Escherichia coli. *Applied and environmental microbiology* **2006,** *72* (7), 4735-4742.

301. Nishino, K.; Nikaido, E.; Yamaguchi, A., Regulation of multidrug efflux systems involved in multidrug and metal resistance of Salmonella enterica serovar Typhimurium. *Journal of bacteriology* **2007,** *189* (24), 9066-9075.

302. Yu, C.-P.; Roh, H.; Chu, K.-H., 17β-Estradiol-Degrading Bacteria Isolated from Activated Sludge. *Environmental Science & Technology* **2007,** *41* (2), 486-492.

303. Li, Z.; Nandakumar, R.; Madayiputhiya, N.; Li, X., Proteomic Analysis of 17β-Estradiol Degradation by Stenotrophomonas maltophilia. *Environmental Science & Technology* **2012,** *46* (11), 5947-5955.

304. Neuberger, A.; Du, D.; Luisi, B. F., Structure and mechanism of bacterial tripartite efflux pumps. *Research in Microbiology* **2018,** *169* (7), 401-413.

305. Kim, Y.-S.; Min, J.-H.; Hong, H.-N.; Park, J.-H.; Park, K.-S.; Gu, M.-B., Analysis of the stress effects of endocrine disrupting chemicals (EDCs) on Escherichia coli. *Journal of microbiology and biotechnology* **2007,** *17* (8), 1390-1393.

306. Witte, G.; Urbanke, C.; Curth, U., DNA polymerase III chi subunit ties single-stranded DNA binding protein to the bacterial replication machinery. *Nucleic acids research* **2003,** *31* (15), 4434-4440.

307. Hołówka, J.; Zakrzewska-Czerwińska, J., Nucleoid Associated Proteins: The Small Organizers That Help to Cope With Stress. *Front Microbiol* **2020,** *11*, 590-590.

308. Lodish, H.; Zipursky, S. L., Molecular cell biology. *Biochem Mol Biol Educ* **2001,** *29*.

309. Martin, R. G.; Rosner, J. L., Binding of purified multiple antibiotic-resistance repressor protein (MarR) to mar operator sequences. *Proc Natl Acad Sci U S A* **1995,** *92* (12), 5456-5460.

310. El Meouche, I.; Siu, Y.; Dunlop, M. J., Stochastic expression of a multiple antibiotic resistance activator confers transient resistance in single cells. *Scientific Reports* **2016,** *6* (1), 19538.

311. Zou, Y.; Li, C.; Zhang, R.; Jiang, T.; Liu, N.; Wang, J.; Wang, X.; Yan, Y., Exploring the Tunability and Dynamic Properties of MarR-PmarO Sensor System in Escherichia coli. *ACS Synthetic Biology* **2021,** *10* (8), 2076-2086.

312. Hao, Z.; Lou, H.; Zhu, R.; Zhu, J.; Zhang, D.; Zhao, B. S.; Zeng, S.; Chen, X.; Chan, J.; He, C.; Chen, P. R., The multiple antibiotic resistance regulator MarR is a copper sensor in Escherichia coli. *Nature Chemical Biology* **2014,** *10* (1), 21-28.

313. Okusu, H.; Ma, D.; Nikaido, H., AcrAB efflux pump plays a major role in the antibiotic resistance phenotype of Escherichia coli multiple-antibiotic-resistance (Mar) mutants. *Journal of Bacteriology* **1996,** *178* (1), 306-308.

314. Beggs, G. A.; Brennan, R. G.; Arshad, M., MarR family proteins are important regulators of clinically relevant antibiotic resistance. *Protein Science* **2019,** *29* (3), 647-653.

315. Nishino, K.; Yamada, J.; Hirakawa, H.; Hirata, T.; Yamaguchi, A., Roles of TolC-dependent multidrug transporters of Escherichia coli in resistance to beta-lactams. *Antimicrobial agents and chemotherapy* **2003,** *47* (9), 3030-3033.

316. Rosenberg, E. Y.; Ma, D.; Nikaido, H., AcrD of Escherichia coli is an aminoglycoside efflux pump. *Journal of bacteriology* **2000,** *182* (6), 1754-1756.

317. Paulsen, I. T.; Park, J. H.; Choi, P. S.; Saier, M. H., Jr., A family of Gram-negative bacterial outer membrane factors that function in the export of proteins, carbohydrates, drugs and heavy metals from Gram-negative bacteria. *FEMS Microbiology Letters* **1997,** *156* (1), 1-8.

318. Besse, S.; Raff, D.; Thejomayen, M.; Ting, P., Sub-inhibitory concentrations of kanamycin may induce expression of the aminoglycoside efflux pump acrD through the two-component systems CpxAR and BaeSR in Escherichia coli K-12. *J Exp Microbiol Immunol* **2014,** *18*, 1-6.

319. Chu, W.; Fallavollita, A.; Lau, W. B.; Park, J. J. H., BaeR, EvgA and CpxR differentially regulate the expression of acrD in Escherichia coli K-12 but increased acrD

transcription alone does not demonstrate a substantial increase in adaptive resistance against kanamycin. *J. Exp. Microbiol. Immunol* **2013,** *17*, 99-103.

320. Bateni, F.; Dickey, M.; Hanafi, H.; Vickers, B., BaeR Is Required for Upregulation of Expression of acrD in Escherichia coli Following Treatment with Subinhibitory Concentrations of Kanamycin. *Journal of Experimental Microbiology and Immunology (JEMI) Vol* **2016,** *20*, 56-60.

321. Nagakubo, S.; Nishino, K.; Hirata, T.; Yamaguchi, A., The putative response regulator BaeR stimulates multidrug resistance of Escherichia coli via a novel multidrug exporter system, MdtABC. *Journal of bacteriology* **2002,** *184* (15), 4161-4167.

322. Kim, H.-S.; Nikaido, H., Different Functions of MdtB and MdtC Subunits in the Heterotrimeric Efflux Transporter MdtB2C Complex of Escherichia coli. *Biochemistry* **2012,** *51* (20), 4188-4197.

323. Kim, H.-S.; Nagore, D.; Nikaido, H., Multidrug Efflux Pump MdtBC of Escherichia coli Is Active Only as a B₂C Heterotrimer. *Journal of Bacteriology* **2010,** *192* (5), 1377-1386.

324. Shimada, T.; Yamamoto, K.; Ishihama, A., Involvement of the leucine response transcription factor LeuO in regulation of the genes for sulfa drug efflux. *Journal of bacteriology* **2009,** *191* (14), 4562-4571.

325. Meng, Y.-L.; Liu, Z.; Rosen, B. P., As(III) and Sb(III) Uptake by GlpF and Efflux by ArsB in Escherichia coli*. *Journal of Biological Chemistry* **2004,** *279* (18), 18334-18341.

326. Yu, Y.; Chen, J.; Li, Y.; Liang, J.; Xie, Z.; Feng, R.; Alwathnani, H. A.; Rosen, B. P.; Grove, A.; Chen, J.; Rensing, C., Identification of a MarR subfamily that regulates arsenic resistance genes. *Applied and environmental microbiology* **2021,** *0* (ja), AEM.01588-21.

APPENDIX A

SUPPLIMENTAL INFORMATION FOR CHAPTER 2: THE ANAEROBIC EFFLUX PUMP MDTEF-TOLC CONFERS RESISTANCE TO CATIONIC BIOCIDES

A.1. Initial Blast Protein Sequence Alignment.

AcrB 29-339

>sp|P31224|29-339

KLPVAQYPTIAPPAVTISASYPGADAKTVQDTVTQVIEQNMNGIDNLMYMSSNS
DSTGTVQITLTFESGTDADIAQVQVQNKLQLAMPLLPQEVQQQGVSVEKSSSSFL
MVVGVINTDGTMTQEDISDYVAANMKDAISRTSGVGDVQLFGSQYAMRIWMN
PNELNKFQLTPVDVITAIKAQNAQVAAGQLGGTPPVKGQQLNASIIAQTRLTSTE
EFGKILLKVNQDGSRVLLRDVAKIELGGENYDIIAEFNGQPASGLGIKLATGANA
LDTAAAIRAELAKMEPFFPSGLKIVYPYDTTPFVKISIHE

AcrB 29-339

>sp|P37637|29-339

NLPVAQYPQIAPPTITVSATYPGADAQTVEDSVTQVIEQNMNGLDGLMYMSSTS
DAAGNASITLTFETGTSPDIAQVQVQNKLQLAMPSLPEAVQQQGISVDKSSSNIL
MVAAFISDNGSLNQYDIADYVASNIKDPLSRTAGVGSVQLFGSEYAMRIWLDPQ
KLNKYNLVPSDVISQIKVQNNQISGGQLGGMPQAADQQLNASIIVQTRLQTPEEF
GKILLKVQQDGSQVLLRDVARVELGAEDYSTVARYNGKPAAGIAIKLAAGANA
LDTSRAVKEELNRLSAYFPASLKTVYPYDTTPFIEISIQE

Blast results

```
67.4% identity in 310 residues overlap; Score: 1112.0; Gap frequency:
0.0%
AcrB            2
LPVAQYPTIAPPAVTISASYPGADAKTVQDTVTQVIEQNMNGIDNLMYMSSNSDSTGTVQ
MdtF            2
LPVAQYPQIAPPTITVSATYPGADAQTVEDSVTQVIEQNMNGLDGLMYMSSTSDAAGNAS
                 ******* ****  * ** ****** ** * *********** * ******
**  *

AcrB           62
ITLTFESGTDADIAQVQVQNKLQLAMPLLPQEVQQQGVSVEKSSSSFLMVVGVINTDGTM
MdtF           62
ITLTFETGTSPDIAQVQVQNKLQLAMPSLPEAVQQQGISVDKSSSNILMVAAFISDNGSL
                 ****** **  *************** **  ***** **
****  ***   *   *

AcrB          122
TQEDISDYVAANMKDAISRTSGVGDVQLFGSQYAMRIWMNPNELNKFQLTPVDVITAIKA
MdtF          122
NQYDIADYVASNIKDPLSRTAGVGSVQLFGSEYAMRIWLDPQKLNKYNLVPSDVISQIKV
                 * ** **** * **  *** *** ****** ******  *  ***  * *
***  **

AcrB          182
QNAQVAAGQLGGTPPVKGQQLNASIIAQTRLTSTEEFGKILLKVNQDGSRVLLRDVAKIE
```

```
MdtF         182
QNNQISGGQLGGMPQAADQQLNASIIVQTRLQTPEEFGKILLKVQQDGSQVLLRDVARVE
                 ** *   ***** *    ******** ****   ********** ****
*******  *

AcrB         242
LGGENYDIIAEFNGQPASGLGIKLATGANALDTAAAIRAELAKMEPFFPSGLKIVYPYDT
MdtF         242
LGAEDYSTVARYNGKPAAGIAIKLAAGANALDTSRAVKEELNRLSAYFPASLKTVYPYDT
                 ** * *   *  ** ** *  **** *******  *   **      **  **
******

AcrB         302 TPFVKISIHE
MdtF         302 TPFIEISIQE
                 ***  *** *

71.1% identity in 1035 residues overlap; Score: 3809.0; Gap frequency:
0.2%

P31224|ACR     1
MPNFFIDRPIFAWVIAIIIMLAGGLAILKLPVAQYPTIAPPAVTISASYPGADAKTVQDT
P37637|MDT     1
MANYFIDRPVFAWVLAIIMMLAGGLAIMNLPVAQYPQIAPPTITVSATYPGADAQTVEDS
                 * * ***** **** *** ********  ******* ****  * ** ******
** *

P31224|ACR    61
VTQVIEQNMNGIDNLMYMSSNSDSTGTVQITLTFESGTDADIAQVQVQNKLQLAMPLLPQ
P37637|MDT    61
VTQVIEQNMNGLDGLMYMSSTSDAAGNASITLTFETGTSPDIAQVQVQNKLQLAMPSLPE
                 *********** * ****** **  *   ******
**  ***************** **

P31224|ACR   121
EVQQQGVSVEKSSSSFLMVVGVINTDGTMTQEDISDYVAANMKDAISRTSGVGDVQLFGS
P37637|MDT   121
AVQQQGISVDKSSSNILMVAAFISDNGSLNQYDIADYVASNIKDPLSRTAGVGSVQLFGS
                 ***** ** ****  ***   *   *   * ** **** * **  *** ***
******

P31224|ACR   181
QYAMRIWMNPNELNKFQLTPVDVITAIKAQNAQVAAGQLGGTPPVKGQQLNASIIAQTRL
P37637|MDT   181
EYAMRIWLDPQKLNKYNLVPSDVISQIKVQNNQISGGQLGGMPQAADQQLNASIIVQTRL
                 ******  *  ***  * * ***  ** ** *   *****
*    ******** ****

P31224|ACR   241
TSTEEFGKILLKVNQDGSRVLLRDVAKIELGGENYDIIAEFNGQPASGLGIKLATGANAL
P37637|MDT   241
QTPEEFGKILLKVQQDGSQVLLRDVARVELGAEDYSTVARYNGKPAAGIAIKLAAGANAL
                   ********** **** *******  *** * *   *  ** ** *  ****
*****
```

```
P31224|ACR   301
DTAAAIRAELAKMEPFFPSGLKIVYPYDTTPFVKISIHEVVKTLVEAIILVFLVMYLFLQ
P37637|MDT   301
DTSRAVKEELNRLSAYFPASLKTVYPYDTTPFIEISIQEVFKTLVEAIILVFLVMYLFLQ
                  **  *   **      **  ** *********  *** **
******************

P31224|ACR   361
NFRATLIPTIAVPVVLLGTFAVLAAFGFSINTLTMFGMVLAIGLLVDDAIVVVENVERVM
P37637|MDT   361
NFRATIIPTIAVPVVILGTFAILSAVGFTINTLTMFGMVLAIGLLVDDAIVVVENVERVI
                  ***** ********* ***** * * **
******************************

P31224|ACR   421
AEEGLPPKEATRKSMGQIQGALVGIAMVLSAVFVPMAFFGGSTGAIYRQFSITIVSAMAL
P37637|MDT   421
AEDKLPPKEATHKSMGQIQRALVGIAVVLSAVFMPMAFMSGATGEIYRQFSITLISSMLL
                  **  ******* ******* ****** ****** ****  * **
********  * * *

P31224|ACR   481
SVLVALILTPALCATMLKPIAKGDHGEGKKGFFGWFNRMFEKSTHHYTDSVGGILRSTGR
P37637|MDT   481 SVFVAMSLTPALCATILKAAPEGGHKPN--
ALFARFNTLFEKSTQHYTDSTRSLLRCTGR
                  ** **  ******** **    * *       *  **  *****
*****    ** ***

P31224|ACR   541
YLVLYLIIVVGMAYLFVRLPSSFLPDEDQGVFMTMVQLPAGATQERTQKVLNEVTHYYLT
P37637|MDT   539
YMVVYLLICAGMAVLFLRTPTSFLPEEDQGVFMTTAQLPSGATMVNTTKVLQQVTDYYLT
                  * * ** *  *** ** * * **** ********  *** ***   *
***  ** ****

P31224|ACR   601
KEKNNVESVFAVNGFGFAGRGQNTGIAFVSLKDWADRPGEENKVEAITMRATRAFSQIKD
P37637|MDT   599
KEKDNVQSVFTVGGFGFSGQGQNNGLAFISLKPWSERVGEENSVTAIIQRAMIALSSINK
                  *** ** *** * **** * *** * ** *** *  * **** * **  **  *
* *

P31224|ACR   661
AMVFAFNLPAIVELGTATGFDFELIDQAGLGHEKLTQARNQLLAEAAKHPDMLTSVRPNG
P37637|MDT   659
AVVFPFNLPAVAELGTASGFDMELLDNGNLGHEKLTQARNELLSLAAQSPNQVTGVRPNG
                  * ** *****  ***** *** ** *   ********** **  **  *   *
*****

P31224|ACR   721
LEDTPQFKIDIDQEKAQALGVSINDINTTLGAAWGGSYVNDFIDRGRVKKVYVMSEAKYR
```

```
P37637|MDT   719
LEDTPMFKVNVNAAKAEAMGVALSDINQTISTAFGSSYVNDFLNQGRVKKVYVQAGTPFR
                 ***** **      ** * **   *** *   * *
******   ********      *

P31224|ACR   781
MLPDDIGDWYVRAADGQMVPFSAFSSSRWEYGSPRLERYNGLPSMEILGQAAPGKSTGEA
P37637|MDT   779
MLPDNINQWYVRNASGTMAPLSAYSSTEWTYGSPRLERYNGIPSMEILGEAAAGKSTGDA
                 **** *  **** * * * * ** **  * ********** ******* **
***** *

P31224|ACR   841
MELMEQLASKLPTGVGYDWTGMSYQERLSGNQAPSLYAISLIVVFLCLAALYFSWSIPFS
P37637|MDT   839
MKFMADLVAKLPAGVGYSWTGLSYQEALSSNQAPALYAISLVVVFLALALALYFSWSIPFS
                 *  *  *  *** **** *** **** ** **** ****** ****
*************

P31224|ACR   901
VMLVVPLGVIGALLAATFRGLTNDVYFQVGLLTTIGLSAKNAILIVEFAKDLMDKEGKGL
P37637|MDT   899
VMLVVPLGVVGALLATDLRGLSNDVYFQVGLLTTIGLSAKNAILIVEFAVEMMQKEGKTP
                 ********* *****   *** ***************************   *
****

P31224|ACR   961
IEATLDAVRMRLRPILMTSLAFILGVMPLVISTGAGSGAQNAVGTGVMGGMVTATVLAIF
P37637|MDT   959
IEAIIEAARMRLRPILMTSLAFILGVLPLVISHGAGSGAQNAVGTGVMGGMFAATVLAIY
                 ***   * ***************** *****
******************  ******

P31224|ACR  1021 FVPVFFVVVRRRFSR
P37637|MDT  1019 FVPVFFVVVEHLFAR
                 *********   * *
```

Periplasm 1

```
67.4% identity in 307 residues overlap; Score: 1103.0; Gap frequency:
0.0%

AcrB           2
LPVAQYPTIAPPAVTISASYPGADAKTVQDTVTQVIEQNMNGIDNLMYMSSNSDSTGTVQ
MdtF           2
LPVAQYPQIAPPTITVSATYPGADAQTVEDSVTQVIEQNMNGLDGLMYMSSTSDAAGNAS
                 ******* ****  * ** ****** ** * ********** * ******
**  *

AcrB          62
ITLTFESGTDADIAQVQVQNKLQLAMPLLPQEVQQQGVSVEKSSSSFLMVVGVINTDGTM
MdtF          62
ITLTFETGTSPDIAQVQVQNKLQLAMPSLPEAVQQQGISVDKSSSNILMVAAFISDNGSL
```

```
                  ****** **  ********************* **  ***** **
****  ***   *   *

AcrB         122
TQEDISDYVAANMKDAISRTSGVGDVQLFGSQYAMRIWMNPNELNKFQLTPVDVITAIKA
MdtF         122
NQYDIADYVASNIKDPLSRTAGVGSVQLFGSEYAMRIWLDPQKLNKYNLVPSDVISQIKV
                   * ** **** * **  *** *** ****** ******  *  ***  * *
***  **

AcrB         182
QNAQVAAGQLGGTPPVKGQQLNASIIAQTRLTSTEEFGKILLKVNQDGSRVLLRDVAKIE
MdtF         182
QNNQISGGQLGGMPQAADQQLNASIIVQTRLQTPEEFGKILLKVQQDGSQVLLRDVARVE
                  ** *   ***** *    ******** ****   ********** ****
*******  *

AcrB         242
LGGENYDIIAEFNGQPASGLGIKLATGANALDTAAAIRAELAKMEPFFPSGLKIVYPYDT
MdtF         242
LGAEDYSTVARYNGKPAAGIAIKLAAGANALDTSRAVKEELNRLSAYFPASLKTVYPYDT
                  ** * *   *  ** ** *  **** *******  *   **      **  **
******

AcrB         302 TPFVKIS
MdtF         302 TPFIEIS
                  ***  **
```

Periplams 1 Emboss Needle

```
#=======================================
#
# Aligned_sequences: 2
# 1: EMBOSS_001
# 2: EMBOSS_001
# Matrix: EBLOSUM62
# Gap_penalty: 10.0
# Extend_penalty: 0.5
#
# Length: 311
# Identity:     207/311 (66.6%)
# Similarity:   256/311 (82.3%)
# Gaps:           3/311 ( 1.0%)
# Score: 1103.0
#
#
#=======================================

EMBOSS_001         1 KLPVAQYPTIAPPAVTISASYPGADAKTVQDTVTQVIEQNMNGIDNLMYM     50
                     .|||||||.||||.:|:||:|||||:||:|:||||||||||:|.||||
EMBOSS_001         1 NLPVAQYPQIAPPTITVSATYPGADAQTVEDSVTQVIEQNMNGLDGLMYM     50

EMBOSS_001        51 SSNSDSTGTVQITLTFESGTDADIAQVQVQNKLQLAMPLLPQEVQQQGVS    100
                     ||.||:.|...||||||:||..|||||||||||||.||:.||||||:|
EMBOSS_001        51 SSTSDAAGNASITLTFETGTSPDIAQVQVQNKLQLAMPSLPEAVQQQGIS    100
```

```
EMBOSS_001       101 VEKSSSSFLMVVGVINTDGTMTQEDISDYVAANMKDAISRTSGVGDVQLF    150
                     |:||||:.|||...|:.:|::.|.||:||||:|:||.:|||:|||.||||
EMBOSS_001       101 VDKSSSNILMVAAFISDNGSLNQYDIADYVASNIKDPLSRTAGVGSVQLF    150

EMBOSS_001       151 GSQYAMRIWMNPNELNKFQLTPVDVITAIKAQNAQVAAGQLGGTPPVKGQ    200
                     ||:|||||::|.:|||:.|.|.|||:.||.||.|::.|||||.|....|
EMBOSS_001       151 GSEYAMRIWLDPQKLNKYNLVPSDVISQIKVQNNQISGGQLGGMPQAADQ    200

EMBOSS_001       201 QLNASIIAQTRLTSTEEFGKILLKVNQDGSRVLLRDVAKIELGGENYDII    250
                     |||||||.||||.:.||||||||||.||||:|||||||::|||.|:|..:
EMBOSS_001       201 QLNASIIVQTRLQTPEEFGKILLKVQQDGSQVLLRDVARVELGAEDYSTV    250

EMBOSS_001       251 AEFNGQPASGLGIKLATGANALDTAAAIRAELAKMEPFFPSGLKIVYPYD    300
                     |.:||:||:|:.||||.|||||||:.|::.||.::..:||:.||.|||||
EMBOSS_001       251 ARYNGKPAAGIAIKLAAGANALDTSRAVKEELNRLSAYFPASLKTVYPYD    300

EMBOSS_001       301 TTPFVKIS---    308
                     ||||::||
EMBOSS_001       301 TTPFIEISIQE    311
```

Cytoplasm 4

```
47.4% identity in 38 residues overlap; Score: 88.0; Gap frequency: 0.0%

AcrBC4            11 AKGDHGEGKKGFFGWFNRMFEKSTHHYTDSVGGILRST
MdtFC4             3 AAPEGGHKPNALFARFNTLFEKSTQHYTDSTRSLLRCT
                       *    *      *  **  ***** *****    ** *
```

Cytoplasm 4 alternate

```
52.1% identity in 48 residues overlap; Score: 108.0; Gap frequency:
4.2%

Acr                1 ALCATMLKPIAKGDHGEGKKGFFGWFNRMFEKSTHHYTDSVGGILRST
Mdt                1 ALCATILKAAPEGGHKPN--ALFARFNTLFEKSTQHYTDSTRSLLRCT
                       ***** **    * *       *  **  ***** *****    ** *

#=======================================
#
# Aligned_sequences: 2
# 1: EMBOSS_001
# 2: EMBOSS_001
# Matrix: EBLOSUM62
# Gap_penalty: 10.0
# Extend_penalty: 0.5
#
# Length: 25
# Identity:      15/25 (60.0%)
# Similarity:    17/25 (68.0%)
# Gaps:           0/25 ( 0.0%)
# Score: 80.0
#
#
#=======================================
```

```
EMBOSS_001         1 FFGWFNRMFEKSTHHYTDSVGGILR     25
                     .|..||.:|||||.|||||...:||
EMBOSS_001         1 LFARFNTLFEKSTQHYTDSTRSLLR     25
```

Periplasm 4

```
65.3% identity in 314 residues overlap; Score: 1114.0; Gap frequency:
0.0%

AcrBP4         3
RLPSSFLPDEDQGVFMTMVQLPAGATQERTQKVLNEVTHYYLTKEKNNVESVFAVNGFGF
MdtFP4         1
RTPTSFLPEEDQGVFMTTAQLPSGATMVNTTKVLQQVTDYYLTKEKDNVQSVFTVGGFGF
                 * * **** ********  *** ***   * ***  ** ******* ** ***
* ****

AcrBP4        63
AGRGQNTGIAFVSLKDWADRPGEENKVEAITMRATRAFSQIKDAMVFAFNLPAIVELGTA
MdtFP4        61
SGQGQNNGLAFISLKPWSERVGEENSVTAIIQRAMIALSSINKAVVFPFNLPAVAELGTA
                 * *** * ** *** *  * **** * **  **  * * *  * **
*****  *****

AcrBP4       123
TGFDFELIDQAGLGHEKLTQARNQLLAEAAKHPDMLTSVRPNGLEDTPQFKIDIDQEKAQ
MdtFP4       121
SGFDMELLDNGNLGHEKLTQARNELLSLAAQSPNQVTGVRPNGLEDTPMFKVNVNAAKAE
                 *** ** *   ********** **  **  *   * **********
**      **

AcrBP4       183
ALGVSINDINTTLGAAWGGSYVNDFIDRGRVKKVYVMSEAKYRMLPDDIGDWYVRAADGQ
MdtFP4       181
AMGVALSDINQTISTAFGSSYVNDFLNQGRVKKVYVQAGTPFRMLPDNINQWYVRNASGT
                 * **   *** *   * * ******   ********      *****
*  **** * *

AcrBP4       243
MVPFSAFSSSRWEYGSPRLERYNGLPSMEILGQAAPGKSTGEAMELMEQLASKLPTGVGY
MdtFP4       241
MAPLSAYSSTEWTYGSPRLERYNGIPSMEILGEAAAGKSTGDAMKFMADLVAKLPAGVGY
                 * * ** **  * ********** ******* ** *****
**  *  *  *** ****

AcrBP4       303 DWTGMSYQERLSGN
MdtFP4       301 SWTGLSYQEALSSN
                  *** **** ** *
```

Transmembrane 1

```
78.9% identity in 19 residues overlap; Score: 82.0; Gap frequency: 0.0%

AcrB-T1        1 IFAWVIAIIIMLAGGLAIL
```

```
MdtF-T1         1 VFAWVLAIIMMLAGGLAIM
                  **** *** ********
```

Transmembrane 2

```
94.1% identity in 17 residues overlap; Score: 72.0; Gap frequency: 0.0%

AcrB-T2         4 VVKTLVEAIILVFLVMY
MdtF-T2         1 VFKTLVEAIILVFLVMY
                  * ***************
```

Transmembrane 3

```
80.0% identity in 20 residues overlap; Score: 84.0; Gap frequency: 0.0%

AcrB-T3         1 LIPTIAVPVVLLGTFAVLAA
MdtF-T3         1 IIPTIAVPVVILGTFAILSA
                  ********* ***** * *
```

Transmembrange 4

```
100.0% identity in 22 residues overlap; Score: 102.0; Gap frequency:
0.0%

AcrB-T4         1 TLTMFGMVLAIGLLVDDAIVVV
MdtF-T4         1 TLTMFGMVLAIGLLVDDAIVVV
                  **********************
```

Cytoplasm 3

```
84.0% identity in 25 residues overlap; Score: 105.0; Gap frequency:
0.0%

AcrB-C3         1 ENVERVMAEEGLPPKEATRKSMGQI
MdtF-C3         1 ENVERVIAEDKLPPKEATHKSMGQI
                  ****** **  ******* ******
```

Transmembrane 5

```
87.5% identity in 16 residues overlap; Score: 66.0; Gap frequency: 0.0%

AcrB-T5         4 LVGIAMVLSAVFVPMA
MdtF-T5         1 LVGIAVVLSAVFMPMA
                  ***** ****** ***
```

Transmembrane 6

```
58.8% identity in 17 residues overlap; Score: 50.0; Gap frequency: 0.0%

AcrB-T6         9 IVSAMALSVLVALILTP
MdtF-T6         1 LISSMLLSVFVAMSLTP
                    * * *** **  ***
```

Transmembrane 7

```
64.7% identity in 17 residues overlap; Score: 59.0; Gap frequency: 0.0%

AcrB-T7         1 GRYLVLYLIIVVGMAYL
MdtF-T7         1 GRYMVVYLLICAGMAVL
                  *** * ** *  *** *
```

Transmembrane 8

```
81.2% identity in 16 residues overlap; Score: 64.0; Gap frequency: 0.0%
```

```
AcrB-T8         2 APSLYAISLIVVFLCL
MdtF-T8         1 APALYAISLVVVFLAL
                  ** ****** **** *
```

Transmembrane 9
94.1% identity in 17 residues overlap; Score: 77.0; Gap frequency: 0.0%

```
AcrB-T9         1 FSVMLVVPLGVIGALLA
MdtF-T9         1 FSVMLVVPLGVVGALLA
                  *********** *****
```

T10
100.0% identity in 19 residues overlap; Score: 91.0; Gap frequency: 0.0%

```
AcrB-T10        1 VYFQVGLLTTIGLSAKNAI
MdtF-T10        1 VYFQVGLLTTIGLSAKNAI
                  ******************
```

Cytoplasm 6
61.5% identity in 26 residues overlap; Score: 77.0; Gap frequency: 0.0%

```
AcrB-C6         4 EFAKDLMDKEGKGLIEATLDAVRMRL
MdtF-C6         1 EFAVEMMQKEGKTPIEAIIEAARMRL
                  ***   * ****  ***   * ****
```

T11
94.4% identity in 18 residues overlap; Score: 79.0; Gap frequency: 0.0%

```
AcrB-T11        3 ILMTSLAFILGVMPLVIS
MdtF-T11        1 ILMTSLAFILGVLPLVIS
                  ************ *****
```

T12
83.3% identity in 12 residues overlap; Score: 46.0; Gap frequency: 0.0%

```
AcrB-T12        9 VMGGMVTATVLA
MdtF-T12        1 VMGGMFAATVLA
                  *****  *****
```

Table A.1. Complete binding site predictions with respective amino acid, region of AA, Z score, and Probability and Ranking of Binding Site predictions. Color represents respective colors associated with Figure 2.5.

Region	AA	Score	Z score	Probability	Pocket Rank	Pocket Rank	Probability	Z score	Score	AA	Region
274	ASP	2.7009	0.8815	0.5268	36	15	0.5843	1.0603	3.1014	ASN	274
459	MET	1.5738	0.3783	0.3014	9	7	0.44	0.6606	2.2062	PHE	459
460	SER	1.5998	0.39	0.3078	9	7	0.4683	0.7298	2.3611	GLY	460
461	GLY	1.0038	0.1239	0.153	0	0	0.3656	0.5008	1.8482	GLY	461
462	ALA	0.8272	0.045	0.1077	12	7	0.3515	0.473	1.7859	SER	462
463	THR	1.4244	0.3116	0.2637	9	7	0.4359	0.6511	2.1848	THR	463
464	GLY	0.4356	-0.1298	0.0321	0	0	0.1629	0.1407	1.0414	GLY	464
465	GLU	0.8017	0.0337	0.1016	0	0	0.1728	0.1573	1.0786	ALA	465
498	LYS	2.1155	0.6202	0.4223	0	0	0.1917	0.1895	1.1507	LYS	498
499	ALA	0.181	-0.2434	0.0076	0	0	0.0053	-0.2613	0.1411	PRO	499
500	ALA	0.1896	-0.2396	0.0081	0	0	0.0114	-0.219	0.2357	ILE	500
501	PRO	0.1058	-0.277	0.0037	0	0	0.1199	0.0668	0.876	ALA	501
502	GLU	0.7777	0.023	0.0959	0	28	0.4261	0.6286	2.1344	LYS	502
503	GLY	1.1695	0.1979	0.1967	0	0	0.3467	0.4635	1.7646	GLY	503
504	GLY	1.4629	0.3288	0.2736	0	0	0.3026	0.3804	1.5784	ASP	504
505	HIS	1.9772	0.5584	0.3935	0	0	0.3794	0.5283	1.9098	HIS	505
506	LYS	0.5811	-0.0648	0.0547	0	0	0.0069	-0.2487	0.1692	GLY	506
507	PRO	0.6092	-0.0523	0.0599	0	0	0.1676	0.1486	1.0591	GLU	507
508	ASN	1.9831	0.561	0.3947	0	0	0.0022	-0.2943	0.067	GLY	508
509	ALA	0.6807	-0.0204	0.0743	0	0	0.0499	-0.0772	0.5535	LYS	509
510	LEU	0.5358	-0.0851	0.0469	0	0	0.5166	0.8528	2.6366	LYS	510
511	PHE	0.856	0.0579	0.1149	0	0	0.0995	0.0296	0.7927	GLY	511
512	ALA	0.5431	-0.0818	0.0481	0	0	0.1883	0.1837	1.1377	PHE	512
513	ARG	0.4369	-0.1292	0.0323	0	0	0.3449	0.46	1.7567	PHE	513
						0	0.3585	0.4869	1.817	GLY	514
						0	0.3338	0.4383	1.7081	TRP	515
615	PHE	3.9474	1.438	0.6823	0	12	0.6173	1.1748	3.3578	PHE	617
616	SER	1.7964	0.4777	0.3539	0	12	0.2791	0.3386	1.4847	ALA	618
617	GLY	0.8164	0.0402	0.1051	0	0	0.1148	0.0577	0.8554	GLY	619
618	GLN	2.0822	0.6053	0.4157	21	36	0.5942	1.0938	3.1765	ARG	620
863	GLN	0.8678	0.0631	0.1178	9	7	0.3486	0.4674	1.7732	GLN	865
864	GLU	2.7755	0.9148	0.5383	9	7	0.4406	0.6619	2.209	GLU	866
865	ALA	1.1472	0.1879	0.1908	6	0	0.1676	0.1485	1.059	ARG	867
866	LEU	1.3374	0.2728	0.2409	6	0	0.2962	0.3691	1.5531	LEU	868
867	SER	0.8659	0.0623	0.1174	9	7	0.2079	0.2169	1.2121	SER	869
868	SER	1.1915	0.2077	0.2026	9	7	0.2163	0.2306	1.2429	GLY	870
869	ASN	0.7331	0.003	0.0856	0	0	0.0431	-0.096	0.5112	ASN	871
870	GLN	0.8958	0.0756	0.1251	0	7	0.267	0.3175	1.4376	GLN	872
274	ASP	1.2987	0.2555	0.2309	13	20	0.2969	0.3703	1.5557	ASN	274
459	MET	1.0272	0.1343	0.1592	0	0	0.2862	0.3511	1.5127	PHE	459
460	SER	0.9992	0.1218	0.1517	0	0	0.1592	0.1343	1.0272	GLY	460
461	GLY	0.9718	0.1096	0.1445	0	0	0.1023	0.035	0.8046	GLY	461
462	ALA	1.1931	0.2084	0.203	37	57	0.0975	0.0259	0.7843	SER	462
463	THR	0.5311	-0.0871	0.0462	37	57	0.023	-0.1632	0.3607	THR	463
464	GLY	0.0937	-0.2824	0.0031	0	0	0.0342	-0.1229	0.4511	GLY	464
465	GLU	0.8991	0.0771	0.1259	0	0	0.0603	-0.0516	0.6108	ALA	465
498	LYS	0.5753	-0.0674	0.0537	41	0	0.1102	0.0495	0.8371	LYS	498
499	ALA	0.167	-0.2497	0.0068	0	0	0.0177	-0.1859	0.3099	PRO	499
500	ALA	0.4388	-0.1283	0.0325	41	0	0.1488	0.117	0.9883	ILE	500
501	PRO	0.2561	-0.2099	0.0129	0	0	0.0063	-0.2529	0.1598	ALA	501
502	GLU	0.2519	-0.2118	0.0126	0	0	0.0681	-0.0335	0.6512	LYS	502
503	GLY	0.1035	-0.278	0.0036	0	0	0.0192	-0.1793	0.3246	GLY	503
504	GLY	0.4826	-0.1088	0.0387	41	0	0.2841	0.3475	1.5047	ASP	504
505	HIS	1.2222	0.2214	0.2106	41	67	0.199	0.2017	1.1782	HIS	505
506	LYS	0.2362	-0.2188	0.0114	0	0	0.101	0.0325	0.7992	GLY	506
507	PRO	0.9259	0.0891	0.1326	0	0	0.1044	0.0389	0.8135	GLU	507
508	ASN	2.1212	0.6227	0.4234	41	0	0.0513	-0.0737	0.5611	GLY	508
509	ALA	0.9317	0.0917	0.1341	0	0	0.0065	-0.2515	0.1629	LYS	509
510	LEU	0.5092	-0.0969	0.0428	0	0	0.0267	-0.1492	0.3921	LYS	510
511	PHE	1.9213	0.5335	0.3819	0	67	0.0088	-0.2348	0.2004	GLY	511
512	ALA	1.4715	0.3327	0.2758	0	67	0.1261	0.0773	0.8995	PHE	512
513	ARG	0.5921	-0.0599	0.0567	0	67	0.2781	0.3368	1.4807	PHE	513
						67	0.2035	0.2093	1.1953	GLY	514
						0	0.2333	0.2598	1.3082	TRP	515
615	PHE	2.7546	0.9055	0.5352	16	4	0.5009	0.8121	2.5454	PHE	617
616	SER	2.2673	0.6879	0.4514	16	4	0.2886	0.3552	1.5219	ALA	618
617	GLY	0.6118	-0.0511	0.0605	0	0	0.0145	-0.2019	0.274	GLY	619
618	GLN	2.5638	0.8203	0.5041	13	4	0.3823	0.5344	1.9233	ARG	620
863	GLN	1.5124	0.3509	0.2861	37	57	0.0968	0.0247	0.7815	GLN	865
864	GLU	1.3005	0.2564	0.2314	37	57	0.2046	0.2112	1.1995	GLU	866
865	ALA	2.3257	0.714	0.4619	0	0	0.2316	0.2568	1.3015	ARG	867
866	LEU	1.5753	0.379	0.3018	0	0	0.19	0.1866	1.1444	LEU	868
867	SER	0.3065	-0.1874	0.0174	0	0	0.046	-0.0877	0.5298	SER	869
868	SER	1.5063	0.3482	0.2846	39	26	0.1613	0.138	1.0355	GLY	870
869	ASN	1.3707	0.2877	0.2497	0	26	0.218	0.2336	1.2496	ASN	871
870	GLN	0.6057	-0.0538	0.0593	0	0	0.2218	0.2402	1.2644	GLN	872
274	ASP	2.5847	0.8296	0.5079	1	1	0.3486	0.4674	1.7733	ASN	274
459	MET	1.5738	0.3783	0.3014	9	34	0.2726	0.327	1.4589	PHE	459
460	SER	1.5998	0.39	0.3078	9	0	0.113	0.0545	0.8483	GLY	460
461	GLY	1.0038	0.1239	0.153	0	0	0.2977	0.3718	1.5592	GLY	461
462	ALA	0.8272	0.045	0.1077	12	0	0.3445	0.4592	1.755	SER	462
463	THR	1.4244	0.3116	0.2637	9	34	0.3862	0.5429	1.9425	THR	463
464	GLY	0.4356	-0.1298	0.0321	0	0	0.0305	-0.1353	0.4232	GLY	464
465	GLU	0.8017	0.0337	0.1016	0	0	0.0795	-0.0091	0.7058	ALA	465
498	LYS	0.4873	-0.1067	0.0394	55	0	0.0131	-0.2093	0.2575	LYS	498
499	ALA	0.3319	-0.1761	0.0199	0	0	0.0056	-0.2591	0.1459	PRO	499
500	ALA	0.2473	-0.2138	0.0122	0	39	0.1489	0.117	0.9884	ILE	500
501	PRO	0.4663	-0.1161	0.0363	55	0	0.0606	-0.0508	0.6126	ALA	501
502	GLU	0.4158	-0.1386	0.0296	0	0	0.042	-0.0991	0.5044	LYS	502
503	GLY	0.3748	-0.1569	0.0246	0	0	0.1044	0.0389	0.8134	GLY	503
504	GLY	0.7012	-0.0112	0.0785	0	0	0.0313	-0.1326	0.4292	ASP	504
505	HIS	0.7394	0.0059	0.087	55	39	0.2905	0.3586	1.5297	HIS	505
506	LYS	0.2384	-0.2178	0.0116	0	0	0.0779	-0.0125	0.6983	GLY	506
507	PRO	0.3077	-0.1869	0.0175	0	0	0.0327	-0.1277	0.4402	GLU	507
508	ASN	1.1689	0.1976	0.1965	0	0	0.0125	-0.2123	0.2507	GLY	508
509	ALA	0.2846	-0.1972	0.0155	55	0	0.0137	-0.2061	0.2646	LYS	509
510	LEU	0.1941	-0.2376	0.0084	0	0	0.0138	-0.2055	0.266	LYS	510
511	PHE	0.9997	0.122	0.1519	0	0	0.0094	-0.2311	0.2086	GLY	511
512	ALA	0.2085	-0.2311	0.0094	0	0	0.0503	-0.0763	0.5554	PHE	512
513	ARG	0.3224	-0.1803	0.019	0	0	0.1205	0.0679	0.8784	PHE	513
						0	0.0374	-0.1126	0.4741	GLY	514
						0	0.1251	0.0758	0.8961	TRP	515
615	PHE	2.1648	0.6422	0.432	1	10	0.5758	1.0319	3.0378	PHE	617
616	SER	2.0559	0.5936	0.4102	1	23	0.4655	0.7228	2.3455	ALA	618
617	GLY	0.8148	0.0395	0.1047	1	1	0.2243	0.2445	1.2741	GLY	619
618	GLN	2.8676	0.9559	0.5514	1	1	0.3727	0.5149	1.8798	ARG	620
863	GLN	2.0407	0.5868	0.4071	7	14	0.4872	0.7768	2.4663	GLN	865
864	GLU	2.4672	0.7771	0.4874	0	0	0.4861	0.7739	2.4599	GLU	866
865	ALA	0.701	-0.0113	0.0785	0	11	0.0718	-0.0256	0.6689	ARG	867
866	LEU	0.6058	-0.0538	0.0593	7	0	0.1457	0.1116	0.9763	LEU	868
867	SER	1.854	0.5034	0.3669	44	34	0.4167	0.6075	2.087	SER	869
868	SER	1.3819	0.2927	0.2526	44	34	0.135	0.0932	0.935	GLY	870
869	ASN	1.1995	0.2112	0.2046	0	0	0.2845	0.3482	1.5063	ASN	871
870	GLN	0.2748	-0.2016	0.0146	0	0	0.0595	-0.0533	0.6068	GLN	872

Table A.2. Chemical substrates of AcrAB and MdtEF from chemical sensitivity assay and associated charges from Chemicalize.

AcrAB				MdtEF			
Panel	**Well**	**Chemical**	**Charge**	**Charge**	**Chemical**	**Panel**	**Well**
PM12	E1	2,4-Diamino-6,7-diisopropyl-pteridine	0	0	2,4-Diamino-6,7-diisopropyl-pteridine	PM12	E1
PM16	A9	5-Chloro-7-iodo-8-hydroxyquinoline	0	0	5-Chloro-7-iodo-8-hydroxyquinoline	PM16	A9
PM20	A1	Amitriptyline	1	1	Amitriptyline	PM20	A1
Pm12	E9	Benzethonium chloride	1	1	Benzethonium chloride	Pm12	E9
PM16	C9	Cetylpyridinium chloride	1	1	Cetylpyridinium chloride	PM16	C9
PM14	G1	Chelerythrine	1	1	Chelerythrine	PM14	G1
PM20	E1	Crystal violet	1	1	Crystal violet	PM20	E1
PM13	A5	Dequalinium chloride	1	1	Dequalinium chloride	PM13	A5
Pm12	H9	Dodecyltrimethyl ammonium bromide	1	1	Dodecyltrimethyl ammonium bromide	Pm12	H9
PM20	E5	Dodine	1	1	Dodine	PM20	E5
PM15	D5	Domiphen bromide	1	1	Domiphen bromide	PM15	D5
PM11	F5	Erythromycin	1	1	Erythromycin	PM11	F5
PM19	A1	Josamycin	1	1	Josamycin	PM19	A1
PM17	E1	Niaproof	-1	-1	Niaproof	PM17	E1
PM15	F5	Oleandomycin	1	1	Oleandomycin	PM15	F5
PM20	F9	Pridinol	1	1	Pridinol	PM20	F9
PM14	A9	Sanguinarine	1	1	Sanguinarine	PM14	A9
Pm12	H1	Spiramycin	1	1	Spiramycin	Pm12	H1
PM20	C1	Thioridazine	1	1	Thioridazine	PM20	C1
PM13	G9	Trifluoperazine	1	1	Trifluoperazine	PM13	G9
PM20	H9	Troleandomycin	1	1	Troleandomycin	PM20	H9
PM13	H9	Tylosin	1	1	Tylosin	PM13	H9
PM15	C9	1,10-Phenanthroline	0	2	Bleomycin	PM11	C1
PM18	H5	2-Phenylphenol	0	-1	Cefmetazole	PM15	A9
PM15	B9	5,7-Dichloro-8-hydroxyquinaldine	0	2	Chlorhexidine	PM19	C1
PM15	C1	5,7-Dichloro-8-hydroxyquinoline	0	1	Lidocaine	PM18	D9
PM20	G9	8-Hydroxy-quinoline	0	0	Minocycline	PM11	C9
PM14	B1	9-Aminoacridine	1				
PM14	A1	Acriflavine	1				
PM11	F1	Chloramphenicol	0				
PM17	D9	Chlorpromazine	1				
PM11	A5	Chlortetracycline	0				
PM20	D5	Ciprofloxacin	0				
PM13	C5	Doxycycline	0				
PM11	E5	Enoxacin	0				
PM15	C5	Fusidic acid	-1				
PM19	B5	Harmane	0				
PM20	E9	Hexa-chlorophene	-1				
PM19	D5	Iodonitro Tetrazolium Violet	1				
PM19	G1	Lauryl sulfobetaine	0				
PM19	E9	Lawsone	-1				
PM18	D9	Lidocaine	1				
PM11	A9	Lincomycin	0				
PM11	B9	Lomefloxacin	0				
PM15	G9	Menadione	0				
PM19	B1	Methyltrioctyl-ammonium chloride	1				
PM11	E9	Nalidixic Acid	-1				
PM15	D9	Nordihydroguaia retic acid	0				
PM16	B1	Norfloxacin	0				
Pm12	D9	Novobiocin	-1				
PM11	H9	Ofloxacin	-1				
PM20	B1	Orphenadrine	1				
PM13	B9	Oxolinic acid	-1				
PM20	F5	Oxytetracycline	0				
PM18	C9	Pentachloro-phenol	-1				
PM20	D1	Proflavine	1				
PM16	E9	Rifamycin SV	-1				
PM13	D9	Rolitetracycline	0				
Pm12	A5	Tetracycline	0				
PM20	B9	Tetrazolium violet	1				
PM18	A9	Thiamphenicol	0				
PM18	G1	Triclosan	0				
PM16	B9	Trimethoprim	1				

APPENDIX B

SUPPLEMENTAL INFORMATION FOR CHAPTER 3: HIGH-THROUGHPUT SCREENING OF SYNERGISTIC GROUP IB-BIOCIDE COMBINATIONS FOR E. COLI INACTIVATION

B.1. Chemcial Sensitivy Assay.

Under each metal concentration (as µM or mM) are four squares (per biocide) representing four increasing concentrations of that biocide. Thus, twelve concentrations were tested per metal/antibiotic pair for a total of 2,520 combinations of Ag (I)/biocide, Cu (II)/biocides, and Au (III)/biocides for 7,560 total combinations tested. Samples were tesed in duplicate.

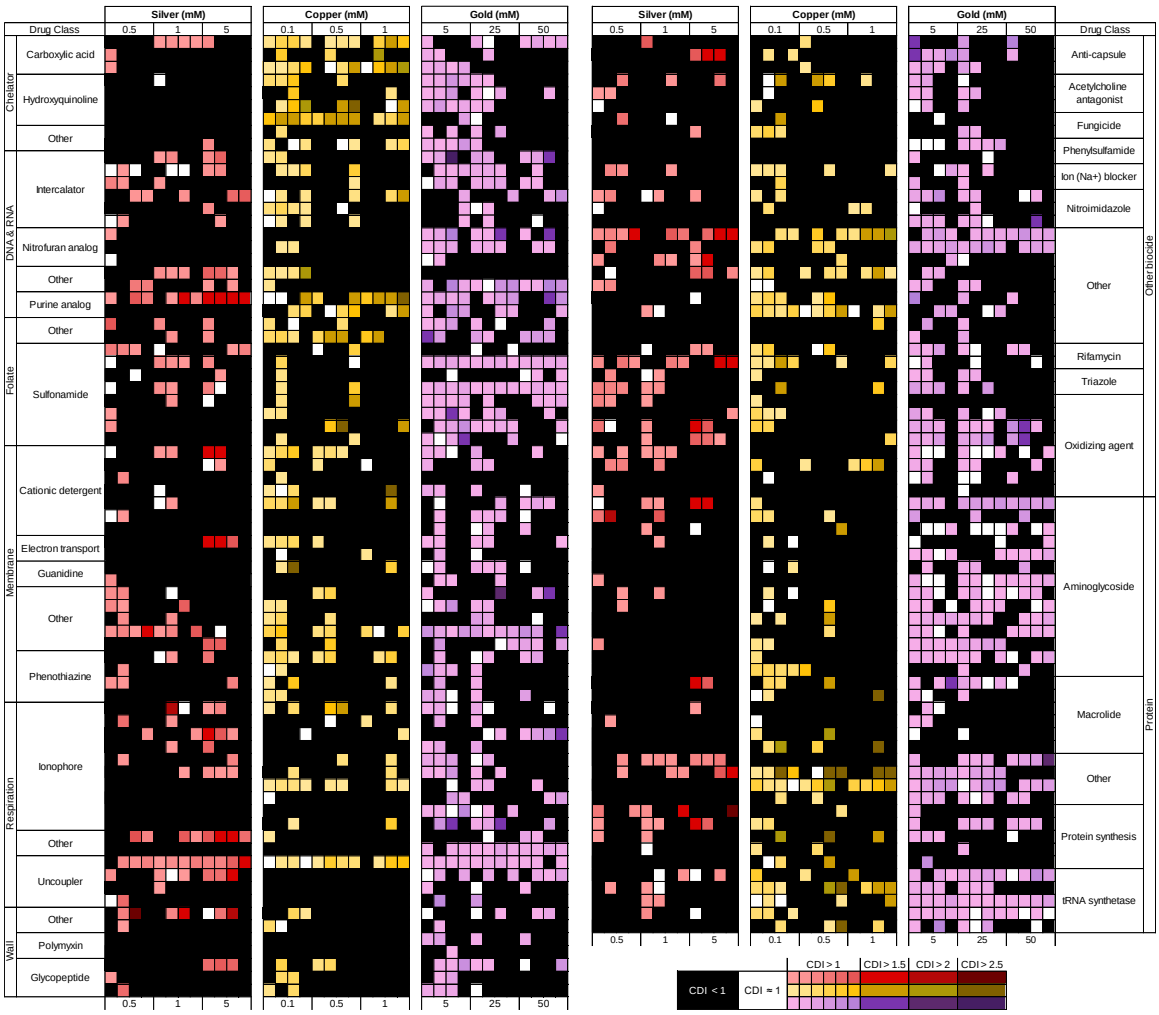

Figure B.1. Heat map of antagonistic responses as determined by the coefficient of drug interaction. 630 combinations of Group IB metals with biocides present in a commercially available 96-well panel set are displayed. Antagonistic responses are highlighted with shades of red, yellow or purple. White squares are considered additive (within 1% of CDI =1). Black shaded regions include synergistic (CDI < 1) or undefined CDI calculations.

Table B.1. Minimum inhibition concentrations of Cu (I), Ag (I), and Au (III) ions with *E. coli*. MIC was carried out using the micro-titer broth dilution method.

	Copper Sulphate	**Silver Nitrate**	**Gold Chloride Trihydrate**
MIC_{90}	> 4 mM	40 uM	50 uM

APPENDIX C

SUPPLIMENTAL INFORMATION FOR CHAPTER 4: SYNERGY AND ANTAGONISM OF GROUP IB METAL AND PHENOTHIAZINE COMPLEXES AND MIXTURES ON E. COLI

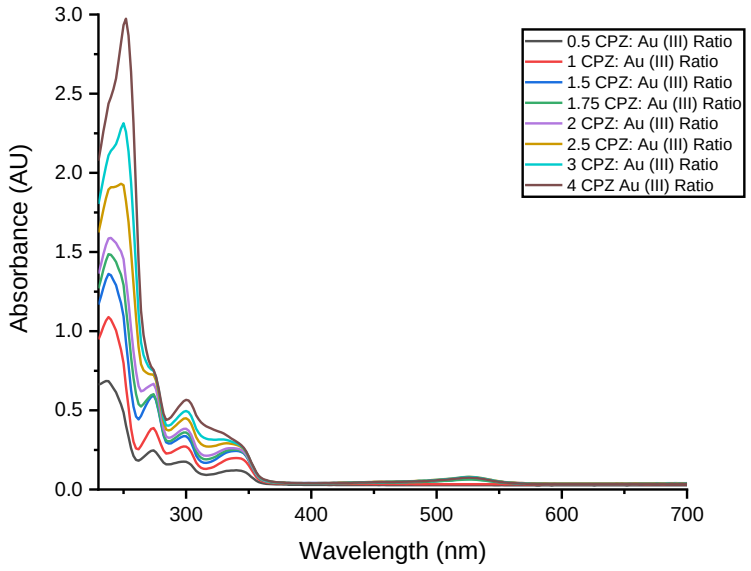

Figure C.1 UV-vis scans of CPZ and Au (III) under increasing molar ratios of PTZ-Metal. Scans were conducted with a base Au (III) concentration of 0.1 mM

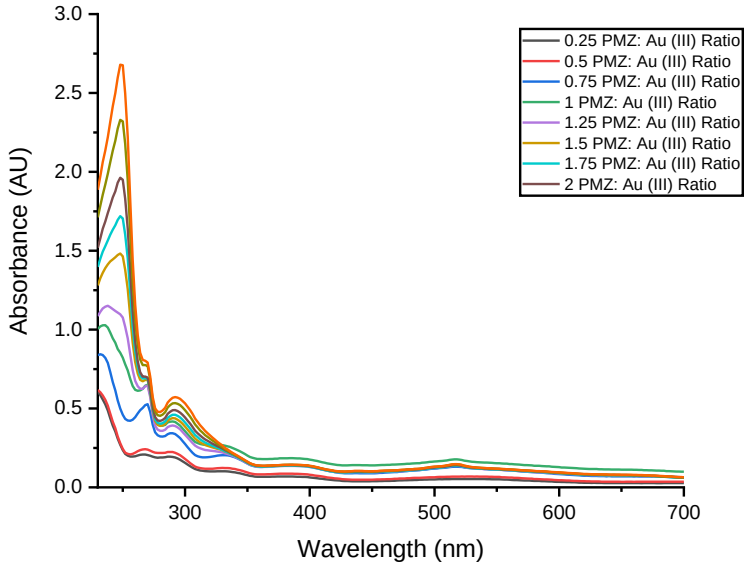

Figure C.2. UV-vis scans of PMZ and Au (III) under increasing molar ratios of PTZ-Metal. Scans were conducted with a base Au (III) concentration of 0.15 mM

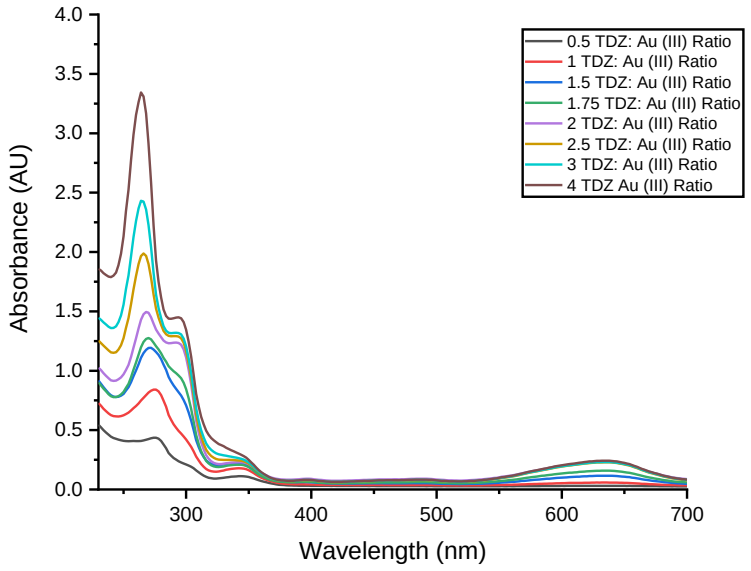

Figure C.3. UV-vis scans of TDZ and Au (III) under increasing molar ratios of PTZ-Metal. Scans were conducted with a base Au (III) concentration of 0.1 mM

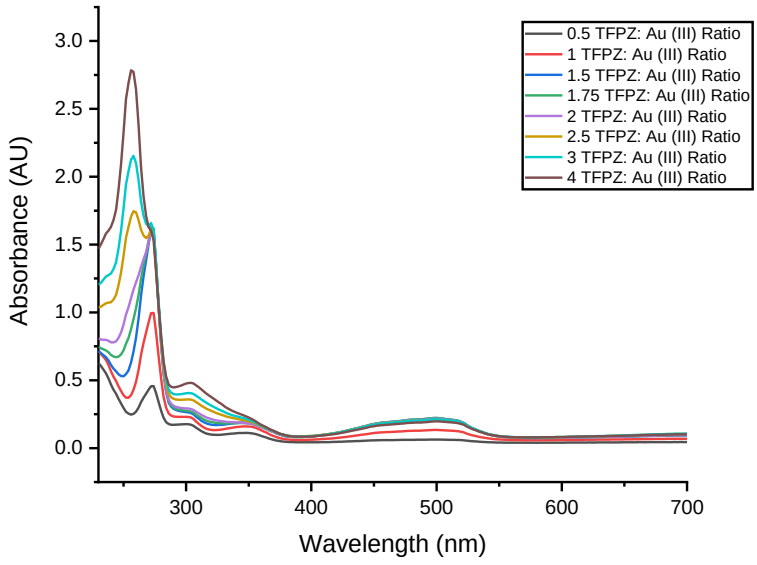

Figure C.4. UV-vis scans of TFPZ and Au (III) under increasing molar ratios of PTZ-Metal. Scans were conducted with a base Au (III) concentration of 0.1 Mm

		Chlorpromazine										
	µM	180	90.1	45.0	22.5	11.3	5.63	2.81	1.41	0.704	0.352	0
Ag (I)	40	90.1556	90.1556	90.1556	90.1556	90.3651	90.3651	90.2603	90.2603	90.4698	90.2603	90.3651
	20	90.3651	90.5745	79.5781	38.6296	31.2986	28.471	30.9844	36.2208	10.772	19.5691	11.4004
	10	90.4698	90.4698	90.4698	52.3489	48.9976	46.5889	46.4841	45.5416	37.1634	6.05925	30.0419
	5.0	90.4698	90.5745	90.2603	51.3016	28.5757	17.684	18.4171	15.0658	27.1095	16.1131	13.9138
	2.5	90.5745	90.4698	87.2232	29.3088	18.836	14.6469	20.8259	10.5625	16.2178	9.93417	16.9509
	1.3	90.3651	90.6792	68.5817	25.6433	13.4949	15.0658	17.5793	12.4476	15.9037	14.9611	11.6098
	0.63	90.8887	90.784	69.9431	16.7415	12.7618	8.88689	12.4476	8.78217	7.52543	10.0389	10.9814
	0	90.3651	90.6792	54.5482	10.772	13.9138	6.16397	3.12687	2.60323	4.27887	7.0018	
Cu (II)	4000	73.4749	73.2868	73.0986	73.4749	73.5689	73.0986	73.1927	72.6283	73.0986	72.8164	72.4402
	2000	80.9057	79.871	64.5391	68.8659	63.5044	69.9946	79.6829	79.6829	79.7769	80.3413	58.0489
	1000	85.7028	85.4206	69.5243	50.8062	38.6724	40.0833	40.3655	41.7764	39.8952	41.5883	40.6477
	500.0	88.5246	77.8017	57.2964	37.2615	27.4792	28.3257	25.0336	28.1376	32.2763	33.7812	29.6426
	250.0	90.1236	89.8414	59.1776	35.6625	26.9148	26.9148	29.6426	22.588	27.197	23.8108	23.0583
	125.0	91.0642	81.0938	51.8409	29.3604	17.6969	22.8702	20.1424	23.7167	19.0137	17.5087	16.0038
	62.50	91.5345	81.376	49.5834	27.6673	22.6821	23.6227	15.7216	19.6721	17.3206	17.7909	15.8156
	0	91.7227	82.975	52.5934	19.2018	12.8057	11.4888	6.78581	10.8304	9.70169	7.82048	
Au (III)	100	87.8035	2.72779	87.0037	90.6027	91.1025	91.1025	91.0026	90.9026	91.2025	90.7027	89.0031
	50.0	90.0029	20.9226	1.22822	61.3111	66.6095	75.9069	62.3108	80.7055	65.3099	66.1097	90.9026
	25.0	90.0029	54.513	0.12853	2.62782	12.7249	14.4245	8.82605	6.02685	19.8229	25.6213	28.9203
	12.5	89.2031	64.91	13.8246	2.32791	2.02799	4.42731	4.42731	5.92688	6.02685	6.72665	8.02628
	6.25	90.3028	74.6073	20.2228	5.72694	0.92831	6.42674	1.72808	3.72751	-0.97115	2.72779	6.22679
	3.13	90.9026	75.3071	25.6213	11.6252	6.22679	7.72636	1.42816	6.22679	1.12825	3.82748	-4.07027
	1.56	91.1025	74.0074	23.022	4.72722	3.82748	7.12654	4.02742	3.12768	-0.47129	-4.97001	1.32819
	0	91.1025	88.0034	50.7141	3.02771	7.62639	8.52614	2.42788	6.52671	3.72751	1.62811	

	High									Low
Inhibition	100	90	80	70	60	50	40	30	20	10

Figure C.5. Heat map of the inhbition of *E. coli* growth from dually appled CPZ and metals corresponding to duplicate experiments

		Promethazine										
	µM	180	90.1	45.0	22.5	11.3	5.63	2.81	1.41	0.704	0.352	0
Ag (I)	40	89.9577	89.9577	90.0634	90.1691	90.2748	90.2748	90.0634	89.9577	89.9577	90.0634	90.1691
	20	90.2748	90.3805	34.1438	33.4038	27.5899	28.7526	32.3467	24.7357	13.5307	34.8837	37.5264
	10	90.3805	89.2178	56.1311	48.0973	44.0803	44.8203	39.2178	31.9239	37.315	33.6152	36.2579
	5.0	90.4863	89.1121	24.9471	24.4186	20.296	17.759	17.8647	20.0846	6.13108	18.6047	19.1332
	2.5	89.9577	79.9154	25.37	20.6131	10.0423	19.3446	2.43129	14.2706	15.6448	7.29387	13.6364
	1.3	90.4863	77.3784	16.4905	10.0423	12.5793	6.76533	10.7822	5.81395	6.87104	15.1163	10.9937
	0.63	90.8034	79.1755	18.0761	7.18816	8.77378	3.59408	4.96829	6.23679	5.81395	8.13953	10.2537
	0	90.4863	67.5476	24.9471	10.3594	5.074	1.16279	-0.42283	1.79704	3.17125	2.32558	
Cu (II)	4000	71.0248	70.6252	70.6252	70.5253	71.7242	71.5244	71.1248	70.825	71.3246	70.825	69.9258
	2000	77.819	77.0197	78.6183	78.5184	78.5184	78.0188	78.0188	78.6183	78.6183	74.2221	77.6192
	1000	81.316	60.2341	48.8438	43.0488	45.7465	42.6492	43.7482	43.5484	42.6492	42.1496	40.6509
	500.0	87.7105	63.0317	43.4485	38.7525	25.8635	27.4622	38.3528	38.7525	35.7551	27.662	31.6586
	250.0	89.3092	63.4313	40.1513	29.1607	25.2641	24.0651	23.2658	24.4647	24.0651	17.0711	22.8661
	125.0	90.3083	61.3331	29.3605	24.9643	25.364	26.3631	22.3665	15.2726	21.2675	17.171	18.0702
	62.50	91.0077	57.0368	30.8593	21.3674	18.4699	15.8721	17.171	19.469	12.7748	13.674	10.7765
	0	91.0077	51.7414	25.8635	26.3631	18.37	11.4759	13.7739	11.9754	8.47845	8.1787	
Au (III)	100	77.6358	35.4487	16.2358	59.0328	85.5649	88.6146	89.7328	90.1394	90.7493	90.7493	90.7493
	50.0	79.3639	40.4299	17.1507	10.8481	10.7464	42.463	76.7209	71.7398	83.5318	83.1252	85.4633
	25.0	86.1748	46.7325	18.4723	12.1696	10.0349	12.6779	10.8481	15.7276	17.7607	17.964	13.4911
	12.5	87.1914	48.359	19.0822	13.4911	11.0514	10.6448	7.59512	9.83154	13.0845	14.406	18.4723
	6.25	88.9195	50.1888	21.6236	12.7796	18.5739	8.81499	11.2547	11.2547	10.3398	9.0183	12.6779
	3.13	90.6477	61.0659	20.7087	16.3375	11.9663	19.6921	15.016	8.71333	3.5289	13.3895	11.9663
	1.56	90.6477	46.2242	21.6236	23.4534	22.0302	19.3872	12.7796	7.79843	8.61168	7.69678	10.9498
	0	90.851	54.56	23.7584	16.4392	12.068	4.03718	3.22393	4.54545	5.86698	1.08917	

	High									Low
Inhibition	100	90	80	70	60	50	40	30	20	10

Figure C.6. Heat map of the inhbition of *E. coli* growth from dually appled PMZ and metals corresponding to duplicate experiments

		Thioridazine										
	µM	180	90.1	45.0	22.5	11.3	5.63	2.81	1.41	0.704	0.352	0
Ag (I)	40	80.9917	89.6694	90.3926	90.5992	90.3926	90.4959	90.2893	90.2893	90.4959	90.3926	90.3926
	20	80.9917	89.9793	90.4959	90.5992	90.4959	79.3388	69.1116	71.281	70.4545	65.9091	69.8347
	10	81.3017	90.0826	90.7025	90.7025	51.1364	49.5868	46.7975	47.5207	48.5537	48.5537	47.1074
	5.0	79.5455	90.2893	90.7025	78.3058	48.1405	33.5744	28.8223	15.186	22.8306	25.3099	24.3802
	2.5	79.9587	90.2893	90.8058	68.6983	5.47521	15.7025	24.5868	22.314	20.0413	28.2025	31.095
	1.3	82.0248	90.4959	90.8058	52.376	28.4091	14.9793	20.3512	12.6033	14.1529	15.5992	22.4174
	0.63	81.1983	90.4959	90.7025	33.6777	17.2521	9.29752	7.95455	8.78099	8.36777	11.7769	6.61157
	0	80.9917	90.3926	78.3058	33.6777	18.8017	13.1198	7.02479	7.95455	9.19421	4.23554	
Cu (II)	4000	71.5695	71.1633	70.9603	71.3664	69.9449	71.3664	70.5541	71.1633	71.1633	70.9603	70.5541
	2000	78.271	79.4894	79.2863	78.0679	59.1819	79.0833	79.0833	78.8802	78.6771	78.474	78.474
	1000	84.3632	84.1601	63.0403	46.1851	37.4529	35.8283	26.6899	38.4682	36.2344	34.8129	32.9852
	500.0	87.8155	66.0865	50.8558	36.0313	27.7053	25.8776	4.75776	28.9237	30.1422	29.5329	26.4868
	250.0	89.4401	67.3049	48.2158	28.3145	14.3023	18.973	26.2837	21.2068	-6.81752	15.1146	21.0038
	125.0	90.4555	61.4157	38.0621	16.333	14.3023	7.39774	9.22541	5.97621	-3.16217	18.7699	18.1607
	62.50	90.0493	51.465	35.016	16.7392	15.3177	1.71163	-6.2083	-2.34987	16.9423	12.4746	6.99159
	0	90.4555	44.5605	27.2991	9.22541	3.53931	-4.98985	4.75776	7.60081	6.99159	5.77314	
Au (III)	100	89.5184	89.1942	89.9506	90.2748	90.2748	90.3828	90.2748	90.1667	90.4909	90.3828	90.2748
	50.0	88.762	78.1723	19.0645	63.5844	89.3023	90.2748	90.1667	70.176	90.1667	90.1667	87.7894
	25.0	87.1411	73.3097	28.6817	-1.35844	7.61037	14.9583	11.3924	16.0389	24.1433	29.1139	26.0883
	12.5	83.7913	71.4727	42.5131	14.31	-4.27601	-3.41155	-2.7632	9.87959	2.42359	12.9052	24.4674
	6.25	84.1155	67.1504	49.9691	17.8759	-1.57456	-4.27601	0.15437	-3.62766	-2.33097	5.77339	7.61037
	3.13	85.5202	82.7107	53.1028	21.766	8.69095	5.77339	-0.92621	1.23495	-6.43717	6.31368	2.74776
	1.56	82.2785	84.5477	42.9454	19.8209	5.12504	16.7953	3.61223	13.2294	13.5536	11.0682	4.69281
	0	85.7363	68.2309	47.6999	23.0627	4.26057	-5.57271	-2.54708	4.47669	4.47669	2.09941	

	High									Low
Inhibition	100	90	80	70	60	50	40	30	20	10

Figure C.7. Heat map of the inhbition of *E. coli* growth from dually appled TDZ and metals corresponding to duplicate experiments

		Trifluoperazine										
	µM	180	90.1	45.0	22.5	11.3	5.63	2.81	1.41	0.704	0.352	0
Ag (I)	40	89.541	89.6488	89.8644	89.9723	90.0801	90.1879	90.0801	89.8644	90.0801	89.9723	89.9723
	20	89.4331	90.1879	90.2957	67.5447	20.4251	29.0511	24.846	36.9224	25.0616	36.5989	31.7468
	10	89.541	90.0801	89.7566	53.2039	50.5083	49.8614	48.8909	45.4405	48.3518	40.0493	50.9396
	5.0	89.8644	88.7862	62.9082	48.6753	29.2668	30.4529	18.053	36.0598	18.6999	11.5835	23.5521
	2.5	90.0801	90.4036	63.8786	38.7554	25.7086	26.4633	7.37831	12.2304	3.06531	7.16266	11.1522
	1.3	90.2957	90.5114	56.87	21.6112	15.8965	7.70179	12.2304	4.89834	4.25139	5.22181	13.74
	0.63	90.1879	90.2957	66.0351	9.53481	8.45656	4.35921	0.58534	3.71226	6.19224	5.43746	5.76094
	0	89.0018	90.1879	45.5484	14.9261	9.21134	3.17314	3.92791	6.30006	2.09489	2.09489	
Cu (II)	4000	71.1633	70.7572	70.5541	70.9603	70.351	71.1633	70.6556	70.8587	70.7572	70.351	70.0464
	2000	78.5756	78.9817	78.7786	77.9663	68.828	78.8802	78.6771	76.2402	78.474	78.1694	78.0679
	1000	84.3632	83.8555	66.7972	47.4035	42.4282	39.0775	35.219	41.6159	41.3113	38.3667	38.6713
	500.0	87.6124	71.1633	53.8004	41.1082	29.3299	19.9884	18.6684	28.6191	22.5268	17.653	27.8068
	250.0	89.1355	70.5541	51.262	33.2898	19.8869	20.1915	27.6037	23.7453	7.19466	17.7546	19.7853
	125.0	89.8462	68.7264	39.9913	19.2776	16.7392	10.0377	12.8808	12.6777	7.60081	18.4653	19.7853
	62.50	90.1509	62.5326	42.9359	24.9637	19.6838	12.3731	9.63156	11.6623	21.1053	16.0284	12.4746
	0	90.4555	45.982	31.5637	13.5915	6.07775	-1.94372	1.10241	8.61619	7.39774	4.96084	
Au (III)	100	88.2278	15.2205	38.8638	87.0407	91.2945	91.2945	91.0967	91.0967	91.2945	91.0967	91.0967
	50.0	88.5246	89.8106	87.931	87.931	90.1074	91.0967	91.0967	91.0967	90.7999	90.9977	90.8988
	25.0	89.4149	90.2063	88.4257	72.2018	17.9904	19.7711	22.4421	40.5455	29.9604	33.1261	57.5608
	12.5	88.4257	88.5246	88.8214	86.4471	18.6829	13.6376	11.4613	17.7925	17.1001	16.8033	19.6721
	6.25	89.1181	89.5138	89.4149	38.4681	12.2527	7.40531	-1.00339	7.40531	4.04183	11.2634	15.2205
	3.13	90.2063	90.4042	48.6574	29.169	15.6162	10.5709	5.22894	7.70209	5.22894	10.1752	13.3409
	1.56	90.4042	90.7999	50.7349	21.9474	13.6376	17.5947	14.1323	9.48276	12.5495	4.43754	12.2527
	0	77.6427	70.9158	37.3799	19.1775	15.5172	12.7473	5.13002	10.0763	9.97739	8.29565	

	High									Low
Inhibition	100	90	80	70	60	50	40	30	20	10

Figure C.8. Heat map of the inhbition of *E. coli* growth from dually appled TDZ and metals corresponding to duplicate experiments

APPENDIX D

SUPPLEMENTAL INFORMATION FOR CHAPTER 5: MEMBRANE PROTEOMIC ANALYSIS REVEALS ENDOCRINE-DISRUPTING CHEMICALS INDUCE ANTIBIOTIC-RESISTANCE TOWARD KNOWN BIOCIDES

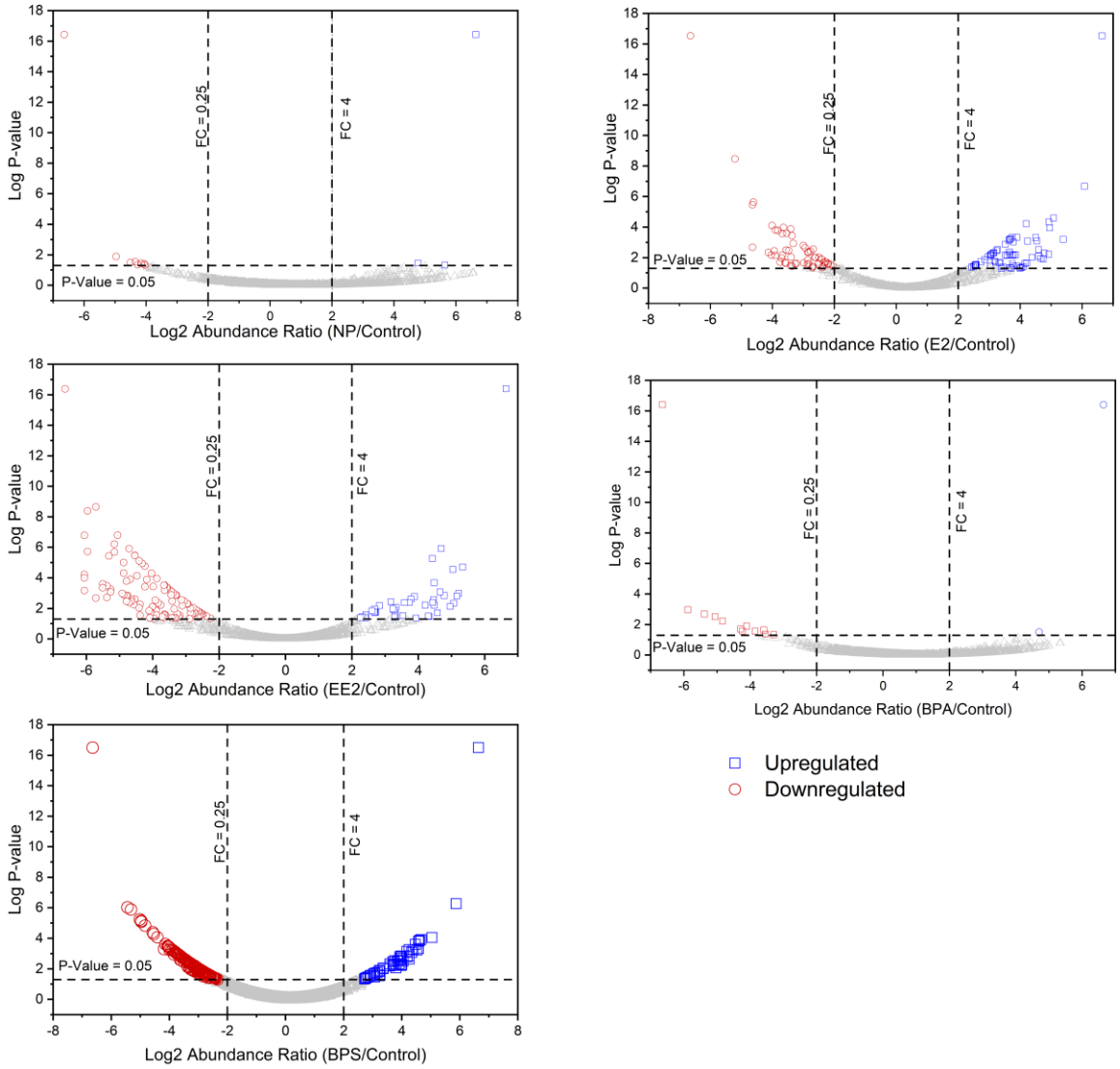

Figure D.1. Total and significantly identified relative proteins from triplicate extractions of respective EDC (0.01% w/v) grown *E. Coli*. Samples were from biological triplicate protein extractions as separate injections in the mass-spec. The solvent for NP, EE2, BPA, BPS is EtOH and the solvent for E2 was DMSO. Samples of just W3110 with no exposure were also processed and compared to solvent controls (data not shown)

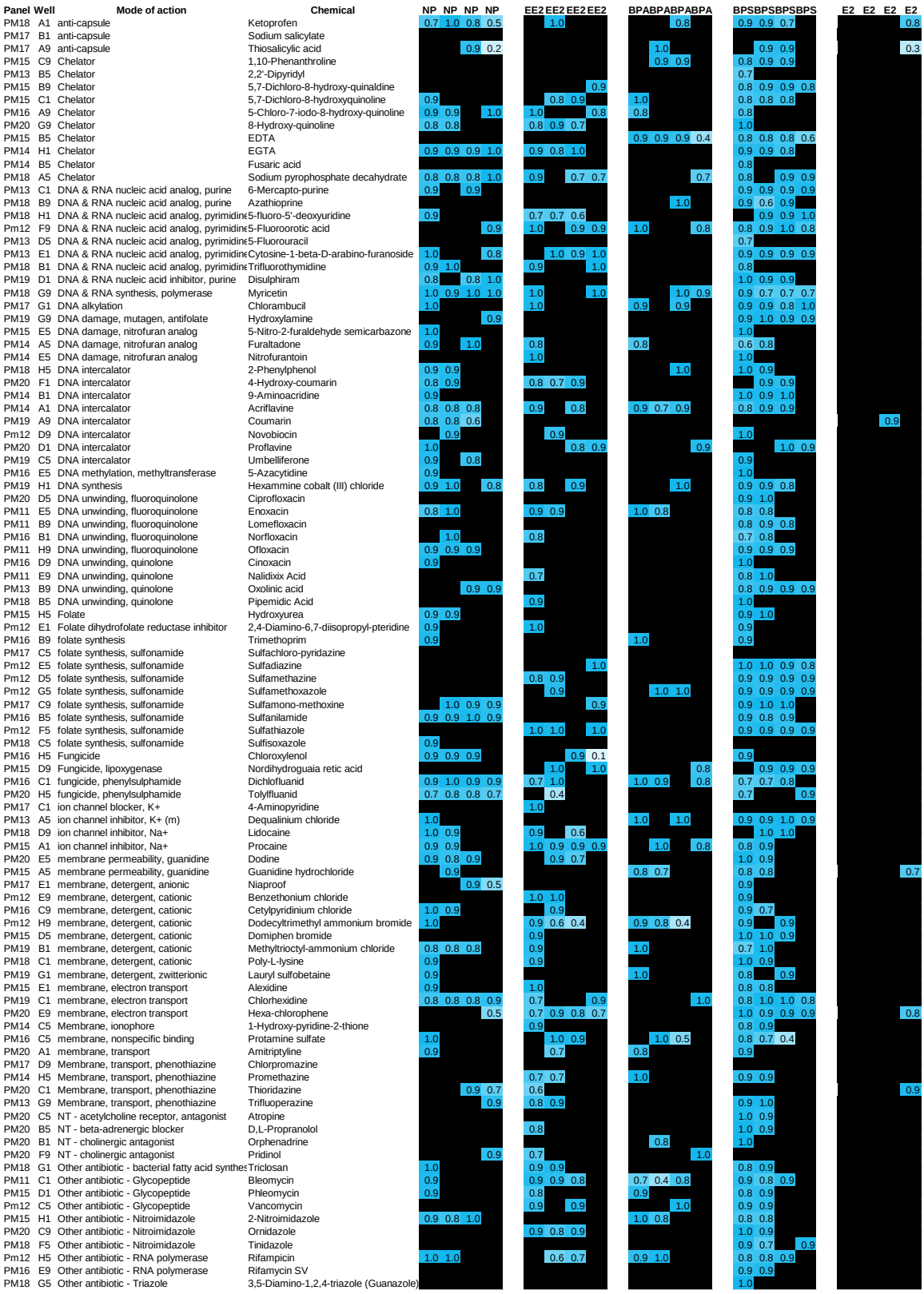
Panel Well Mode of action Chemical NP NP NP NP EE2 EE2 EE2 EE2 BPABPABPABPA BPSBPSBPSBPS E2 E2 E2 E2
PM18 A1 anti-capsule Ketoprofen 0.7 1.0 0.8 0.5 1.0 0.8 0.9 0.9 0.7 0.8
PM17 B1 anti-capsule Sodium salicylate
PM17 A9 anti-capsule Thiosalicylic acid 0.9 0.2 1.0 0.9 0.9 0.3
PM15 C9 Chelator 1,10-Phenanthroline 0.9 0.9 0.8 0.9 0.9
PM13 B5 Chelator 2,2'-Dipyridyl 0.7
PM15 B9 Chelator 5,7-Dichloro-8-hydroxy-quinaldine 0.9 0.8 0.9 0.9 0.8
PM15 C1 Chelator 5,7-Dichloro-8-hydroxyquinoline 0.9 0.8 0.9 1.0 0.8 0.8 0.8
PM16 A9 Chelator 5-Chloro-7-iodo-8-hydroxy-quinoline 0.9 0.9 1.0 1.0 0.8 0.8 0.8
PM20 G9 Chelator 8-Hydroxy-quinoline 0.8 0.8 0.8 0.9 0.7 1.0
PM15 B5 Chelator EDTA 0.9 0.9 0.9 0.4 0.8 0.8 0.8 0.6
PM14 H1 Chelator EGTA 0.9 0.9 0.9 1.0 0.9 0.8 1.0 0.9 0.9 0.8
PM14 B5 Chelator Fusaric acid 0.8
PM18 A5 Chelator Sodium pyrophosphate decahydrate 0.8 0.8 0.8 1.0 0.9 0.7 0.7 0.7 0.8 0.9 0.9
PM13 C1 DNA & RNA nucleic acid analog, purine 6-Mercapto-purine 0.9 0.9 0.9 0.9 0.9 0.9
PM18 B9 DNA & RNA nucleic acid analog, purine Azathioprine 1.0 0.9 0.6 0.9
PM18 H1 DNA & RNA nucleic acid analog, pyrimidine 5-fluoro-5'-deoxyuridine 0.9 0.7 0.7 0.6 0.9 0.9 1.0
Pm12 F9 DNA & RNA nucleic acid analog, pyrimidine 5-Fluoroorotic acid 0.9 1.0 0.9 0.9 1.0 0.8 0.8 0.9 1.0 0.8
PM13 D5 DNA & RNA nucleic acid analog, pyrimidine 5-Fluorouracil 0.7
PM13 E1 DNA & RNA nucleic acid analog, pyrimidine Cytosine-1-beta-D-arabino-furanoside 1.0 0.8 1.0 0.9 1.0 0.9 0.9 0.9
PM18 B1 DNA & RNA nucleic acid analog, pyrimidine Trifluorothymidine 0.9 1.0 0.9 1.0 0.8
PM19 D1 DNA & RNA nucleic acid inhibitor, purine Disulphiram 0.8 0.8 1.0 1.0 0.9 0.9
PM18 G9 DNA & RNA synthesis, polymerase Myricetin 1.0 0.9 1.0 1.0 1.0 1.0 1.0 0.9 0.9 0.7 0.7 0.7
PM17 G1 DNA alkylation Chlorambucil 1.0 1.0 0.9 0.9 0.9 0.9 0.8 1.0
PM19 G9 DNA damage, mutagen, antifolate Hydroxylamine 0.9 0.9 1.0 0.9 0.9
PM15 E5 DNA damage, nitrofuran analog 5-Nitro-2-furaldehyde semicarbazone 1.0 1.0
PM14 A5 DNA damage, nitrofuran analog Furaltadone 0.9 1.0 0.8 0.8 0.6 0.8
PM14 E5 DNA damage, nitrofuran analog Nitrofurantoin 1.0 1.0
PM18 H5 DNA intercalator 2-Phenylphenol 0.9 0.9 1.0 1.0 0.9
PM20 F1 DNA intercalator 4-Hydroxy-coumarin 0.8 0.9 0.8 0.7 0.9 0.9 0.9
PM14 B1 DNA intercalator 9-Aminoacridine 0.9 1.0 0.9 1.0
PM14 A1 DNA intercalator Acriflavine 0.8 0.8 0.8 0.9 0.8 0.9 0.7 0.9 0.8 0.9 0.9
PM19 A9 DNA intercalator Coumarin 0.8 0.8 0.6 0.9
Pm12 D9 DNA intercalator Novobiocin 0.9 0.9 1.0
PM20 D1 DNA intercalator Proflavine 1.0 0.8 0.9 0.9 1.0 0.9
PM19 C5 DNA intercalator Umbelliferone 0.9 0.8 0.9
PM16 E5 DNA methylation, methyltransferase 5-Azacytidine 0.9 1.0
PM19 H1 DNA synthesis Hexammine cobalt (III) chloride 0.9 1.0 0.8 0.8 0.9 1.0 0.9 0.9 0.8
PM20 D5 DNA unwinding, fluoroquinolone Ciprofloxacin 0.9 1.0
PM11 E5 DNA unwinding, fluoroquinolone Enoxacin 0.8 1.0 0.9 0.9 1.0 0.8 0.8 0.8
PM11 B9 DNA unwinding, fluoroquinolone Lomefloxacin 0.8 0.9 0.8
PM16 B1 DNA unwinding, fluoroquinolone Norfloxacin 1.0 0.8 0.7 0.8
PM11 H9 DNA unwinding, fluoroquinolone Ofloxacin 0.9 0.9 0.9 0.9 0.9 0.9
PM16 D9 DNA unwinding, quinolone Cinoxacin 0.9 1.0
PM11 E9 DNA unwinding, quinolone Nalidixix Acid 0.7 0.8 1.0
PM13 B9 DNA unwinding, quinolone Oxolinic acid 0.9 0.9 0.8 0.9 0.9 0.9
PM18 B5 DNA unwinding, quinolone Pipemidic Acid 0.9 1.0
PM15 H5 Folate Hydroxyurea 0.9 0.9 0.9 1.0
Pm12 E1 Folate dihydrofolate reductase inhibitor 2,4-Diamino-6,7-diisopropyl-pteridine 0.9 1.0 0.9
PM16 B9 folate synthesis Trimethoprim 0.9 1.0 0.9
PM17 C5 folate synthesis, sulfonamide Sulfachloro-pyridazine
Pm12 E5 folate synthesis, sulfonamide Sulfadiazine 1.0 1.0 1.0 0.9 0.8
Pm12 D5 folate synthesis, sulfonamide Sulfamethazine 0.8 0.9 0.9 0.9 0.9 0.9
Pm12 G5 folate synthesis, sulfonamide Sulfamethoxazole 0.9 1.0 1.0 0.9 0.9 0.9 0.9
PM17 C9 folate synthesis, sulfonamide Sulfamono-methoxine 1.0 0.9 0.9 0.9 1.0 0.9 1.0
PM16 B5 folate synthesis, sulfonamide Sulfanilamide 0.9 0.9 1.0 0.9 0.9 0.8 0.9
Pm12 F5 folate synthesis, sulfonamide Sulfathiazole 1.0 1.0 1.0 0.9 0.9 0.9 0.9
PM18 C5 folate synthesis, sulfonamide Sulfisoxazole 0.9
PM16 H5 Fungicide Chloroxylenol 0.9 0.9 0.9 0.9 0.1 0.9
PM15 D9 Fungicide, lipoxygenase Nordihydroguaia retic acid 1.0 1.0 0.8 0.9 0.9 0.9
PM16 C1 fungicide, phenylsulphamide Dichlofluanid 0.9 1.0 0.9 0.9 0.7 1.0 1.0 0.9 0.8 0.7 0.7 0.8
PM20 H5 fungicide, phenylsulphamide Tolylfluanid 0.7 0.8 0.8 0.7 0.4 0.7 0.9
PM17 C1 ion channel blocker, K+ 4-Aminopyridine 1.0
PM13 A5 ion channel inhibitor, K+ (m) Dequalinium chloride 1.0 1.0 1.0 0.9 0.9 1.0 0.9
PM18 D9 ion channel inhibitor, Na+ Lidocaine 1.0 0.9 0.9 0.6 1.0 1.0
PM15 A1 ion channel inhibitor, Na+ Procaine 0.9 0.9 1.0 0.9 0.9 0.9 1.0 0.8 0.8 0.9
PM20 E5 membrane permeability, guanidine Dodine 0.9 0.8 0.9 0.9 0.7 1.0 0.9
PM15 A5 membrane permeability, guanidine Guanidine hydrochloride 0.9 0.8 0.7 0.8 0.8 0.7
PM17 E1 membrane, detergent, anionic Niaproof 0.9 0.5 0.9
Pm12 E9 membrane, detergent, cationic Benzethonium chloride 1.0 1.0 0.9
PM16 C9 membrane, detergent, cationic Cetylpyridinium chloride 1.0 0.9 0.9 0.9 0.7
Pm12 H9 membrane, detergent, cationic Dodecyltrimethyl ammonium bromide 1.0 0.9 0.6 0.4 0.9 0.8 0.4 0.9 0.9
PM15 D5 membrane, detergent, cationic Domiphen bromide 0.9 1.0 1.0 0.9
PM19 B1 membrane, detergent, cationic Methyltrioctyl-ammonium chloride 0.8 0.8 0.8 0.9 1.0 0.7 1.0
PM18 C1 membrane, detergent, cationic Poly-L-lysine 0.9 0.9 1.0 0.9
PM19 G1 membrane, detergent, zwitterionic Lauryl sulfobetaine 0.9 1.0 0.8 0.9
PM15 E1 membrane, electron transport Alexidine 0.9 1.0 0.8 0.8
PM19 C1 membrane, electron transport Chlorhexidine 0.8 0.8 0.8 0.9 0.7 0.9 1.0 0.8 1.0 1.0 0.8
PM20 E9 membrane, electron transport Hexa-chlorophene 0.5 0.7 0.9 0.8 0.7 1.0 0.9 0.9 0.9 0.8
PM14 C5 Membrane, ionophore 1-Hydroxy-pyridine-2-thione 0.9 0.8 0.9
PM16 C5 membrane, nonspecific binding Protamine sulfate 1.0 1.0 0.9 1.0 0.5 0.8 0.7 0.4
PM20 A1 membrane, transport Amitriptyline 0.9 0.7 0.8 0.9
PM17 D9 Membrane, transport, phenothiazine Chlorpromazine
PM14 H5 Membrane, transport, phenothiazine Promethazine 0.7 0.7 1.0 0.9 0.9
PM20 C1 Membrane, transport, phenothiazine Thioridazine 0.9 0.7 0.6 0.9
PM13 G9 Membrane, transport, phenothiazine Trifluoperazine 0.9 0.8 0.9 0.9 1.0
PM20 C5 NT - acetylcholine receptor, antagonist Atropine 1.0 0.9
PM20 B5 NT - beta-adrenergic blocker D,L-Propranolol 0.8 1.0 0.9
PM20 B1 NT - cholinergic antagonist Orphenadrine 0.8 1.0
PM20 F9 NT - cholinergic antagonist Pridinol 0.9 0.7 1.0
PM18 G1 Other antibiotic - bacterial fatty acid synthes Triclosan 1.0 0.9 0.9 0.8 0.9
PM11 C1 Other antibiotic - Glycopeptide Bleomycin 0.9 0.9 0.9 0.8 0.7 0.4 0.8 0.9 0.8 0.9
PM15 D1 Other antibiotic - Glycopeptide Phleomycin 0.9 0.8 0.9 0.8 0.9
Pm12 C5 Other antibiotic - Glycopeptide Vancomycin 0.9 0.9 1.0 0.9 0.9
PM15 H1 Other antibiotic - Nitroimidazole 2-Nitroimidazole 0.9 0.8 1.0 1.0 0.8 0.8 0.8
PM20 C9 Other antibiotic - Nitroimidazole Ornidazole 0.9 0.8 0.9 1.0 0.9
PM18 F5 Other antibiotic - Nitroimidazole Tinidazole 0.9 0.7 0.9
Pm12 H5 Other antibiotic - RNA polymerase Rifampicin 1.0 1.0 0.6 0.7 0.9 1.0 0.8 0.8 0.9
PM16 E9 Other antibiotic - RNA polymerase Rifamycin SV 0.9 0.9
PM18 G5 Other antibiotic - Triazole 3,5-Diamino-1,2,4-triazole (Guanazole) 1.0

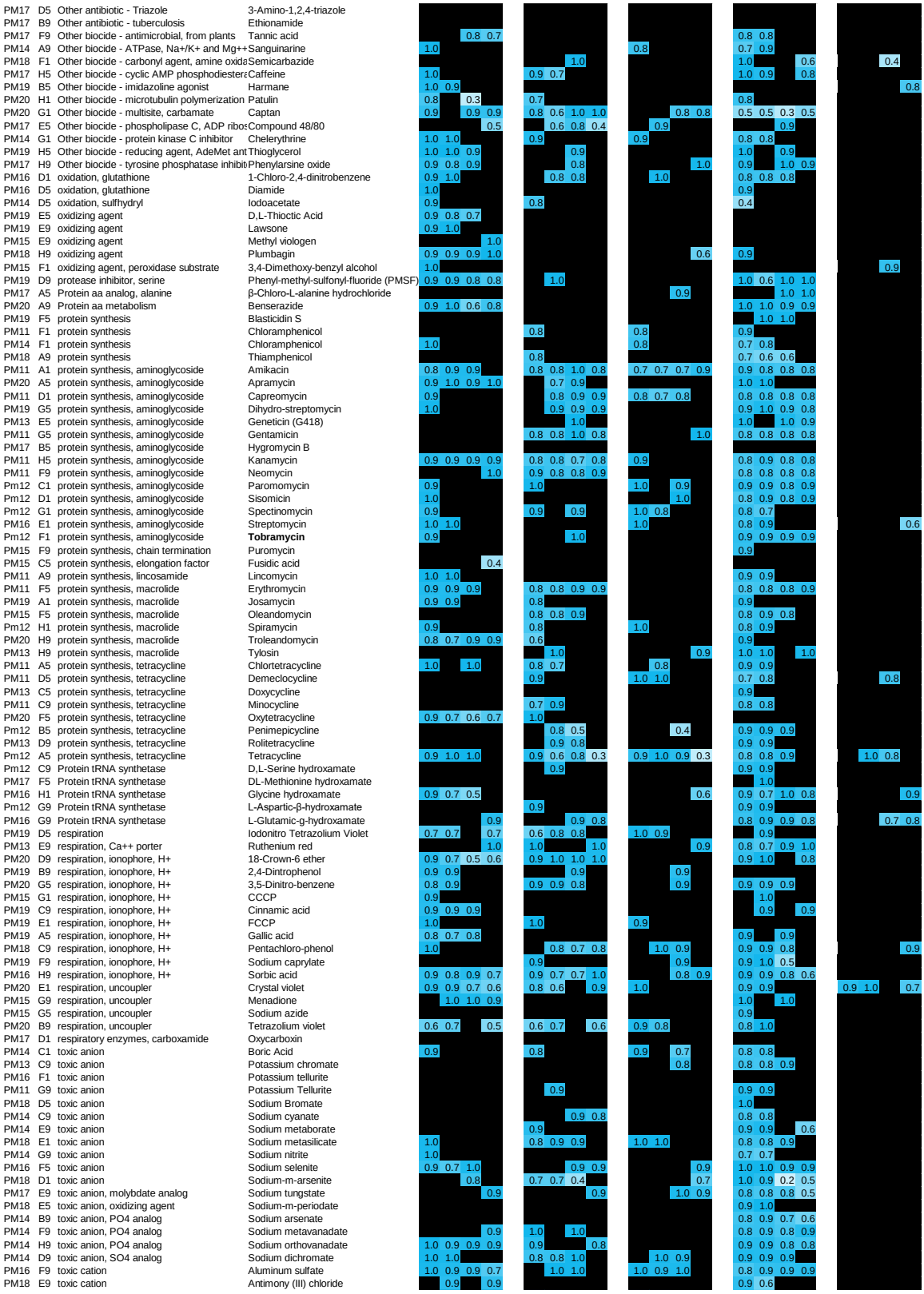
PM17 D5 Other antibiotic - Triazole 3-Amino-1,2,4-triazole
PM17 B9 Other antibiotic - tuberculosis Ethionamide
PM17 F9 Other biocide - antimicrobial, from plants Tannic acid
PM14 A9 Other biocide - ATPase, Na+/K+ and Mg++ Sanguinarine
PM18 F1 Other biocide - carbonyl agent, amine oxida Semicarbazide
PM17 H5 Other biocide - cyclic AMP phosphodiesterz Caffeine
PM19 B5 Other biocide - imidazoline agonist Harmane
PM20 H1 Other biocide - microtubulin polymerization Patulin
PM20 G1 Other biocide - multisite, carbamate Captan
PM17 E5 Other biocide - phospholipase C, ADP ribos Compound 48/80
PM14 G1 Other biocide - protein kinase C inhibitor Chelerythrine
PM19 H5 Other biocide - reducing agent, AdeMet ant Thioglycerol
PM17 H9 Other biocide - tyrosine phosphatase inhibit Phenylarsine oxide
PM16 D1 oxidation, glutathione 1-Chloro-2,4-dinitrobenzene
PM16 D5 oxidation, glutathione Diamide
PM14 D5 oxidation, sulfhydryl Iodoacetate
PM19 E5 oxidizing agent D,L-Thioctic Acid
PM19 E9 oxidizing agent Lawsone
PM15 E9 oxidizing agent Methyl viologen
PM18 H9 oxidizing agent Plumbagin
PM15 F1 oxidizing agent, peroxidase substrate 3,4-Dimethoxy-benzyl alcohol
PM19 D9 protease inhibitor, serine Phenyl-methyl-sulfonyl-fluoride (PMSF)
PM17 A5 Protein aa analog, alanine β-Chloro-L-alanine hydrochloride
PM20 A9 Protein aa metabolism Benserazide
PM19 F5 protein synthesis Blasticidin S
PM11 F1 protein synthesis Chloramphenicol
PM14 F1 protein synthesis Chloramphenicol
PM18 A9 protein synthesis Thiamphenicol
PM11 A1 protein synthesis, aminoglycoside Amikacin
PM20 A5 protein synthesis, aminoglycoside Apramycin
PM11 D1 protein synthesis, aminoglycoside Capreomycin
PM19 G5 protein synthesis, aminoglycoside Dihydro-streptomycin
PM13 E5 protein synthesis, aminoglycoside Geneticin (G418)
PM11 G5 protein synthesis, aminoglycoside Gentamicin
PM17 B5 protein synthesis, aminoglycoside Hygromycin B
PM11 H5 protein synthesis, aminoglycoside Kanamycin
PM11 F9 protein synthesis, aminoglycoside Neomycin
Pm12 C1 protein synthesis, aminoglycoside Paromomycin
Pm12 D1 protein synthesis, aminoglycoside Sisomicin
Pm12 G1 protein synthesis, aminoglycoside Spectinomycin
PM16 E1 protein synthesis, aminoglycoside Streptomycin
Pm12 F1 protein synthesis, aminoglycoside Tobramycin
PM15 F9 protein synthesis, chain termination Puromycin
PM15 C5 protein synthesis, elongation factor Fusidic acid
PM11 A9 protein synthesis, lincosamide Lincomycin
PM11 F5 protein synthesis, macrolide Erythromycin
PM19 A1 protein synthesis, macrolide Josamycin
PM15 F5 protein synthesis, macrolide Oleandomycin
Pm12 H1 protein synthesis, macrolide Spiramycin
PM20 H9 protein synthesis, macrolide Troleandomycin
PM13 H9 protein synthesis, macrolide Tylosin
PM11 A5 protein synthesis, tetracycline Chlortetracycline
PM11 D5 protein synthesis, tetracycline Demeclocycline
PM13 C5 protein synthesis, tetracycline Doxycycline
PM11 C9 protein synthesis, tetracycline Minocycline
PM20 F5 protein synthesis, tetracycline Oxytetracycline
Pm12 B5 protein synthesis, tetracycline Penimepicycline
PM13 D9 protein synthesis, tetracycline Rolitetracycline
Pm12 A5 protein synthesis, tetracycline Tetracycline
Pm12 C9 Protein tRNA synthetase D,L-Serine hydroxamate
PM17 F5 Protein tRNA synthetase DL-Methionine hydroxamate
PM16 H1 Protein tRNA synthetase Glycine hydroxamate
Pm12 G9 Protein tRNA synthetase L-Aspartic-β-hydroxamate
PM16 G9 Protein tRNA synthetase L-Glutamic-g-hydroxamate
PM19 D5 respiration Iodonitro Tetrazolium Violet
PM13 E9 respiration, Ca++ porter Ruthenium red
PM20 D9 respiration, ionophore, H+ 18-Crown-6 ether
PM19 B9 respiration, ionophore, H+ 2,4-Dintrophenol
PM20 G5 respiration, ionophore, H+ 3,5-Dinitro-benzene
PM15 G1 respiration, ionophore, H+ CCCP
PM19 C9 respiration, ionophore, H+ Cinnamic acid
PM19 E1 respiration, ionophore, H+ FCCP
PM19 A5 respiration, ionophore, H+ Gallic acid
PM18 C9 respiration, ionophore, H+ Pentachloro-phenol
PM19 F9 respiration, ionophore, H+ Sodium caprylate
PM16 H9 respiration, ionophore, H+ Sorbic acid
PM20 E1 respiration, uncoupler Crystal violet
PM15 G9 respiration, uncoupler Menadione
PM15 G5 respiration, uncoupler Sodium azide
PM20 B9 respiration, uncoupler Tetrazolium violet
PM17 D1 respiratory enzymes, carboxamide Oxycarboxin
PM14 C1 toxic anion Boric Acid
PM13 C9 toxic anion Potassium chromate
PM16 F1 toxic anion Potassium tellurite
PM11 G9 toxic anion Potassium Tellurite
PM18 D5 toxic anion Sodium Bromate
PM14 C9 toxic anion Sodium cyanate
PM14 E9 toxic anion Sodium metaborate
PM18 E1 toxic anion Sodium metasilicate
PM14 G9 toxic anion Sodium nitrite
PM16 F5 toxic anion Sodium selenite
PM18 D1 toxic anion Sodium-m-arsenite
PM17 E9 toxic anion, molybdate analog Sodium tungstate
PM18 E5 toxic anion, oxidizing agent Sodium-m-periodate
PM14 B9 toxic anion, PO4 analog Sodium arsenate
PM14 F9 toxic anion, PO4 analog Sodium metavanadate
PM14 H9 toxic anion, PO4 analog Sodium orthovanadate
PM14 D9 toxic anion, SO4 analog Sodium dichromate
PM16 F9 toxic cation Aluminum sulfate
PM18 E9 toxic cation Antimony (III) chloride

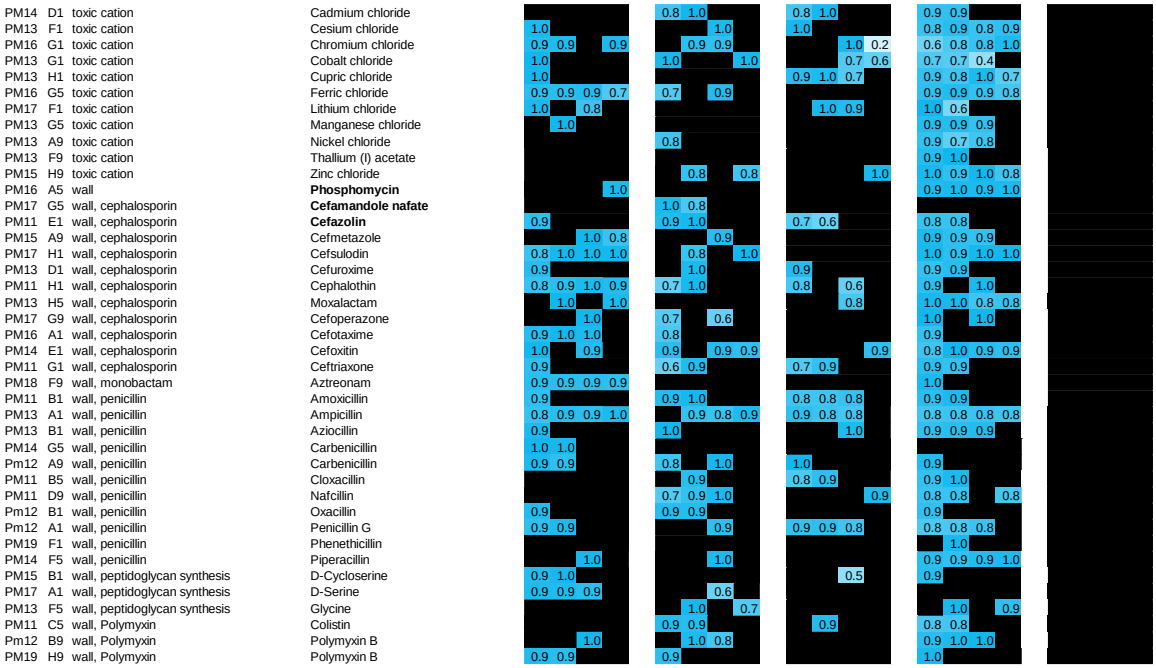

Figure D.2. Heatmap of CDI values of EDC (0.01% w/v) induced Syergism and additve effects to Biolog (Blue shading).

Table D.1. All identified proteins from triplicate biological injections of *E. coli* grown in all respective EDCs and control testing conditions.

Protein List
Q8XE62 , P39180 , P0ADW3 , P0ADA7 , P75818 , P0A905 , W1FVW9 , A0A0H3JH44 , P0AAC0 , P0ABC3 , P69807 , P0AE08 , P46130 , P37749 , P0ABT2 , P0A7Z4 , P0A7G6 , P0A8N5 , P0A6Y8 , P0AAI3 , P10408 , P0A853 , P12758 , P0C8J6 , P05847 , P0A9M8 , P0ABF6 , P0AFG8 , P69741 , P0ACE0 , P08839 , P0ABJ9 , P09152 , P60422 , P09323 , P0A8F4 , P00393 , P0A9A6 , P00363 , P00961 , P0A9B2 , P07001 , P0CE47 , P61175 , P68187 , P0ABB4 , P0ABB0 , P0A9V1 , P0A6M8 , P0A940 , P77774 , P06959 , P09373 , P0A7A7 , P39177 , P0A7K2 , P69797 , P69786 , P0C8J8 , A0A0H3JQ75 , P0ABA0 , A0A0H3JMR3 , P0AG67 , P60723 , P0A7V0 , P06996 , P0ADY3 , P37194 , P0A915 , P0A917 , P0A912 , P0AC02 , P31554 , P69776 , P0A908 , P0AEH5 , P0ADB1 , P64581 , P02943 , P60438 , P0A7R9 , P02359 , P0A7L0 , P0A7W1 , P02413 , P0A7V8 , P0A910 , P25714 , P02931 , P02930 , P28635 , P0AG44 , P62399 , P0ADY7 , P0A7X3 , W1FZ84 , W1G3V3 , P37636 , P58229 , P64604 , P0A927 , W1FUB4 , P0ADQ7 , P09424 , P0A9M0 , P37617 , P0A921 , P77293 , W1FU14 , A0A0H3JJM9 , P0A9Q7 , P0ACD8 , P0ADG4 , P11349 , P0A7M2 , P31224 , P09127 , P26459 , P69739 , P63284 , P76576 , P0A7S9 , P0A7L3 , P37637 , P0A7K6 , P0AG59 , P0AFR2 , P37665 , P77330 , P06129 , P0ADZ7 , P60955 , P76578 , P45464 , W1FSW5 , P0A6P9 , P69783 , P0ABH9 , P0AB98 , P08194 , P69828 , P0AGF6 , P0AB26 , P0AEX9 , P0A742 , P0AC41 , P76507 , P0ACF4 , P09169 , P10384 , P0ADB7 , P20966 , Q8XE41 , P24182 , Q8XC31 , W1G708 , P36659 , P0A9S3 , A0A0H3JJZ5 , P0AC47 , P23173 , W1FS73 , P0A7D7 , P11868 , P0A7B1 , P52647 , A0A0H3JJ32 , Q8X5R4 , P10100 , P77338 , A0A0H3JCY2 , P30844 , P77625 , P41036 , P06609 , P0AEJ4 , P15005 , Q8X578 , P0A6E1 , P38506 , P23890 , W1FQZ7 , P0AFD4 , P0A9C0 , P08956 , P0AAG5 , P0A9Q5 , A0A0H3JRG4 , P13035 , P0AAH0 , P77529 , P04805 , P33232 , A0A0H3JS22 , A0A0H3JI64 , P0AGG0 , P0ACL9 , Q8X660 , P75691 , P0AFB5 , P22524 , Q46803 , A0A0H3JCY6 , P76251 , P0A8W2 , P0A6Z1 , P25665 , P09372 , P60720 , P0ADN0 , P39409 , A0A0H3JI35 , P08660 , P75800 , P27242 , P0AA93 , P0AGI8 , P20083 , P15034 , P0A8U0 , P0A7A9 , P69503 , P05852 , W1FTM3 , Q8X5T0 , P23839 , P16433 , P0A9D4 , P00887 , Q8XC00 , W1G0W6 , A0A0H3JDL6 , W1FUN7 , P37648 , W1G8R8 , P0AAJ5 , P27243 , P75839 , A0A0H3JEB9 , P0DMC5 , P0AAC4 , P52644 , P75946 , P0AAK7 , Q8X5N1 , P24207 , P09391 , P0AE74 , P0A8S1 , A0A0H3JKI8 , P27836 , P75828 , P76237 , P0A935 , P76185 , P37639 , P76421 , P0AFD1 , P0AEJ0 , P0A8R9 , P09549 , W1G7L0 , Q2MB16 , P52101 , A0A0H3JQB0 , P37327 , A0A0H3JFG8 , P54746 , P17315 , P0AG71 , P31697 , P0AER0 , P32681 , P77485 , A0A0H3JRM4 , P0AFU0 , P0AAD6 , P76406 , Q46793 , P33358 , P76561 , P0A3R8 , P0AGC7 , P0AFA9 , A0A0H3JM80 , P77475 , P75831 , W1FV91 , Q8XDU3 , P0ABU0 , P07913 , W1FYM8 , W1FUN1 , Q8X781 , P04846 , Q8X809 , P33941 , P02918 , P0AAE0 , W1FUR2 , A0A0H3JS36 , W1G0T2 , P0C066 , P37691 , Q8XDB1 , A0A0H3JH37 , Q8XAZ8 , Q46920 , P24224 , W1FUT9 , P03819 , P0ACS9 , A0A0H3JCC8 , P75870

, P07021 , P33591 , P0AG96 , A0A0H3JIX3 , P06971 , P37692 , P0AF20 , A0A0H3JCX1 , P0A843 , A0A0H3JFT3 , P00903 , P05041 , A0A0H3JHD7 , P76053 , P06999 , A0A0H3JEY2 , P65958 , P33011 , W1G2V7 , W1G489 , W1G4E3 , P64616 , P31475 , P0AE18 , P75913 , Q8XCJ1 , W1FUA9 , P0AB20 , A0A0H3JDY3 , A0A0H3JGZ0 , W1G2R5 , P0AFU4 , Q46861 , P26648 , W1FPX3 , P46853 , Q8XC75 , W1FZ17 , P25536 , A0A0H3JCJ9 , P60546 , P0ABU5 , P0A6D0 , Q8X7Y7 , P45568 , P02358 , P0A8I5 , P76145 , P0A7X6 , P0AB61 , P0ACD4 , P0AF67 , P0A9G8 , P37634 , P41407 , Q8X9W9 , P0AF63 , P18133 , P0AF50 , P0ADN2 , Q8XDX3 , A0A0H3JGJ3 , P29680 , P0A6K1 , P08179 , P15254 , P31806 , P0A9J0 , W1FTH4 , P32143 , P67701 , W1G653 , P0A978 , P30748 , P0A4D1 , P67603 , P0A752 , P0A9I8 , P19624 , A0A0H3JH97 , W1G5W0 , Q8X901 , A0A0H3JC69 , W1G253 , Q8X5P5 , W1G1V0 , P0ADF6 , A0A0H3JDN2 , P37013 , P21693 , W1G2K1 , A0A0H3JFW2 , P0AEC8 , P18196 , P67601 , W1G5H1 , W1FT75 , P0AB93 , P42626 , A0A0H3JEC1 , P17888 , P77510 , W1FZ49 , W1G039 , P55135 , W1FT47 , P11454 , W1G778 , P75796 , P43261 , W1FTV9 , W1FUP5 , P0A6T5 , W1FZ33 , W1FRC2 , P0A8Z7 , P07762 , W1FXJ7 , A0A0H3JHC2 , P33234 , Q06067 , P60664 , P76187 , P25550 , P06960 , P19642 , A0A0H3JIZ2 , P05827 , P76469 , P26649 , P69791 , P39829 , P64599 , P09053 , W1FV03 , P37623 , P62623 , Q8XA02 , P0A8E5 , P0A814 , A0A0H3JJ08 , P37590 , Q8XA99 , P41409 , P06989 , W1FRD3 , Q8XCT1 , P75782 , P0AAN9 , P0A884 , P0AFW0 , P13669 , Q8X7B0 , P0A7C6 , P0A8W5 , P28905 , P0AA39 , W1FPC6 , P76055 , P0A8B2 , P52076 , P0AC19 , P0AAU7 , P13001 , P0A8U6 , P0A8D9 , P0AEZ9 , P05706 , P07649 , P77559 , P0A7H6 , P22106 , P76502 , P0AB43 , Q8XA92 , P0AB28 , P22255 , P36995 , P0AC84 , P0AF10 , P0A6K3 , P0AE48 , P23882 , P77247 , P75849 , P27828 , P25539 , P27848 , P76550 , P0ABK9 , Q8X994 , P0ACK2 , P0AEM0 , P69829 , P39377 , P24232 , P0AEH3 , P0A722 , Q8X5J6 , P67553 , Q46857 , P0A6I3 , W1FZX2 , P0AEF4 , W1FU28 , P76073 , P0AAR3 , P0AF18 , P0ACE7 , P12008 , Q46927 , Q8XDJ1 , P0AAT6 , P0AAL3 , P58344 , P21189 , A0A0H3JGR3 , P32664 , P75931 , P52697 , P0ADA1 , P38489 , Q46799 , P39410 , Q46810 , P0AFC0 , P03030 , P30749 , W1FV36 , P27298 , P0A8I8 , W1FSB6 , P0A7D1 , P0A898 , P45799 , P37182 , P24178 , Q8X5J2 , P75952 , P24171 , P68567 , P0AF61 , P38051 , W1G3Q3 , P68398 , P0ACG8 , P00893 , Q8XCB9 , P0A720 , P21515 , P14900 , P38684 , P64426 , P77182 , A0A0H3JQY5 , W1FZP9 , Q8XD14 , P07026 , P0AAL6 , P0A9J8 , P03007 , P0A6W0 , P37671 , Q8XDB6 , P0AE76 , W1FTJ7 , W1FUV4 , W1G595 , P64432 , P39376 , P0AEE8 , P77544 , P0A7I7 , P25526 , P0A8G3 , P65556 , W1FZU6 , P21365 , P37641 , P0A8B0 , A0A0H3JII1 , P0A9S1 , A0A0H3JHT3 , P46144 , Q46814 , P0ABY4 , P11458 , Q8X8B9 , P75825 , P64559 , P76291 , W1G1U2 , P30863 , P0AGA6 , P38038 , P0ADP9 , W1G4E2 , P76273 , P64455 , P62601 , P25744 , Q8XB52 , A0A0H3JEL6 , P45475 , P40719 , A0A0H3JJE9 , P0A8Y5 , P15977 , P33593 , P0AFE8 , Q8XCA1 , P09126 , P64610 , P0A9N8 , P61316 , P0AFP6 , P0A8P8 , A0A0H3JMN3 , P39304 , P56258 , P0AD24 , P0AB91 , P0A8P3 , Q8X9I4 , P0A8Y3 , P0AB18 , P0A8A0 , P0AGK4 , P0C0R7 , P0A9Z1 , P00926 , P0A6W9 , P52006 , Q46919 , P0AAT2 , P09162 , P64622 , W1FX53 , Q8X776 , P75874 , P0A8N7 , P42599 , P0AGB3 , A0A0H3JER1 , P05459 , P00490 , P19931 ,

Q8XBL0 , P75959 , P05523 , Q8X7J9 , P04693 , P76483 , P0AEN4 , P15286 , P36767 , P32716 , P0A8W8 , Q2M7R5 , P0AGE9 , P0AEQ3 , W1FX82 , P77552 , P75876 , P0AEN1 , P39173 , P69222 , P45544 , P0AA78 , P0A7I0 , P31129 , P0A8D6 , P0A8I3 , P76046 , P0A8D0 , P45578 , P0A8D3 , P33934 , P64545 , A0A0H3JRT5 , P77400 , P69490 , P0A951 , P07117 , P60782 , P67660 , P0A924 , Q8XE32 , P0ABG1 , P77335 , P39176 , W1G0V9 , P0ADP7 , W1FUN6 , A0A0H3JG15 , P0AFY8 , Q8X6L8 , P0A725 , P32162 , W1FUQ9 , P58323 , P0A8Z0 , P37650 , P0AFQ2 , W1FRG3 , A0A0H3JH40 , P58319 , P0ADS9 , P0A7Y8 , P0A6L2 , W1FTP1 , A0A0H3JJ58 , P12282 , P52061 , P0ACY1 , A0A0H3JE38 , P22525 , P39286 , P37666 , P11875 , P32173 , P0AD68 , P75824 , P0AC53 , P52598 , P17115 , A0A0H3JGN4 , P37180 , P0ADV1 , W1FTQ7 , P0AD59 , P0A932 , P66948 , P29745 , P33937 , P76909 , P0AD01 , P77304 , A0A0H3JK93 , P64606 , P02932 , P39836 , W1FSV8 , P0AA60 , P07821 , Q8X5S4 , W1FS83 , P30855 , P76398 , W1G269 , P60932 , P76402 , W1FTS2 , P0AFM9 , P0AFX9 , P27241 , P0A998 , P63201 , P45955 , A0A120LVQ1 , Q8X7Y9 , Q2EET2 , P31547 , P0AF36 , P0AAE2 , P12295 , P07102 , P0ACL2 , P37001 , P0ABL5 , P0A948 , W1FS10 , P24177 , P32709 , P0AE30 , W1G7I3 , P0ABZ6 , P0A996 , P30177 , P0A6F9 , P32129 , P0A8H6 , A0A0H3JDU9 , P76143 , P0A9W0 , P0ACJ0 , W1G0R6 , P07024 , P77499 , P14175 , P30843 , P33919 , Q46835 , P0A6S5 , P0AFY6 , P76146 , P00888 , P45523 , P0A7N4 , P0ACM2 , P77504 , P31663 , W1FXQ5 , P68191 , P0AFM6 , A0A0H3JIR1 , P0A738 , P0A6Y5 , Q8XA37 , P64476 , P63204 , P30143 , Q8XE61 , P0ACZ4 , P0AAK4 , Q8XB22 , P0A6W5 , P0AGB6 , P0A7M9 , P0A988 , P0AAD8 , P0AET8 , P62768 , P0A763 , W1FWT0 , P0AFN2 , P75822 , P39407 , A0A0H3JJK9 , P0AAA9 , P0A873 , A0A0H3JI70 , P06610 , P07395 , P64540 , P37355 , P77808 , P39336 , Q8X7Q1 , P0AED9 , P29208 , P69228 , P07862 , P0A9E0 , P30128 , P0AFW4 , P19930 , P00370 , P0A9Q9 , P76270 , Q8X7Z0 , P0A9J4 , P52636 , P63020 , P0A9D2 , P0ABK5 , P0ADX9 , W1FPE5 , P21866 , P76194 , W1G3E5 , P77150 , P63228 , P61949 , P27126 , W1G5U4 , Q8XAK7 , W1FVJ7 , Q8XDD3 , P0AES2 , P29217 , P32099 , P33030 , P0A9E2 , P0ADU2 , P75867 , P0AFU8 , P06612 , W1FTK6 , P0A6Q6 , Q8XDH4 , P69434 , P08373 , P0A8X0 , P0A8S5 , P0AD19 , W1G5G3 , P77183 , P0A9X1 , P10346 , P0AAE8 , P52645 , P45800 , P0ABN1 , W1FVR7 , Q8XCI1 , P0AD65 , W1G2T5 , P0ADX7 , P0AFP4 , P39297 , A0A0H3JK35 , P0ABF1 , P37019 , P0ADV7 , P69423 , P0ABM9 , P0ACV4 , P46474 , P16432 , A0A0H3JD10 , W1FU90 , P45537 , P37615 , P63340 , Q8XA28 , Q8XD04 , P46118 , Q7DFV3 , P23837 , P76397 , Q8XE89 , P0AFF0 , P0AC78 , P0AC75 , P30011 , P77536 , P0AGH5 , P0A7A5 , P0AF48 , P46022 , P39453 , Q8XDX9 , P0A6A6 , A0A0H3JKB7 , A0A0H3JJI1 , P0A9J6 , P0A8W0 , P63177 , P0A9L8 , Q8XEB1 , P0AG76 , Q8XBA0 , P39406 , P39334 , P04982 , Q47150 , P27830 , A0A0H3JKJ3 , P0AF90 , P21893 , P42596 , P28630 , P27245 , P75933 , P39385 , P14375 , W1FYT1 , P0A7J0 , P61887 , P0AGF2 , A8B1I2 , P0A6U5 , P32134 , P33018 , P23908 , W1FX37 , P23874 , A0A0H3JGU9 , P76535 , A0A0H3JID1 , P09147 , Q8XBT8 , P10908 , A0A0H3JCK2 , Q8X9L1 , P15770 , P0AFV4 , P0AAI9 , P76245 , P08244 , P0AEZ1 , P75915 , P36566 , Q8X7G9 , P0A800 , P64554 , P0ACN4 , P0AFH6 , P0A6Q3 , W1FXF6 , A0A0H3JFI9 , P0A6P7 , P0AGH3 , W1FT60 , P33025 ,

P0AA43 , P0AF03 , P67095 , P62615 , P76235 , P21514 , P30864 , P60716 , P0ADL3 , P21645 , P0A805 , P52129 , P37908 , P0A955 , P03841 , P45577 , P27247 , P26646 , P0AAX8 , P07023 , P56580 , P45527 , P30870 , A0A0H3JNM3 , P71298 , W1G016 , W1FXQ7 , P0C058 , P0AFZ3 , P76256 , P0ACC7 , P0AC69 , W1FR76 , P0ACB0 , P06710 , P0AF12 , P0AEI4 , P64483 , P09030 , P0A862 , P76440 , P0C054 , P33136 , P32166 , P22634 , P37774 , P0AAF6 , P25535 , P0A9R7 , P76220 , P0A9F6 , P37340 , P0AEC5 , P52643 , P23886 , P0AC35 , P24192 , P31119 , P0ABP3 , P0AGD3 , P69856 , P0AFI2 , P0A6J5 , P0ABP8 , P27303 , Q8XCA4 , P0ABV6 , P0AF98 , P0ABU7 , P04335 , P64499 , P0AEQ6 , P04128 , P0A8J8 , P28224 , P08550 , P15877 , P0AGC3 , P0AFB8 , P0AED5 , A0A0H3JGQ0 , P08312 , P0A9P0 , P0A6U8 , Q8XCI5 , Q47710 , P0A7G2 , P0ABQ4 , P26458 , Q8X7I9 , P0AET5 , P0AAH8 , P33607 , P0AB01 , P64448 , P31677 , Q8XAM6 , P60293 , P08394 , P75780 , P33920 , P76446 , A0A0H3JH08 , P33931 , P0ADS6 , P19934 , P0AFI9 , P13024 , P25742 , P06709 , W1G4G9 , P27306 , P77689 , P28631 , W1FYA7 , P76034 , P77334 , P13458 , P0A6T9 , P0A7F6 , P0A8T1 , P0AG40 , P50465 , P0AEY3 , P0AFX4 , P67087 , P24230 , P0AEI6 , P46859 , W1FT41 , P0ACL0 , P0AEJ6 , P25745 , A0A0H3JMT8 , Q06065 , P64588 , P0AGG8 , P07648 , P0AE39 , P0AC81 , P37758 , A0A0H3JCA2 , P76268 , P75863 , P58585 , P0A6E4 , P0A944 , P17109 , P0A9P4 , W1FS31 , P0A9F1 , P0A7C2 , P00968 , P23003 , P0A7F9 , P0AGE6 , P06987 , P75809 , P39356 , P25516 , Q8XDA2 , P75949 , P0A6X3 , Q8XE71 , P0AE52 , P0AEV4 , P24215 , P11880 , A0A0H3JHF5 , P24186 , P0AF24 , P04425 , P0AG24 , P0A6P1 , P34209 , P0A9F3 , P0AAB6 , P58345 , P08555 , P31802 , P06149 , P0AD33 , P0AE34 , A0A0H3JM35 , P0ADR8 , P37642 , P0A7E5 , P0A9D8 , P0AAN3 , Q8X7C0 , P24251 , P64590 , P0AEH1 , Q8XE81 , P69910 , P64463 , P0A9C9 , P0AAY1 , P30871 , P24228 , P0ACR9 , P27248 , P0A6X1 , P0AD99 , P32680 , P0ACC1 , P31057 , P77279 , P0A8Z3 , P0AEF0 , P0A729 , P27300 , P37746 , P10441 , P0AC59 , P0AFS7 , P0ACQ4 , W1G1P2 , P0A776 , P0AF43 , P0A6J3 , P63224 , P0A812 , P0A9K7 , P0ACU5 , P0A6D7 , P0A6U3 , P0A780 , P33643 , P37745 , P76002 , P29013 , P76491 , P0A761 , P0AAI5 , P0A7A2 , P03018 , P16095 , P60906 , P64612 , P0AAB4 , P63417 , A0A0H3JFP5 , P23893 , P31658 , P24193 , Q8XE73 , P0AE88 , P00946 , P37744 , P07650 , P25397 , P0A9L5 , P28246 , P51025 , P39831 , P30744 , P08200 , A0A0H3JR68 , P69441 , P0ADE8 , P36680 , P24202 , P0A962 , P0A832 , Q8X643 , P76243 , P0A8U2 , Q8X5N6 , Q8X703 , P00936 , P64596 , P0AG27 , P31063 , Q8XBD3 , P08997 , A0A0H3JH39 , P0A8T7 , A0A0H3JER5 , P23894 , P00957 , P05055 , P0ABK2 , P0AEZ3 , P00960 , P33599 , P60785 , P06993 , P76506 , P77804 , P69411 , P0A7R5 , P0A7J7 , P0AE06 , W1G7I8 , P0ABN5 , A0A0H3JEB0 , P0ABI4 , W1FTZ0 , P0ADK0 , P0A8K1 , P0AG14 , P0A8V2 , P0C0S1 , P0AA53 , P76372 , P0AEB2 , P0A6H5 , P21513 , P0AGD7 , P0AG55 , P02919 , P0AEE3 , P0ADY1 , P0A937 , P0ABC7 , Q8XB65 , P0AAA1 , P37751 , P0A6H1 , P0A7E1 , P10121 , P00452 , P0A7J3 , P0AFL6 , P0ACJ8 , P0AG86 , P0ABU9 , P0A6V8 , P0ACF0 , P61889 , P0AFD6 , P0ACP1 , P0A953 , P76389 , P0AB67 , P31433 , P64451 , A0A0H3JLY7 , P0AC86 , P39835 , P0AFB1 , P0AGA2 , P04994 , P0AES6 , P0A9W3 , P77737 , P0A850 , P0ACY3 , P0A799 , P0AB89 , P0ABA4 , P0ABH0 , P42632 , P07118 , P0A7M6 , P39838 , P11350 ,

P64564 , P76170 , P0ACI0 , P0A9H3 , P22333 , P28903 , P76658 , P33218 , P21507 , P0AEI1 , P13445 , P29018 , P39414 , P77717 , Q8X9F5 , P0A8V6 , P37177 , P23865 , P0AEK7 , P39342 , P68699 , P0AE45 , P76272 , P60872 , P13029 , P31680 , P15038 , P04983 , P0A901 , P06616 , P46837 , P36979 , P69908 , P69874 , P0AE42 , P00864 , P0A7L8 , P0A705 , P75864 , P33594 , P0AAM1 , P07014 , P21170 , P0A8F8 , P0DMC7 , P0AG51 , P0ADI9 , P62620 , P0A6G7 , Q46808 , W1FS28 , W1G3P2 , P27129 , P0A9C5 , P0A749 , P0AD12 , P0A7Y0 , P0AFG3 , P21889 , P60240 , P0ADG7 , P64624 , P0A8E7 , P0ACR4 , P0AE14 , P0ADS2 , P0AED0 , P0A8N3 , Q7DKW4 , P0A8F0 , P63389 , P0A6I0 , A0A0H3JHA3 , P30958 , P69924 , P33226 , P21345 , P0A6X7 , P67662 , P77454 , Q8X6U4 , P75801 , P42641 , P22188 , P68919 , A0A0H3JIZ3 , P0AF26 , P0ACZ8 , P0AG20 , P08390 , P22939 , P37759 , P37613 , W1G4N9 , P06992 , P15042 , Q8XDR0 , Q8X6P6 , P08506 , P27434 , P0AG90 , Q8X9J8 , Q59385 , P43329 , P0AG00 , P62517 , P0AEK4 , P0AA10 , P68183 , P0A8G6 , A0A0H3JL26 , P0ABN9 , P02916 , P61320 , P76537 , P76471 , P0ADC3 , A0A0H3JJ52 , P0AG30 , P03004 , A0A0H3JHB8 , P24183 , P00579 , P0A6H8 , P0ADN6 , P0ABD5 , P69811 , P0AAJ3 , P0A9Q1 , P21829 , P75957 , P09980 , P0AFC3 , A0A0H3JEF4 , P36683 , P0A870 , P0AEC3 , P0A6P5 , P39285 , P39830 , P37624 , Q46802 , P0AFA2 , P00582 , P0A796 , P0AFK0 , P0ACG1 , P0ABJ1 , P28249 , P0A8Q0 , P37747 , P0A8R7 , P16926 , P0A6N4 , P0C0L7 , P0A8M3 , P21499 , P0ABB8 , P0AFG6 , P08395 , P0A7S3 , P0A7D4 , P23930 , P0A9P6 , P0AFV2 , P0AD57 , P0AGI1 , P0AFF6 , P0A715 , P75958 , P0AEC0 , P0AAD2 , P0AFY2 , P77265 , P23842 , P24255 , P09833 , W1FYH2 , P28303 , P30014 , W1FYN4 , P30178 , P33195 , P0AAS0 , P66899 , P0CG19 , P21865 , P14081 , P0A9U3 , P76330 , P0A817 , P75829 , P00934 , P04079 , P31473 , P26616 , P37342 , Q47146 , P77272 , P21888 , P0AA84 , P00954 , P24203 , P30847 , P23367 , P77735 , A5A613 , P0AF16 , P0A8B5 , P17952 , P0ABD3 , P26602 , P0AEW6 , P13033 , P0A8N0 , P0AFA5 , P76594 , P0A6A0 , P19932 , P28304 , Q46856 , P23836 , P0ACP7 , P0AAB8 , P0A7I4 , P0A825 , P10443 , A0A0H3JDX3 , W1FW14 , P00963 , P0AE22 , P76086 , A8B1I1 , P0A6L7 , P03024 , P0A703 , A0A0H3JIU0 , P69451 , P60340 , P30015 , P11447 , A0A0H3JMN1 , P14294 , P03817 , P75793 , P58220 , A0A0H3JEF8 , P77434 , W1G4N8 , P0A759 , P77509 , W1FXC4 , Q8X945 , P27829 , P77570 , P23898 , A0A0H3JIH5 , P0A6L9 , P0AFT5 , P77667 , P0A7N9 , P17993 , P19323 , P23305 , P64493 , P0AFH2 , P0A9H1 , P05825 , P31678 , P76510 , P39353 , P39401 , P62707 , P25522 , P0A6J8 , P52062 , P76222 , P32662 , P07639 , P0AA04 , P23871 , P33224 , P76549 , P17117 , P05707 , A0A0H3JLT0 , P31142 , P07004 , P0AF28 , P0ACT6 , P08192 , P68066 , Q8XBT4 , P41052 , P0A6Z3 , A0A0H3JIW9 , P0AFA7 , P69801 , P0ADV9 , P75820 , P0A959 , P00803 , Q8XA79 , P0A7W7 , P0A7P5 , P0AAT4 , P00350 , Q8X4T2 , W1G7K4 , P21420 , P0ADZ0 , P69853 , P0A8A2 , P17169 , P55734 , P0A6T1 , P0AFG0 , P00962 , P0A6R0 , P27240 , P42630 , P0A6B7 , A0A0H3JHM7 , P0A855 , P0ACB4 , P58603 , P0A8Q3 , P02925 , P18776 , P0A7E9 , P77775 , P0A6L4 , W1G0F7 , P0A8G0 , P0A7B3 , P0AAQ2 , P0ABS5 , P0A809 , P0A821 , P09394 , P76141 , P0A6T3 , A0A0H3JNF7 , W1G2V3 , P0ABG7 , W1G301 , P0AB85 , P0AG16 , P23869 , P0ACA3 , Q8X904 , P0ABS1 , P37095 , P0A7T3 , P32132 , P11557 , P0AB71 , P00805 , W1G7Q0 , P0AGE0 ,

P0AFJ7 , P0AC38 , P0AC30 , P0A7U7 , P60752 , P0AA91 , P43671 , P0AAJ8 , P0ADC1 , W1FT65 , P0AB38 , P0AEU7 , P0ACV0 , P0AD27 , P31600 , P77173 , P0AG99 , P0AEB5 , P15288 , P69831 , P0A8M6 , P22523 , P76027 , P24205 , P31120 , Q8X7H3 , P68767 , P60061 , P13036 , P0AE01 , P0AB12 , P0AES9 , P0AE82 , P0A9B6 , P36879 , P0A9E5 , P75777 , P33602 , P0ACB7 , P0A8M0 , P0ADE4 , Q46841 , P37188 , P18775 , P69380 , P0AD44 , P0AG48 , P77562 , P63386 , P31979 , P37197 , A0A0H3JHE3 , P0A8E1 , P37903 , P0ABU2 , P0AAJ1 , P0A6V1 , P64423 , P25894 , P25746 , P07658 , P0A8J4 , P0A698 , P0A6F5 , P0AB77 , A0A0H3JCM9 , P75728 , P0A717 , P0AGJ9 , P07012 , P0A887 , P39321 , P0A9K3 , Q46868 , P75960 , P0A7R1 , A0A0H3JIG0 , P40710 , P37750 , P0ADT8 , P37765 , P0ADU5 , P0AG93 , P17443 , P0AB10 , P0A6Y1 , W1FZ58 , P69428 , P0ADA3 , P30750 , P0A6E9 , A0A0H3JEX7 , P00561 , P07003 , P0A6F3 , P0A7U3 , P0AGJ5 , P76177 , P0AD42 , P64585 , P0ADT2 , P0AC23 , P06282 , W1FU40 , P0ABI8 , P00509 , P0AFP9 , P26647 , P37649 , P0A7Q1 , P0ADZ4 , P0AEW9 , P0A858 , P65294 , P77739 , A0A0H3JHM3 , P00959 , P0AFC7 , P0ABA6 , P28306 , P63183 , P0CK95 , P0AEK2 , P23909 , P28904 , P0A8L1 , P0A6A3 , P67910 , P0A9H7 , P69425 , P0AAK1 , P64429 , A0A0H3JP03 , P75830 , P29131 , P13009 , P0ACQ7 , P0A8C1 , P22259 , W1G754 , P05052 , P0ADQ2 , W1G4S0 , P0AAD4 , P0AB58 , P77374 , P13518 , A0A0H3JGB9 , P0A6E6 , W1G5M8 , P0AA86 , P37325 , A0A0H3JMC7 , P45469 , P37760 , P0AFK6 , P04825 , W1FRK5 , P0AB03 , P0AE78 , P39383 , A0A0H3JH12 , P37686 , A0A0H3JIA4 , Q8X5H9 , P77488 , P0ADR6 , Q93K97 , A0A0H3JHY6 , Q8X876 , P33362 , P27128 , P23721 , Q57261 , P0A9S5 , P39160 , P0A6S7 , Q8X570 , P05719 , P63264 , Q8XB21 , Q8XDE2 , P0A6N8 , P0AES0 , P25437 , P0AAT9 , P0A6L0 , P16456 , P0A6M2 , P0AAU2 , P07000 , P0A867 , P0A8A4 , P0C093 , P36929 , P0AG63 , P0A7B5 , P0AD61 , P0AFX0 , P60869 , A0A0H3JFA8 , P0A993 , P76014 , P16659 , P30850 , P0A6W3 , P0AAH4 , P07813 , P77718 , P0AD49 , P25519 , A0A0H3JGP7 , P08957 , P0CB39 , P39411 , P77756 , Q46811 , P0ACF8 , P27249 , P0C0V0 , P36938 , P0CE53 , P75906 , P0A836 , P0A9N4 , P37349 , P37773 , P52108 , A0A0H3JEX9 , P36655 , P60624 , P0A707 , P0A6K6 , P31064 , P37689 , P60390 , P0A9K9 , P0A734 , P08622 , P08201 , P0AGL5 , P00956 , P45395 , P67244 , P36561 , P77754 , P0AA97 , P45463 , P14407 , W1FW53 , P37440 , P76536 , P0AEP3 , P0AD05 , Q8XAF3 , P0A7B8 , P75838 , P76329 , P76290 , P76346 , W1FVM8 , P16384 , P18777 , P77748 , W1FPV6 , P0A894 , P0A8C4 , P76403 , P25666 , P33225 , A0A0H3JCN9 , P0AFI7 , P0A731 , P31808 , P39199 , P18843 , P61714 , P12281 , P00562 , P65807 , P0A9A9 , P37195 , A0A0H3JCT3 , W1FWC3 , P02666 , P00761 SWISS-PROT:P00761 , P04264 , P02769 , P13645 , P35527 , P35908 , Q3SZR3 , P02768-1 , ENSEMBL:ENSBTAP00000038329 , ENSBTAP00000024146 , P02672 , Q2UVX4 , ENSBTAP00000018574 , Q8IUT8 , P19012 , P08730-1 , Q9C075 , P02668 , P02662 , P78386 , Q15323 , Q6KB66-1 , Q1RMN8 , P02663 , P19013 , Q14533 , O95678 , Q32MB2 , P02676 , Q86YZ3 , P04259 , ENSBTAP00000038253 , Q5D862 , P02535-1 , P00735 , P01966 , P02538 , P02533 , P13647 , P07477 , Q04695 , P08779 , Q8N1N4-2 , Q7Z794